IDO-16666
Reactors-General
TID-4500, Ed. 15

PROPOSAL FOR AN ADVANCED ENGINEERING TEST REACTOR - ETR II

D. R. deBoisblanc et al.

March 17, 1960

AEC RESEARCH AND DEVELOPMENT REPORT

PHILLIPS PETROLEUM CO.
ATOMIC ENERGY DIVISION
(UNDER CONTRACT NO. AT (10-1)-205)
IDAHO OPERATIONS OFFICE
U. S. ATOMIC ENERGY COMMISSION

DISCLAIMER

PRICE $3.50

Available from the
Office of Technical Services
U. S. Department of Commerce
Washington 25, D. C.

LEGAL NOTICE

PAGES 1 to 2

WERE INTENTIONALLY

LEFT BLANK

PROPOSAL FOR AN ADVANCED ENGINEERING TEST REACTOR - ETR II

D. R. deBoisblanc, Director

March 17, 1960

ETR II Conceptual Design Group

R. L. Barnett
J. M. Beeston, Materials
A. W. Braun
A. W. Brown
E. S. Brown
E. E. Burdick, ETRC Experiment
M. L. Burkholder
W. J. Byron, Hazards Evaluation
S. E. Craig, Heat Transfer
J. M. Crighton
L. S. Cutler
G. M. Davis
H. W. Davis
R. M. Eckert
E. N. Ekstrand
D. W. Elison
R. S. Fisher
R. J. Flygare
R. M. Fors
*T. L. Francis
W. C. Francis, Fuel Element Design
S. R. Gossmann
L. C. Grantier
M. L. Griebenow
R. A. Grimesey
R. L. Gump
F. C. Haas, Utilities and Heat Dissipation
D. C. Hanson
G. H. Hanson, Co-ordinator and General Editor
L. J. Harrison
O. M. Hauge
J. W. Henscheid
G. Homer
L. F. Hunt
D. V. Jensen
R. D. Johnston
L. H. Jones
F. R. Keller, Operations Requirements
R. S. Kern
*B. H. Leonard
J. L. Liebenthal
W. S. Little
R. S. Marsden, Physics
P. J. Martell
K. D. Metcalf
D. W. Miller
K. V. Moore
D. R. Mousseau
R. F. Mull
K. A. McCollom, Reactor Control
R. S. McPherson
R. J. Nertney, Exp. Facilities
E. C. Newman, Eng. Design
K. L. Nilsson
V. L. Overstreet
F. L. Petree
D. L. Reid
R. E. Rhoads
J. A. Roland
J. H. Ronsick
L. W. Scarbrough
A. M. Schellenberg
O. K. Shupe
E. H. Smith
E. O. Smith
A. H. Spano, Physics
M. V. Stanton
H. M. Sullivan
B. D. Tackett
J. L. Taylor
J. M. Waage
**V. A. Walker
L. G. Wells
D. F. Whitney
L. R. Woolf
L. A. Zaladonis

ETR II Consultants

M. H. Bartz
E. F. Berry
J. W. Dykes
*O. J. Elgert
W. M. Hawkins
J. R. Huffman

* Internuclear Company
** Now with AEC Division of Inspection

THIS PAGE

WAS INTENTIONALLY

LEFT BLANK

PROPOSAL FOR AN ADVANCED ENGINEERING TEST REACTOR - ETR II

S U M M A R Y

This report presents the results of a study which was directed at providing additional experimental loop irradiation space for the AEC-DRD testing program. It was a premise that the experiments allocated to this reactor were those that could not be accommodated in the MTR, ETR or in existing commercial test reactors.

To accomplish the design objectives called for a reactor producing perturbed neutron fluxes exceeding 10^{15} thermal neutrons per square centimeter per second and 1.5×10^{15} epithermal neutrons per square centimeter per second. To accommodate the experimental samples, the reactor fuel core is four feet long in the direction of experimental loops. This is twice the length of the MTR core and a third longer than the ETR core.

The reactor concept herein proposed represents an advance in test reactor technology and can be expected to contribute a substantial body of information to reactor development as has been the case with the MTR and ETR.

The vertical arrangement of reactor and experiments permits the use of straight and vertical loops penetrating the top cap of the reactor vessel. The design offers a high degree of accessibility of the exterior portions of the experiments and offers very convenient handling and discharge of experiments. Since the loops are to be integrated into the reactor design and the in-pile portions installed before reactor startup, it is felt that many of the problems encountered in MTR and ETR experience will cease to exist. Installation of the loops prior to startup will have an added advantage in that the flux variations experienced in experiments in ETR every time a new loop is installed will be absent.

ETR II (formerly called ETR IV) has a core configuration which provides essentially nine flux-trap regions in a geometry which is almost optimum for cylindrical experiments. The geometry is similar to that of a four-leaf clover with one flux trap in each leaf, one at the intersection of the leaves, and one between each pair of leaves. The nominal power level is 250 megawatts.

This study was carried out in enough detail to permit the establishment of the design parameters and to develop the power requirement which, conservatively rated, will definitely reach the flux specifications. A critical mockup of an arrangement similar to ETR II was loaded into the Engineering Test Reactor Critical Facility. A two-dimensional calculation of this actual test provided a confirmation of validity of these computer techniques in predicting the behavior of this reactor.

The study of the remainder of the plant layout and the engineering performance of the plant incorporated the large body of test reactor experience developed at the MTR and ETR site. This design contemplates an integrated, self-sufficient site, including all service facilities required for the operation and maintenance of the reactor and experiments.

THIS PAGE

WAS INTENTIONALLY

LEFT BLANK

TABLE OF CONTENTS

TABLE OF CONTENTS (CONT.)

1.0 INTRODUCTION

1.1 Historical

On August 5, 1959 Phillips Petroleum Company was asked to undertake the conceptual design of an advanced engineering test reactor capable of satisfying the needs of the Division of Reactor Development for additional high flux irradiation space. Phillips was asked to examine and employ the most advanced technology available, and to bring forth a design with sufficient flexibility and flux capabilities to meet the Commission's needs for some time to come. This report is a technical description of the resulting reactor designated ETR II.*

Previous studies[1-10] concerning advanced testing reactors were carefully reviewed before deciding the direction the design should take.** The most detailed studies were those carried out under AEC contract in 1956 and 1957. These studies included many advanced reactor types, ranging from a heavy water homogeneous system to the light-water moderated flux-trap system. All of these studies were directed at providing high fluxes in large loop facilities. This reactor is aimed at providing extremely high flux environment for a multiplicity of high-pressure loops whose greatest sample diameter is about 2 in. In this study, an attempt has been made to bring a fresh viewpoint to the problem. The cylindrical symmetry of the experimental loops, their small diameter and the large number of samples to be irradiated at one time were factors which strongly influenced the choice of the reactor type.

Operational experience in multi-facility reactors such as the MTR and ETR set an upper limit of loops at about nine, to avoid an unduly large amount of down time. In a program where many samples are being irradiated simultaneously, each with a reasonable chance of failure and in which each sample is capable of causing the reactor to be shut down, downtime becomes a dominant factor. ETR II is considered a reasonable compromise.

1.2 Choice of Reactor Type

In considering the reactor design, various combinations of reflector and moderator materials were evaluated. It was necessary to make some arbitrary selection where comparative studies showed more than one system to be promising. For example, light water, heterogeneous reactors were chosen in preference to homogeneous types, in spite of the superior heat removal situation in the latter, because of the development problems in

---

* Designated ETR IV in IDO-16555.

** Appendix 8.2.

NOTE: References 1-12 are given at end of Section 1.0.

the homogeneous system. These problems were considered so formidable that the Fluid Fuel Task Force of the AEC, in their report of February 27, 1959, did not consider this type ready for power applications in the near future.

Light-water moderated and cooled, plate type systems were chosen and advantage was taken of the power density reductions possible with the flux concentration principle (flux trap). The use of the flux trap lowers the power density to an extent that satisfactory fuel elements can be fabricated with a limited amount of metallurgical development.

Other designers of high flux reactors have reached similar conclusions regarding the choice of systems, after they also considered use of Be, D_2O, H_2O, and C. The Argonne High Flux Research Reactor[12], the Oak Ridge High Flux Isotope Reactor[10], and the Advanced Engineering Test Reactor proposed by the Internuclear Company[11] all employ light water as moderator and flux-trap material and are heterogeneous.

A system cooled and moderated by H_2O, with beryllium as the external and internal reflector was considered.[8] With clean beryllium, fast and thermal fluxes equal to those obtained with the H_2O system result in a reactor having a lower operating power. However, beryllium was not selected as a flux-trap material because of the deleterious buildup of Li^6, He^3, He^4, H^3 in the Be due to (n,α) reaction of the fast neutrons on beryllium.

For the convenience of the reader, the important properties and parameters of the selected design, and of the plant, are collected in Tables 1.3A and 1.3B. The design velocity of 44 ft/sec (see Table 1.3A) contains allowances for all non-uniformities in heat generation in the reactor, for the hot spot - hot channel analysis in heat transfer calculations and for all uncertainties in the physics calculations which would affect the nominal power. This velocity is lower than the velocity of 50 ft/sec used in IDO-16555 because all of the physics data in IDO-16555 were not available when it was necessary to freeze the 1959 rating of the primary coolant system.

TABLE 1.3A

ETR II DESIGN SUMMARY

Reactor Configuration	Four-Lobe
Length of Reactor Core, ft	4
Power Level (Nominal), Mw	250
Fuel Region Volume, Liters	262
Fuel Loading, kg U-235	36
Estimated Operating Cycle, Days	30
Power Density, Mw/Liter	
Maximum	2.1***
Average	0.954
Vertical Power Distribution,	
Maximum-to-Average	1.40
Radial Power Distribution,	
Maximum-to-Average	1.56***
Fuel Annulus Metal-to-Water Ratio	0.75-0.80
Typical Fluxes in Experiments*	
Maximum Thermal**	0.8×10^{15}
Maximum > .6 ev	1.5×10^{15}
Primary Cooling Water	
Flow Rate, gpm	30,000
Velocity in Fuel Channels, ft/sec	44
Inlet Temperature, °F	130
Inlet Pressure, psig	300
Reactor Δt, °F	57
Core Pressure Drop, psi	92

* Since the manner in which this test reactor meets the requirements of each of the intended experiments cannot be shown in this abbreviated table, the reader is referred to Sections 2.0 and 3.0.

** These are not the maximum attainable fluxes, but rather represent fluxes attained in particular experiments chosen as examples.

***These values do not contain the 1.15 factor (see Fig. 314K) which allows for flux peaking near the side plates.

TABLE 1.3B

DESIGN SUMMARY OF UTILITIES*

Raw Water	3000 gpm
Demineralized Water	150 gpm
Steam, 135 psig	20,000 lb/hr
Plant and Instrument Air	600 scfm
Electric Power	
Commercial, 132 kv	15,000 kva
Failure-Free, 4160 volts	1500 kva
Hot Waste Storage	15,000 gal
Hot Waste Treatment (Resin Beds)	50 gpm
Gaseous Waste Disposal	80,000 scfm
Solid Waste Burial Ground	25 acres

* The above figures are normal maximum utility requirements which serve as the criteria for individual system design. They do not, however, reflect total system capacity when considering spares, stand-by units, etc.

REFERENCES

1. O. J. Elgert, C. F. Leyse, D. G. Ott, "Preliminary Investigations for an Advanced Engineering Test Reactor", Internuclear Company, Inc., Clayton, Missouri, Report AECU-3427, February 22, 1957.

2. R. G. Mallon, J. Saldick, R. E. Gibbons, "Conceptual Design of an Advanced Engineering Test Reactor", Advanced Scientific Techniques Research Associates, Milford, Connecticut, Report NYO-4849, March 1, 1957.

3. "A Selection Study for an Advanced Engineering Test Reactor", Aeronutronic Systems, Inc., "A Subsidiary of Ford Motor Company", Glendale, California, Report AECU-3478, March 29, 1957.

4. "A Conceptual Design Study of an Advanced Engineering Test Reactor", Research Division, Curtiss-Wright Corporation, Quehanna, Pennsylvania, Report CWR-464 (Del.), May 1, 1957.

5. C. F. Leyse, B. H. Leonard, Jr., "Preliminary Investigations for an Advanced Engineering Test Reactor", Internuclear Company, Clayton, Missouri, Report AECU-3427 (Add.), April 16, 1957.

6. W. L. Carter, et al., "Design Study of an Advanced Test Reactor - Reactor Design and Feasibility Study", Oak Ridge School of Reactor Technology, Oak Ridge, Tennessee, Report CF-57-8-5, August, 1957.

7. J. R. Huffman, W. P. Connor, G. H. Hanson, "Advanced Testing Reactors", Phillips Petroleum Company, Idaho Falls, Idaho IDO-16353, May 28, 1956.

8. R. J. Howerton, G. H. Hanson, W. P. Connor, "Parameters of High Flux Testing Reactors", Phillips Petroleum Company, Idaho Falls, Idaho, Report IDO-16406, August 23, 1957.

9. Marvin McVey, et al., "Evaluation of an Advanced Engineering Test Reactor Design", American-Standard, Atomic Energy Division, American Radiator and Standard Sanitary Corporation, Mountain View, California Report ASAE-S-11, July 15, 1958.

10. James A. Lane, "The Design and Need for Ultra High Flux Reactors", Oak Ridge National Laboratory, Oak Ridge, Tennessee, Paper presented at the Symposium On Experiences in the Use of Research Reactors, Harwell, England, June 11, 1959.

11. C. F. Leyse, et al., "An Advanced Engineering Test Reactor Design", Internuclear Company, Inc., Clayton, Missouri, Report AECU-3775, March 15, 1958.

12. L. E. Link, et al., "Argonne High-Flux Research Reactor - AHFR Conceptual Design Study", Argonne National Laboratory, Lemont, Illinois, Report ANL-5983, June, 1959.

2.0 REACTOR CORE DESIGN

In order to design a core best suited to fit the experimental requirements, it was necessary first to determine desirable and undesirable reactor core features. As has already been stated, concepts involving features such as homogeneous fuel and the use of plutonium were considered undesirable in view of the limited present day stage of the art. To achieve a relatively large amount of test space and efficient absorption of neutrons in experiments, the ETR II design (Fig. 2.0A) features a high leakage core, re-entrant core geometry, flux trapping, and a favorable geometrical arrangement of the fuel around the experiment.

With the four-lobe reactor, many of the advantages of the single annulus flux trap have been preserved and additional flux traps have been provided thus greatly increasing the available test space per reactor. Furthermore, the nuclear coupling reduces the mass of fissionable material needed for criticality below that required in four separate single annulus reactors. The philosophy of the multi-lobe reactor core geometry is applicable to essentially any number of fuel lobes. The four-lobe reactor with its nine excellent experimental locations was selected because it provides the optimum ratio of good experimental positions per fuel lobe and a reasonable number of loop facilities.

2.1 Fuel Disposition

Fuel elements whose cross sections are segments of a circular ring are arranged to form four partially complete right cylindrical shells, or annuli of fuel, so oriented to one another that they may be connected together by four other partially complete annuli of fuel thus forming a continuous serpentine fuel configuration.

2.2 Irradiation Spaces

The light water filled space within the fuel configuration provides five very attractive flux traps--one in the center of each of the four lobes and one in the center of the total fuel configuration as defined by the convex surfaces of the connecting fuel elements. The concave surfaces of these same connecting elements provide four additional valuable test spaces. The desired flux spectrum in each location is achieved by varying the metal-water ratio (by means of aluminum filler pieces) in the flux-trapping region between the fuel and the experiment.

2.3 Reflector Arrangement

Several reflector schemes are practical. One method utilizes a two region heavy water system. The first region consists of annular tanks of heavy water which partially surround each fuel lobe and thus may be used for control. The second region is only a continuation of the heavy water to the required reflector thickness. The use of a D_2O reflector imparts important kinetic properties discussed in Section 6.0.

A second reflector scheme also utilizes two regions, the first of which may be used for control and consists of heavy water cooled beryllium pieces outlining the periphery of the core. The second region surrounds the first and consists of an annulus of light water.

2.4 Reactor Control

As shown in Fig. 2.0A, a safety control blade is located at the neck of each lobe as well as borated D_2O shim control tubes. Partially surrounding each lobe is an individual borated heavy water region for shim control. Beryllium reflector pieces partially surround the external test spaces and are in turn surrounded by the heavy water reflector.

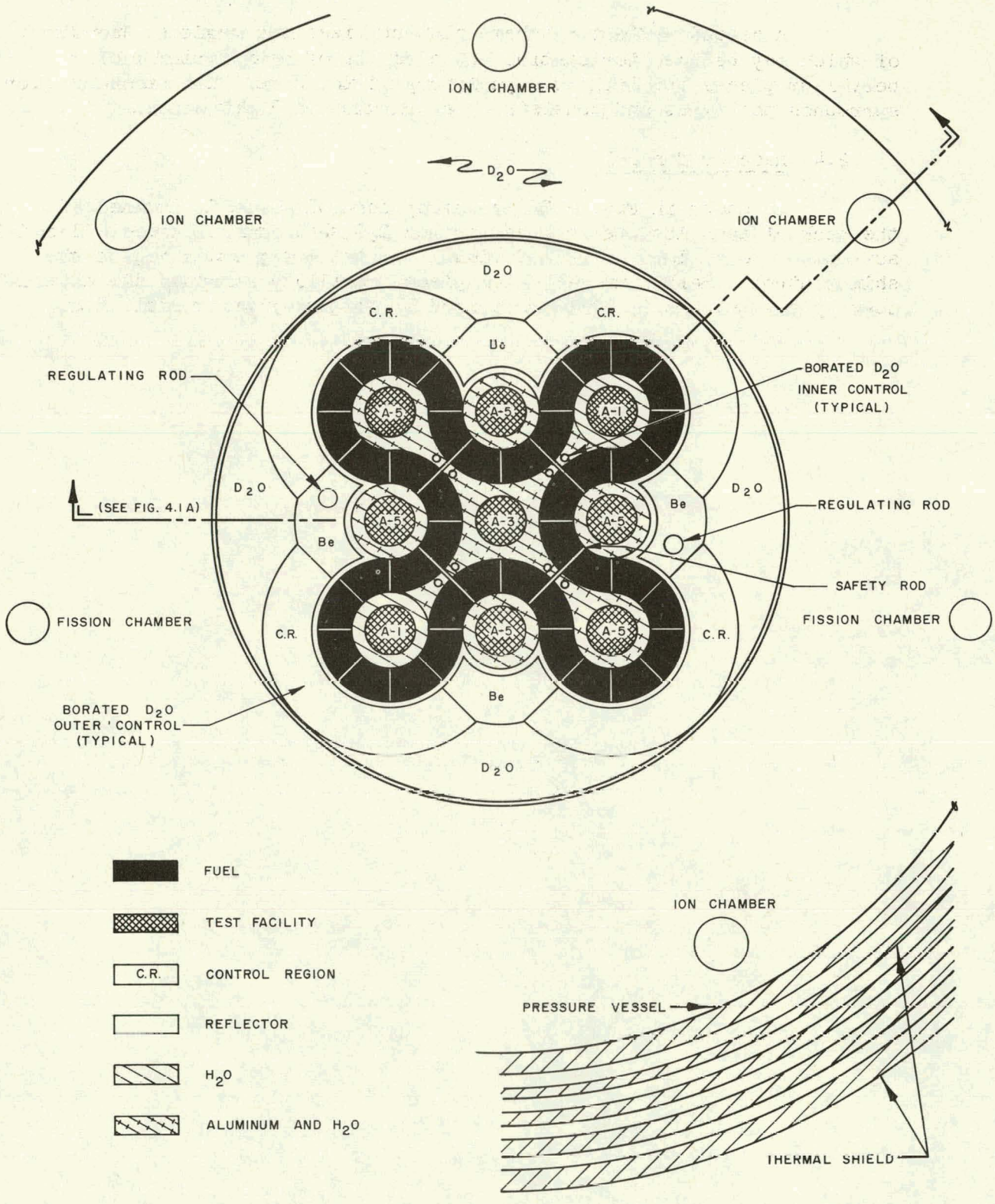

FIG. 2.0A
CORE CROSS SECTION
ETR II: FOUR-LOBE REACTOR

PPCo.-C-2700

3.0 REACTOR PHYSICS

3.1 Scope and Objectives

This section presents part of the reactor physics studies carried out during the course of this conceptual design. The aim of the work has been to develop enough information to permit selection of a core geometry which, while known not to be optimized, is known to be capable of meeting the flux and spectral requirements of the assigned experiments.

The calculations for ETR II were made by two-group diffusion theory using the IBM-704 PDQ two-dimensional code. A number of supporting studies were made on a one-dimensional model of an individual flux trap. Flux measurements were made in the Engineering Test Reactor Critical Facility on a mockup of a five flux-trap version of the ETR. These measurements provided an experimental verification of the computational methods and justified the assumption that each region can be approximated by a cylindrical flux trap. Constants for the two-dimensional calculations were developed using MUFT and DONATE routines. Constants for the one-dimensional studies were obtained from tables and semi-empirical formulas.

Previous studies on high flux reactors by Phillips Petroleum Company and others have been used to restrict the range of variables considered.[1,2,3] The work of Internuclear Company has been particularly valuable for this purpose.[4,5]

3.2 Basis for Selection

3.21 General Considerations

In this section a description is given of the parametric studies which formed a basis for determining a reactor arrangement capable of providing the requisite high fast and thermal fluxes in the test spaces of the Engineering Test Reactor II (ETR II). The fission power densities,

---

1. R. J. Howerton, G. H. Hanson, W. P. Conner, "Parameters of High Flux Testing Reactors", IDO-16406, August 28, 1957.
2. L. E. Link, "The Mighty Mouse Research Reactor Preliminary Design Study", ANL-5600, March, 1957.
3. J. A. Lane, et al., "High Flux Isotope Reactor Preliminary Design Study", CF-59-2-65, March 20, 1959.
4. C. F. Leyse, et al., "An Advanced Engineering Test Reactor", AECU-3775, March 15, 1958.
5. O. J. Elgert, et al., "Preliminary Investigations for an Advanced Engineering Test Reactor", AECU-3427, February 22, 1957.

fast flux levels, and fast-to-thermal flux ratios selected as the design objectives for this test reactor are summarized in Tables 3.2A and 3.2C. These values are considered to be the requirements to be met by the reactor.

TABLE 3.2A

DESIGN OBJECTIVES FOR ETR II

Loop Type	Nominal Loop Diameter, in.	Total Length, ft	Fission Heat in Test Specimen, Kw/g U-235	Fast Neutron Flux, 10^{15} n/cm^2-sec
A-1	2	6	30	1.0
A-3	2	6	15	1.5
A-5	2	6	10	1.0

For calculational purposes, two geometrically similar reference reactor models were adopted, which were characterized primarily by the thickness of the annular core region. Core thicknesses considered were 2 in. and 3 in. Study of these two cases provided design information of the effects on maximum power density, fuel loading and requisite system power level, due to changes in core thickness. In the actual conceptual design, described in Section 2.0, the selected core thickness of 2.5 in. represented a compromise between the flux-trap advantages of the thinner fuel annulus in reducing total power requirements and the decreased power density and heat removal problems of the thicker core.

The reference calculational cores were taken to be 4 ft in length, with end reflector regions consisting of H_2O and aluminum structural material. The cross sectional composition structure was considered constant in the axial direction so that, for a specified axial buckling, solution of the few-group diffusion equations reduced to a two-dimensional diffusion calculation. The calculational results obtained correspond to a group-independent axial buckling of 0.00043 cm^{-2}; this is computed from the physical core height of 121.9 cm and an estimated axial reflector savings of 15 cm, which results from the Al-H_2O axial reflector and end effects of the radial D_2O reflector.

3.22 Review of Calculational Procedure

The calculational procedure considered a simplified reactor model with a radial cross section having quarter-section reflective symmetry. The assumptions of an equivalently bare core in the axial

direction and of separability of the axial and radial flux distributions reduces the three-dimensional two-group neutron diffusion equations to a two-dimensional set, which can be solved conveniently by application of the IBM-704 PDQ code. This code computes the eigenvalue, the flux distributions and the fission source distribution throughout the core, and from a knowledge of the source distribution the peak and average power densities are obtained. Tabulations of the PDQ calculations made for the conceptual study are given in Tables 8.3E and 8.3F. For these PDQ problems the core storage of the computer used permitted a maximum of 3750 interior mesh points. To describe the unusual geometry of the ETR II core in sufficient detail, a square grid of 55 x 55 mesh points was used to cover one quadrant of the reactor. The physically curved portions of the core regions were approximated in the reactor model by rectangular segments of variable length.

Two-group reactor constants were developed by means of the MUFT III and DONATE codes for all reactor compositions with the exception of Be, and D_2O and borated water solutions, for which, handbook values were utilized. (See Section 8.31.) Fast fission effects were included in obtaining the fuel constants.

3.23 Geometric and Compositional Structure of the Reactor Model

A section through the reactor model used in the calculational program for the ETR II reactor is shown in Fig. 3.2A. In this figure, only one quadrant of the symmetrical reactor model is shown; the reference case illustrated is that of the 2 in. thick core. The 3 in. reference core is similar in structure to the 2 in. core, but with a slightly narrower "neck" region (Region 11 in Fig. 3.2A) and a thicker core. The 6 in. diameter of the flux trap in the lobe is identical in both reference models.

Regions 1, 2, and 3 in Fig. 3.2A represent the 3 in. diameter experimental test spaces at, respectively, the center of the reactor, the center of the lobe region, and at the outside flux trap. In the major portion of the calculations, a single test specimen composition was assumed for all test loops, having a metal-to-water ratio (M/W) of 0.4 and a mean temperature of 200°F. In the final calculations the specimen M/W ratio was increased to unity and the effective neutron temperature increased to 400°F because of changes in the experiments assumed to be in the loops. In estimating the effective neutron temperature of neutrons captured in the test specimen fuel, consideration must be given to the fact that on a volumetric basis most of the neutrons captured in the specimen fuel suffer their last scattering collision in the 200°F flux-trap moderator annulus region rather than in the 650°F test cell region. In addition, the number density of hydrogen scatterers is greater in the surrounding annulus than in the test hole. With allowance made for some spectral hardening in traversing the stainless steel pressure tube, an effective test cell neutron temperature is estimated which is more nearly equal to the median temperature of the two regions. For these reasons, a temperature of 400°F has been applied in obtaining the two-group constants for the test cell compositions.

Region 4 is the curved fuel region of thickness equal to 2 in. The fuel composition consists of a homogenized mixture (M/W = 0.69) of enriched uranium-aluminum fuel plates and light water at a temperature of 200°F. Four different fuel concentrations were considered: 20, 30, 40, and 50 weight per cent of 93.2 per cent enriched U in the U-Al meat alloy.

The entire reflector region surrounding the core is shown divided into three parts: an inner 1 in. thick reflector adjacent to the core (Region 5), an intermediate 3 in. thick reflector region (Region 6), and an outer 18 in. thick D_2O reflector (Region 7). Generally, however, Regions 5 and 6 were treated compositionally together as a single region. Reflector compositions considered consisted of H_2O, D_2O, and a mixture (M/W ≈ 4.0) of Be and D_2O. For calculations involving poisoned reflectors, saturated solutions of borated heavy water were used.

Explicit moderator annular regions were defined surrounding each of the test holes to permit individual specification of the moderator compositions occupying these regions. This allowed for adjustment of the fast-to-thermal flux ratio in the test holes by varying the M/W ratio of the moderator material. The combination of test loop space and surrounding moderator annulus constitutes the flux-trap unit. Regions 8, 9, and 10 are the respective flux-trap moderator regions for the center, lobe and side experimental spaces. The inner moderator Region 11 at the neck of the lobe was also regionally specified in order to investigate its effectiveness as a control region. Flux-trap moderator compositions considered consisted of H_2O, Be + D_2O (M/W = 4) and Al-H_2O mixtures with M/W ratios of 0.11 and 1.5.

The annular Regions 12, 13, and 14 represent the stainless steel pressure tubes for the test loops. In particular, the half-cylinder Regions 12 and 13 contain stainless steel or B^{10}-stainless steel (1.25 weight per cent B^{10}) compositions. By alternating the stainless steel and B^{10}-stainless steel composition of these regions, the control worth of rotating rods in the side regions was investigated.

An additional means of rapid reactor control was also considered using cadmium blades located in the neck region of the fuel. These blades, represented by Region 15, calculationally amount to fuel-bearing rods, since they are replaced by fuel material when withdrawn from the core. Since the blade region is small, however, the fuel-bearing character of the control blades is of little importance in the calculations.

3.24 Effect of Core Loading on Reactivity

The calculated results for the dependence of k_{eff} on the U-235 concentration in the fuel are summarized in the two curves of Figure 3.2B. A curve is given for each reference core thickness. To compare the results for both cores, the k_{eff} values of the 3 in. case have been adjusted to make its reactor conditions, aside from that of core thickness, identical to that of the 2 in. core. The 7 per cent difference in k_{eff} at 30 weight per cent concentration is due to the presence of the additional fuel inventory arising in the case of the thicker core. The slopes of

both curves at 30 weight per cent concentration are nearly identical, indicating that changes in fuel concentration have approximately the same effect for either core thickness. In Figure 3.2C the related plot of k_{eff} as a function of core loading is presented. The smooth transition shown here between the curve for the 2 in. core and that for the 3 in. core shows that the reactivity for a given core inventory is relatively independent of core thickness for the range of core thicknesses investigated.

3.25 Core Thickness Effects

The results of the previous section show that the fuel density requirements for ETR II do not present obstacles to the acceptance of the 2 in. core thickness since the estimated excess reactivity requirements of 21 per cent ($k_{eff} = 1.27$) can be met in this case by a fuel density of 40 weight per cent, a value consistent with existing fuel element technology. For this reason the nuclear criteria governing the selection of core thickness rest primarily on examination of the changes in power density and in the available test loop fluxes as the core thickness is varied.

Calculations performed for several reactor cases show that the available fluxes per megawatt of reactor power in the test holes increase significantly with decreasing core thickness. For thermal test loop fluxes in the 2 in. core, an increase of 40 per cent is obtained over those for the 3 in. core, while for fast fluxes an increase of about 33 per cent is found. Thus, the requisite system power level required to meet the specified test fluxes can be decreased by approximately 1/3 with the thinner core. This advantage is offset by the significant increase in the peak power density as the core annulus is made thinner. Analysis of the two-dimensional calculational results indicates that the maximum power density is found in the neighborhood of the neck of the lobe at the interface between core and neck-moderator. If the moderator consists of H_2O, a decrease in core thickness from 3 to 2 in. results in a 50 per cent increase in peak power density. If the moderator composition consists of Be + D_2O, with M/W = 4, the increase in peak power density is still larger, approximately 60 per cent. On the other hand, for a moderator composition of Al + H_2O the increase in peak power density with decrease in core thickness may be expected to be smaller than the 50 per cent value for pure H_2O -- the amount depending on the M/W ratio of the moderator. In addition, for a given core thickness the peak power density may be lowered by borating the neck-moderator region (see Section 3.26).

The calculational results on the ETR II on the changes in test loop fluxes and in power density with changes in core thickness are consistent with the results of supplementary one-dimensional calculations.

3.26 Reactor Control Effects

3.261 Reactivity Worth of Cadmium Blades

The use of cadmium blades, as regulating control rods or as a means of providing fast shutdown, was studied by determining the total worth of black blades located in a representative region of importance in the core but effectively far from the test spaces. Calculations were made for the 2 and 3 in. cases with the blades located in the neck portion of the core between the center and lobe flux-trap regions. The results show reactivity difference, $\Delta\rho = \frac{k_2 - k_1}{k_2 k_1}$, between rods-in and rods-out of 6.9 per cent for the 2 in. core and 5.6 per cent for the 3 in. core. From these results it is estimated that for an intermediate thickness case of 2.5 in., a total reactivity effectiveness of about 6.3 per cent is made available by means of control blades.

With the control blades located in the neck region of the core, the perturbation on the fast-to-thermal flux ratio in the three test locations is found to be less than 1 per cent as the rods are inserted or withdrawn.

A notable effect of the control blades is the general shift of the reactor power distribution from the central region to the outer lobe region as the cadmium blades are inserted. This is indicated by the fact that the loop fluxes attainable per megawatt of total reactor power decrease by approximately 23 per cent in the central reactor region and increase by 7 per cent in each of the lobe regions as the rods are inserted. This shift is accompanied by about a 22 per cent decrease in the maximum power density in the core, the location of the hot spot normally occurring in the neighborhood of the neck of the core.

3.262 Reactivity Effect of Rotating Boron-Stainless Steel Control Rods

The reactivity effectiveness of rotational control rods located in the side flux-trap regions was calculated and compared with the worth of the cadmium blades. The calculation was made by alternating the stainless steel and B^{10}-stainless steel compositions in Regions 12 and 13. The results obtained for the 3 in. reference case only, show a reactivity difference of 2.0 per cent. Within the control rod, at the center of the experimental test space, the fast-to-thermal flux ratio increases by 6 per cent as the poison half-cylinders of the control rods are rotated to the inner less reactive position.

Because the control rod effectiveness of the side rotational rods is about 1/3 of that of the cadmium blades and because the perturbation on the side loop test fluxes by the rotating rods is not negligible, the use of cadmium blades is a more favorable method of exercising fast control.

3.263 Effects of Borating the Neck-Moderator Region

Calculations of the effectiveness of borating the neck-moderator region (Region 11) for use as a chemical shim control were made for both reference cores. The neck-moderator was poisoned using saturated borated solutions of H_2O and D_2O. The calculated results for two different moderator compositions are shown in Table 3.2B.

TABLE 3.2B

REACTIVITY WORTH OF BORATED SOLUTIONS IN THE NECK MODERATOR

Reference Core	Moderator Composition	M/W	$\frac{k(\text{clean}) - k(\text{borated})}{k(\text{clean}) \cdot k(\text{borated})}$
3 in.	Be + Heavy Water	4.0	4.7%
2 in.	Be + Light Water	1.5	4.8%

As discussed above in connection with the cadmium control blades, a similar shift in power distribution to the outer regions is again found as borated solution is introduced in the neck-moderator region. In this case, the test loop fluxes per megawatt of reactor power are decreased by about 20 per cent in the central test hole and by about 9 per cent in the side loops. In the lobe test hole the fluxes are increased by approximately 3 per cent (see Table 3.2D, Cases 22 and 24). In all test regions the change in the fast-to-thermal flux ratio is 5 per cent or less.

The neck-moderator region is of interest as an auxiliary independent shim control, supplementing the borated reflector control but having a response (inversely related to the water volumes to be poisoned) which is more rapid than that of the slower acting reflector control. It is anticipated that a gray control of this type, located in the inner moderator region, will make it possible to adjust for changes in power distribution which may occur during the reactor cycle or as a result of reactor perturbations.

3.264 Effects of Borated D_2O in the Reflector

Calculations were made to determine the reactivity control worth of a saturated boron solution of heavy water in the reflector Regions 5 and 6. For the 2 in. reference core, the results obtained indicate a net reactivity worth of 17.0 per cent.

The effect of a reactor control poison on power distribution is seen in the present case of a reflector poison to effect an inward shift in power distribution, in contrast to the outward shift caused by borating the neck moderator. The increase in the central test fluxes is about 60 per cent while the decrease in the lobe test fluxes is approximately 10 per cent. At the side loops, fast fluxes are increased by 27 per cent and thermal fluxes are increased by 10 per cent (Cases 22 and 23, Table 3.2D). The most drastic change in the fast-to-thermal flux ratio is seen to occur in the side test holes, where an increase of 15 per cent takes place as the reflector is poisoned.

For the 2 in. core, the combination of borating the neck-moderator region, which yields a reactivity control worth of 4.8 per cent, and of borating the D_2O radial reflector (Regions 5 and 6) yields a total worth of about 22 per cent. No calculations have been made for the 3 in. core with heavy water in the reflector. However, an estimate of the shim control worth for the 3 in. case can be obtained by extrapolation from the results of calculations for the total reactivity change in borating to saturation a composition of Be and D_2O (M/W = 4.0) assigned to the neck region and in borating the reflector. The results obtained show a reactivity difference of 20.6 per cent for the 2 in. core and a difference of 14.0 per cent for the 3 in. core as a result of neck and reflector poisoning. Thus, the control effectiveness of these two regions decreases by approximately 32 per cent as the core thickness is increased from 2 to 3 in. Assuming this effect to be linear with thickness, a decrease of 16 per cent in effectiveness may be expected for the intermediate thickness case of 2.5 in. Applying this factor to the 22 per cent total worth found for the 2 in. core above, yields a total shim worth of about 18.5 per cent reactivity for the 2.5 in. thick core. This amount of shim control appears conceptually sufficient to meet the estimated needs of 21 per cent for excess reactivity. Further, if approximately 10 per cent reactivity is accounted for by means of a burnable poison in the fuel, it is clear that the available chemical shim control is more than adequate in the present concept. The need for shim control in the neck-moderator region as well as in the reflector appears necessary to counteract the effects of one another on the core power distribution.

3.265 Effects of Borating Reflector and Neck Regions on Peak Power Density

The effect of shifting the power inward, toward the center of the reactor when the reflector is poisoned, or outward, toward the lobe when the neck-moderator region is poisoned, results in a corresponding increase or decrease in the peak power density at the neck of the core. Calculations made for the 2 in. reference core, in which the neck-moderator consisted of an Al-H_2O (M/W = 1.5) composition, indicated that the peak power density is increased by 56 per cent when only the reflector is borated to saturation. When the neck-moderator alone is borated, the peak power density decreases by 34 per cent. Calculations of the effect of simultaneous poisoning of neck and reflector

regions were made only for the case of a neck-moderator composition consisting of Be + D_2O (M/W = 4.0). For the 2 in. core, a net decrease of about 2 per cent in peak power density was obtained when both regions were borated and for the 3 in. core the decrease was 14 per cent.

3.27 Effects of Flux-Trap Moderator Compositions in Determining the Fast-to-Thermal Flux Ratio in the Test Holes

The required fast-to-thermal flux ratios specified for the various test loops in ETR II are as follows:

TABLE 3.2C

DESIGN FAST-TO-THERMAL FLUX RATIOS

IN ETR II TEST LOOPS

Test Loop and Location	ϕ_f/ϕ_{th}
A-3 Center Test Hole	3.6
A-1 Lobe Test Holes	1.2
A-5 Lobe Test Holes	3.6
A-5 Side Test Holes	3.6

Adjustment of the flux ratio in the test hole of the flux trap can be made by variation of the moderator-gap thickness separating the fuel and the test hole and by variation of the M/W ratio in the moderator composition. The former method has not been considered because the separate flux ratio requirements of A-1 and A-5 would necessitate use of two different fuel elements in the lobe regions. The latter method is straight forward and has been investigated in some detail for a one-dimensional cylindrical representation of a flux trap. The results of this study are summarized in Figure 3.2J. In this figure the flux ratio in the flux trap is seen to be dependent on the water fraction of the aluminum-water moderator. For ETR II, the two design flux ratios of 1.2 and 3.6 for the lobe test holes (Table 3.2C) are shown in this curve to be given by moderator water fractions of approximately 90 per cent and 40 per cent, respectively.

Calculations performed for ETR II have shown that with pure H_2O in the flux-trap annulus a flux ratio of about 0.7 is obtained in the center test hole and a slightly higher ratio of 0.8 is obtained for the lobe test hole. For an aluminum light-water composition (water fraction = 0.40) in the flux-trap annulus, a fast-to-thermal ratio of 3.5 is found in the center test hole and 4.0 in the lobe test space. These results are in agreement with those of Figure 3.2J. Additional

ETR II calculational results show that use of a Be-D_2O (M/W = 4.0) flux-trap moderator yields a fast-to-thermal ratio of 1.1 in the lobe test space. This value is much lower than the corresponding value for Al-H_2O due to the moderating power of Be. It is also found that changes in the M/W ratio of the neck-moderator region does not affect the flux ratio in the test spaces. This indicates that in regard to the flux spectrum of the test hole each flux-trap region in ETR II acts as a relatively isolated unit, with the flux spectrum determined by the moderator composition surrounding each test cell. This conclusion is also borne out by the fact that the flux ratios of the side test spaces are found to remain unaffected even by changes of composition throughout the entire interior moderator region of the reactor.

3.28 Power Balancing in Reactor Operation

The ETR II loop requirements for fast fluxes and fast-to-thermal ratios (Tables 3.2A and 3.2C) pose two problems. First, the fast flux required (1 x 10^{15} n/cm^2-sec) is the same in all loops except A-3, where a 50 per cent greater value is called for. Secondly, the value of 3.6 for fast-to-thermal flux ratio is specified to be the same in all loops except A-1, where the required value is 1.2.

In regard to the first condition, since the fast flux available in the test loop is proportional to the power level, the flux specification in the centrally located A-3 loop can be met simultaneously with those of the test loops located in the lobes and side positions by shifting the general power distribution of the reactor toward the center. The possibility of this has already been suggested in Section 3.26 in noting the control effects on power distribution.

In regard to the second condition, the feasibility of adjusting the flux ratio in the test space by varying the M/W ratio of the moderator annulus surrounding the test loop has been discussed in Section 3.27. In varying the M/W ratio in the flux-trap annulus, however, the available fast flux at the test loop is also changed. The dependence of the fast flux on the water fraction of the annulus moderator has been derived from supplementary one-dimensional studies and is shown in Figure 3.2D. It is seen that the available fast flux in the test hole decreases by a factor of 2.2 as the water fraction in the moderator increases from 40 per cent to 90 per cent. Consequently, the power level necessary to meet the same fast flux requirement of 1 x 10^{15} n/cm^2-sec in both the A-1 and A-5 lobe test loops, will be a factor of 2.2 higher in the A-1 lobe, where the required flux ratio is 1.2, than in the A-5 lobe, where the flux ratio is 3.6. To meet both lobe requirements simultaneously, the power distributions may be shifted in the direction of the A-1 lobes and away from the A-5 lobes.

The power shifting demands of the A-3 center loop can be correlated to a certain extent with those of the different lobe loops by an appropriate balance of the reflector and neck shim controls in each quadrant of the reactor. To do this, it is necessary to exercise individual

control of the concentration of the borated solution in each of the quadrants. The fact that the power developed in each lobe can be measured separately because of exit flow division makes this individual control feasible.

3.29 Reactor Performance in the Two-Inch Reference Core

To determine reactor performance in the two-inch core by means of power balancing, the twin problems of shifting power toward the center of the reactor and of shifting it in the direction of the A-1 lobes have been treated separately. Calculations have been made to determine the system power level necessary to meet the flux requirements in a balanced reference reactor consisting of an A-3 center test loop, four A-5 lobe test loops and four type A-5 side lobe loops. A calculation was then made to determine the increase in system power level to meet flux requirements when A-1 loops are substituted for two A-5 lobe loops.

For the first part of this analysis of reactor performance, a single Al-H_2O (M/W = 1.5) flux-trap moderator was assumed for all loop annuli. Three PDQ calculations were made in which the neck and reflectors were first considered unborated and then individually borated. The calculated results for the available loop fluxes per megawatt of reactor power are given in Table 3.2D. For this unborated core (Case 22), plots of the fast and thermal flux distributions are illustrated in Figures 3.2E, F, and G. In Figure 3.2E, the radial distributions along the 45° diagonal line are shown. In Figure 3.2F, the radial distribution is taken along the reactor center line joining the center and side test holes. In Figure 3.2G, the flux distributions shown are along the line joining the side and lobe test holes. The fast and thermal flux shifting effects accompanying the poisoning of the reflector and neck regions are illustrated in Figures 3.2H and 3.2I, respectively. The ratio of the required fast flux at the center loop to that of the lobe loop is 1.5. The available ratio for the clean reactor (Case 22) is 1.02, whereas the ratio for the borated reflector case is 1.80. Thus, borating the reflector to saturation has shifted the power distribution to the center more than the optimum value for meeting the required ratio of 1.5. Assuming to a first approximation that the power distribution shift is linear with boron concentration in the reflector, a boron concentration equal to 64 per cent of that of saturation is determined which will provide the desired ratio of 1.5 to 1.0 for these two loops. At this concentration, the fast flux in the center test loop is found to be 9.23×10^{12} n/cm^2-sec per megawatt of reactor power. The requisite power level for meeting the specified value of 1.5×10^{15} n/cm^2-sec is therefore 162 Mw. The estimated performance characteristics for this partially optimized reference reactor at 162 Mw have been obtained and are compared with the design objectives in Table 3.2E.

TABLE* 3.2D

FAST AND THERMAL FLUXES AVAILABLE AT MIDPLANE OF TEST LOOP

PER MEGAWATT OF REACTOR POWER

PDQ Case Number	Neck Region 11	Reflector Regions 5 and 6	Center Test			Lobe Test			Side Test			Peak Power Density Kw/liter
			ϕ_f, 10^{12} n/cm^2-sec	ϕ_{th}, 10^{12} n/cm^2-sec	$\frac{\phi_f}{\phi_{th}}$	ϕ_f, 10^{12} n/cm^2-sec	ϕ_{th}, 10^{12} n/cm^2-sec	$\frac{\phi_f}{\phi_{th}}$	ϕ_f, 10^{12} n/cm^2-sec	ϕ_{th}, 10^{12} n/cm^2-sec	$\frac{\phi_f}{\phi_{th}}$	
22	Unbor.	Unbor.	6.63	1.90	3.49	6.53	1.64	3.98	6.26	1.61	3.89	7.82
23	Unbor.	Borated	10.7	3.05	3.51	5.96	1.47	4.06	7.95	1.77	4.49	12.2
24	Borated	Unbor.	5.40	1.47	3.67	6.73	1.66	4.06	5.71	1.50	3.80	5.13

* Peak-to-average axial flux ratio is equal to 1.35. (Note: In Table 1.3A the value of 1.40 is given, which is a more recent value; however, this change was not considered of sufficient magnitude to necessitate changing the information given in Table 3.2D.)

TABLE 3.2E

REFERENCE REACTOR FLUXES AT 162 Mw

Loop Location and Number	Fast Flux 10^{15} n/cm^2-sec		Thermal Flux 10^{15} n/cm^2-sec		Fast-to-Thermal Flux Ratio	
	Design Objectives	Avail.	Design Objectives	Avail.	Design Objectives	Avail.
A-3 Central Loop (1)	1.5	1.5	0.41	0.43	3.6	3.5
A-5 Lobe Loop (4)	1.0	1.0	0.28	0.25	3.6	4.0
A-5 Side Loop (4)	1.0	1.2	0.28	0.28	3.6	4.3

For this reactor the peak power density at 162 Mw is estimated to be 1.4 Mw/liter.

In considering the replacement of two A-5 lobe test loops by two A-1 loops, in which the M/W ratio of the A-1 moderator annuli is 0.11 in order to achieve the required fast-to-thermal ratio of 1.2, the lobe power previously associated with the A-5 loop must now be increased by a factor of 2.2 in order to maintain the same fast flux level. In the balanced reference reactor discussed above, the power associated with each lobe is estimated at 29.4 Mw, hence, an increase by a factor of 2.2 in two of these lobes raises the system power level to approximately 230 Mw. This local power increase in the two A-1 lobes is achieved by means of the power distribution regulating control system of the reactor. In regard to the maximum power density in the core, the location of which is in the neighborhood of the center of the reactor, it is not believed that an increase in local power distribution in the two A-1 lobes will greatly enhance the value found in the balanced reference core. However, this question must be resolved in future studies. For the side test loops, it is estimated that the performance characteristics are increased by approximately 10 per cent due to the local power increase in each of the A-1 lobes. On this basis, the test fluxes for each type of loop are determined and are presented in Table 3.2F.

TABLE 3.2F

REFERENCE REACTOR FLUXES AT 230 Mw

BY CONTROL OF POWER DISTRIBUTIONS

Loop Location and Number	Fast Flux		Thermal Flux		Fast-to-Thermal	
	Design Objectives	Est. Performance	Design Objectives	Est. Performance	Design Objectives	Est. Performance
A-3 Center Loop (1)	1.5	1.5	0.41	0.43	3.6	3.5
A-1 Lobe Loop (2)	1.0	1.0	0.83	0.83	1.2	1.2
A-5 Lobe Loop (2)	1.0	1.0	0.28	0.25	3.6	4.0
A-5 Side Loop (4)	1.0	1.3	0.28	0.30	3.6	4.3

For this reference reactor, the peak power density at 230 Mw is estimated to be 2.1 Mw/liter.

In the final design selection, the core thickness chosen is 2.5 in. rather that 2 in. As discussed in Section 3.25 on core thickness effects and in Section 3.27 on effects of flux-trap moderators, the overall effect of an increase in core thickness from 2 to 2.5 in. is a decrease in the available fast flux at the test loop of approximately 17 per cent and a decrease in the peak power density of less than 25 per cent, with the flux ratio in the loop being essentially determined by the nature of the moderator. For the purpose of the study, a nominal increase of 10 per cent has been applied in estimating the increase in power level between the 2 in. reference design and the proposed 2.5 in. core; this results in raising the system power level up to the nominal value of 250 Mw. In addition, it is believed that the peak power density will not change substantially from the value of 2.1 Mw/liter as the power level is raised from 230 Mw and the core thickness increased from 2 to 2.5 in.

3.3 ETR II Design Selection

The Engineering Test Reactor II has a single fuel annulus shaped to provide five interior and four exterior flux traps. A plan view is shown in Figure 2.0A and a general description is given in Section 2.0.

3.31 Reactivity Requirements and Core Loading

Typical excess reactivity requirements for the hot clean core are estimated to be 21 per cent. These requirements are apportioned as follows:

Equilibrium Xe and Sm	4%
Partial Xe override	6%
Burnup and other fission products	11%
Total	21%

The reactivity loss with burnup is based on a 30-day lifetime cycle at 250 Mw system power level, using an estimated factor of 1.5 to take account of non-uniform burnup effects (in the MTR a typical non-uniform burnup factor of 1.7 is found to apply). From Figure 3.2B the excess reactivity requirement of 21 per cent (k_{eff} = 1.27) is satisfied in the 2.5 in. core by an estimated fuel concentration of 33 weight per cent U-235 in the meat alloy. At this concentration the required total core loading is 36 kg of U-235.

3.32 Control Requirements

Use of chemical shim controls in the neck-moderator region and in the reflector yield total reactivity worth of 18.5 per cent. Additional analysis should make it possible to further optimize this. Burnable poison will also furnish an additional 10 per cent control reducing the shim control needed to 11 per cent.

3.33 Core Thickness

The core thickness selected for the ETR II conceptual design is 2.5 in. Following initial calculations on the 2 in. reference core, which indicated excessive peak power densities for this core, the value of 2.5 in. was adopted early in the nuclear design study in order to initiate work on the mechanical layout of the reactor. Later calculations on the 2 in. core revealed that proper choice of the interior flux-trap moderator would lead to a reduction in reactor power level and consequently reduce the peak power density to an acceptable value. On the basis of the present study, it appears that a considerable reduction in reactor power can be achieved by use of a thinner core than the proposed 2.5 in. thickness.

3.34 Flux-Trap Moderator Compositions

The required fast-to-thermal flux ratios of 1.2 in the A-1 loop and of 3.6 in the other loops are obtained by aluminum-water flux-trap moderators having M/W ratios of 0.11 and 1.5, respectively.

3.35 Summary of Nuclear Characteristics of ETR II

Table 3.3A presents a summary of the nuclear characteristics of the conceptual design of ETR II.

TABLE 3.3A

NUCLEAR CHARACTERISTICS OF ETR II

Core	
Height	48 in.
Thickness	2.5 in.
Volume	262 liters
Metal-to-Water Ratio	0.75
Power	250 Mw
Average Power Density	0.954 Mw/liter
Maximum Power Density	2.1 Mw/liter
Core Life (Full Power)	30 days
Initial Loading	36.0 kg
Final Loading	27.4 kg
Burnup	24%
Fuel Concentration	33 wt. %
Excess Reactivity Requirements	
Equilibrium Xenon and Samarium	4%
Xenon Override	6%
Burnup and Other Fission Products	11%
Total	21%
Reactivity Control Capability	
Compensation Control in Neck	4.8%
Reflector Shim Control	13.7%
Cadmium Blades	6.3%
Average Mid-plane Test Hole Fluxes for One Assumed Loading	
One Central Test Hole; A-3 Loop	
Fast	1.5×10^{15} n/cm^2-sec
Thermal	0.43×10^{15} n/cm^2-sec
Fast-to-Thermal Ratio	3.5
Two Lobe Test Holes; A-1 Loops	
Fast	1.0×10^{15} n/cm^2-sec
Thermal	0.83×10^{15} n/cm^2-sec
Fast-to-Thermal Ratio	1.2
Two Lobe Test Holes; A-5 Loops	
Fast	1.0×10^{15} n/cm^2-sec
Thermal	0.25×10^{15} n/cm^2-sec
Fast-to-Thermal Ratio	4.0
Four Side Test Holes; A-5 Loops	
Fast	1.3×10^{15} n/cm^2-sec
Thermal	0.30×10^{15} n/cm^2-sec
Fast-to-Thermal Ratio	4.3

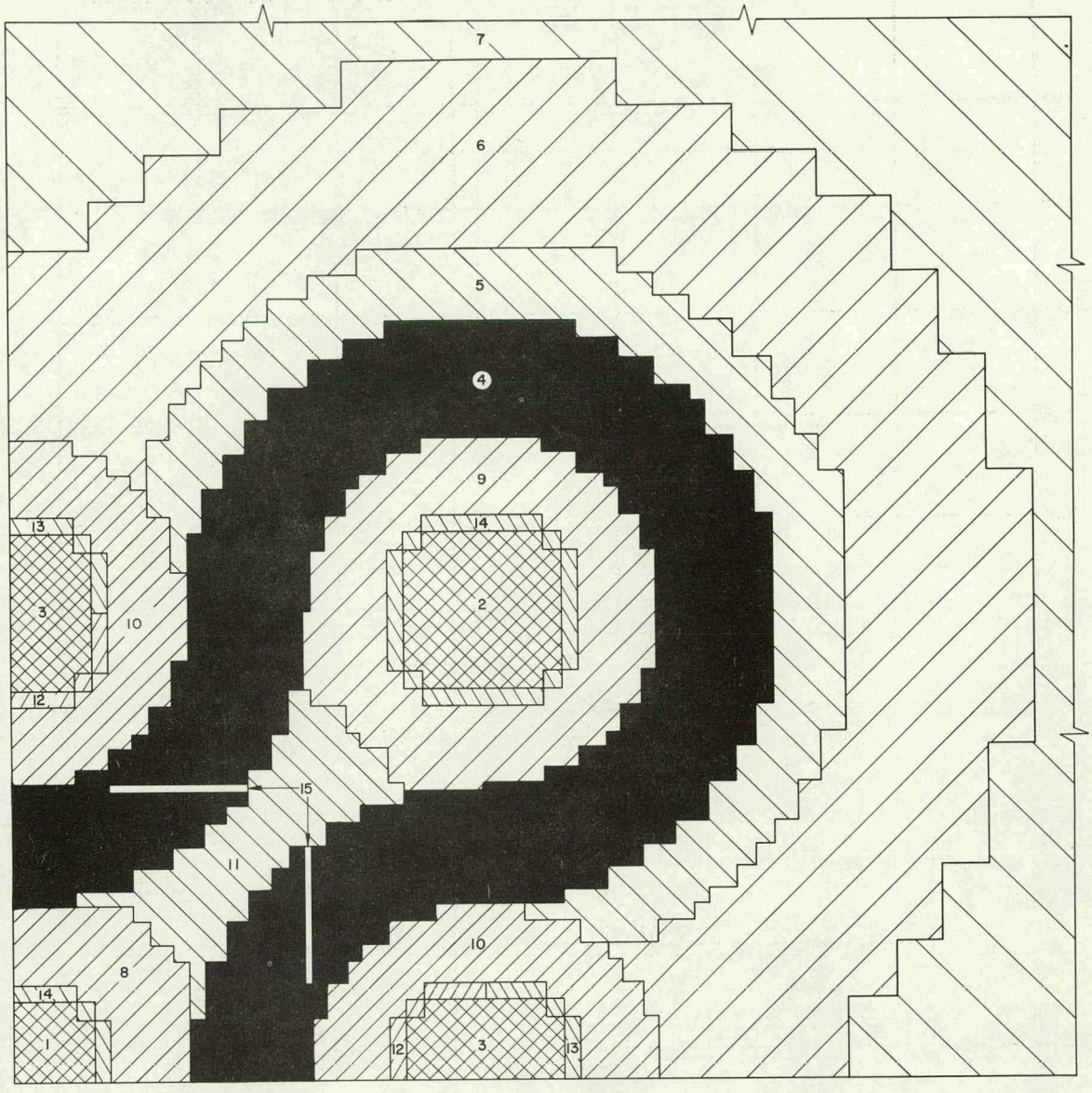

REGION

1. CENTER TEST HOLE
2. LOBE TEST HOLE
3. SIDE TEST HOLE
4. FUEL
5. INNER REFLECTOR
6. INTERMEDIATE REFLECTOR
7. OUTER REFLECTOR
8. CENTER FILLER ANNULUS
9. LOBE FILLER ANNULUS
10. SIDE FILLER ANNULUS
11. NECK MODERATOR
12. BORATED STAINLESS STEEL HALF PRESSURE TUBE
13. STAINLESS STEEL HALF PRESSURE TUBE
14. STAINLESS STEEL PRESSURE TUBE
15. CADMIUM BLADE

PPCo.-D - 2701

FIG. 3.2A

RADIAL CROSS SECTION FOR REACTOR CALCULATIONAL MODEL
(ONE QUADRANT)

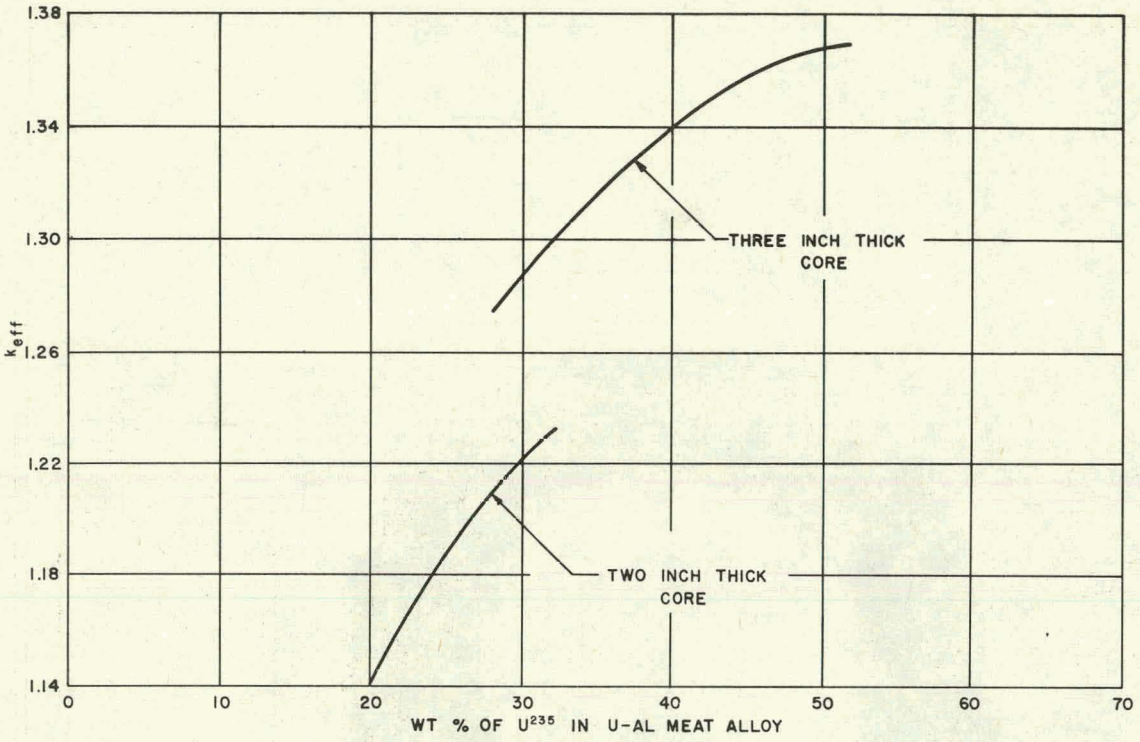

FIG. 3.2B

EFFECT OF FUEL CONCENTRATION ON k_{eff}

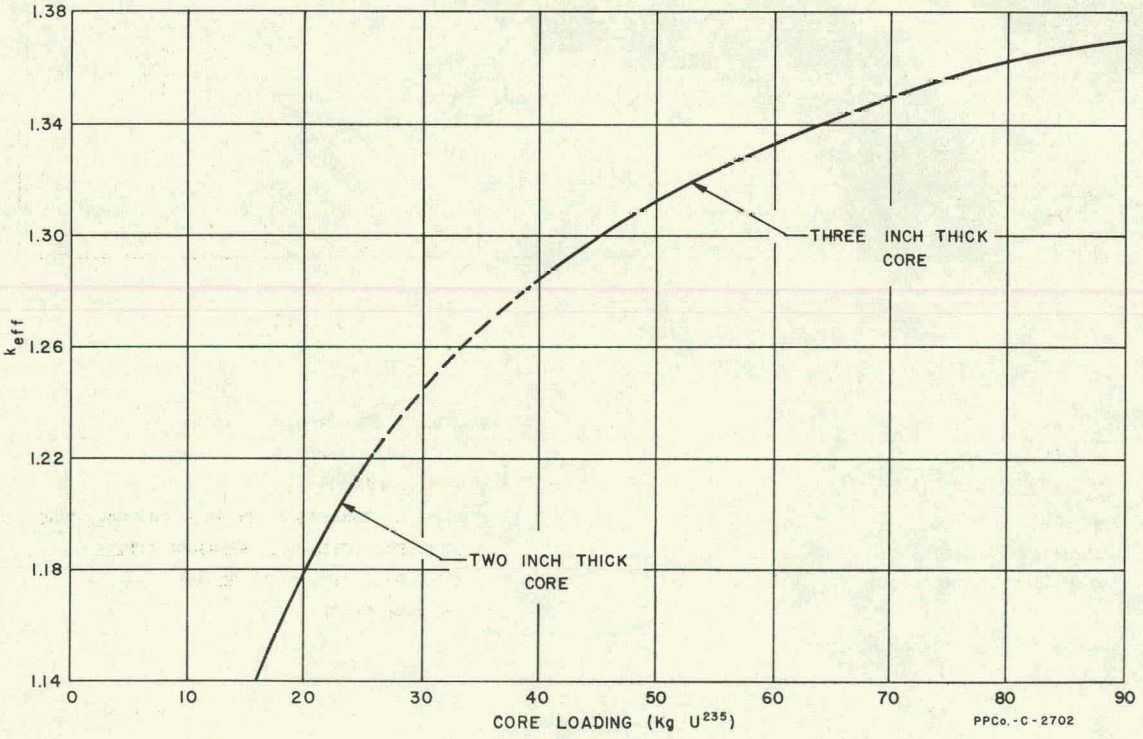

FIG. 3.2C

EFFECT OF FUEL LOADING ON k_{eff}

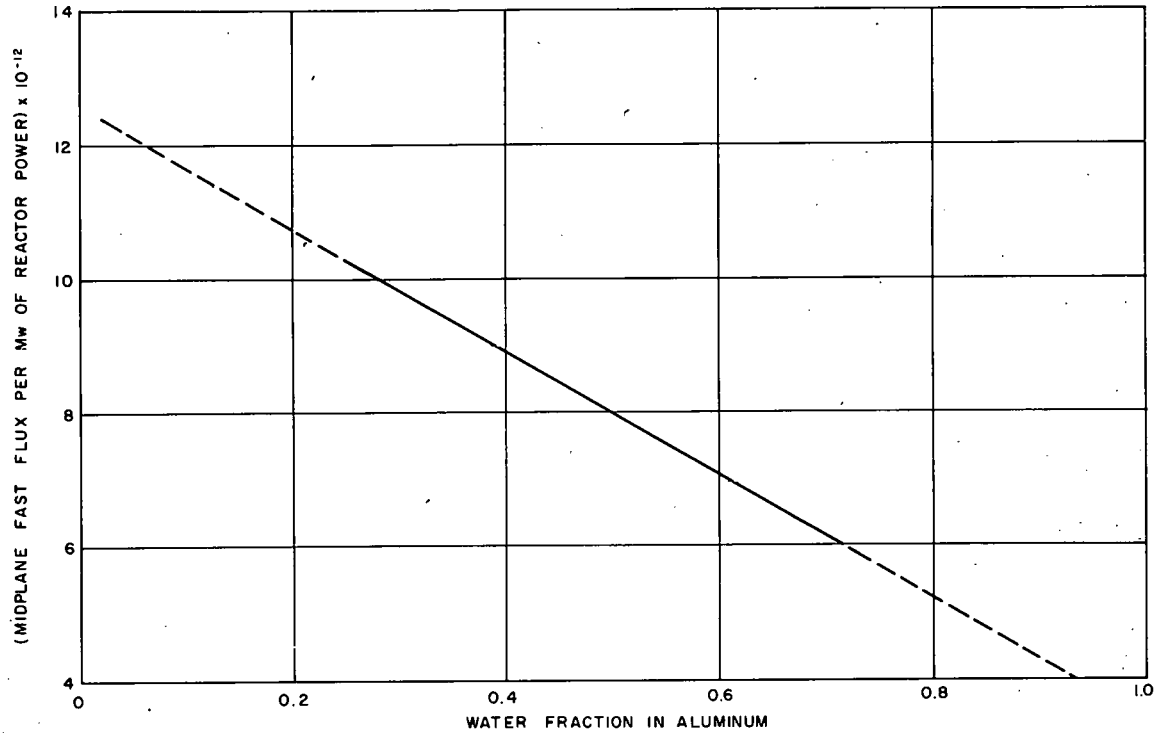

FIG. 3.2 D

DEPENDENCE OF FAST FLUX PER Mw OF REACTOR POWER ON MODERATOR COMPOSITION (ONE DIMENSIONAL STUDIES)

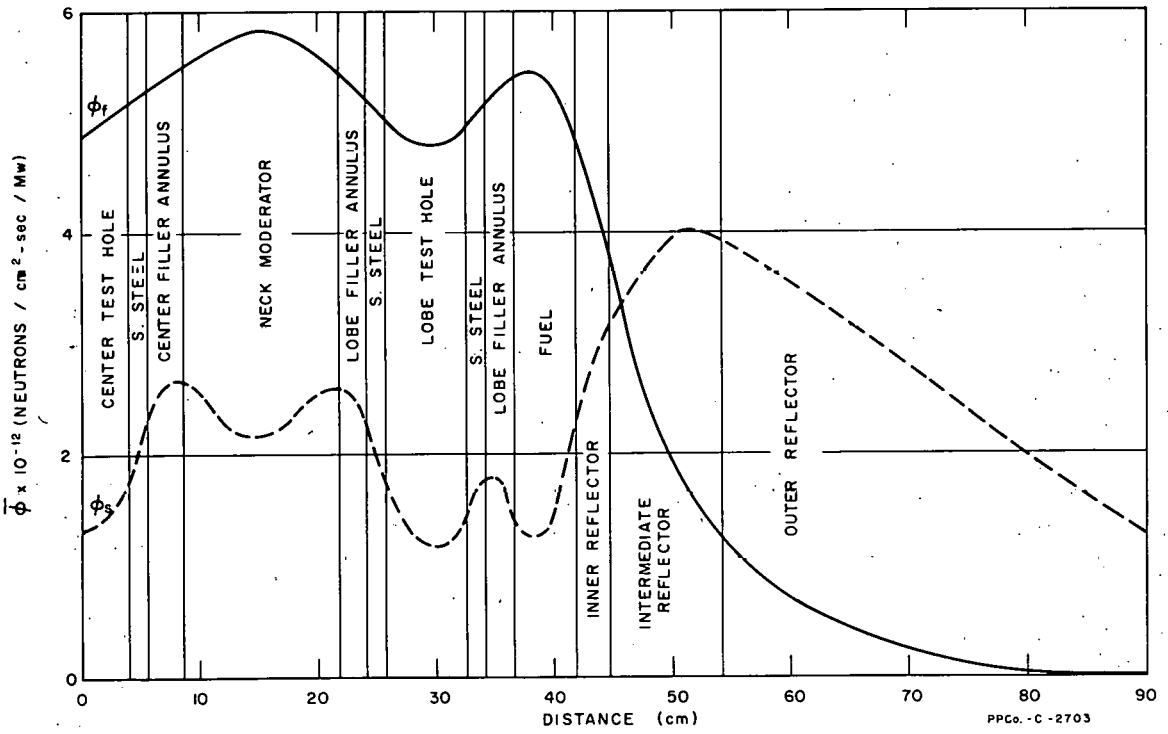

FIG. 3.2 E

AXIALLY-AVERAGED FLUX PROFILES ALONG A 45° DIAGONAL LINE (PDQ CASE 22--CLEAN CORE)

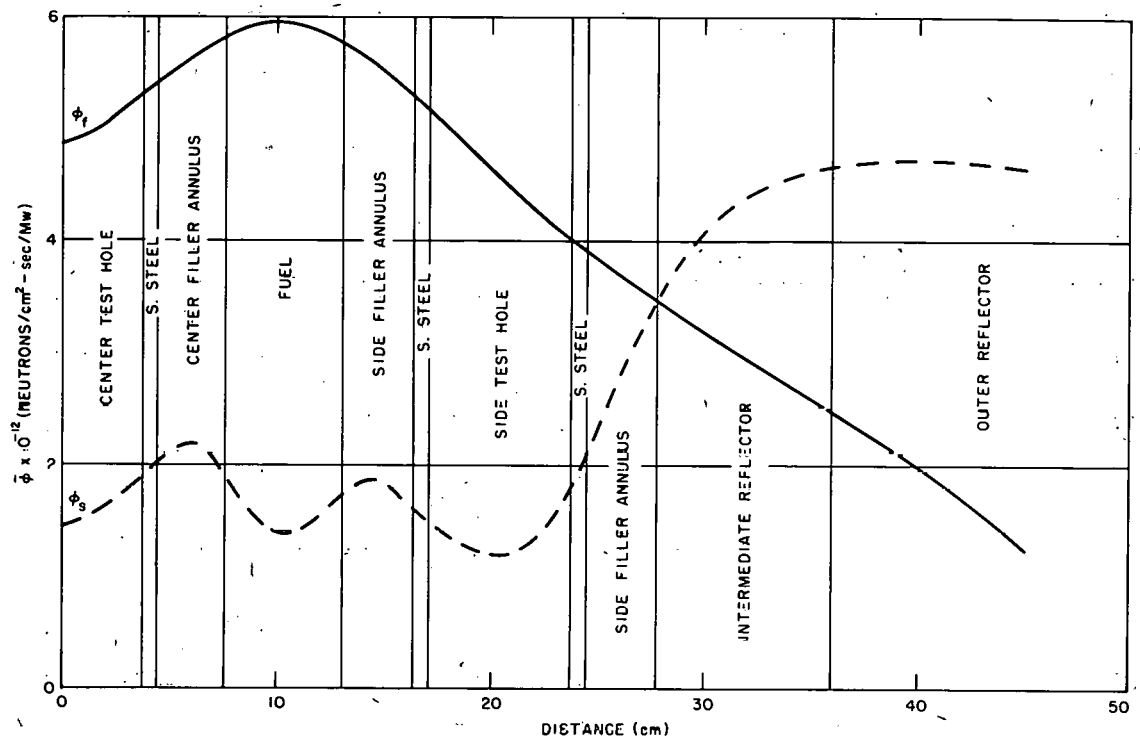

FIG. 3.2 F

AXIALLY - AVERAGED FLUX PROFILES ALONG REACTOR CENTER LINE
(PDQ CASE 22 - CLEAN CORE)

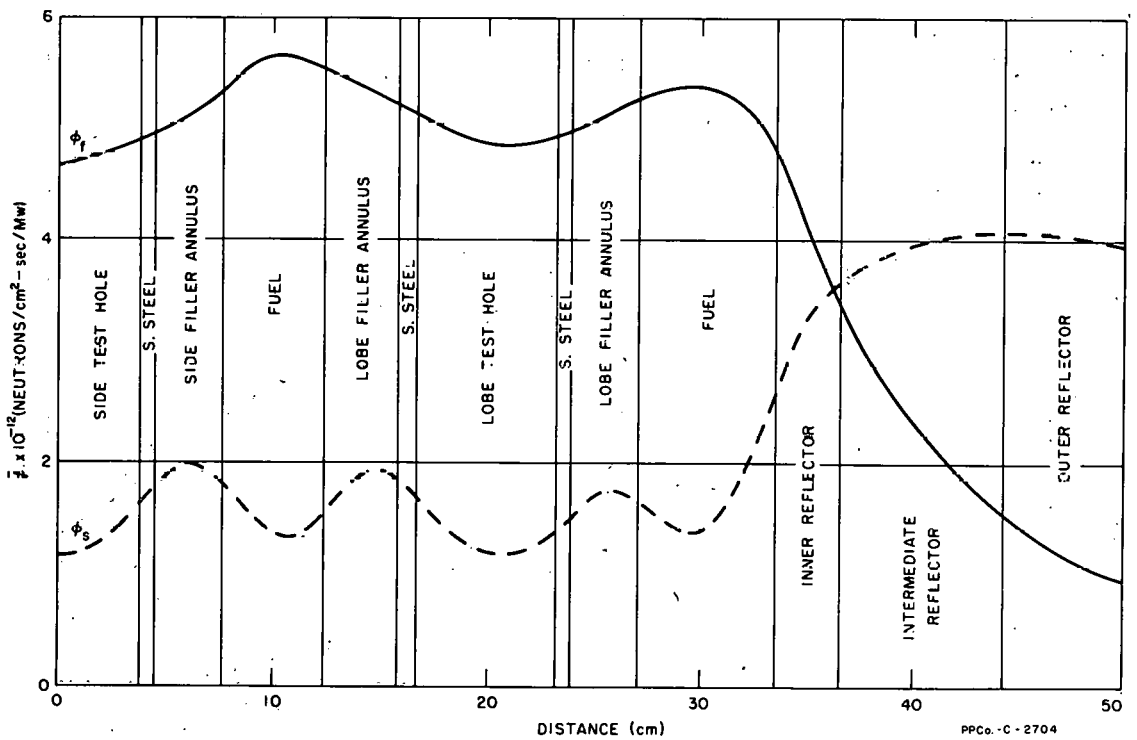

FIG. 3.2 G

AXIALLY - AVERAGED FLUX PROFILES ALONG LINE JOINING CENTERS
OF SIDE AND LOBE TEST HOLES (PDQ CASE 22 - CLEAN CORE)

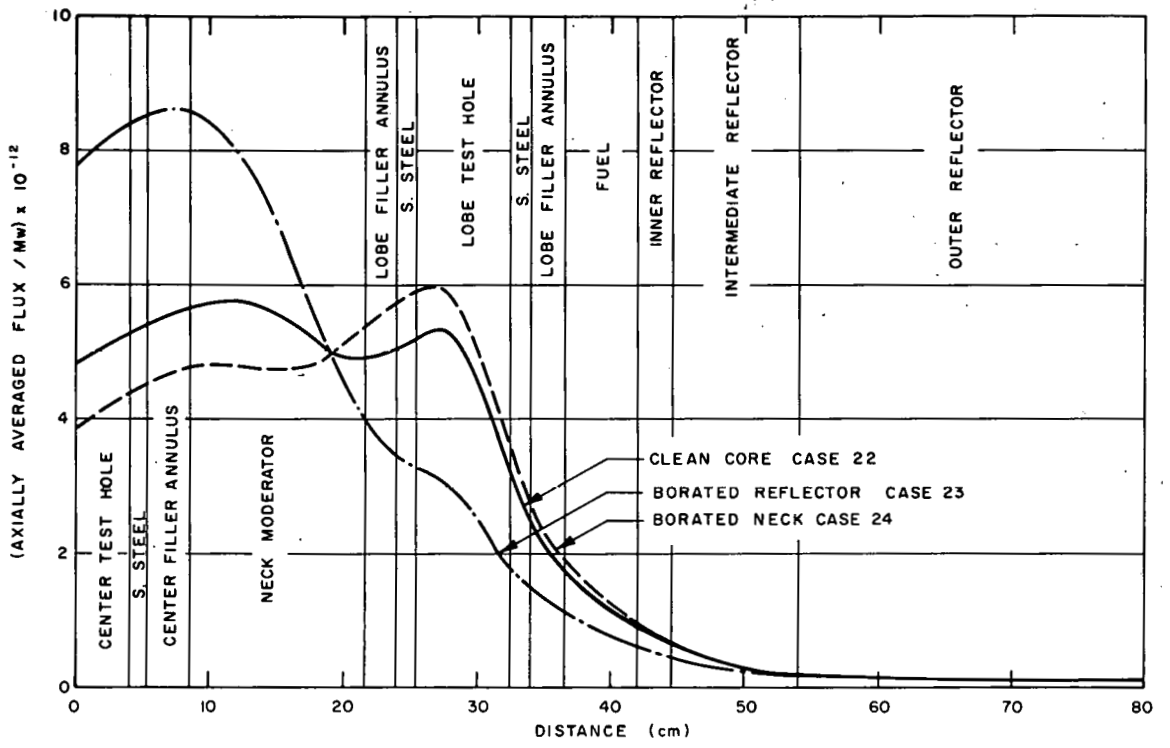

FIG. 3.2 H

EFFECTS OF BORATED REFLECTOR AND BORATED NECK-MODERATOR REGION ON FAST FLUX DISTRIBUTION ALONG A 45° DIAGONAL LINE

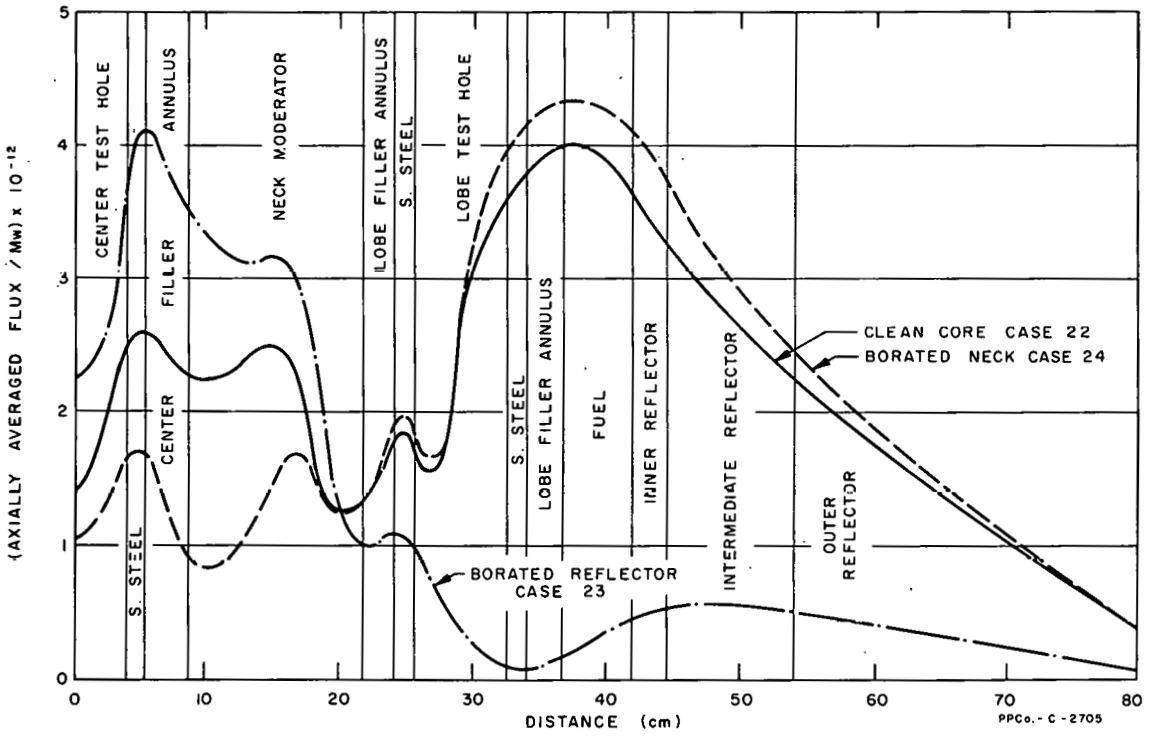

FIG. 3.2 I

EFFECTS OF BORATED REFLECTOR AND BORATED NECK-MODERATOR REGION ON THERMAL FLUX DISTRIBUTION ALONG A 45° DIAGONAL LINE

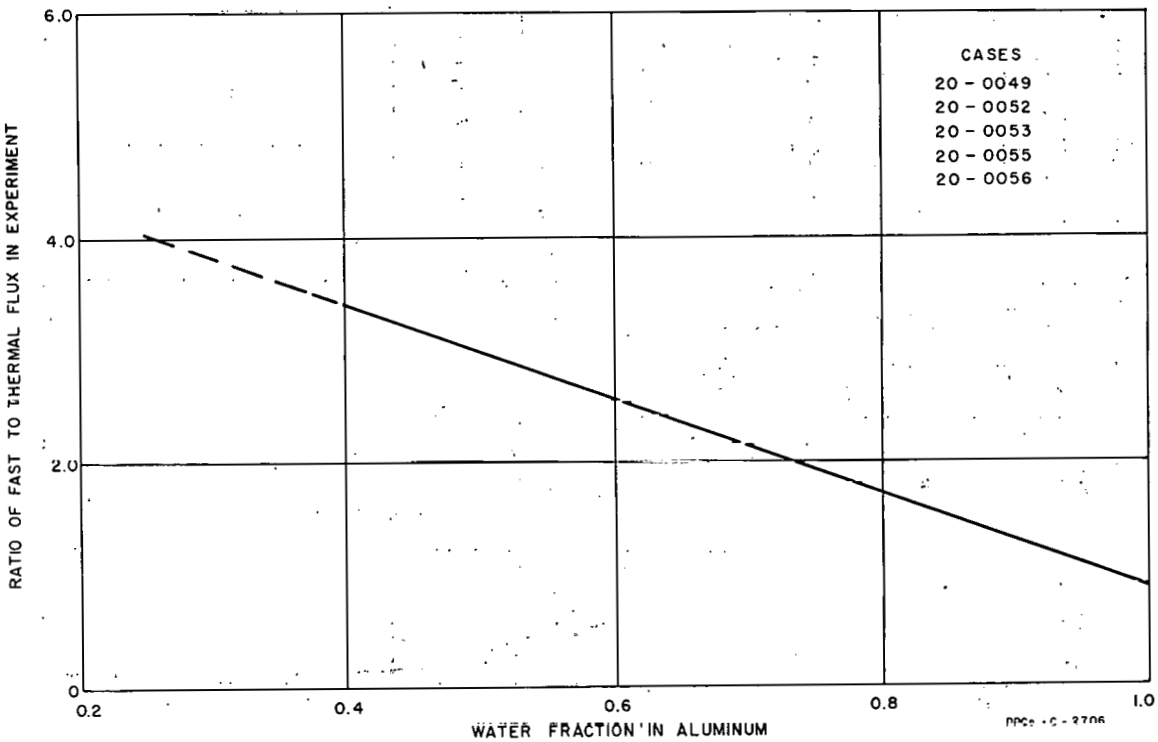

FIG. 3.2 J

DEPENDENCE OF FAST TO THERMAL FLUX RATIO ON MODERATOR COMPOSITION IN FLUX TRAP (ONE DIMENSIONAL STUDIES)

4.0 ENGINEERING DESCRIPTION

Section 2.0 presents the core design for ETR II, and Section 3.0 discusses its reactor physics. It is the objective of this part of the report to give an engineering description of the entire plant, beginning with a discussion of the reactor itself.

4.1 Reactor

See Figures:

4.1A - ETR II Four-Lobe Reactor Installation - Vertical Cross Section

4.1B - ETR II Four-Lobe Reactor - Horizontal Cross Section

4.1C - ETR II Four-Lobe Reactor - Top Plan

4.1D - ETR II Four-Lobe Reactor - Rod Access Room - Horizontal Cross Section

4.1E - ETR II Four-Lobe Reactor - Sub-Pile Room - Cross Sectional Elevation

4.1F - ETR II Four-Lobe Reactor - Sub-Pile Room - Alternate Arrangement

The four-lobe reactor resembles ETR I in the arrangement of reactor, canal, etc., except that special consideration was given to experimental facilities, experiment handling, and meeting much more exacting flux specifications. The reactor core is physically smaller than that of ETR I. ETR II consists basically of four flux traps in a cloverleaf arrangement of circular segment fuel assemblies. This arrangement provides a reactor with nine excellent experimental facilities.

The following sections give a brief description of the pressure vessel, active lattice and reflector, loop and capsule facilities, fuel handling, reactor structure, and the process piping.

4.11 Pressure Vessel

The multi-diameter reactor vessel, Fig. 4.1A, is vertically mounted and has a spider-shaped top head with an integral shielding sleeve for loop experiments, inlet and outlet cooling water openings, a flow distributor for inlet coolant water, a rotary fuel handling rack built as a part of the flow distributor, a discharge chute, supports for reactor grid plate and experimental in-pile equipment, and a bottom head which incorporates openings for various drive rods and loop piping.

The reactor vessel is to be constructed in accordance with appropriate ASME Codes. Operating pressures of 300 psig and temperatures in the range of 200°F indicate that the pressure vessel may be made of

either aluminum or stainless steel. The upper section of the pressure vessel is about 12 ft in diameter and contains facility nozzles and supports for experiment flow tubes, flanged nozzles for capsule leads, a flow distributor, and the two 24 in. inlet cooling water lines. A rotary fuel rack is also provided for passing fuel elements around the reactor to the discharge chute. The lower section, approximately 6 ft 9 in. in diameter, contains the reactor core, and a grid plate for support of fuel elements and the shim control and reflector tanks. Suitable baffling is provided to divide the flow from the fuel elements in order to permit individual flow and temperature-rise measurements for each lobe. Four 16 in. cooling water outlet lines are located below the grid. The over-all length of the pressure vessel is about 32 ft. In the detailed design, consideration should be given to the possibility of placing the pressure vessel wall just inside the D_2O reflector. Nuclear considerations in this case suggest an aluminum pressure vessel.

The top head is fabricated in the form of a large spider. This spider contains four fueling ports for access into the vessel. The central area of the vessel head contains loop facility penetrations and lead shielding both above and below the head. The shielding protects personnel working adjacent to the head during the periods that experiment samples are being drawn into the loop cask. Experiment instrumentation lead return tubes run from the center of the head downward into the vessel, and bend to enter nozzles in the vessel wall leading to a nozzle trench. Thus, the leads can run into the experiment cubicles via the same passages that are provided for top-re-entrant of through-loop type experiments.

The vessel bottom head contains drive-rod penetrations for the regulating rods, the safety rods, and the fission and ion chambers. Top and bottom head penetrations should contain double-gland or equivalent seals that allow pure process water to be introduced between the glands. The nine re-entry loop pipes also enter this head through similar seals (see Fig. 5.1B). Seals should be designed in a manner which will permit re-packing during a normal reactor shutdown, and must be capable of operating reliably in their environment.

4.12 Active Lattice and Reflector

Circular segment fuel elements (see Fig. 4.3A - Circular Segment Fuel Element, Fig. 4.3B - Plan View of Fuel Element for ETR II, and Fig. 2.0A - ETR II Four-Lobe Reactor - Core Cross Section) are used in this reactor. They are supported by a grid plate with sockets for the fuel element side plate extension. Surrounding the fuel elements are an aluminum supporting tank, a borated D_2O shim control tank, beryllium reflector segments and a D_2O reflector tank. Four safety rods and two regulating rods are located in the core and borated D_2O shim control regions, respectively, and are driven from the rod access room below the reactor. Fission and ion chambers are located in thimbles penetrating the D_2O reflector tank. All drives must be reliable units fully meeting all operating requirements while operating in their environments. Adequate

factors of safety are to be incorporated in all designs. Mechanical, electrical-mechanical, or other drives may be considered for this reactor, but the performance of these units should be proved prior to actual use on the reactor.

4.13 Loop and Capsule Facilities

Loop experiment and capsule facilities for the reactor are shown in Figures 2.0A, 4.1A, 4.1B, 4.1C, 4.1D, 4.1E, 4.1F, and 5.1B.

Bottom re-entrant type pressurized water loops (see Fig. 5.1B) extend vertically through the reactor. The top pressure tube closure penetrates the top reactor head and permits removal, insertion, or reinsertion of test specimen trains with instrumentation leads intact during one normal reactor shutdown period.

The in-pile tube consists of three concentric pipes or tubes. The inner tube, of 2 in. inside diameter, serves as a support for the experiment sample and as a coolant flow channel. The intermediate pipe contains the loop pressure and also serves as a coolant flow channel. The outer tube contains the insulating gas space surrounding the pressure tube.

In-pile tubes extend vertically through the core and downward through the reactor vessel bottom head. Top and bottom head penetrations are sealed by a double-gland type seal. Pure coolant water is applied between the glands at a pressure slightly higher than that of the reactor vessel. The seals should be designed so that they may be repacked during a normal reactor shutdown. The in-pile tube continues vertically downward through the rod access room. In-pile tube extensions through the rod access room may be shielded with limited amounts of lead shielding, dependent on actual clearances between rod drives and in-pile tubes, maintenance and operating requirements of these items, and other factors. The rod access room is located directly below the vessel bottom head and incorporates traps which are imbedded in lead shielding in the rod access room floor (see Figures 4.1E and 4.1F). Traps are designed to catch radioactive particulate matter that may be lost from experiment samples. Loop piping is routed from the rod access room to the piping corridors via insulated pipes in shielded trenches radiating outward from the center of the rod access room.

The arrangement of the experimental out-of-pile piping and reactor control rod drives must be fully optimized at the time of final reactor design. Toward this end, preliminary design layouts of these items are presented on Figures 4.1D, 4.1E, and 4.1F.

As shown on Fig. 4.1D, facility tubes and rod drives are adequately separated just as they leave the reactor bottom head. However, in order to improve the operability, servicing, etc., of the experiments and the reactor, drives and experimental tubes should be physically separated as soon as feasible below the bottom head. This can be accomplished in any one of the following ways:

1. (See Fig. 4.1E) In-pile tube extensions proceed vertically downward to the catcher sections situated in the lead shielding built into the rod access room floor. Rod drives are of the quick-disconnect, flexible, push-pull type, and are routed radially outward to the rod access room side walls.

2. (See Fig. 4.1F) In-pile tube extensions extend vertically downward and are gently curved outward as they proceed to the catchers located in the sub-pile room floor. These extensions might also be fitted with remotely-operated vibrators to insure that all solids settle into the catchers. Rod drives extend vertically downward through the sub-pile room floor into a rod access room where they are serviced, removed, etc., in the same manner as in ETR I.

3. (No figure) In-pile tube extensions proceed vertically downward to the catcher sections situated in the sub-pile room floor. Rod drives also extend vertically downward through the sub-pile room floor, and the drive mechanism is located in the rod access and catcher removal room. In this instance, rod drives would be fitted with quick-disconnects relatively close to the reactor vessel bottom head. It would be necessary to disconnect and physically remove one or more rod drives in order to service individual loop catchers.

Capsule experiment leads, if any, would be brought out through nozzles in the reactor vessel into the capsule trench. These leads could also be brought out through the reactor vessel top head, if desired.

The design of the reactor also permits installation of top re-entry loops and through loops. Piping above the reactor core would be brought out of the reactor vessel via radial nozzles located 10 to 12 ft above the reactor core. Experimental leads would also be brought through the reactor top head penetrations in these cases.

Refueling of the reactor would be accomplished through off-axis ports also located in the reactor top head. This particular arrangement may mean that loop experiment insertion or removal and experiment instrumentation work will be done before or after the refueling operation of the reactor, but this arrangement appears acceptable if all of these operations are optimized in the final reactor and experiment design and are carefully planned and scheduled when these facilities go into operation. Factors which will significantly affect the length of a reactor shutdown are discussed below.

Experiment removal or insertion times might be significantly reduced by utilizing an experiment handling cask and dolly which would operate on straight rails extending over the reactor and reactor working canal. This cask and its dolly would be motorized, and could be positioned over any reactor loop or capsule location, could be elevated or lowered as desired, and could include provisions for water cooling of experiments, etc.

Experiment lead connections should be of a type which would require a minimum of time to make of break connections in the shielded, pressurized terminal boxes located above the reactor vessel top head loop closures.

4.14 Fuel Handling

Fuel handling (Figures 4.1A, 4.1B, and 4.1C) is accomplished through fueling ports in the top head. A rotary fuel storage rack is built inside the flow distributor so that fuel may be passed around the reactor, under the loop flow and lead tubes, and under the top head spider arms to the discharge chute.

One important feature of the fuel storage rack is its ability to hold an entire fuel element charge, thereby making it possible to refuel for an emergency shutdown without having to discharge each element into the working canal until the next regular shutdown.

4.15 Reactor Structure

Figures 4.1A, 4.1B, and 4.2D show the structural features around the reactor.

A capsule handling cask is supported on the top structure and would service any of the capsule installations and would also operate over and discharge into the reactor working canal. A loop experiment handling cask is also provided for discharge of loop experiments into the working canal. Consideration should be given to placing this cask on rails straddling the top head of the reactor and the canal.

Shielded tunnels, cubicles, etc., are located in the reactor structure and around the periphery of the reactor vessel as necessary to service capsule nozzles, D_2O piping, and top re-entrant or through loop flow tubes. Piping corridors and suitable reactor vessel support structures are also provided. The outer thermal shield is shown outside the reactor vessel in this instance, but this might be placed inside of the reactor vessel and cooled with process water. Joining the reactor on the north side is a working canal with transfer tubes for fuel and experiment handling and a canal viewing window for underwater inspection of fuel assemblies, experimental equipment, etc. The long experiment transfer tube is slotted its full length so that discharge into the canal is possible.

4.16 Process Piping

A main header from the process water area (Fig. 4.2D, Reactor Building Section A-A) brings cooling water to the reactor vessel by way of a piping tunnel beneath the canal. The two 24 in. inlet lines then run to the flow distributor in the vessel where the water is dispersed through the upper section of the vessel. The water flows downward through the core and leaves the vessel through four 16 in. exit water lines. The process water then returns to the process water area by way of the piping tunnel.

FIG. 4.1 A

ETR II FOUR-LOBE REACTOR INSTALLATION VERTICAL CROSS SECTION

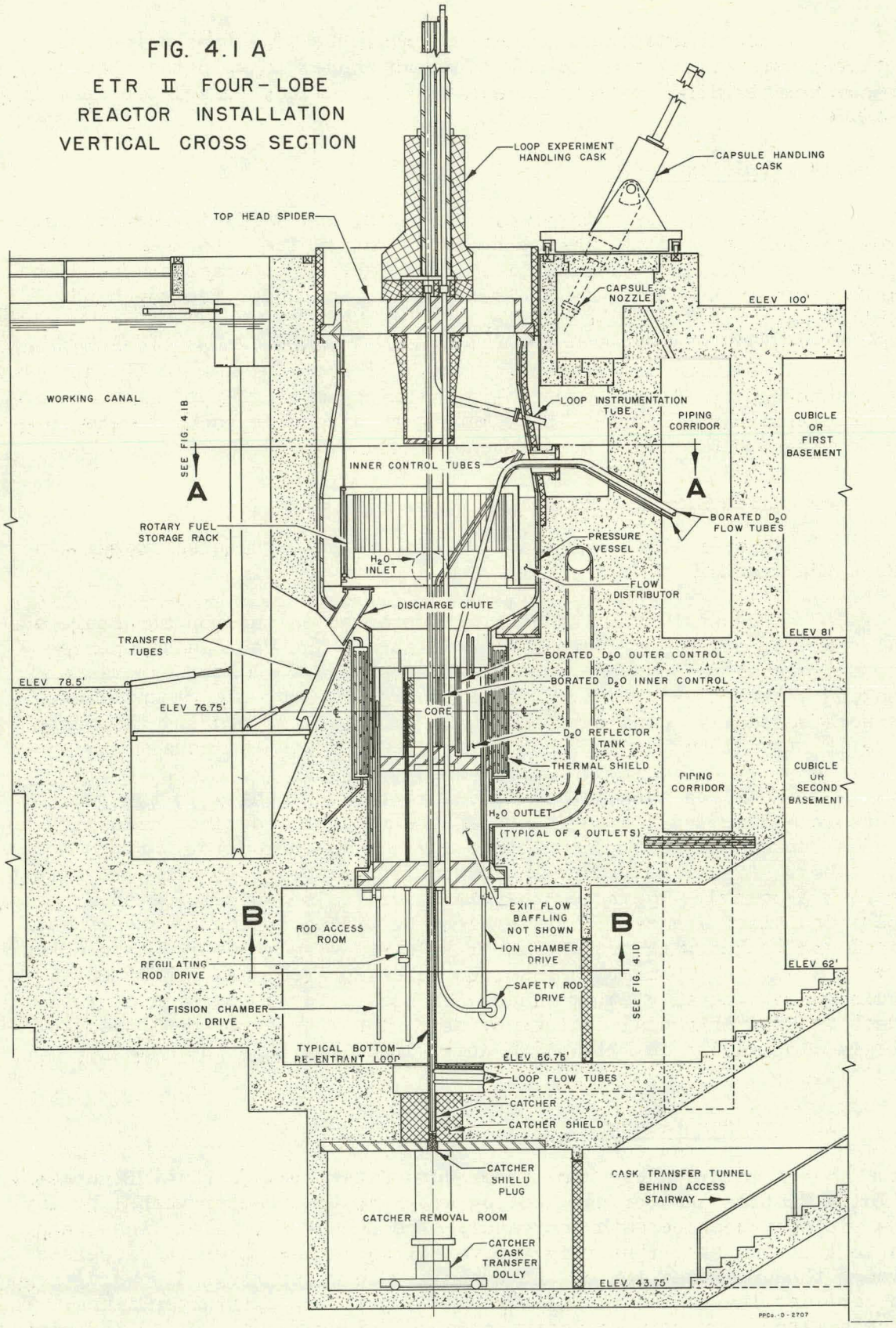

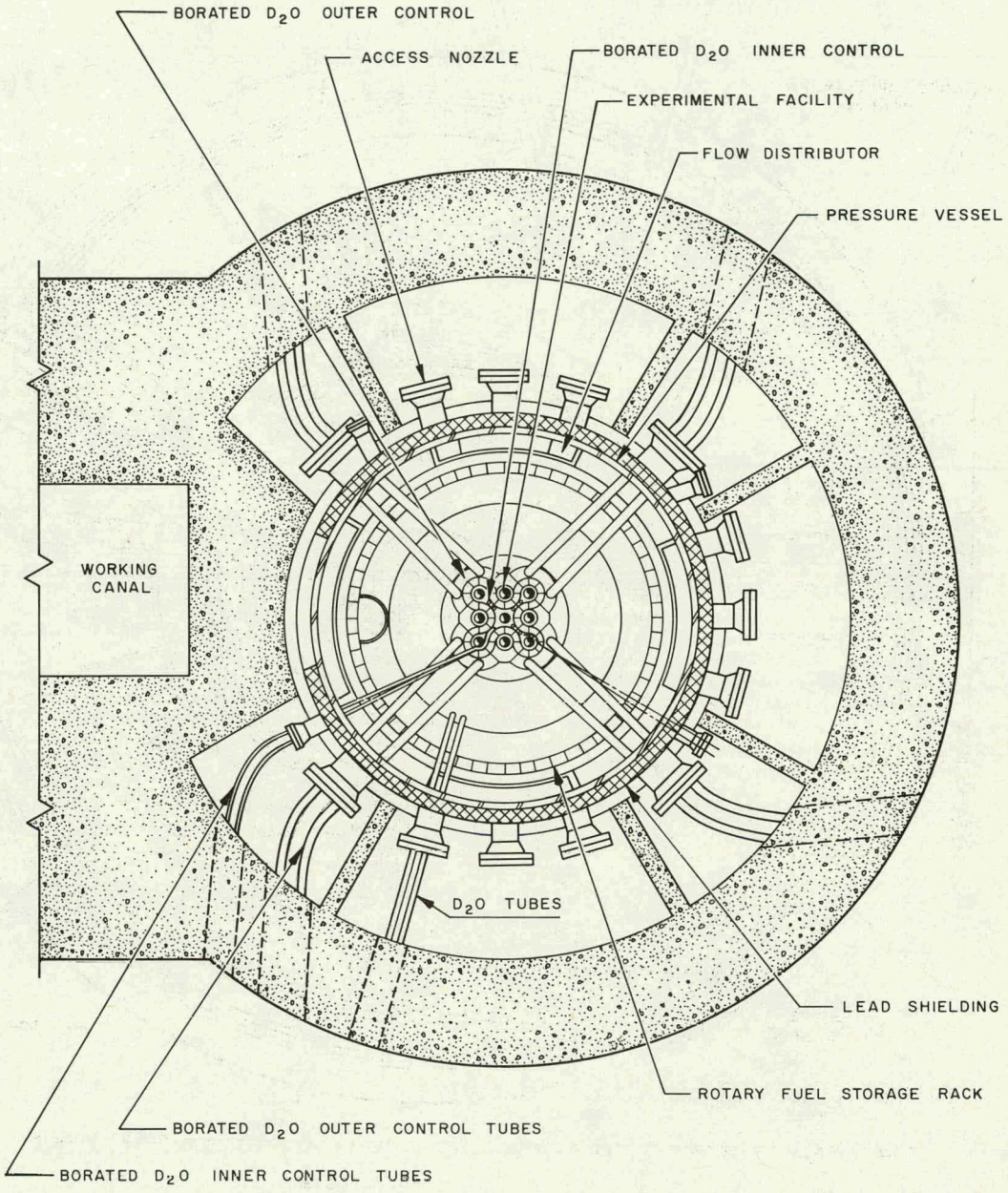

PPCo. -C - 2708

FIG. 4.1B

ETR II FOUR-LOBE REACTOR
HORIZONTAL CROSS SECTION
SECTION **A-A** FIG. 4.1A

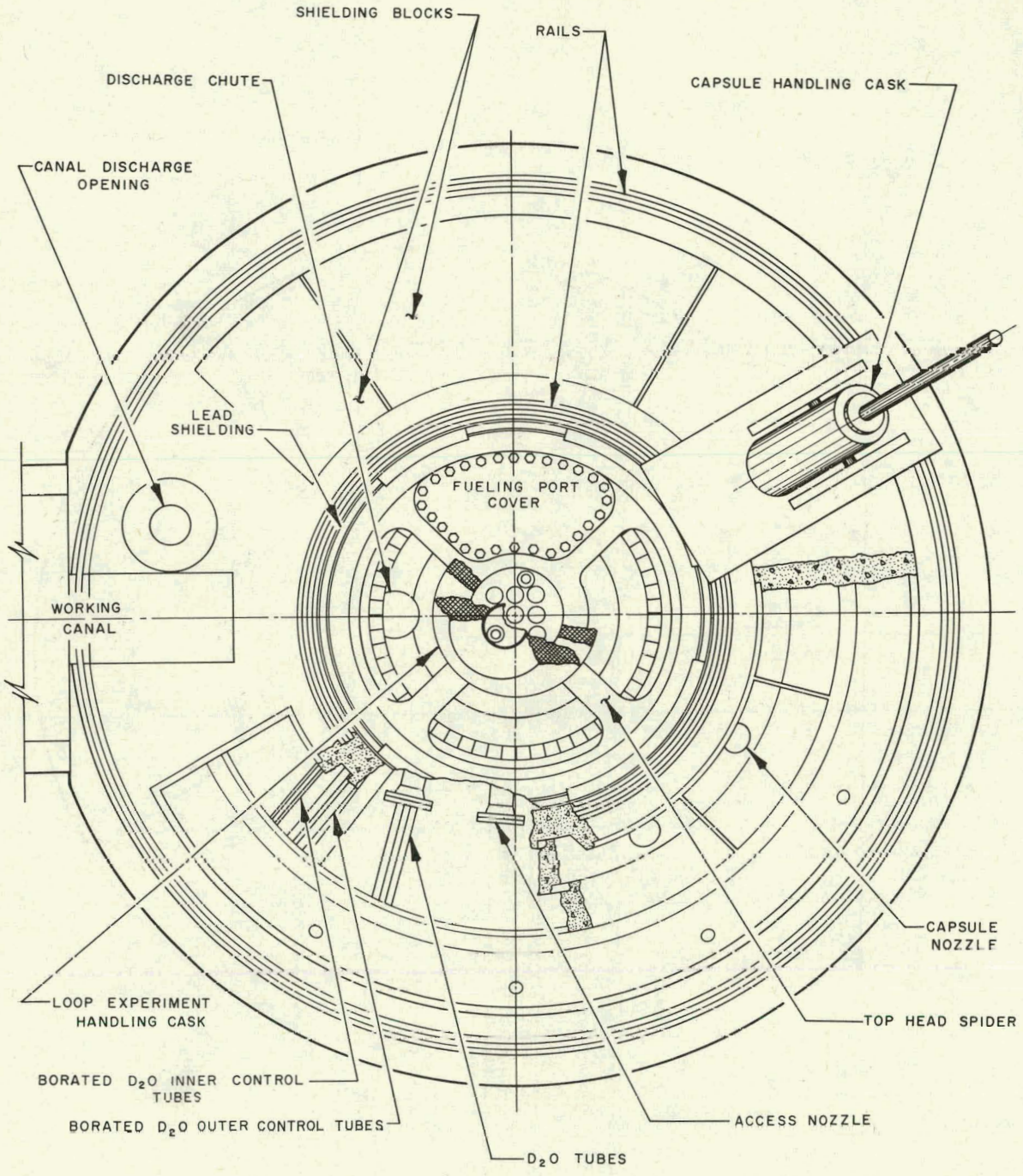

FIG. 4.1 C

ETR II FOUR-LOBE REACTOR

TOP PLAN

SEE FIG. 4.1 A

PPCo.-C-2708

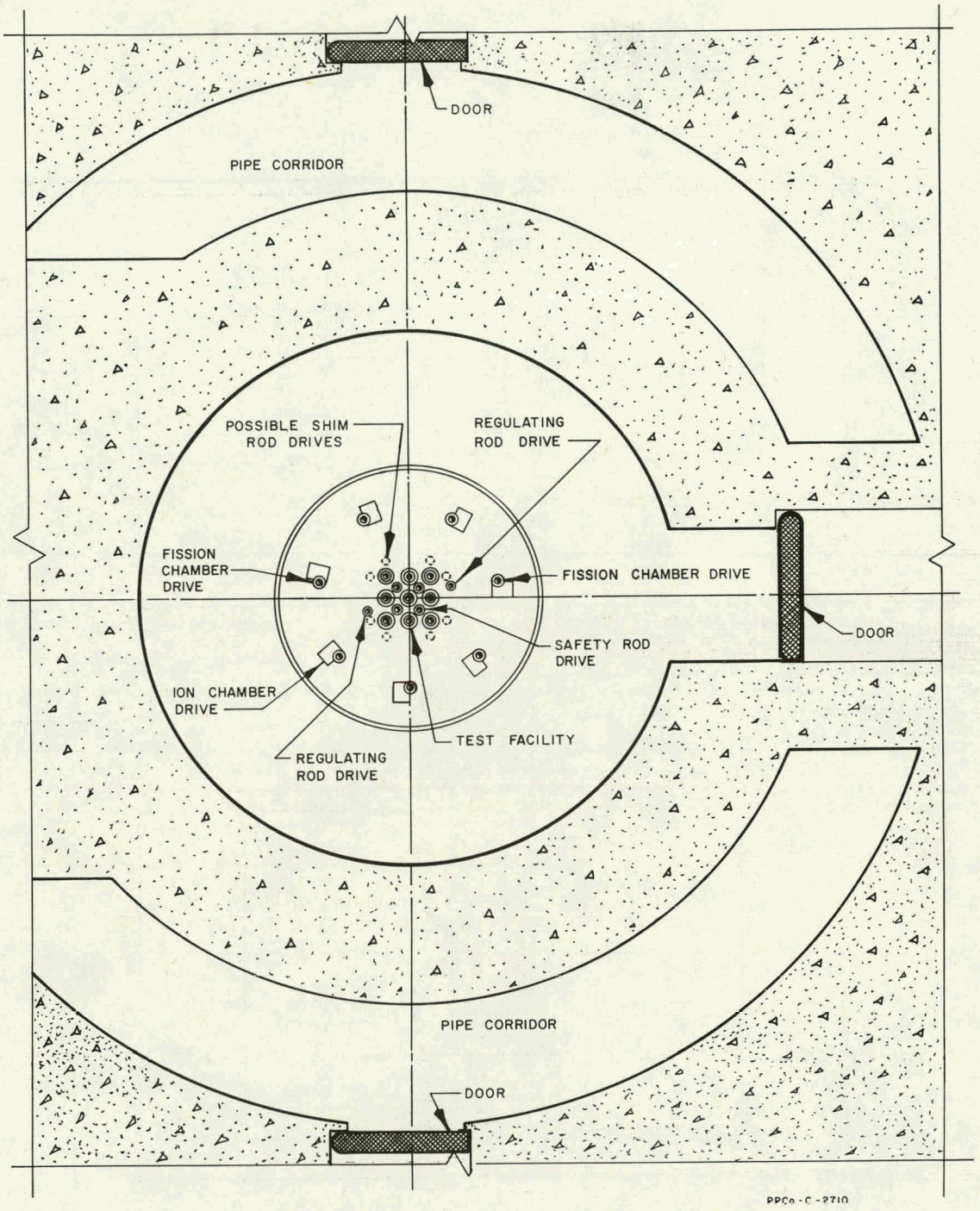

FIG. 4.1D

ETR II FOUR-LOBE REACTOR
ROD ACCESS ROOM
HORIZONTAL CROSS SECTION
SECTION **B-B** FIG. 4.1A

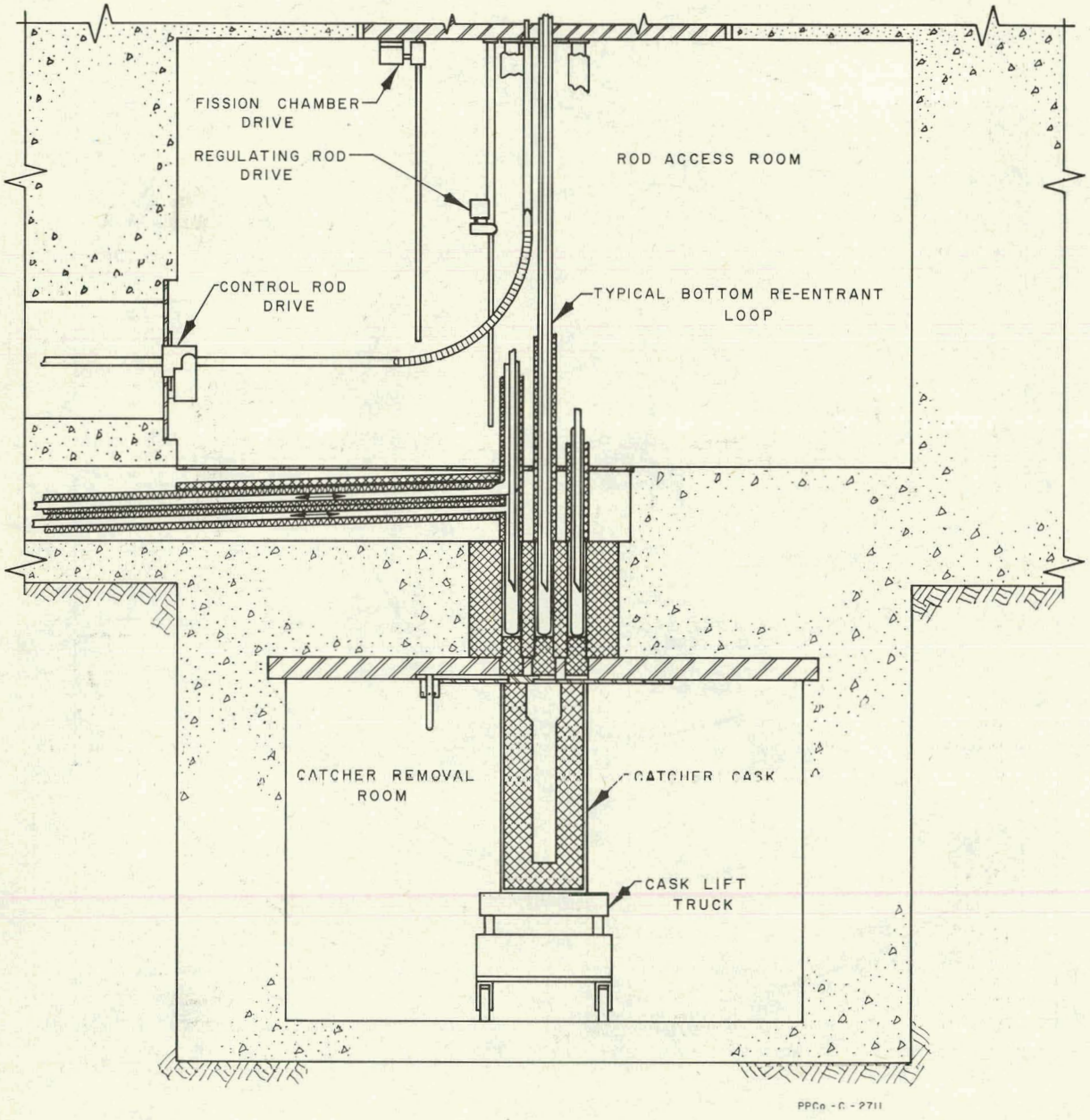

FIG 4.1 E

ETR II

FOUR LOBE REACTOR SUB-PILE ROOMS

CROSS SECTIONAL ELEVATION

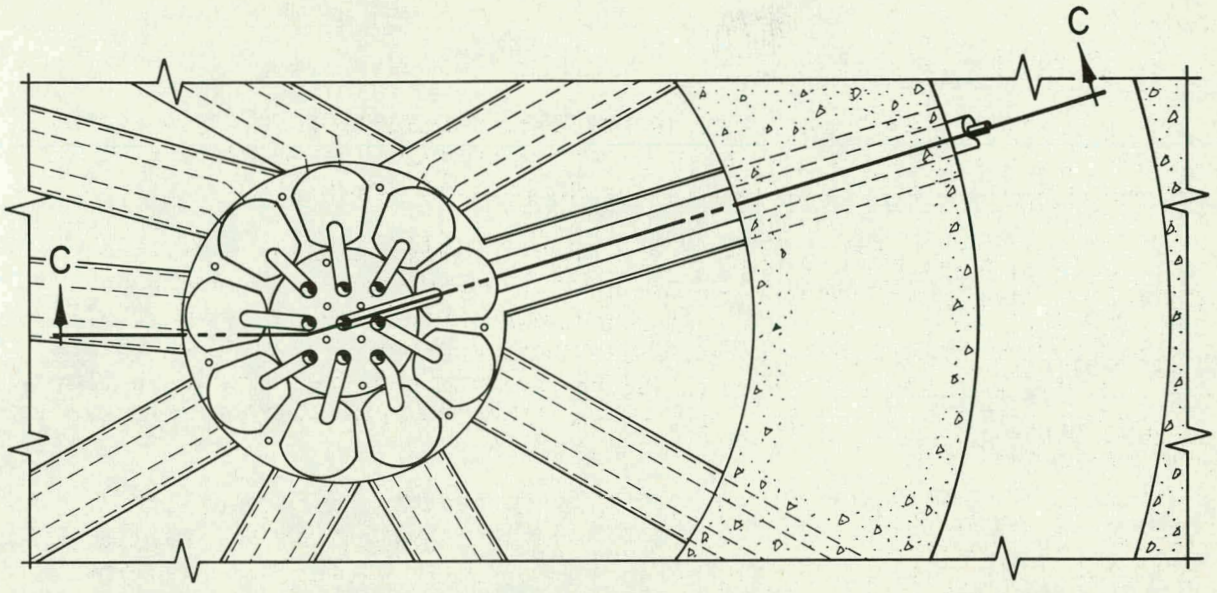

PLAN VIEW SUB-PILE ROOM

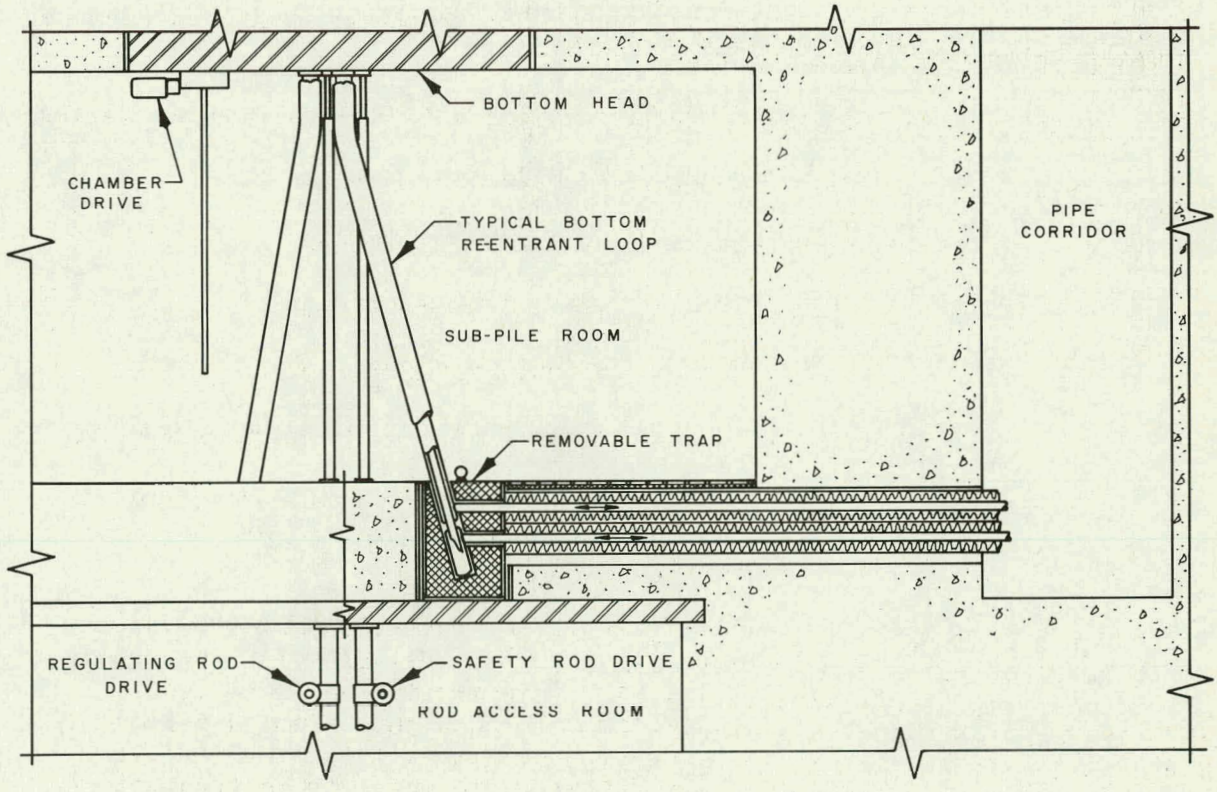

SECTION C-C

PPCo.-C-2712

FIG 4.1F

ETR II

FOUR LOBE REACTOR SUB-PILE ROOMS

ALTERNATE ARRANGEMENT

4.2 Reactor Building Complex

Design philosophy leading to the location and relationship of the reactor, critical facility, storage canal, experimenters' section of canal, and the hot cell is discussed in the material following:

1. Common canal access is provided for all of these facilities since it appears likely that there might be considerable interchange of loop experiments, capsules, fuel elements, etc., between any or all of the above facilities. Under such conditions, canal transfer appears more attractive than cask transfer when considering such things as time consumed in effecting a given transfer, likelihood of physical damage during transfer, and other considerations.

2. Each facility should nominally be capable of operating regardless of conditions existing in adjoining facilities. Toward that end, each facility and its access routes would be isolated from every other facility.

3. Actual floor space provided for each facility should take into consideration the experimental programs and the operational and maintenance requirements for that facility.

The above design considerations led to the layouts shown on Figures:

4.2A - Reactor Building - First Floor Plan

4.2B - Reactor Building - First Basement Plan

4.2C - Reactor Building - Second Basement Plan

4.2D - Reactor Building - Sectional Elevation A-A

4.2E - Reactor Building - South and West Building Elevations

As indicated on the above layouts, the reactor, critical facility, experimenters' section of canal, and hot cell are all located on, and connected to, a common storage canal.

The north side of the reactor building contains the storage canal which would be used to store hot experiments, fuel elements, and experimental equipment, to load cut fuel and experimental equipment into shielded carriers, to transfer experimental equipment into shielded carriers, and to transfer experimental equipment, fuel elements, etc., between facilities located in the reactor building. Gamma irradiations might also be conducted in this storage canal. The entire storage canal area would be serviced by a 50 ton bridge crane.

The south side of the reactor building is divided into six areas. Starting at the east end of the building, the first area is a service area containing a freight elevator, decontamination room, stairwell, and

entrances to the critical facility area, storage canal area, and mockup area. The second area from the east end of the reactor building is the critical facility area and contains a 24 ft long canal in which the four-lobe critical facility would be located. The critical facility canal is connected to the storage canal by a short canal extension. Transfer of heavy materials through this connecting section would be accomplished by means of a mechanical cart or other device located in the bottom of the connecting canal and operated from the canal parapet on both sides of the north sliding isolation curtain. The critical facility is served by a 15 ton bridge crane running in a north-south direction.

Located south of the critical facility is the mockup and pressure testing area. A 15 ton bridge crane running in an east-west direction will serve this area.

In the center section of the reactor building is the reactor area. A reactor working canal extends from the storage canal through the north wall of the reactor area to the reactor structure. Transfer from the reactor working canal to the storage canal would be accomplished by means of a mechanical cart or other device located in the bottom of the connecting canal and operated from the canal parapet on both sides of the north isolation wall. This isolation wall will extend a nominal distance below water level to form an air seal between the reactor area and the storage canal area. The reactor area is serviced by a 50 ton bridge crane running in a north-south direction and by a 2 ton handling crane located above the 50 ton crane and operating over the reactor and working canal. Truck access to the reactor area is provided through a truck door located on the south wall of the reactor area. The reactor area, the critical facility area, hot cell area, and the experimenters' canal area are to be designed so that air or surface contamination in one area can be contained in that area and will not affect operations in any of the other reactor building areas.

The extreme west area of the reactor building contains the experimenters' canal and the hot cell areas. The experimenters' canal is 60 ft long and is connected to the storage canal. Transfer from the reactor working canal to the experimenters' canal would be effected in the same manner as in the reactor area. Hot experiments and experimental equipment could be visually examined and remotely worked on from the top of the canal parapet or from behind shielding windows located below water level on the west side of the experimenters' canal (see Figures 4.2A and 4.2B). This area is served by a bridge crane, probably 15 ton, running in a north-south direction. Located south of the experimenters' canal area is the hot cell area. The hot cell itself is located over a narrow extension from the experimenters' canal and it is possible to transfer experiments, capsules, etc., directly from the experimenters' canal to the hot cell, where hot cell metallurgical examinations and other work could be conducted in air.

A two-story office building, attached to the south side of the reactor building, provides additional office and service space for functions essential to operation of the reactor and the experimental program.

The two basement levels in the reactor area of the reactor building are utilized for experimental cubicles, consoles, sample and mockup areas, etc., for the process equipment directly associated with the borated D_2O reflector circulation system, and for reactor instrument repair rooms.

Other basement areas are utilized for heating and ventilating equipment, a fuel storage vault, experimental emergency cooling loop equipment, and D_2O reflector process equipment.

Location of the reactor process water and other process equipment is also indicated on the above figures, but will be more fully discussed in Section 4.7, "Site, Buildings, and Facilities".

Building floor loads and canal floor loads should be specified at time of final design. In many instances, these loadings have tended to be inadequate in facilities built to date. Representative loadings for various areas might approach the following:

Reactor Area - All Floors	5000 lb/sq ft
Storage Canal Area	5000 lb/sq ft
Critical Facility Area	3000 lb/sq ft
Hot Cell Area	3000 lb/sq ft
Experimenters' Canal Area	3000 lb/sq ft
All Canals	3000 lb/sq ft + water load

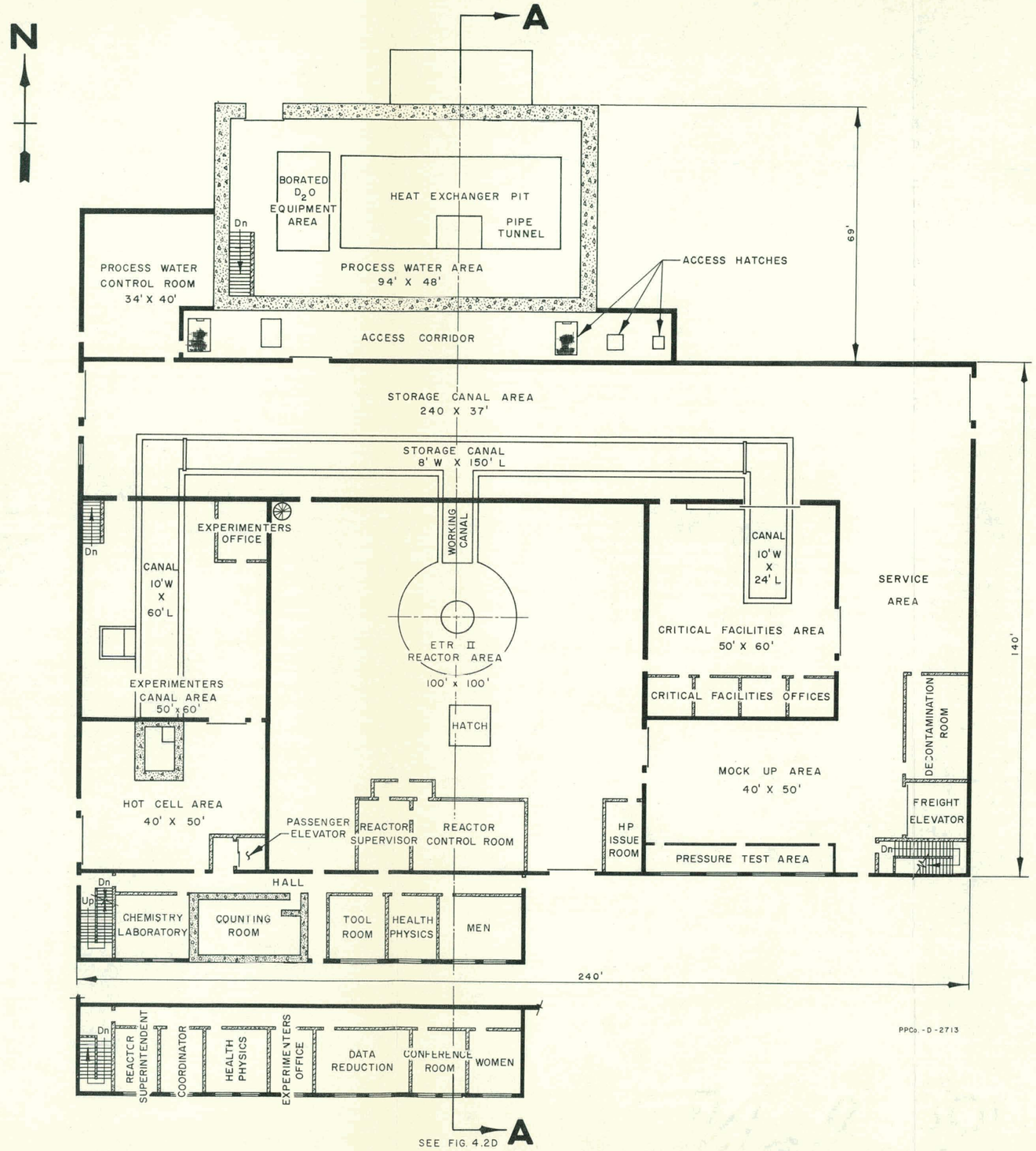

FIG. 4.2 A
REACTOR BUILDING
FIRST FLOOR PLAN

THIS PAGE

WAS INTENTIONALLY

LEFT BLANK

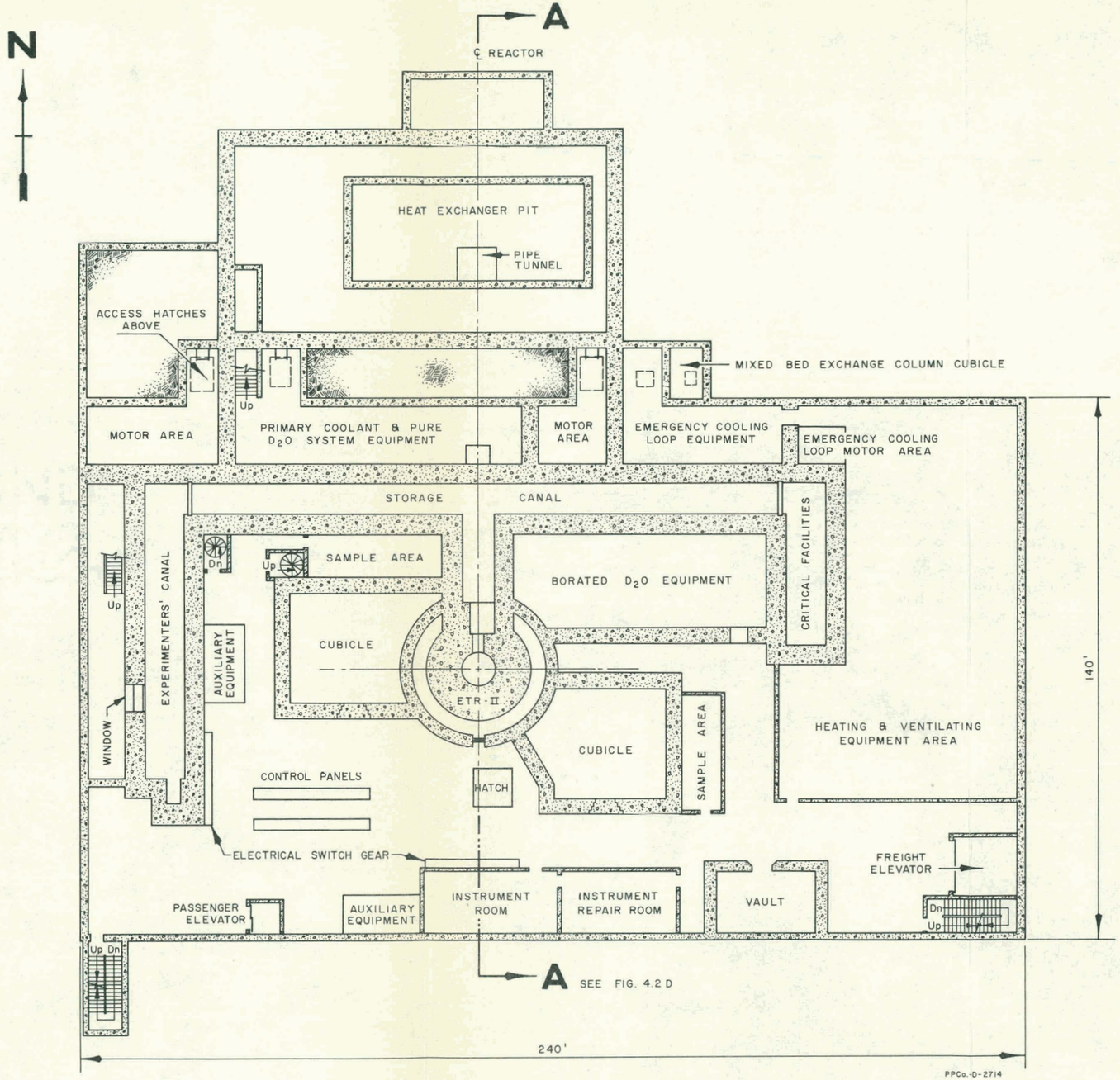

FIG. 4.2B
REACTOR BUILDING
FIRST BASEMENT PLAN

THIS PAGE

WAS INTENTIONALLY

LEFT BLANK

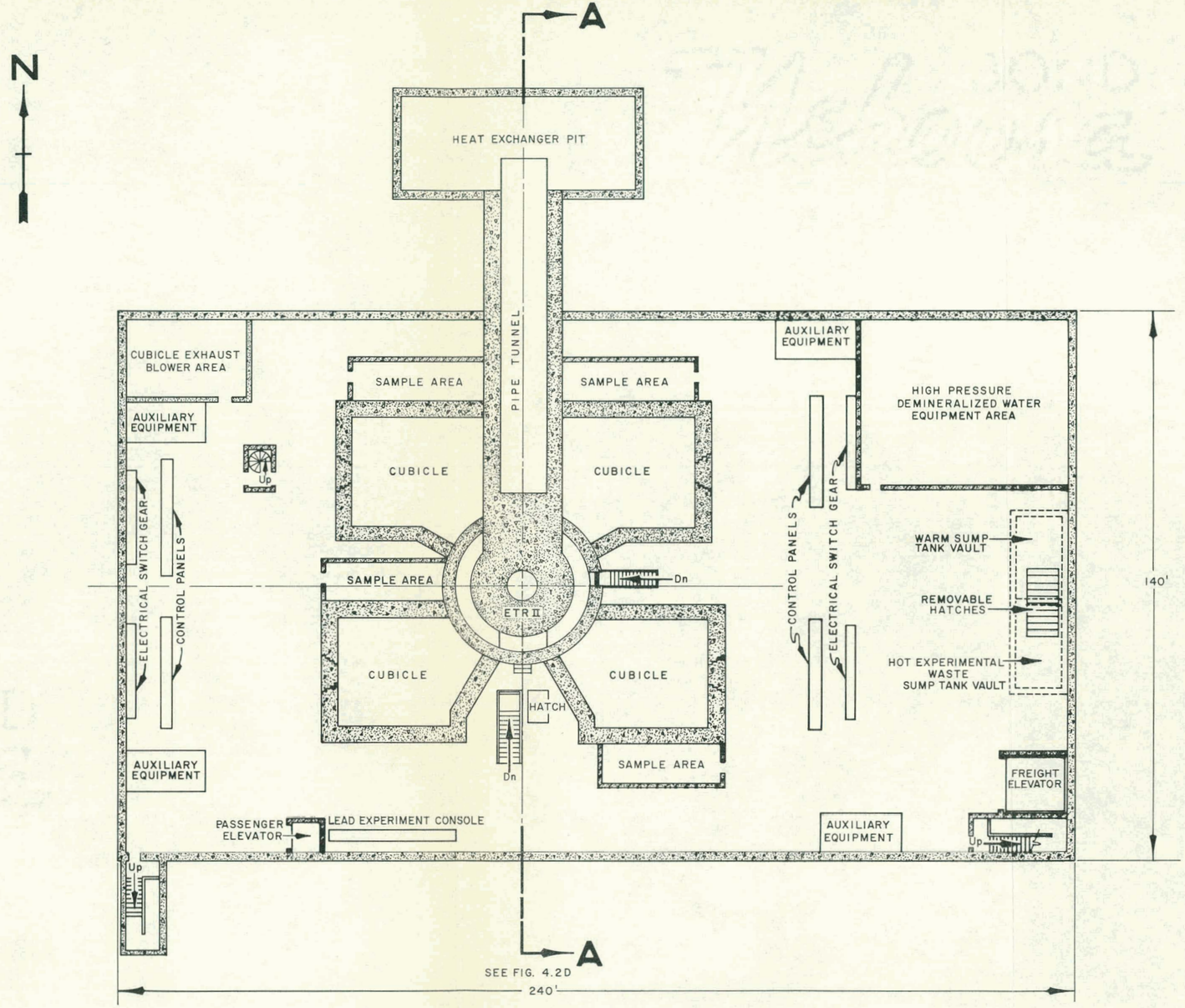

FIG. 4.2C
REACTOR BUILDING
SECOND BASEMENT PLAN

THIS PAGE

WAS INTENTIONALLY

LEFT BLANK

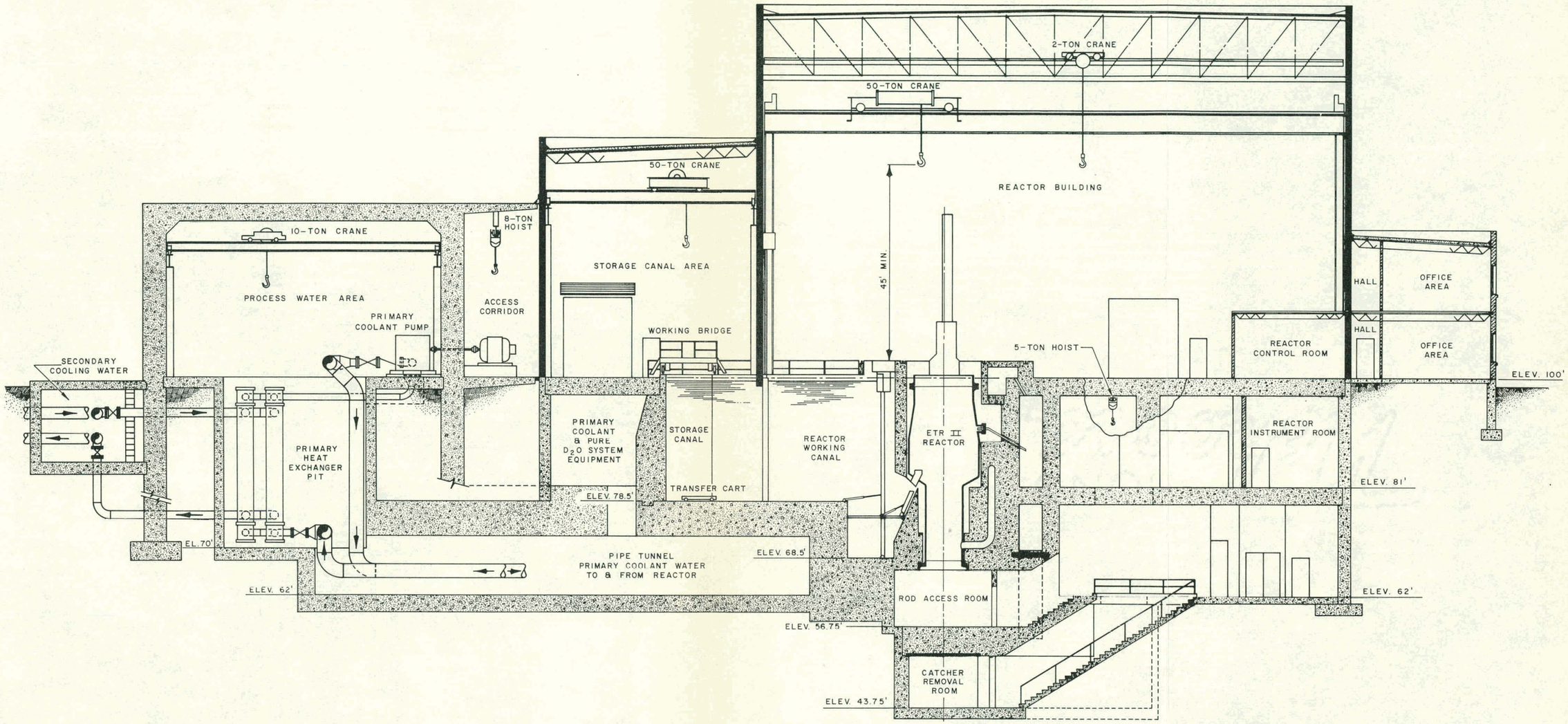

PPCo.-D-2716

FIG. 4.2D
REACTOR BUILDING
SECTIONAL ELEVATION "A-A"

THIS PAGE

WAS INTENTIONALLY

LEFT BLANK

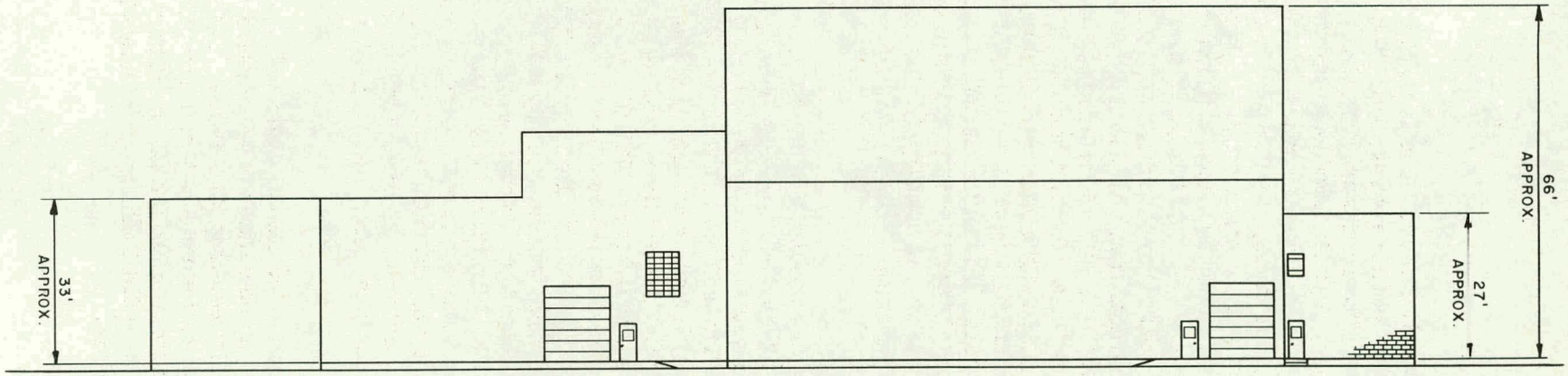

REACTOR BUILDING WEST ELEVATION

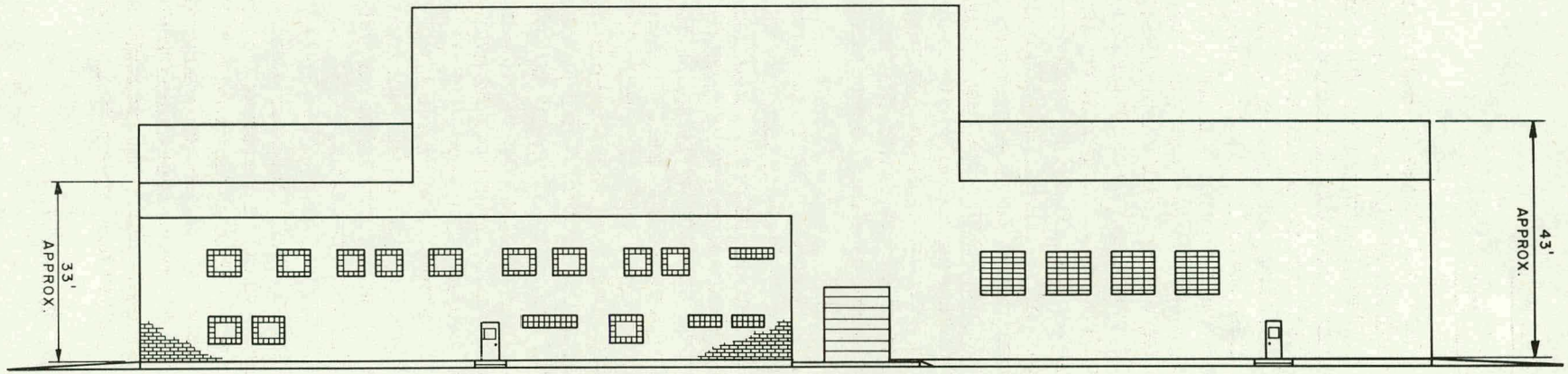

REACTOR BUILDING SOUTH ELEVATION

PPCo. - C - 2717

FIG. 4.2E
REACTOR BUILDING - BUILDING ELEVATIONS

4.3 Fuel Element

4.31 General

The fuel element design for the proposed reactor has been based on criteria dictated by the core physics, cooling requirements, and materials technology. The high neutron flux and associated power density in the reactor specifications indicated advanced fuel technology, yet it has been desired to achieve the immediate objectives with a minimum of development effort. An attempt has also been made to select a design offering adequate flexibility for future increases in reactor power. Computations of core physics have produced such parameters for the fuel element design as maximum and average power density, metal-to-water ratio, and critical mass. Heat transfer considerations have provided channel size, coolant velocity, core pressure drop, pressure differential across the fuel plates, and maximum wall temperature. With the maximum wall temperature in the 400-500°F range, aluminum technology is applicable. Fuel loading has necessarily been high to accommodate the high power density. Uranium-aluminum alloys of 35 weight per cent uranium have been considered as the present fabrication limit but with 45 weight per cent possible with some development. The rolled "picture frame" plate has been retained as an adequate and well developed fabrication technique. To retain the strength of the hardened aluminum alloy, assembly by brazing has been eliminated in favor of roll swaging or pinning. This technique has been verified by ETR I operating experience.

In general, the fuel element features desirable for optimum heat removal are contradictory to those features required for the best structural characteristics. Heat removal considerations indicate that both the side plates and fuel plates should be thin and that the span of the fuel plates should be large. However, strength requirements dictate that the side plates and fuel plates should be relatively thick and that the unsupported span of the fuel plates should be minimized. Fluid velocities and wall temperatures have a direct effect upon both the heat removal and the structural properties of the element. For example, increasing the nominal fluid velocity from 30 to 40 ft/sec increases the heat removal capabilities by a factor of approximately 1.2, while the lateral core pressure differential is increased by a factor of 1.8. Similarly, increasing the wall temperature by 50°F will increase the heat removal ability of the element by about 20 per cent while the structural strength of the fuel plate is reduced by about 40 per cent. High velocities and high temperatures increase the rate of corrosion of the cladding and therefore necessitate the use of thicker cladding.

From a heat removal standpoint, there are obvious potential methods of improving the element such as decreasing the number of elements per lobe, decreasing the plate thickness and increasing the number of plates per element. However, each of these changes decreases the structural quality of the element and therefore cannot be recommended until sufficient development work is done to establish the complete reliability of the modified element under the specified reactor conditions.

4.32 The Circular Segment Fuel Element

The geometry most nearly meeting the specifications outlined in the previous section appears to be an element composed of circular segment fuel plates (Figures 4.3A and 4.3B). Basically the element consists of curved plates mounted between two side plates to form a 45° segment of a right circular cylinder. The inside radius is 3 in. and the outside radius is 5.5 in. The side plates are extended to form the bottom end box. Each element has nineteen curved plates 0.050 in. thick, mechanically joined to the side plates. Each fuel plate consists of a homogeneous, highly enriched uranium-aluminum alloy core, 0.020 in. thick, completely clad with a 0.015 in. layer of X8001 aluminum alloy which should be sufficient for the corrosion and stress conditions encountered. The overall length of the plates is 49.5 in. and the fuel loading required is 33 weight per cent. Boron is incorporated in the core alloy to compensate for the loss in reactivity due to fuel burnup.

The 20 per cent enriched core loading experience in the MTR indicates that little irradiation testing is needed on the fuel alloy used in the proposed reactor. However, dynamic in-pile corrosion data extending the published data on the X8001 cladding to higher flow rates and temperatures should be obtained.

Some increase in cost of the circular segment fuel element over the present MTR-ETR type elements can be expected due to the number of dies needed to fabricate the individually sized plates, the incorporation of boron, the special alloy cladding, and the reject rate of the high weight per cent core. Recent ETR experience has shown that the boron distribution can be satisfactorily controlled in production. No increase in price is anticipated if it becomes desirable to grade the fuel radially to flatten the power. A slight increase in cost (i.e., 10 per cent) might be expected for axial grading of fuel.

Other fuel element designs and materials which were considered are discussed in Section 8.6.

4.33 Fuel Element Flow Containment

Because the coolant velocity through the fuel (44 ft/sec) is much greater than the velocity through the adjacent H_2O and Al-H_2O regions, some provision is needed either in the design of the fuel element or in the reactor structure to effect adequate cooling of the external plates and to establish flow conditions such that no unacceptable lateral pressure differentials exist across these outside plates. If the flow immediately adjacent to the outside fuel plates were allowed to have the same velocity as the flow through the Al-H_2O and H_2O regions, then a lateral pressure differential of approximately 86 psi would exist across the outside plates.

Three methods are suggested for providing a .0775 in. thick flow channel adjacent to the exterior fuel plates so that the velocity on both sides of these fuel plates is the same and no excess lateral pressure will exist.

1. Where aluminum filler pieces are adjacent to the fuel, as in the center high flux region, these filler pieces will be designed to provide the required flow channel.

2. Where structural members are adjacent to the fuel, as on the outside of the four lobes, these members will be designed to provide the required flow channel for the outer fuel plates. An example of this is the borated D_2O outer control tanks.

3. Where a water region is adjacent to the fuel, as in the flux-trap regions in two of the lobes, complete right circular cylindrical shells will be used to separate the fuel region from the adjacent water region and to provide the necessary flow channels adjacent to the external fuel plates.

If provisions, such as those outlined above, are not made to isolate the low coolant velocity regions from the high coolant velocity fuel region and to provide channels which permit high flow rates along the two outside fuel plates, then relatively thick (0.180 in.) non-fueled outer plates will be required on the fuel elements.

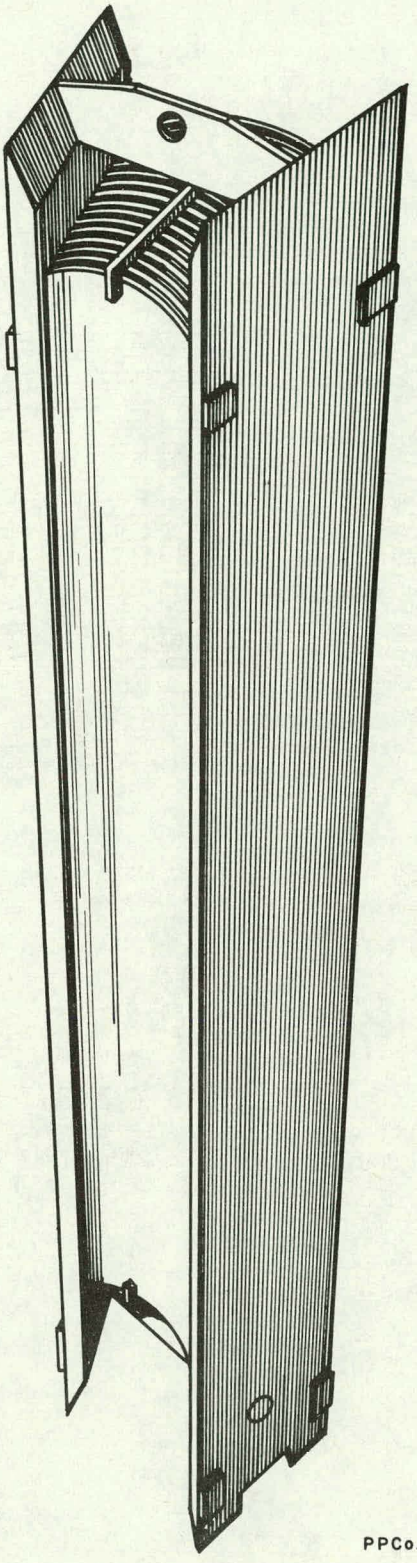

PPCo.-A-2718

FIG. 4.3A
CIRCULAR SEGMENT FUEL ELEMENT

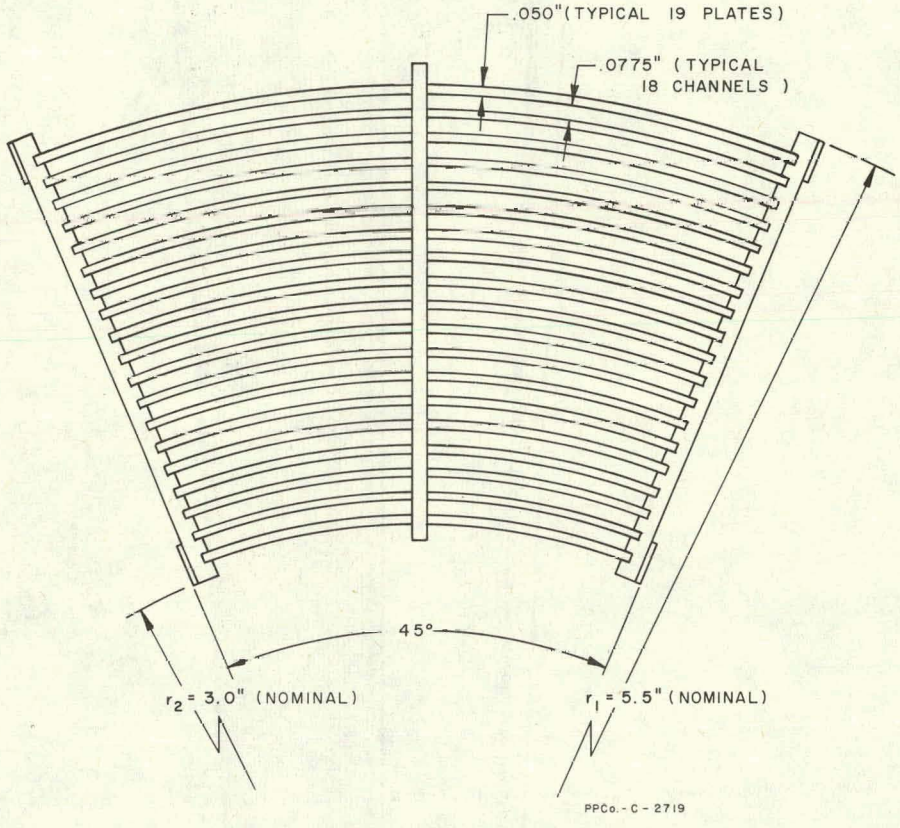

FIG 4.3 B

PLAN VIEW OF FUEL ELEMENT FOR ETR II

4.4 Reactor Controls and Instrumentation

The instrumentation system may be divided into three categories for purposes of discussion: the control system which utilizes regulating rods and shim control to allow automatic operation of the reactor under preset conditions; the safety system which functions to protect the reactor throughout all conceivable operating situations, intended or accidental; and the process instrumentation to allow the proper processing of the reactor coolants according to the reactor requirements.

4.41 Control System

The control system provides a continuous means of measuring the power level and the neutron flux level in the reactor and a means of controlling the long time variations (shim control) and the short time variations (regulating rod control).

4.411 Power Level Instrumentation

There are two systems for determining the integrated power level of the reactor as shown in Fig. 4.4B. The first is a system of water sample tubes spaced around the reactor to bring a sample of the coolant water from five regions out to a gamma ray detector arrangement. This sample is at the detector within approximately 10 sec after passing through the reactor core so that the activity caused by the neutron reaction ${}_8O^{16}(n,p){}_7N^{16}$ which decays with a 7.4 sec half life can be measured. By sampling at five symmetrical regions in the reactor an integration of the reactor neutron flux is obtained. In addition, this measurement allows balancing of the neutron flux in the reactor by shim control when experimental loading causes unbalance.

The second system consists of a conventional computation of the reactor power by measurement of the difference in temperature of the inlet and outlet cooling water and multiplying by the coolant flow rate. Several resistance thermometers are used to allow better integration of the inlet and outlet temperatures reducing the effect of any stratification in the coolant water piping.

A differential galvanometer allows a more sensitive indication of the drift in power level than on a normal full scale indication. The system shown in Fig. 4.4A with a carefully controlled zero offset is quite sensitive in this measurement. With batteries as the high voltage supply, the system is also used as a power level indication independent of a.c. power generation. The chamber for this instrument may be located outside of the thermal shield since it does not require fast response and can thus operate at lower neutron sensitivity.

4.412 Shim Control

A system of shim control is proposed which uses a chemical solution of boron to be added to or taken away from two control regions in each of the four-lobes otherwise containing D_2O as shown in

Fig. 2.0A. This type control has an advantage over the fuel follower type shim rod control in that it perturbs the neutron flux symmetrically in the vertical direction. This in turn relieves an otherwise more critical heat generation problem and allows a more uniform neutron flux throughout the length of the experimental tubes.

A chemical shim control system design for the reflector region only demonstrates the problems and possible solutions encountered. Directly outside the core is a 10 cm thick D_2O reflector annulus to which D_3BO_3 can be added or removed to provide a chemical shim control system. A schematic diagram of such a system is shown in Fig. 4.4D. The shim control annulus is divided into four sections to allow differential control of reactivity unbalances from the experiments, to effect power balancing during reactor operation and to allow special distribution of power among the four-lobes to achieve a special combination of flux levels. Due to the high gamma and neutron heating in the borated D_2O tanks and reflector annulus, the D_2O is cooled in an external heat exchanger. A baffle and orifice is provided to force part of the D_2O at a high velocity past the inner walls of the borated D_2O tanks to increase the heat transfer coefficient and reduce the operating temperatures.

For removal of boron from the reflector stream, a boiler-D_2O recovery system is used. This is preferred to an ion-exchange resin bed because of the high cost of a deuterated resin which cannot feasibly be rejuvenated. The recovery system stores the portion of the borated D_2O withdrawn from the reflector stream and distills off the D_2O as a batch process. Pure D_2O injected into the system during dilution of the borated D_2O shim solution comes from a makeup tank.

For addition of the boron to the system, an injector places a metered amount of 46.5 g D_3BO_3/liter solution into the main D_2O stream just prior to entrance into the reflector tank region.

The equations describing both systems are shown below. For removal of boron from the system,

$$\frac{C}{C_o} = e^{-\frac{\beta v_s}{V_R} t},$$

where

C = concentration of D_3BO_3 at time, t, in g/liter,

C_o = the initial concentration of D_3BO_3 in g/liter,

v_s = the flow rate of the coolant in ft^3/sec,

β = the fraction of flow being drawn off,

V_R = the total reflector volume in ft^3, and

t = the time in sec.

Fig. 4.4E shows the variation in the effective multiplication factor, k_{eff}, for two continuous rates as criticality is approached from $k_{eff} = 0.98$. To achieve criticality in four minutes after starting dilution of the borated D_2O shim solution from a solution which is 70 per cent saturated with D_3BO_3, $\beta v_S/V_R$ must equal 0.512 for an injection flow rate of about 65 gpm. To limit the maximum rate of change of reactivity to less than 10^{-3} in $\delta k/k$ per sec, however, the value of $\beta v_S/V_R = 0.217$ for an injection flow rate of about 28 gpm, which changes the reactor startup time to about 10 min for the same conditions. It is possible that the faster flow rate may be used until nearing criticality and then the slower rate to reach criticality. It is also noted that this can be an intermittent process instead of a continuous one.

The boron injection system is described by the equations,

$$C = C_1 - (C_1 - C_o)\, e^{-\frac{v_S}{V_R} t} \quad \text{and}$$

$$C_1 = \frac{\frac{v_a}{v_S} C_a + C_o}{1 + \frac{v_a}{v_S}},$$

C_a = the D_3BO_3 concentration being injected in g/liter,

C_o = the initial concentration of the system in g/liter,

v_S = the system flow rate in ft^3/sec,

v_a = the injection flow rate in ft^3/sec,

t = the injection time in sec, and

V_R = the total reflector volume in ft^3.

This equation is valid only for a single cycle of the reflector system due to the cycle delay time from starting injection until the concentration increase is felt throughout the system. For times longer than the system cycle time a series of successive approximations must be used to determine the concentration of the fluid entering the reflector. The cycle time effect does not allow injection at a constant rate to maintain a uniform increase in boron concentration. Refinements in injection techniques and mixing in the external system should approximate a uniform rise, however.

It is desirable to have similar sensitivity of control for the addition of boron as occurs for the removal of boron in the reflector. In Fig. 4.4F the value of v_a/v_S required to initiate a 10^{-3}/sec

rate of change of reactivity for the operating reflector boron concentrations is obtained. Then the curve shown in Fig. 4.4G is used to determine what rate of change of injection rate versus time is required to maintain the negative reactivity change at 10^{-3} in $\delta k/k$ per sec. The curve shown in Fig. 4.4G has been divided into three exponentially increasing region corresponding to three regions on the exponential curve of effective multiplication factor as a function of D_3BO_3 concentration. (See Fig. 4.4H.)

In the neck of each lobe straddling each mechanical safety rod is an additional location for boron in D_2O. The one side is inlet and the other the outlet for the solution allowing an easy replacement of a defective unit from the top. This will allow additional control of flux variations and shutdown reactivity.

The preliminary design calculations show that this type of reflector shim system does not perturb the test assembly flux unduly and gives a gradual and stable reactor control. The engineering development work should be directed to provide a smooth, reliable, and proper rates of addition of pure D_2O and concentrated D_3BO_3 solution. The feasibility of this system has been demonstrated in the BORAX Facility located at NRTS.

The boron chemical shim control system is sufficiently flexible to allow adequate compensation for changing reactor conditions. The rate of change of reactivity available in the system is greater than that produced by the maximum rate of change of xenon or temperature under the worst operating conditions. Controlling of each quadrant individually allows suppression of any oscillation in the flux that might be caused by the degree of coupling between the four lobal sections. It also permits adjusting the five major loops individually to unlike operating flux conditions.

4.413 Regulating Rod Control

The regulating rod is a vertically operating rod located in the BeO reflector as shown in Fig. 2.0A. The rod inserts and withdraws neutron absorbing material to damp small reactor power fluctuations as dictated by the servo control system. The servo system which allows automatic control of the reactor power is shown in Fig. 4.4I. The ionization caused by neutrons in the compensated ion chamber allows current to flow through the motor operated rheostat proportional to the neutron flux. The rheostat acts as a set point to produce a voltage from the ion current that is balanced against a fixed voltage in the servo amplifier. As the rheostat is varied a different power level is determined and the hydraulically driven rod allows a correction to be made to bring the voltage into balance. Two decades of power level are controlled by the servo system.

It is possible that with a chemical shim control system as described above a mechanical regulating rod may be unnecessary. To determine this an investigation into the mixing problems, the time response and the practical processing of the chemical solutions is necessary. This proposal is made including a mechanical regulating rod.

As discussed in the kinetic calculations in the Hazards section of this report, there is an added measure of safety in the control of the water reflected reactor. Those neutrons entering the reflector return to the active core with some finite delay in the order of a millisecond. The effect is similar to that of the delayed neutrons which is the mechanism allowing control in a thermal reactor. Only in this case the percentage of neutrons delayed is some 30 per cent instead of the 0.7 per cent normally available. The result is that the performance of the servo system can be relaxed over a thermal reactor that does not have heavy water reflection.

It is noted that the boron in the shim reflector can react on the worth of the regulating rod due to the close proximity of the two. However, at criticality and power where the regulating rod is operating, the amount of boron in the shim reflector will be reduced and the effect should be minimized.

4.42 Safety System

The safety system receives its activation from fission chambers and gamma-compensated ionization chambers, which, either separately or in combination, provide a continuous indication of the neutron level in the reactor from the cold clean reactor (with neutron source) to greater than 150 per cent of full power rating. These channels are adjusted appropriately to give the proper shutdown of the reactor for unsafe operating conditions in whatever region of neutron level the reactor is operating.

4.421 Startup Instrumentation

The startup instrumentation consists of two channels of counting rate instruments to count the fissions in two fission chambers. The output from the log count rate meters as shown in the block diagram in Fig. 4.4C is recorded. On the recorder there are microswitches set so that the control system will not allow the reactor to start up without having at least one of the count rate channels reading on-scale. These channels allow observation of the neutron flux in the cold clean reactor region with a reasonable size neutron source from which to multiply.

4.422 Mechanical Safety Rods

In ETR II the safety rods are blade type curtains which move between adjacent fuel sections in the stem of each of the four-lobes. The rods are driven from below the core by a system similar to that in use in ETR I. During reactor operation the safety rods are withdrawn completely to a position one ft above the core. In the event of a scram signal, the holding magnets are de-energized, releasing the rods which are accelerated by gravity and core pressure into the reactor.

The safety rod drop time is found from the solution of the acceleration equation to be

$$t = \frac{w}{KA\sqrt{\frac{2g}{K}\left(\Delta p + \frac{w}{A}\right)}} \cosh^{-1}\left(2\, e^{\frac{KAL}{w}} - 1\right) ,$$

where

w = the rod weight in lb,

A = the rod cross sectional area in ft^2,

K = a conversion factor,

Δp = the pressure drop across the core in psf, and

L = the length of the core over which pressure drop occurs in ft.

Neglecting dashpot effects at the end of the rod travel, the safety rod drop time is approximately 0.47 sec with a Δp of 75 psi. Assuming a negligible delay time in the instruments and a release time for the magnets of 0.05 sec, the total time required to introduce the complete shutdown reactivity is 0.52 sec.

The shim control system is adjusted to have enough negative reactivity effect that at no time will the reactors go critical on withdrawal of the safety rods during startup. To account for the excess reactivity needed for burnup and the possible additional positive reactivity that might occur from fuel experiments, a value of effective multiplication of 0.98 has been chosen for the cold clean reactor when the safety rods are completely withdrawn.

4.423 Safety Instrumentation

The safety instrumentation for the reactor makes use of many of the desirable features in the MTR. The block diagram of the safety instrumentation is shown in Fig. 4.4J. The signals from three level channels and two period channels originating from five separate chambers are tied to a common sigma bus. This sigma bus acts as an input signal to the nonlinear magnet amplifiers. The magnet amplifiers have the characteristic that as the input from the sigma bus goes either up above a certain voltage or down below a certain voltage, the output current to the magnets goes down. Thus, for a reactor power increase and the resulting sigma bus voltage increase or for shorting of the sigma bus resulting in a voltage decrease, the magnet current decreases sufficiently to release the safety rods into the reactor. This system is commonly referred to as the "Fast Scram" or "Electronic Scram"

instrumentation since it can occur in the millisecond range and does not require any mechanical relay operations. The "Slow Scram", "Setback", and "Reverse" are usually initiated by recorder level switches using relays. A list of typical "Corrective Signals" to be used are given in Table 4.4A.

TABLE 4.4A

CORRECTIVE SIGNALS

Parameter	Setback Signals	Reverse Signals	Scram Signals
Neutron Level	>1.1 N_F*	>1.2 N_F	>1.3 N_F
N-16 Power Level	>1.1 N_F		>1.3 N_F
Water Power	>1.1 N_F		>1.3 N_F
Water Temperature Rise	>105% Normal		>150% Normal
Water Flow	$\geq\pm$ 10% Normal		$\geq\pm$ 20% Normal
Water Pressure	$\geq\pm$ 10% Normal		$\geq\pm$ 20% Normal
Manual Operation	Yes	Yes	
Neutron Level (Manual)		>3 N_L**	
Reactor Period		<5 sec	< 1 sec
Neutron Level (Reactor Period < 1 sec)			> N_L
Loss of Instrument Voltage			Yes
Purchased Power Frequency out of limits			> 3 cps
Loss of Purchased Power			Yes
Loss of Relay Bus Voltage			Yes

* $N_F \equiv$ Full Power

** $N_L \equiv$ 1% Full Power

The Setback is used to bring about a gradual reduction of operating power with the occurrence of an abnormal condition, not necessarily unsafe, but which is either a precursor of an unsafe condition or that which would invalidate some standby protection in the event of a real emergency. The setback is accomplished by the automatic lowering of the control point of the servo system and persists only so long as the condition which provoked action remains. The reactor is always essentially critical. When the trouble has cleared, the servo will respond to the operator's demand for return to the original or desired servo setpoint.

The Reverse is more drastic in that all control elements are driven in the direction of decreasing reactivity and continue this action until the condition has cleared and the operator has removed the reverse command. Depending upon how long the reverse lasts, the reactor may be subcritical by several per cent; the withdrawal of shim rods must be initiated by the operator to restore the reactor to normal operation. Whether this can be done in any particular case will depend upon the neutron level at the time increasing the reactivity is attempted by the operator. If the flux has fallen below some safe, arbitrary value, the system will demand the operator go through the entire startup procedure. Obviously the reverse is used for conditions which require drastic action, such as a 5 sec period.

The Scram is the final and most dramatic corrective action which may be taken by the control system and results in complete shutdown. The ultimate safety of the reactor depends on the existence of numerous independent means for achieving the scram, so that the probability of simultaneous failure of all is made vanishingly small.

4.424 Auxiliary Instrumentation

Fission Product Monitoring System[1] - In a high-flux, water-cooled reactor it is an important consideration to detect contamination of the system from fresh fission products. The detection and localization of such contamination is necessary from an operational viewpoint in order to make decisions regarding reactor operating level, disposition of effluent water, and the operation of experimental facilities.

The instrumentation must discriminate against the high "noise level" caused by radiation from activated impurities in the water, by entrance of radioactive nuclei from structural materials and deposition of radioactive material on the surface of the water system. This problem is alleviated by using fission product iodine isolation by means of ion exchange resins and gamma energy discrimination as indicated in Fig. 4.4K. By looking at the short lived iodine products, past history is not a major factor in the measurement.

---

1. R. L. Heath, "Fission Product Monitoring in Reactor Coolant Streams", IDO-16213, January 1, 1956.

Boron Concentration Instrumentation - The startup of the reactors requires that a 70 per cent saturated solution of D_3BO_3 be present in the D_2O shim control reflector so that the reactor does not go critical on withdrawal of the safety rods. A test should be available to assure the operator that this condition does exist. A primary measurement of the neutron absorption can be made as shown in the block diagram in Fig. 4.4L. A polonium-beryllium neutron source located adjacent to a thermal neutron detector will emit neutrons into the shim reflector region around it. The number of thermal neutrons reflected back to the detector is a function of the concentration of boron in the heavy water. The system must be calibrated at several known points as the measurement is a nonlinear relationship with concentration.

There is a boron instrumentation system on each of the separate segments in the reactor that have variable boron concentration for control purposes. This information is displayed on a recorder calibrated in concentration and coupled into the control system for startup control.

Health Physics Instrumentation - The health physics instrumentation included here is a remote monitoring constant air monitor which has sampling stations in critical regions throughout the reactor buildings. These stations indicate and alarm at a central location in each reactor building. Other health physics instrumentation, such as the portable instruments to measure normal radiation types, will also be available.

4.43 Process Instrumentation

All important process variables are recorded and displayed in the appropriate locations. Since this instrumentation is fairly standard and straightforward as related to reactor operation and control, it is not detailed here. The cost of this instrumentation is, however, included in the final cost estimate.

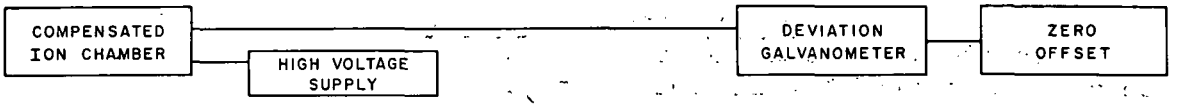

FIG. 4.4A
DIFFERENTIAL GALVANOMETER

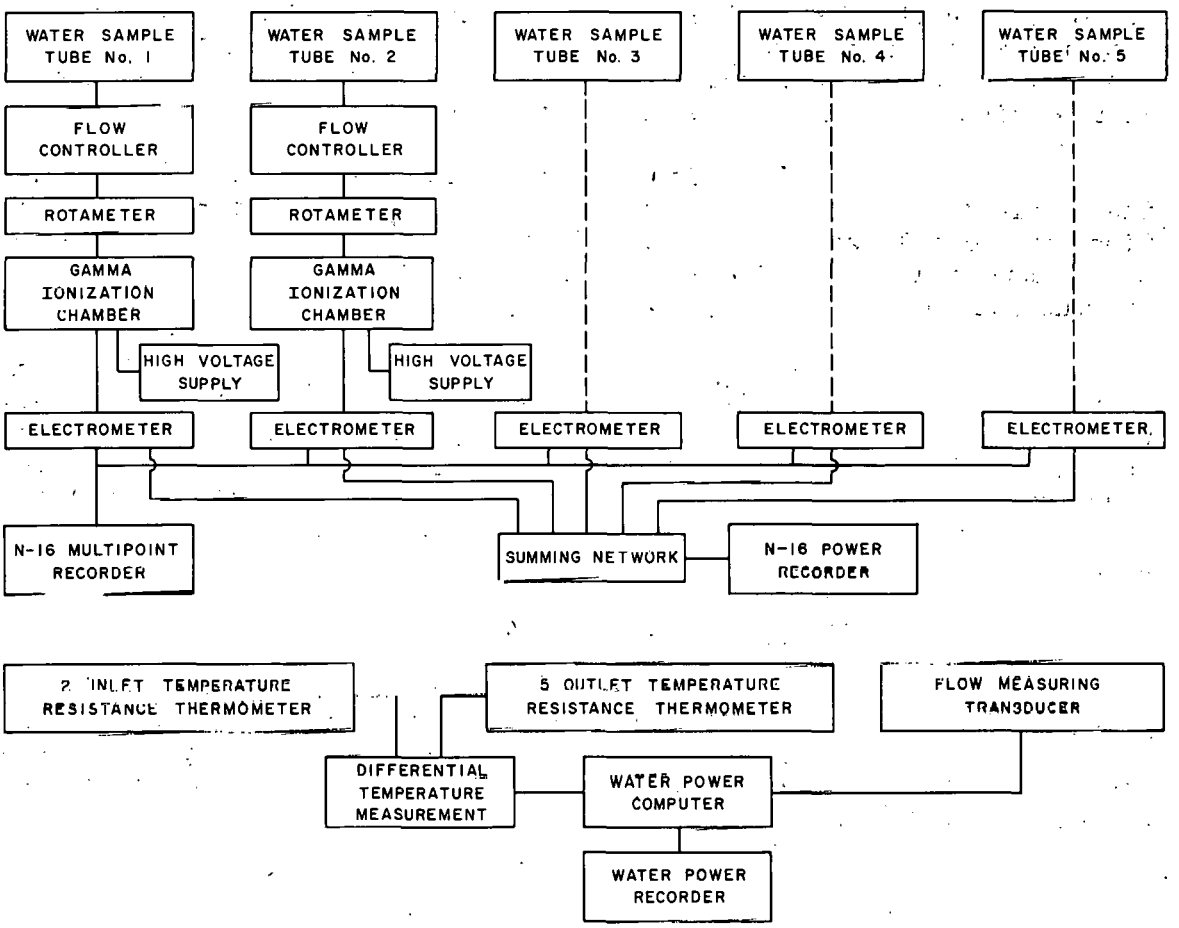

FIG. 4.4B
POWER LEVEL INSTRUMENTATION

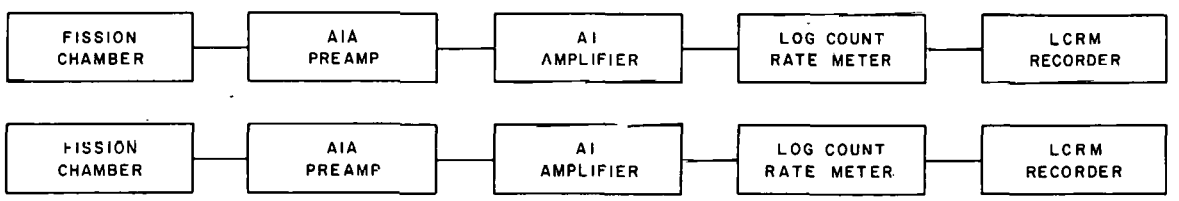

P.P.CO.-C-2720

FIG. 4.4C
STARTUP INSTRUMENTATION

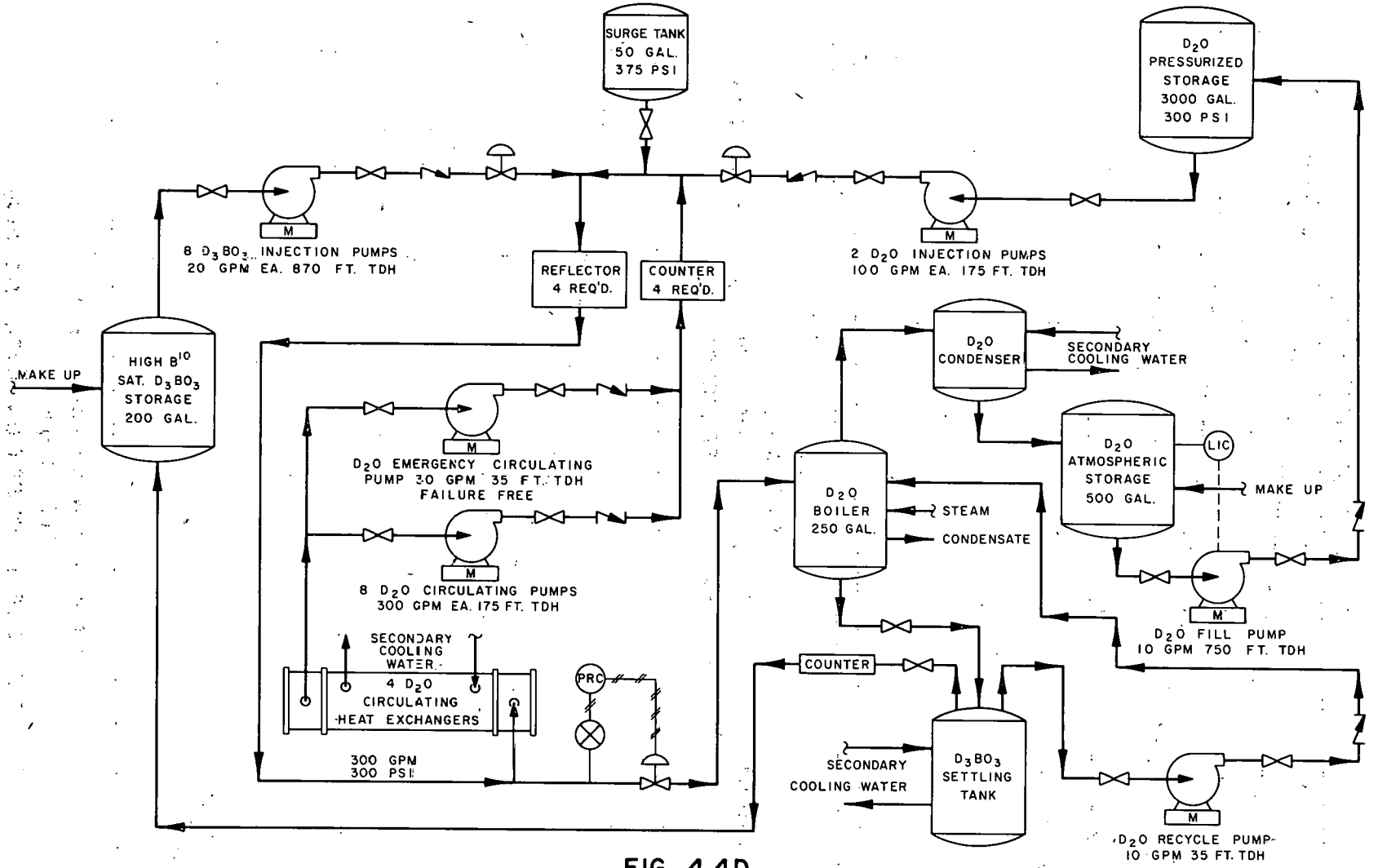

FIG. 4.4D
TYPICAL BORATED D_2O REFLECTOR SYSTEM
FLOW DIAGRAM

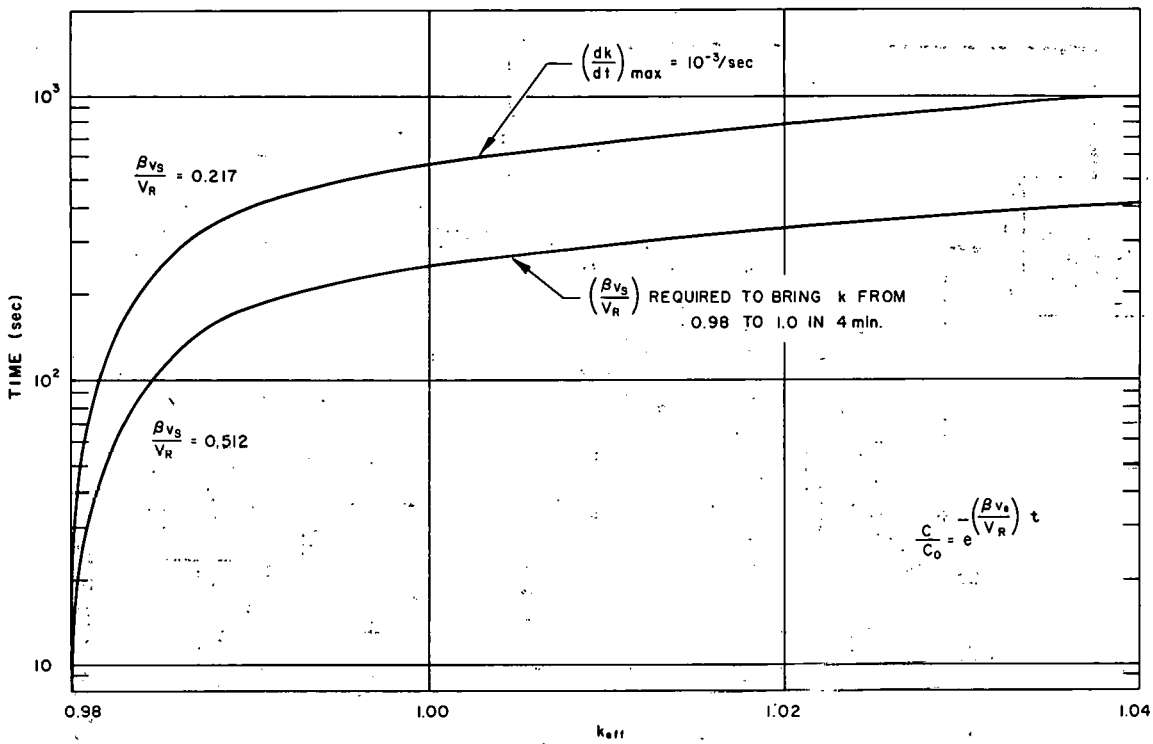

FIG. 4.4E

TYPICAL CURVE OF k_{eff} vs. TIME FOR D_2O DILUTION OF BORATED REFLECTOR

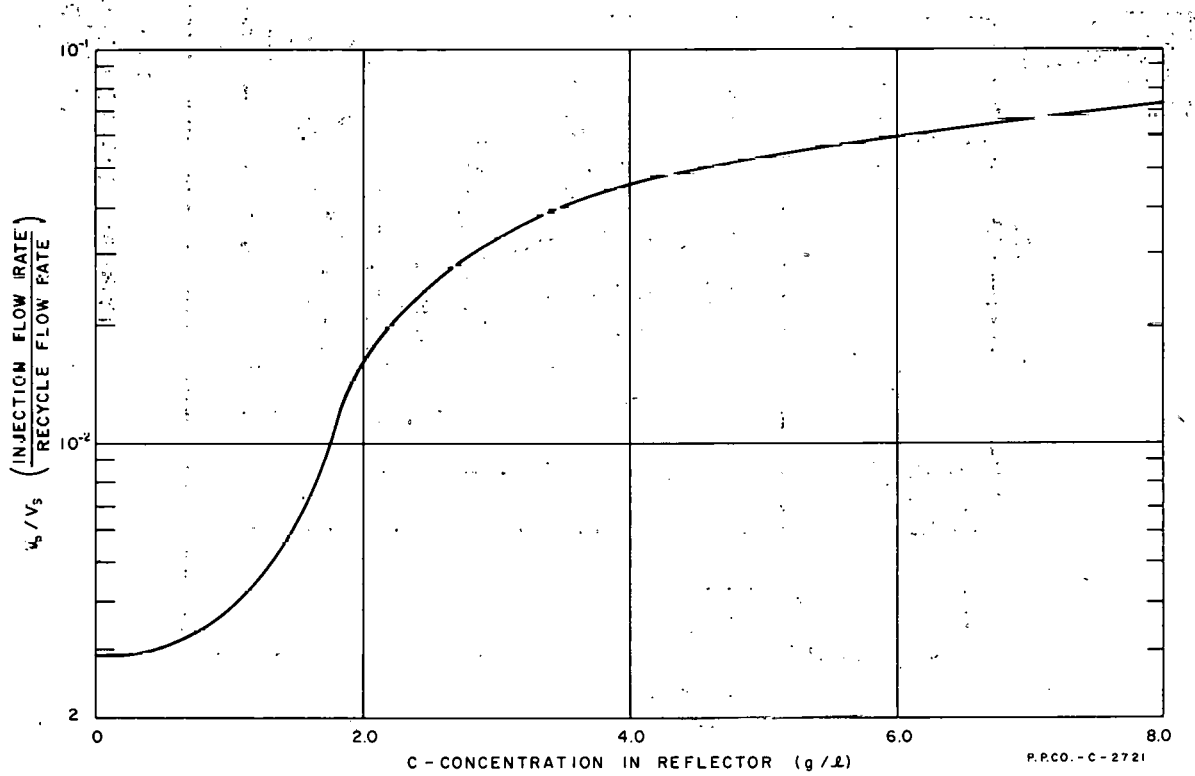

FIG. 4.4F

TYPICAL BORON INJECTION RATE YIELDING $dk/dt = 10^{-3}$ δ k/k-sec AT A GIVEN SYSTEM CONCENTRATION

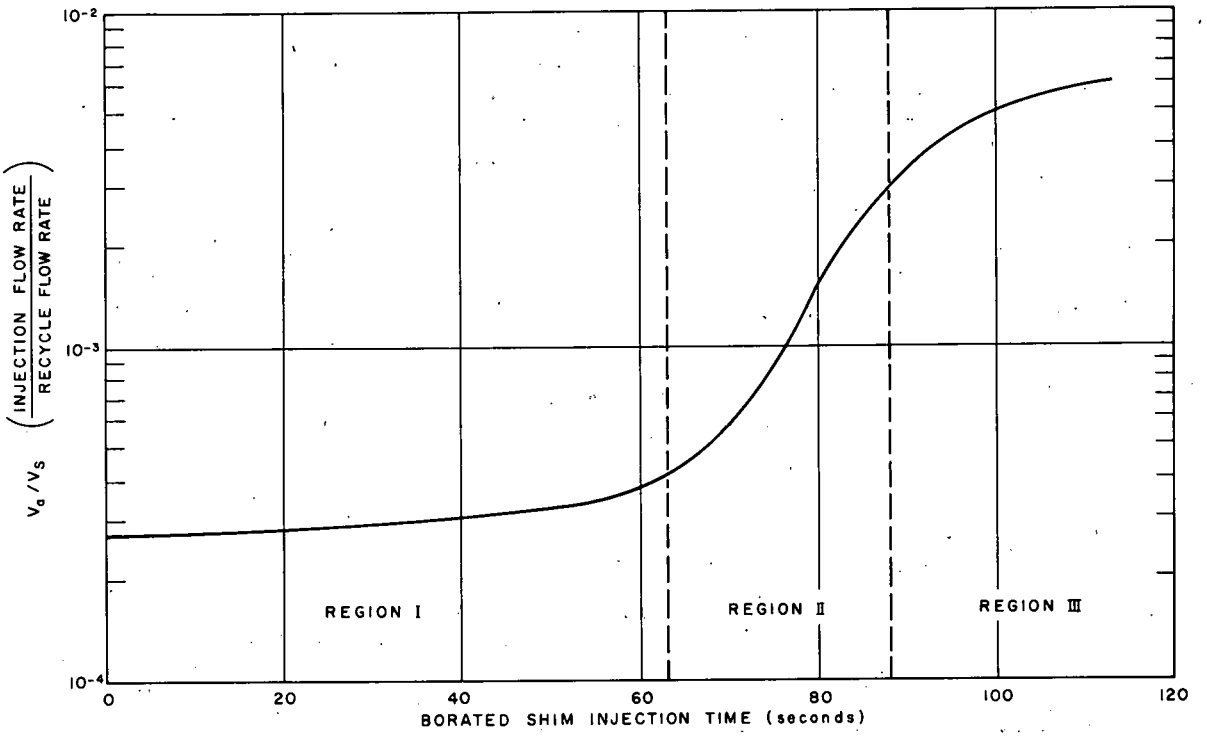

FIG. 4.4 G

TYPICAL RATE OF CHANGE OF INJECTION RATE REQUIRED TO MAINTAIN $10^{-3}\delta$ k/k - sec.

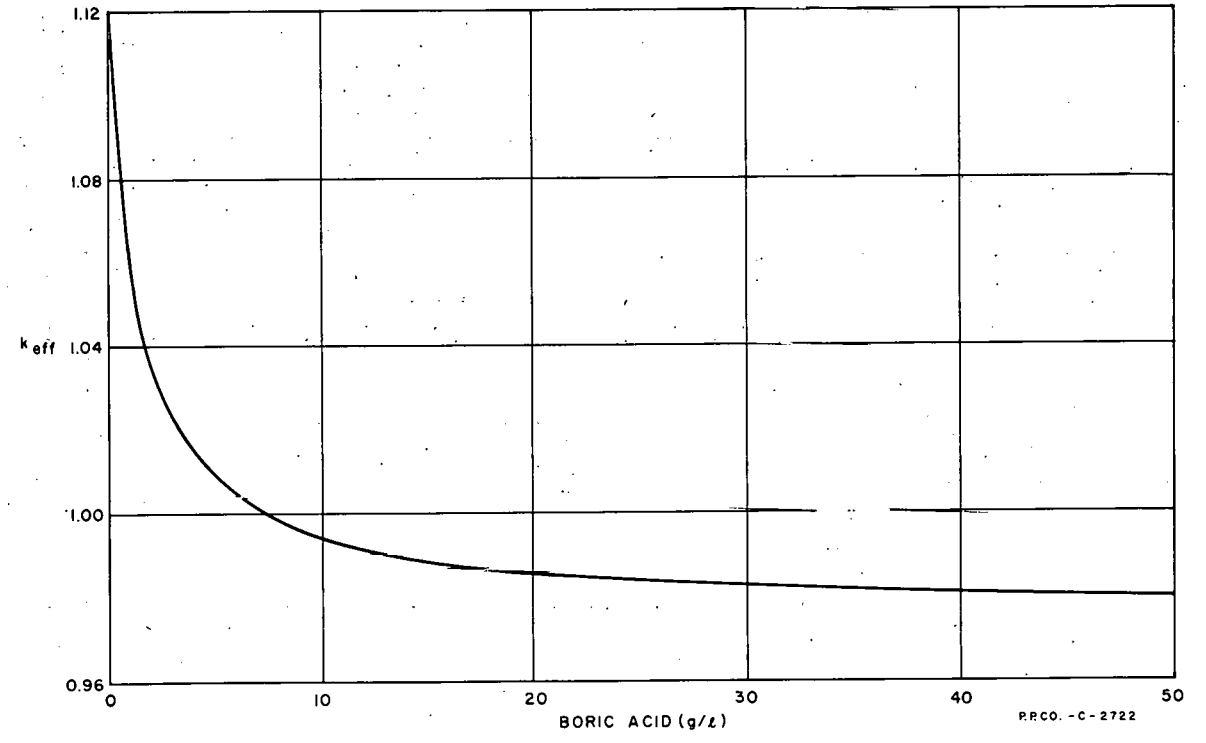

FIG. 4.4 H

TYPICAL k_{eff} v.s. CONCENTRATION FOR BORATED REFLECTOR SYSTEM

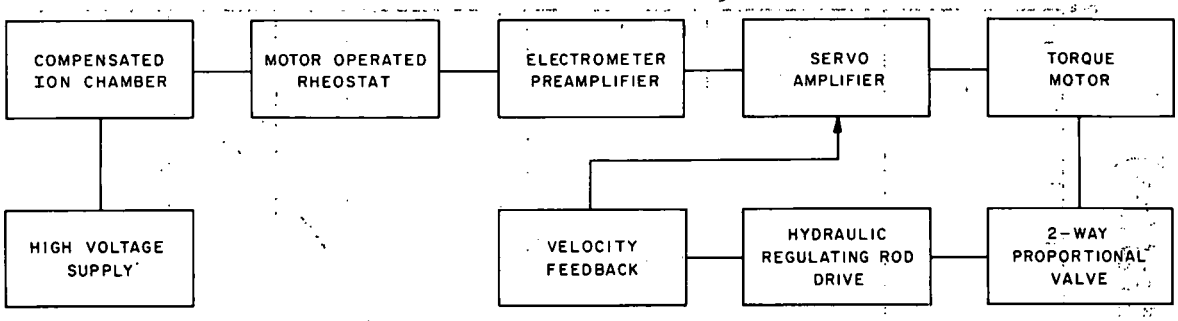

FIG. 4.4I
POWER REGULATING SYSTEM

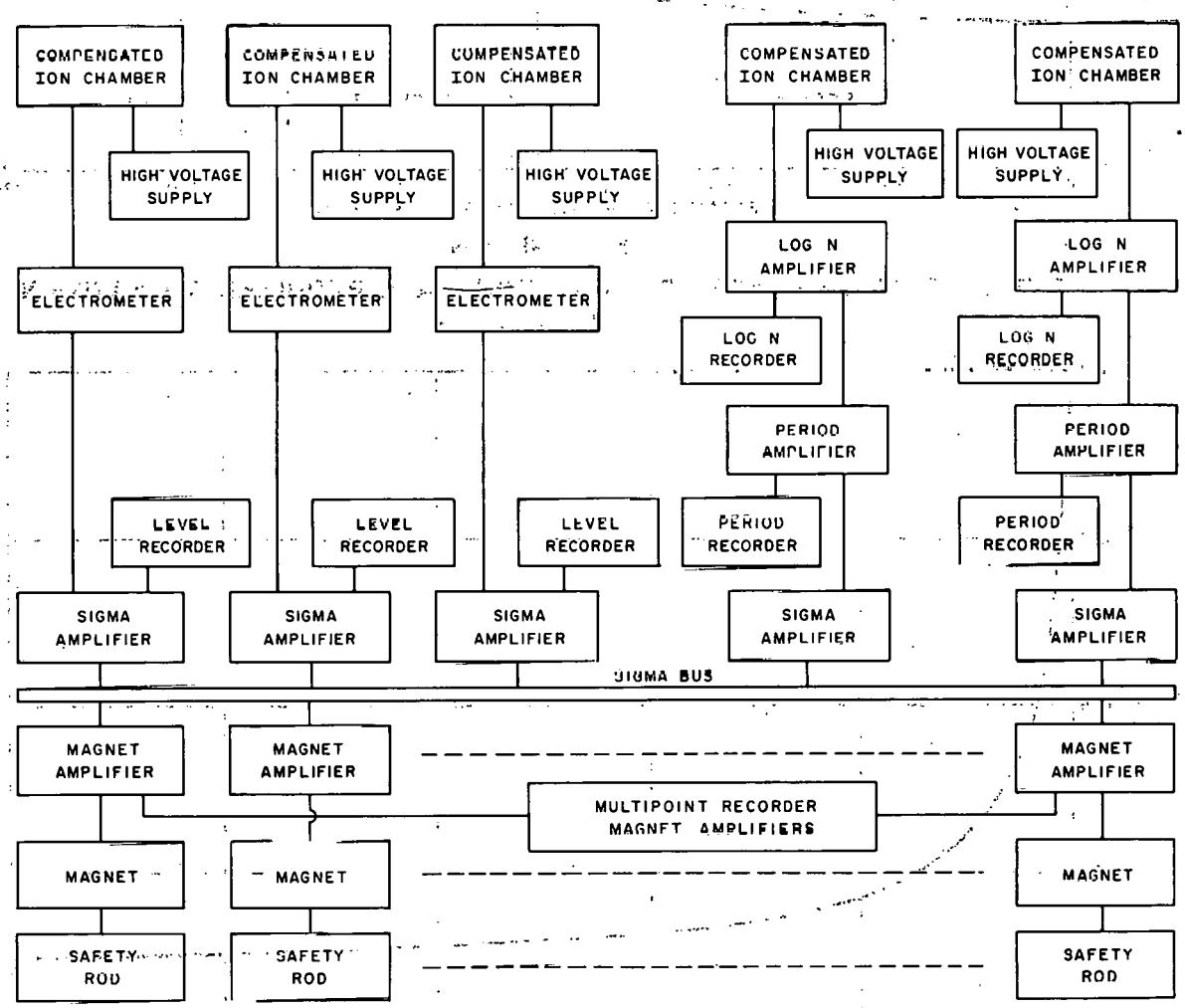

PP CO-C-2723

FIG. 4.4J
REACTOR SAFETY INSTRUMENTATION

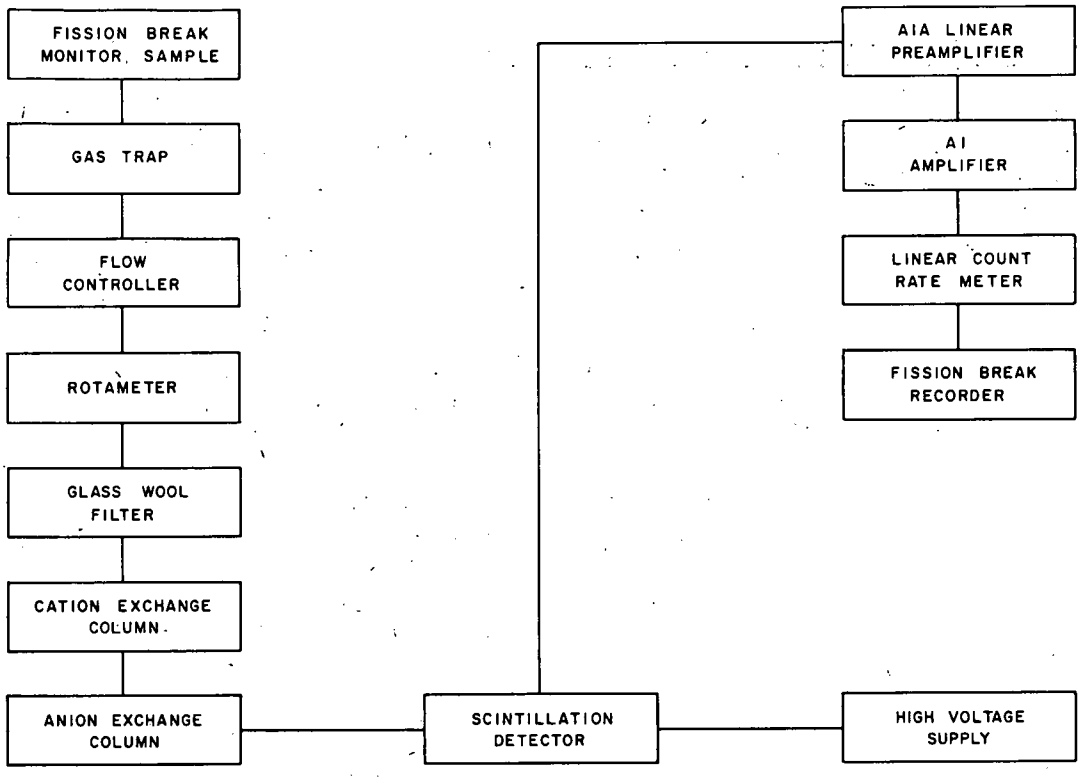

FIG. 4.4K
FISSION BREAK INSTRUMENTATION

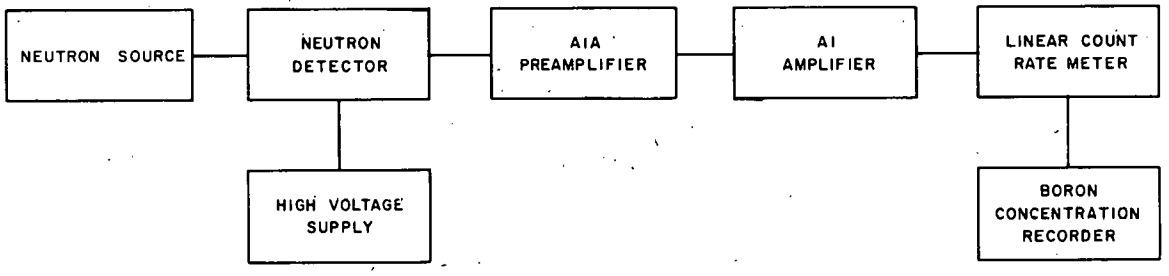

FIG. 4.4L
BORON CONCENTRATION INSTRUMENTATION

P.P. CO.-C-2724

4.5 Reactor Cooling and Heat Dissipation

Moderately pressurized light water flowing at relatively high rates is used to remove the heat generated in the fuel elements and associated hardware in the reactor. Heat is eventually rejected to the atmosphere through forced-draft cooling towers. Shell-and-tube heat exchangers are used to transfer heat from primary to secondary cooling water.

4.51 Reactor Cooling

The operating conditions of the reactor primary coolant system were established by means of a modified hot spot - hot channel analysis together with three other criteria:

1. The maximum pressure differential across any fuel plate at operating conditions is equal to or less than 5 psi.

2. The maximum allowable wall temperature, using the hot spot - hot channel analysis, is the saturation temperature at the hot-spot pressure plus 20°F.

3. The maximum steady state wall temperature with Type X8001 aluminum-alloy cladding is not to exceed 500°F.

The lateral pressure differential across any fuel plate must be limited to insure operability of the fuel element under dynamic conditions. Static pressure testing of several MTR and ETR fuel elements which had fuel plates attached to the side plates by different methods has shown, in general, that about 10 psi is required to obtain a 0.010 in. deformation in the fuel plates. It has also been shown that developing lateral differential pressures of this order under dynamic conditions causes closure of some of the coolant channels between fuel plates. A lateral pressure differential of 5 psi was selected as the maximum permissible since the high fuel plate temperature substantially decreases the yield strength of the aluminum alloy, and operation of the ETR with pressure of about this magnitude has not resulted in failure of the fuel elements.

In both the MTR and ETR the maximum calculated wall temperature is allowed to exceed the saturation temperature at the hot spot by about 20°F. This is obtained through essentially the same modified hot spot - hot channel analysis. Section 8.7 of this report explains this analysis in detail. The hot spot - hot channel and power distribution factors that were used for the reactor are summarized in Table 4.5A.

The factors cited are based on operating data, fuel element inspections, and chemical analysis of the MTR and ETR fuel elements. Therefore, they are considered realistic.

TABLE 4.5A

FACTORS USED IN HEAT TRANSFER CALCULATIONS

Hot Channel Factors	
Fuel Content Per Plate Variation	1.02
Reactor Power Measurement Variation	1.05
Hydraulic Diameter Variation	1.05
Channel Cross Sectional Area Variation	1.10
Velocity Distribution	1.10
Product	1.36
Hot Spot Factors*	
Variation of Fuel Core Alloy Area	1.08
Fuel Content Per Plate Variation	1.02
Variation of Fuel Core Alloy Thickness	1.10
Reactor Power Measurement Variation	1.05
Correlation on Heat Transfer Coefficient	1.25
Velocity Distribution	1.09
Product	1.74
Power Distribution Factors	
Horizontal Power Distribution Max/Avg	1.56
Vertical Power Distribution Max/Avg	1.40
Fraction of Reactor Power Generated in Fuel Plates	0.90
Additive Inlet Water Temperature Variation	$3^{\circ}F$

* Hot Spot is assumed to be 11 in. below core center line.

Exceeding the saturation temperature at the hot spot pressure does not appear to present undue hazard for the following reasons. Release of fission products into either the MTR or ETR primary coolant systems has never been related to overheating of a fuel plate. It is a known fact that the saturation temperature must be exceeded by some margin before nucleate boiling commences. The probability of all the factors cited in Table 4.5A occurring simultaneously is low.

No factors are included in Table 4.5A for uncertainties in the power distribution and maximum power density even though large uncertainties may exist in the physics calculations upon which these values are based. Since final optimization of the core design and fuel loading program is expected to result in lower core power and lower maximum power density than specified, the inclusion of an additional uncertainty factor and the resulting limitation imposed on the fuel element are unjustified at this time. If final optimization fails to decrease the maximum power density below the design level of 2.1 Mw/liter, then a satisfactory coolant velocity may be determined from Fig. 8.7A for the final maximum power density (including a reasonable uncertainty factor). The specified operating velocity of 44 ft/sec allows for all known uncertainties in the maximum power density. The recommended operating conditions for the reactor core are presented in Table 4.5B.

4.52 Primary Coolant System

4.521 General Description (Fig. 4.5A)

Operating conditions of the primary coolant system are summarized in Table 4.5B. The system provides reactor cooling at a total flow of 30,000 gpm and a reactor inlet pressure of 300 psig. The four primary coolant pumps (7500 gpm, 280 ft TDH, 700 hp) discharge water via the 36 in. reactor inlet header into the upper section of the reactor vessel. Water passes down through the core out of four 16 in. outlet pipes which connect to the main 36 in. return header. Because it will probably be desirable to operate the four-lobes of the reactor at different power levels to accommodate specific experimental requirements, the coolant flow through and from the reactor is divided into four parts to permit measurements of the operating power of each quadrant of this reactor. Separate flow and temperature measuring instrumentation is provided on each of the four outlets. The water from the four 16 in. outlet pipes flows into a common 36 in. return header, through four banks of two primary heat exchangers, and then returns to the suction side of the primary pumps.

Two emergency pumps (2000 gpm, 15 ft TDH, 20 hp), one of which is a spare, are connected in parallel with the main primary pumps to provide shutdown cooling. One pump is connected to the diesel power system to provide cooling in the event of commercial power failure.

The four primary pumps are centrifugal, controlled leakage pumps, each connected to a pair of heat exchangers. Heat exchanger characteristics are listed in Table 4.5B. Shell and tube heat

TABLE 4.5B

PRIMARY COOLANT OPERATING CONDITIONS

Reactor Power	250 Mw
Reactor Maximum Power Density	2.1 Mw/liter
Reactor Inlet Temperature	130°F
Reactor Exit Temperature	187°F
Maximum Fuel Surface Temperature	420°F
Reactor Inlet Pressure	300 psig
Core Pressure Drop	92 psi
Average Coolant Velocity in Core	44 ft/sec
Core Flow Rate	26,000 gpm
Total Reactor Flow Rate	30,000 gpm
Number of Primary Coolant Pumps	4
Pump Horsepower	700 each
Number of Heat Exchangers	8
Total Heat Exchange Area	4.7×10^4 ft^2

TABLE 4.5C

HEAT EXCHANGER SPECIFICATIONS

Heat Transfer Area	5,870 ft^2
Tube Side Fluid	Primary Coolant
Shell Side Fluid	Secondary Coolant
Tube Length	21 ft
Tube Outside Diameter	5/8 in.
Tube Wall Thickness	16 BWG
Tube Configuration	Triangular
Tube Pitch	1-1/8 in.
Tube Side Pressure Drop	10 psi
Tube Material of Construction	304 stainless steel
Overall Shell Length	27 ft
Shell Outside Diameter	42 in.
Shell Thickness	1/4 in.
Baffle Type	Segmental
Baffle Spacing	72 in.
Shell Side Pressure Drop	5 psi
Shell Material of Construction	Mild Steel

exchangers with a floating tube sheet are indicated since the temperature differences involved are probably greater than can be sustained by fixed tube sheet construction. This choice probably increases the preventive maintenance necessary to insure that the tube sheets do not permit primary coolant to leak into the secondary coolant. However, preventive maintenance is much more easily accomplished in comparison to the repair of a cracked tube within a fixed tube sheet. The over-all heat transfer coefficient of these exchangers under operating conditions has been set at 400 Btu/hr, ft^2, ^oF; heat transfer rates of this magnitude have been obtained consistently during ETR operation and the coefficient has not shown a decrease as a function of operating time. The specifications for the heat exchangers in ETR II are given in Table 4.5C.

The required coolant flow is controlled by the main butterfly valve, the position of which is set prior to startup. Since only steady flow conditions are required, only minor adjustments of this valve should be required during operation. Primary coolant flow is measured by a Gentile Tube in the reactor inlet line.

A 1000 gal capacity surge tank is connected to the main coolant piping on the pump discharge to dampen pressure transients which could result due to rapid coolant temperature fluctuations, when the reactor is scrammed.

The system is pressurized by means of two pressurizing and degassing pumps (300 gpm, 500 ft TDH, 50 hp), one of which is a spare. The pumps take suction from a 5000 gal capacity degassing tank and discharge coolant into the main system near the suction side of the main coolant pumps. The flow from the two degassing and pressurizing pumps is measured by means of an orifice which, via a flow recorder-controller, positions a flow control valve to maintain a constant flow from the degassing system into the main coolant loop. Primary water is bled from the main loop system via a pressure control valve positioned by means of a pressure recorder-controller which senses the reactor coolant inlet pressure. The volume of coolant flowing through the back pressure control valve to the degassing tank is equal to the volume of liquid being pumped continuously into the main system by the pressurizing pump, so that a constant primary coolant pressure is maintained. The degasifier tank, normally 1/2 full, is equipped with level controls, an overflow, and an air purge to maintain a low concentration of decomposition and fission gases above the water.

Two gland seal and pressurizing pumps (50 gpm, 600 ft TDH, 10 hp) provide demineralized water for the rod seals, experiment tube seals, primary pump glands and the HDW system. Only one pump is used normally with the other pump serving as a spare.

4.522 Primary Cooling Water Chemistry (Fig. 4.5B)

The presence of aluminum, beryllium and stainless steel in the reactor requires that the pH and electrical resistivity of the

light water coolant be rigidly controlled. Due to the possibility of a fuel element rupture, provisions must also be made for removing fisssion products from the coolant.

The purity of the water is controlled by the primary by-pass demineralizer which maintains the pH of the coolant between 5.5 and 6.5, and the specific resistivity at more than 250,000 ohms, in addition to removing fission products. Water is taken from the primary supply header, passed through the demineralizer system and then back into the primary discharge header at a rate of 150 gpm. The system consists of two cation and two anion beds valved so that the water passes through either or both of the cation beds, and then through either or both anion beds. Any one or all of the beds can be by-passed. The system is designed so that in the event of a fission break the primary coolant can be passed through the demineralizer system to the retention basin.

Past experience on similar systems at the ETR and MTR has shown that the cation bed becomes too radioactive to allow resin regeneration. Therefore, the cation beds are designed so that the bed may be changed but not regenerated. Past experience with the ETR demineralizer indicates that it is permissible to regenerate the anion beds. Therefore, the anion beds are designed so that the resin can be regenerated or changed.

A degasifier is provided to remove gaseous oxygen, hydrogen, and oxides of nitrogen from the coolant primary system. Two 1000 gpm demineralized water flush pumps are provided to purge the primary cooling water system after shutdown with demineralized water from a 100,000 gal storage tank.

4.53 Secondary Cooling System (Fig. 4.5C)

Heat generated in the reactor core, experiments, D_2O reflector system, and the borated D_2O control system is transported by the secondary coolant system from heat exchangers to the cooling towers where most of the heat is released by evaporation to the atmosphere. The total secondary coolant flow is 42,000 gpm, including 6000 gpm of utility cooling water. The secondary coolant on-tower and off-tower temperatures are 140°F and 85°F, respectively. Four vertical turbine pumps (9000 gpm, 125 ft TDH, 350 hp) circulate the secondary water to the shell side of the primary heat exchangers, D_2O heat exchangers, and the borated D_2O heat exchangers with flow regulated by temperature controlled butterfly valves. The total secondary flow, and the inlet and outlet temperatures to each of the system heat exchangers, are measured and recorded.

4.531 Cooling Tower

A forced draft cooling tower consisting of eight cells is provided for final heat dissipation to the atmosphere. Each cell is 36 ft long, 36 ft wide and 46 ft high. Each cell contains a reversible fan driven by a 75 hp motor; fans are reversible to permit de-icing

operations during severe winter weather. The tower was selected on the basis of the following parameters:

42,000 gpm Maximum Flow

10^9 Btu/hr

65°F Maximum Wet Bulb

85°F Off-tower Temperature

140°F On-tower Temperature

20°F Approach

4.532 Secondary Cooling Water Treatment

Chemical treatment of the raw water fed to the cooling tower is necessary for four reasons: to inhibit scale formation, to minimize corrosion, to discourage algae formation, and to minimize the degeneration of the cooling tower redwood. Three chemicals are injected: 66° Baume sulfuric acid, gaseous chlorine, and Orocol (a mixture of polyphosphate and dichromate). The injection rates are given in Section 4.814, "Cooling Tower Make-up Water."

4.54 Pure D_2O Reflector System (Fig. 4.5D)

The unborated D_2O reflector material is circulated through a tube-and-shell exchanger (cooled by secondary water) to remove the heat generated therein. The D_2O enters the upper reflector area and exits from the lower area via 6 in. stainless steel supply and return lines. Circulation is accomplished by sealed stainless steel pumps.

The coolant system is provided with by-pass facilities for deuterated-resin ion exchange columns, filtering, distilling, and pH adjustment. A positive helium atmosphere is maintained above the D_2O in the reactor reflector tank and the storage and surge tanks. The auxiliary helium system is required to prevent contamination by the moisture (light water) contained in the atmosphere. Also included in the helium system are facilities to recombine D_2O which has been dissociated in the reactor reflector.

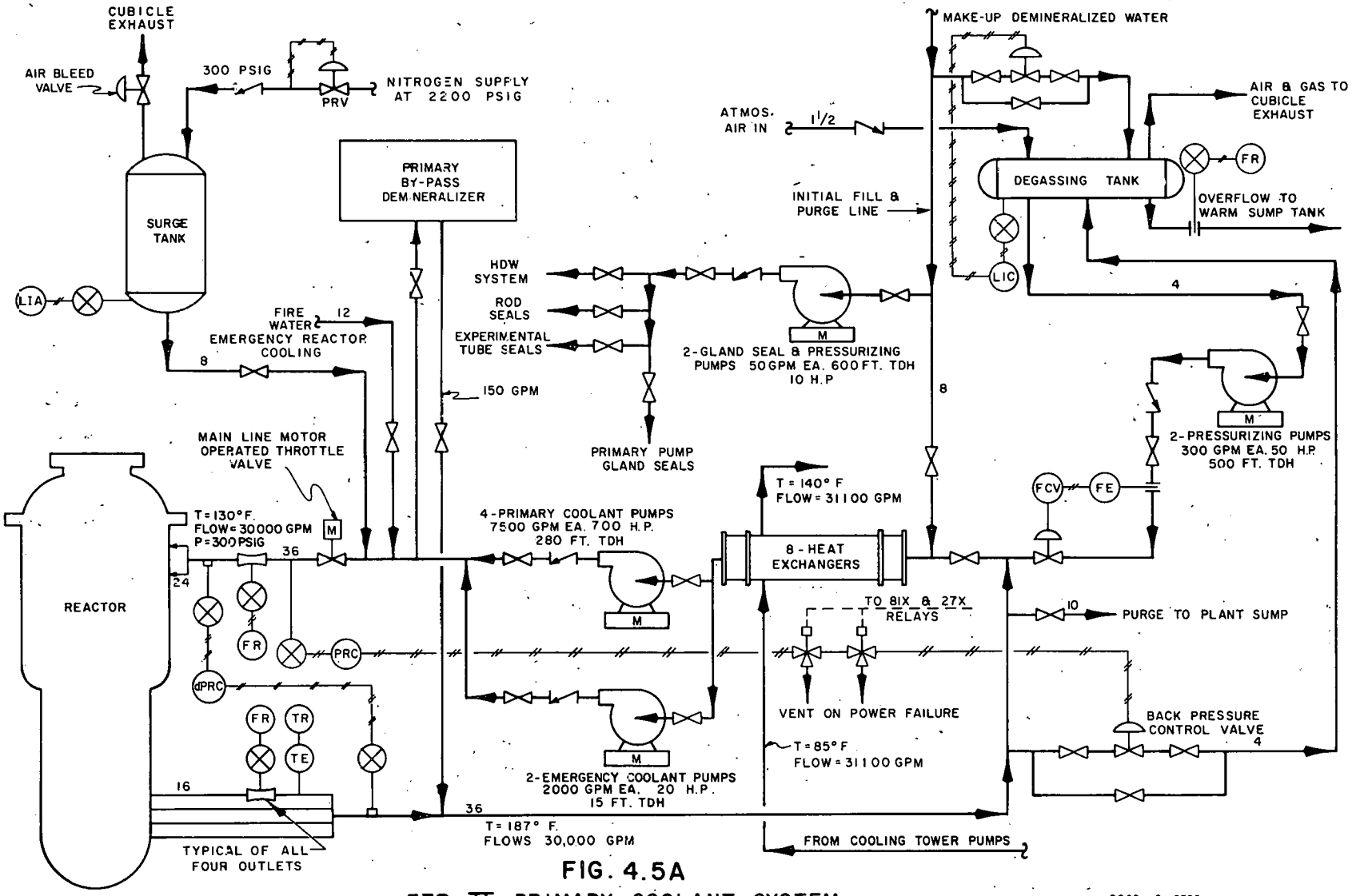

FIG. 4.5A

ETR II PRIMARY COOLANT SYSTEM FLOW DIAGRAM

P.P.CO. - C - 2725

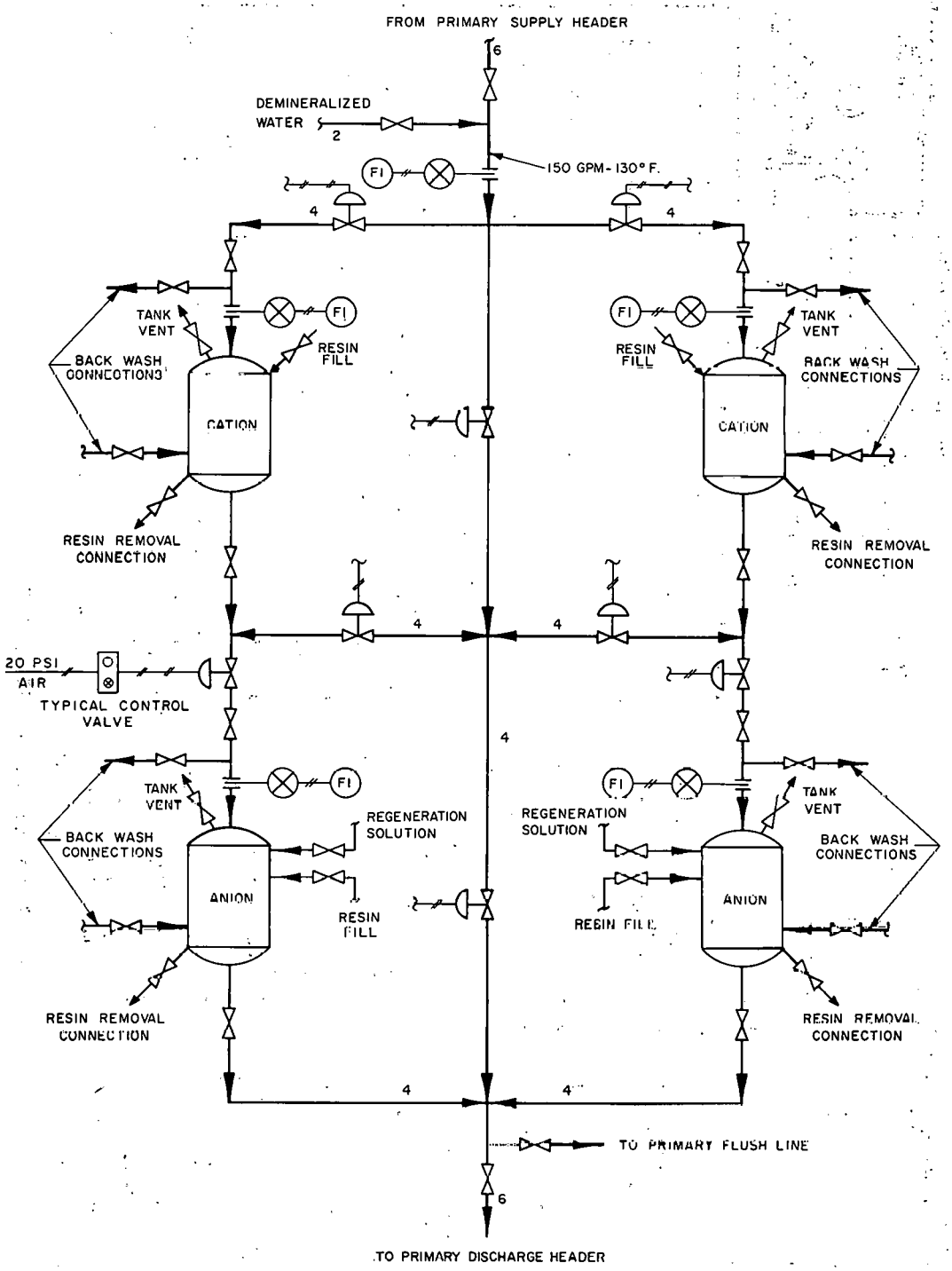

P.P.CO.-C-2726

FIG. 4.5 B

PRIMARY BY-PASS DEMINERALIZER

FLOW DIAGRAM

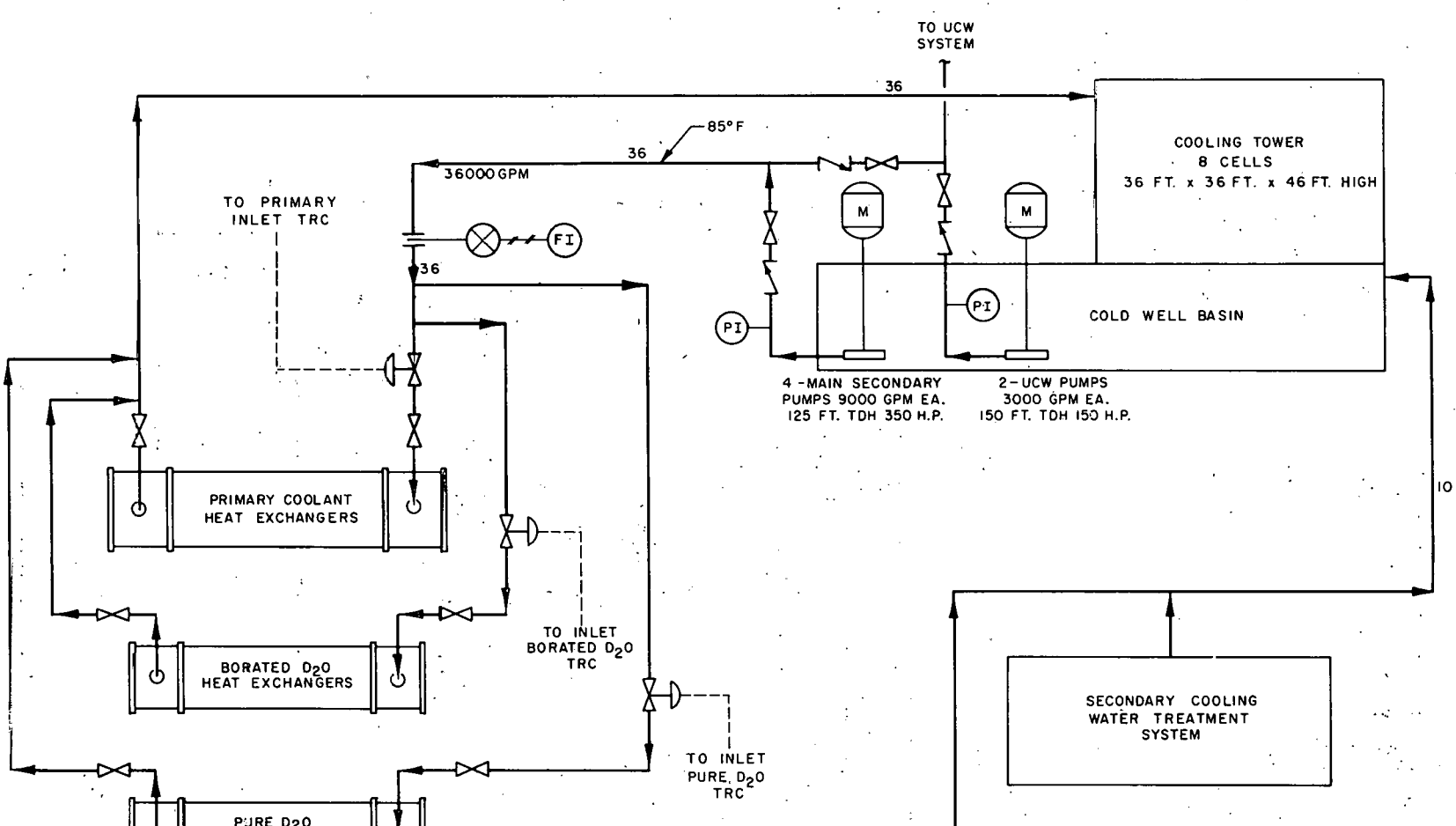

FIG. 4.5C

SECONDARY COOLANT SYSTEM

FLOW DIAGRAM

P.P.CO.-C-2727

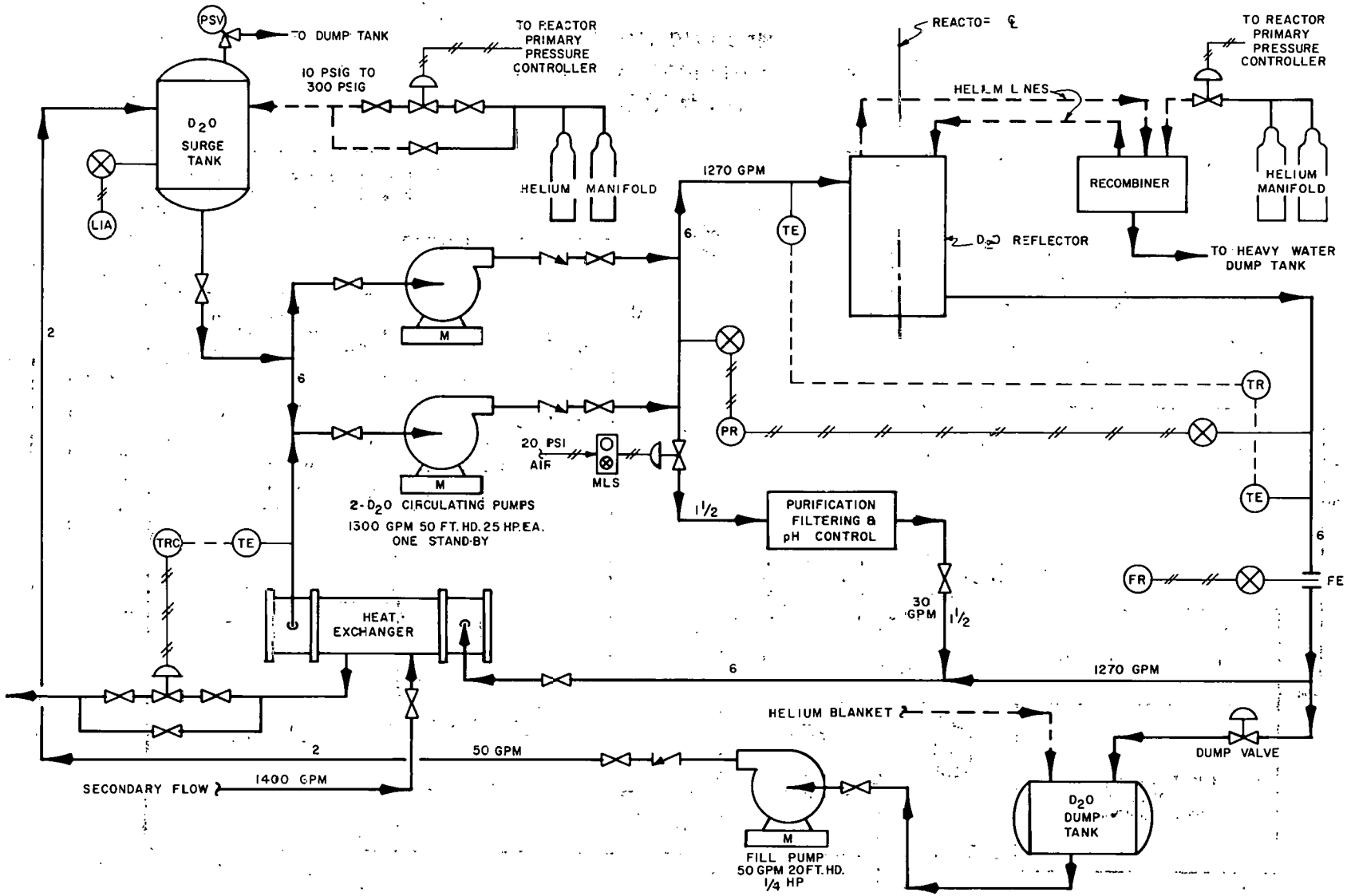

FIG. 4.5D
PURE D_2O REFLECTOR SYSTEM
FLOW DIAGRAM

4.6 Critical Facilities

4.61 Introduction

The performance of the ETR I Critical Facility (ETRC) has aptly demonstrated that an exact nuclear mockup (referred to as a critical facility in this report) is an important adjunct to a high flux test reactor. Since its initial criticality date, May, 1957, the ETRC has been used constantly to support the ETR program.

Parameters which can be determined in a low power reactor to support the operation of a test reactor are: 1) neutron flux distributions, 2) gamma heat generation rates, 3) excess reactivities, and thus charge lifetimes, 4) shutdown reactivities, 5) rod, or control region, calibration, 6) consequences of experiment failures, 7) fuel loading requirements, reactivity and neutron flux, and 8) effects of the insertion or removal of experiments. Many of these measurements are essential to the operation of the reactor and if not made in a critical facility would have to be made in the power reactor itself. Others serve to aid in the design of the experiments and if not available would result in something short of an optimum design.

One of the most difficult reactor parameters to calculate accurately is the critical mass and operational fuel loading. If a critical facility were built far enough in advance of the test reactor, the first core of fuel elements or prototype elements built could be used to determine any required adjustment in the fuel content of the elements. Another possibility considered for the proposed reactor is graduated fuel density within the element. The required non-uniform distribution would be determined from measurements in this preliminary loading. This could be accomplished by having a few special elements with removable plates so that plates with a variety of fuel densities could then be inserted.

At the same time the above determinations were being made, data would be obtained for designing the experiments. These data would be obtained by making neutron and gamma flux measurements in prototypes of the experiments.

Because no reactors have used the type reflector control proposed, probably less is known about this one factor than any other feature of this reactor. From measurements in a critical facility, it will be possible to determine the boron concentrations required to control the excess reactivity and the changes in the flux distributions due to the poisoned reflector.

4.62 Description

The total ground floor space which is recommended for this facility is 3000 sq ft in a room 50 ft x 60 ft. This includes space for a 10 ft x 24 ft x 20 ft deep canal for the facility, floor space

for experiment mockup assembly and storage, reactor console, and office space for the staff. This room should be located in the main reactor building and the canal should be connected to the transfer canal so that radioactive fuel and samples can be transferred from the reactor.

The reactor core should be an exact nuclear mockup of the core proposed. The structural requirements can be relaxed, of course, since the core will not have to withstand the hydraulic pressures created by coolant flow. Since the pressure vessel is close to the core, the nuclear equivalent of these must also be included. It is necessary that it extend only a few inches above and below the core, however.

The mechanical design of the ETR I Critical Facility has been found to be quite adequate. Therefore, it is proposed that this facility be built similarly. Since a quite complete description appears in the Hazards Report[1], only a brief description will be included here.

The grid plate which supports the core, reflectors, and neutron detector tubes rests on the bottom of the canal. A control bridge which contains all rod drives sits on the canal parapet. The control wiring is fed through quick disconnect plugs so that the control bridge can be removed to gain access to the core. The bridge is removed and placed in dry dock with an overhead crane. Although this has been quite satisfactory in the ETRC, an alternate method, which eliminates the use of the crane for this purpose, would be to mount the control bridge on wheels and tracks, and roll the bridge from above the core. The bridge would have to be moved toward the end of the canal so that the fuel could be moved freely from the transfer canal to the core. This would require a slightly longer canal but the additional length would have to be only deep enough to receive the control rod drives. Provisions would also have to be made for servicing the control rod lifting magnets.

A working bridge which permits working directly over the core is mounted on wheels and rests on the parapet.

The control and safety instrumentation of the ETRC is also offered as an example of a suitable system. The ETRC system has proved to be very reliable and easy to maintain. It is composed principally of commercial instruments, many of which are also used in the MTR and ETR. This is especially desirable because repair is easier since the instrument repairmen are familiar with the instruments and since additional spare parts are not required. Since the shim control for the proposed reactor is principally reflector control, pumps will have to substituted for rod drives. This should not change the mode of operation, however.

---

1. D. R. deBoisblanc, "The Engineering Test Reactor Critical Facility Hazards Summary Report", IDO-16332, March 27, 1957.

The reflector control system should have the same range of reactivity control as does its parent reactor. Its rate of change would not have to be as fast, however, since xenon override is not necessary. To avoid unnecessary waste of experimental time, the response should not be unduly slow, however.

It is proposed that the D_2O flow system be similar to that in the parent reactor except that no heat exchangers will be required. The recirculating pump would serve only as a mixer and would operate whenever the reactor is operating.

Using the plant D_2O cleanup system looks attractive from an economical viewpoint and appears to be feasible but has one disadvantage. If the critical facility goes into operation long before the power reactor, the plant D_2O cleanup system may not be completed soon enough. Therefore, since a cleanup system of the capacity required for the critical facility is a small fraction of the cost of the entire facility, a separate system may be advisable. It is estimated that a system with a capacity of 100 gal per day will be adequate to serve this facility. This is based on the assumption that the system contains dump and holdup tanks so that it will not be necessary to remove the boron from the D_2O each time an excess reactivity or some other large reactivity measurement is made. Boron would have to be removed only when it becomes necessary to purify the D_2O.

4.7 Site, Buildings, and Facilities

4.71 Site Plan

The proposed plot plan for the ETR II site is shown on Fig. 4.7A - Site Plan. No specific geographical location for the site has been selected, but the facility has been designed to be self-contained. The more important assumptions made in the layout of the proposed area are:

1. reactor containment shell will not be necessary,
2. prevailing wind direction will be as shown on the plot,
3. an adequate supply of ground water will be available, and
4. liquid and gaseous wastes may be returned to the environment under controlled conditions through a leaching bed and stack.

Buildings and facilities within the area have been oriented so as to provide minimum exposure potential for personnel in the event of an activity release. Cold, or non-radioactive areas, such as the administration building and cafeteria are separated and up wind from the reactor building, stack, and liquid waste leaching pond; as are maintenance and warehousing areas.

The site has been spread out to permit convenient access to each individual area, and to allow reasonable future additions.

4.72 Reactor Building and Canal Area

4.721 Reactor Building Area

Design philosophy leading to the layouts shown on Figures 4.2A, 4.2B, 4.2C, 4.2D, and 4.2E have been discussed in Section 4.2 - Reactor Building Complex. Some of the more important details pertaining to this area are discussed in material following.

The building section housing the reactor, canal, and operating office areas has been kept clean and unencumbered. Means are also provided for isolating any individual area from other areas when required.

The reactor building proper is of insulated panel construction with an overall main floor area of some 34,000 sq ft. Of this area approximately 10,000 sq ft are devoted to the reactor proper, with another 9,000 sq ft occupied by the main canal and its access and operating areas. The reactor is serviced by its own overhead crane; a second crane covers the main canal area. The remainder of the building is occupied by a critical facility, an experimenters' canal and work area, a mockup area, and an office and control room area.

Office areas within the reactor building are intended for shift reactor operating supervisory personnel. A wing building, connected to the reactor building, provides additional office and service space for functions essential to operation of the reactor. Health Physics personnel and counting equipment are housed in this area. One warm chemical laboratory is located in the wing building so that essential water chemistry work may be performed as expeditiously as possible.

It is anticipated that extensive programs of flux determinations will be undertaken in the operation of the reactor. Therefore, a shielded counting room, to be designed to accommodate the most modern counting equipment, is situated in the wing building.

An instrument rack room for the control room is located directly below the control room on the first basement level. A separate instrument repair room is also located on this level for the repair and servicing of instruments from the reactor.

The remainder of the first basement level and the second basement level are devoted to heating and ventilating equipment, experiment cubicles, control panels, switch gear, etc., as described in Section 4.2. Numerous hatchways, stairwells, and elevators provide communication between the three floors for equipment and personnel.

4.722 Canal Area

The reactor is connected to the main canal by means of a lateral. In addition to the critical facility, an experimenters' canal and work area are connected to the main canal. The main canal will be some 18 ft in depth, 8 ft wide and 150 ft long. The experimenters' canal, located in a separate area, will be 18 ft deep, 10 ft wide and approximately 60 ft long. This canal, although connected to the main reactor canal, will be equipped with bulkheads to separate it when required. Similar bulkheads will be provided for the critical facility.

Working areas are provided on both sides of the main canal. A through truck aisle parallels the main canal. This aisle is serviced by the canal crane and permits convenient loading and shipping of experiment casks.

It is anticipated that the canals will be lined with stainless steel to minimize the leak potential and to keep canal water contamination at the lowest possible levels. Demineralized water at a pH of 6.5 will allow storage of fuel elements, experiments, etc., for long periods of time with little or no corrosive attack.

4.73 Process Water Area

The process water area is situated immediately adjacent to the reactor building, with an enclosed motor area separating the two buildings some 12 ft at grade level. The building proper is heavily shielded for

protection against a potential gross fission break into the reactor cooling water stream. The main coolant pumps are located at approximately grade elevation and are connected to drive motors by shaft extensions through the shield wall. A heat exchanger pit 24 ft wide by 60 ft long by 30 ft deep is provided. The pit is sized to accommodate ten vertical heat exchangers and necessary piping. An overhead crane serves the heat exchanger and pump areas and has a lift adequate to pull any exchanger from its pit to the grade level floor for maintenance work. Ion exchange resin beds are located in shielded lean-tos next to heat exchanger pits.

A control room for the reactor cooling system is provided adjacent to the process water building.

4.74 Utilities Building

A utilities building 180 ft long by 140 ft in width, of pumice block or equivalent construction, will house the steam plant, demineralized water production units, compressors, emergency and failure free power units, etc. All equipment will be located substantially at grade elevation and this consolidation and centralization of utilities is suggested to keep operating forces at the smallest number compatible with safe and competent operation.

4.75 Maintenance and Warehousing Building

A single building, divided by function into two areas, is located convenient to the reactor building. The building will be of pumice block or equivalent construction and contains approximately 20,000 sq ft, divided between maintenance and warehousing.

The maintenance portion of the building will be subdivided into machine, welding, pipe, electrical, etc., shop areas as required by the needs of the reactor site. A portion of the building will be high bay area equipped with crane service to handle heavy equipment. It is not planned to provide complete heavy machine tool facilities because it is expected that, regardless of the final location of the reactor site, such services will be available within reasonable distances.

Experience at both MTR and ETR has established conclusively the need for a building to receive, warehouse, and store incoming and idle materials, shipping casks, spare parts, etc. Such a building also will perform the normal warehouse and issue function for the miscellaneous stores and supplies which are a necessary part of any large installation.

Approximately 8,000 sq ft of the Maintenance and Warehousing Building, including access to high bay and crane area, is earmarked for the warehouse function.

It is suggested that construction of this building be scheduled for the earliest possible completion after the reactor project is approved.

4.76 Administration and Cafeteria Building

Since no specific location for the reactor site has been selected, it is necessary to provide space for the administrative, personnel, finance, etc. functions normally connected with an installation of the size projected in this proposal. A pumice block or equivalent administration building with a usable area of approximately 15,000 sq ft is included to meet this need. A portion of the building will be occupied by cafeteria facilities.

4.77 Laboratory and Engineering Building

A one- and two-story pumice block or equivalent building with approximately 20,000 sq ft of usable area is contemplated to house the laboratory, engineering, and technical department personnel necessary to service the reactor. Chemical laboratories, instrument development shops, engineering and metallurgical laboratories, and a computations center will be housed in the single-story area. The two-story portion of the building will comprise offices for engineering and technical group personnel, and will include a large conference room.

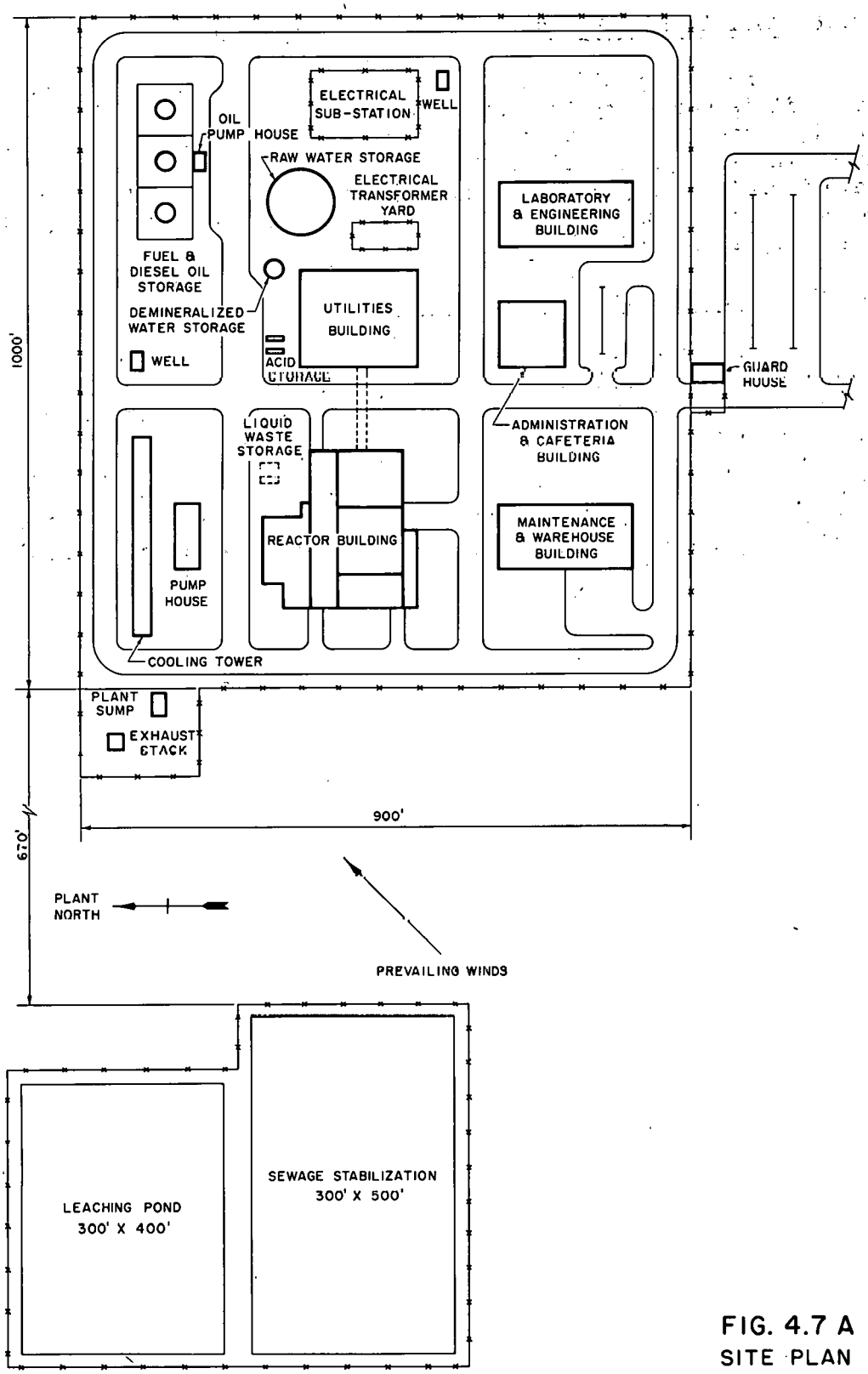

FIG. 4.7 A
SITE PLAN

PP Co -0-2788

4.8 Utilities

The ETR II utilities assume:

1. that sufficient reliable commercial electric power is available,

2. that suitable ground water exists at the site selected, and

3. that fuel oil, diesel oil, and water treating chemicals are transported to the site by truck.

4.81 Water (Ref. Fig. 4.8A)

4.811 Wells and Storage

It is assumed that the water at the site selected is available at 400 to 500 ft below grade and that the water has the following characteristics:

1. dissolved solids, 250 ppm,

2. total hardness as $CaCO_3$, 200 ppm, and

3. alkalinity as $CaCO_3$, 200 ppm.

In addition, it is assumed that the turbidity, silt, and sand of the well water are sufficiently low so that filters are not required.

Well water is pumped by means of two deep well turbine pumps (3000 gpm, 600 ft TDH, 600 hp). Either of the two deep well pumps has sufficient capacity to supply the maximum plant demand. The deep well pumps start and stop automatically by means of a level indicating controller on the ground level water storage tank.

The ground level storage tank has a capacity of 2,000,000 gal. The large capacity is required to satisfy the firewater requirements of the cooling tower, which is estimated to be 5000 gpm. Since no standby power source for any of the deep wells is provided, the ground level storage tank must have a firewater supply at all times of 1,200,000 gal which is sufficient for a four hour supply at maximum demand.

A bypass line is provided around the ground level storage tank so that the tank can be repaired and cleaned without interruption of the raw water supply.

4.812 Firewater

Two 5000 gpm fire pumps are provided to furnish water to the 12 in. firewater loop at 175 ft head. One of the pumps is electric driven (300 hp) and the other is diesel driven (450 hp) to provide firewater in case of commercial power failure. A crosstie from the service water

system to the firewater system maintains system pressure until a fire hydrant is opened. At this time, the system pressure will drop which will automatically start the electric driven fire pump. The diesel driven fire pump is interlocked with the electric driven fire pump, so that if the electric pump fails to start on a low system pressure signal, the diesel driven pump will automatically start.

The plant is looped with a 12 in. firewater main and fire hydrants are placed at strategic locations around the plant. Hydrants have a maximum spacing of 300 ft and each building is serviced by at least two hydrants. Hose stations are provided in all buildings. The cooling tower is protected by a fire detection system which automatically opens the deluge valves to the cooling tower bay or bays involved in a fire and also actuates the deluge valves on the bays adjacent to the fire. The maximum number of tower bays that will have to be flooded at any one time is six. At 0.5 gpm per sq ft of deck area this is about 3900 gpm. In addition, about 500 gpm of firewater are required for spraying six fan motors above the deck and 600 gpm for one fire hydrant. Based on these estimates, firewater pumps with a 5000 gpm rating are adequate.

An interconnection to the primary coolant system is provided to supply raw water to the reactor in case of an incident involving a large loss of primary water.

4.813 Service Water (Fig. 4.8A)

The service water system supplies 200 gpm of raw water for the demineralizer system influent and 100 gpm for all sanitary requirements.

Either of two service water pumps (300 gpm, 175 ft TDH, 20 hp) transfers the raw water from the ground level storage tank to the demineralizer system and also to the 3 in. service water header which serves all of the facility buildings.

To meet sanitary requirements, a chlorinator at each well chlorinates the water before it enters the ground storage tank. The demineralizer is automatically shut down on power failure and demineralized water requirements are met from demineralized storage.

4.814 Cooling Tower Make-up Water (Ref. Fig. 4.8A)

Either one of two cooling tower make-up pumps (2500 gpm, 100 ft TDH, 100 hp) supplies the evaporation, windage, and blowdown water requirements of the cooling tower. The pumps are located in the utilities building and furnish make-up water to the cooling tower through a 10 in. carbon steel line. The cooling tower make-up requirements are based on maintaining four cycles of concentration* in the cooling tower water.

*Cycles of concentration is the term employed to indicate the degree of concentration of the circulating water as compared to the make-up water.

MTR-ETR experience has indicated that seven cycles of concentration are satisfactory at a water temperature of 110°F. However, the secondary on-tower water temperature is 140°F and it is deemed advisable to limit the maximum cycles of concentration to four, thereby minimizing scale formation in the heat exchangers.

Make-up water treatment is needed to inhibit corrosion, scaling and the growth of slime and algae. When the reactor is operating at full power it is estimated that 360 gal of 66° Be. sulfuric acid, 300 lb of Orocol (a corrosion and scale inhibiting chemical), and 40 lb of chlorine are required per day.

4.815 Demineralized Water (Ref. Fig. 4.8B)

The demineralizer produces 150 gpm of demineralized water with a specific resistance of 250,000 to 500,000 ohms. A unit, which is available commercially, will produce water of this quality. The demineralizer system consists of two 100 gpm sulfuric acid regenerated cation units, a degasifier for removing carbon dioxide from the cation effluent, a 10,000 gal plastic lined concrete sump, and two 75 gpm strong base caustic regenerated anion units. The cation unit flow rating was purposely made 25 gpm larger than the anion flow rate since cation effluent is needed for anion regeneration. MTR-ETR experience has indicated that the cation beds should have a larger flow rating than the anion units. The cation and anion regeneration cycles are automatically controlled; however, the operator will initiate the regeneration cycle.

Demineralized water from the anion units is stored in a 100,000 gal ground level, stainless steel storage tank equipped with level indicator and high and low level alarms.

Either of two motor driven demineralized water pumps (150 gpm, 175 ft TDH, 10 hp) pumps the water to the plant through an 8 in. stainless steel line. Two demineralized flush pumps (1000 gpm, 175 ft TDH, 75 hp) supply water for flushing the reactor and primary system after reactor shutdown. Since the flush pumps are used only intermittently, both pumps will normally operate at a combined rate of 2000 gpm. However, if one pump is down for repairs, the other can adequately flush the primary system at a slower rate.

Cation and anion tanks and manifolds for these tanks are rubber-lined carbon steel. The remainder of the system is constructed of 304 stainless steel to minimize contamination of the water with corrosion products.

4.816 Water Treating Chemicals Storage (Ref. Fig. 4.8B)

Sulfuric acid is stored in two 10,000 gal carbon-steel tanks adjacent to the utilities building and pumped to the cation acid measuring tank or the secondary system acid measuring tank by either of two motor-driven acid pumps (20 gpm, 2.5 hp). The acid

requirements for the secondary system and the demineralizer are estimated to be 500 gal per day. The acid storage tanks are not heated since the freezing point of 66°Be acid is -29°F.

Fifty per cent sodium hydroxide solution is stored in two 3000 gal, insulated, steam heated, carbon-steel tanks located in the utilities building. The caustic is pumped from the storage tanks by means of either of two motor-driven caustic pumps (20 gpm, 1.5 hp). The caustic requirements for the demineralizer are estimated to be 95 gal per day. The caustic in the tanks is steam heated to 85°F to facilitate pumping. The tanks are located inside the building to eliminate the necessity of heating the caustic piping.

The acid and caustic storage tanks are equipped with level indicators. Truck unloading facilities adjacent to the storage tanks provide for unloading with plant air. Acid and caustic systems are constructed of carbon steel.

The Orocol is purchased in 400 lb fiber drums and is stored in the warehouse. Chlorine is purchased in ton containers.

4.817 Utility and Emergency Cooling Water (Ref. Fig. 4.8C)

The utility and emergency cooling system is used as the heat transfer medium for final heat removal by the cooling tower on the reactor auxiliary systems. These include the high pressure demineralizer water (2000 gpm), emergency cooling loop (425 gpm), reactor canal cooling (700 gpm), diesel engine cooling (1200 gpm), plant and instrument air compressor cooling (50 gpm), and to provide emergency cooling for the primary heat exchangers in the event of a commercial power outage (1500 gpm).

Two motor-driven, vertical turbine pumps (3000 gpm, 150 ft TDH, 150 hp) are located in the cooling tower pump house and provide the necessary water flow for the system at the design off-tower temperature of 85°F. In the event of a commercial power failure, one utility pump will continue to operate, providing cooling tower water to critical cooling loads. It is anticipated that the total heat load imposed on the cooling towers by the utility cooling system will be 20 to 25 Mw.

4.818 Experimental Emergency Cooling Loop (Ref. Fig. 4.8D)

The experimental emergency cooling loop (ECL) is a system which permits cooling of in-pile tubes and/or fuel elements during periods when the experimenters' coolant circulating system is out of service.

The shielded loop is designed to cool defected specimens under emergency conditions. Therefore, the entire loop system is constructed of stainless steel, which will permit use of various chemical decontamination solutions.

The ECL system circulates high purity demineralized water up to 500 gpm at a pressure of 450 psig and a temperature of 150°F. The experimental loops return the water at 200 psig with temperatures up to 190°F thus forming a closed loop. The heat load of 3 Mw is transferred to the utility cooling water system via shell and tube heat exchangers for final dissipation through the cooling tower.

System pressure is maintained at 450 psig by means of a pressurizing pump, taking suction from the low pressure demineralized water system and discharging through a pressure regulating valve to the circulating pump suction headers. To compensate for system pressure and volume changes during temperature transients, a surge tank with a pressurized nitrogen blanket is installed on the circulating pump discharge header.

A mixed bed ion exchanger column is provided to control cooling water pH and conductivity and to maintain the system demineralized water purity. A removable shielded resin cask is provided to dispose of depleted ion exchange resins.

The loop instrumentation is located on a control panel outside the loop cubicle shield.

4.819 High Pressure Demineralized Water (Ref. Fig. 4.8E)

The high pressure demineralizer water (HDW) system at a supply pressure of 300 psig circulates 3000 gpm of demineralized water of which 2500 gpm is supplied at 150°F and 500 gpm at 100°F. The 2500 gpm system removes fission and gamma heat from the experimental loop circulating water via water-to-water experimental heat exchangers. The 500 gpm system, at 100°F, is used for experimental primary pump and ion exchange cooling, both of which require lower temperature cooling water.

The maximum heat input to this system is estimated to be 16 Mw which is transferred through shell and tube heat exchangers to the utility cooling water for heat removal by the cooling tower. Suitable temperature indicators and flow measuring devices are provided on both the demineralized water side and the utility water side of the heat exchanger to control the system temperature.

The three HDW circulating pumps are horizontal centrifugal, double suction, double volute type with a capacity of 1000 gpm each at 230 ft TDH. The pumps are driven by 100 hp electric motors. A by-pass pneumatic pressure regulator valve is installed between the supply header and the common return header to maintain a constant supply pressure under varying experimental demands. In the event of a commercial power outage, one circulating pump continues to operate providing water at reduced flows to the experimental loops for shutdown heat removal. This necessitates the experimental uses to be automatically trimmed to insure adequate cooling water for critical demands.

Demineralizer water from the gland seal and pressurizing pumps passes through a pressure reducing valve set at 200 psig to control pressure on the suction side of the HDW circulating water pumps. A system fill line by-passing the PRV is incorporated to provide fast filling of the entire system.

4.82 Heating and Ventilating

4.821 Steam Plant (Ref. Fig. 4.8F)

The heating requirements of the plant buildings necessitates the installation of a steam plant. In addition, steam is required for D_2O distillation; however, this requirement is small.

Two 20,000 lb/hr packaged water tube boilers are provided to supply the facility steam requirements. The estimated steam load at an ambient temperature of -20°F is 20,000 lb/hr. One boiler will be required to supply the maximum steam demand, with the other serving as a standby.

The boilers, located in the utilities building, supply 135 psig steam to a 6 in. insulated steam header which loops the reactor building. The 2 in. insulated condensate loop parallels the steam loop. Steam and condensate service to the various buildings and facilities is supplied from these loops.

The steam plant is a conventional low pressure system with a 20,000 lb/hr deareating feed water heater, two motor-driven feedwater pumps (60 gpm, 425 ft TDH, 10 hp), a 500 gal condensate tank located in a pit below the utilities building floor and two motor-driven condensate pumps (60 gpm, 75 ft TDH, 5 hp). The boiler feed is treated with sodium sulfite for oxygen removal and with sodium phosphates for pH control. Since the boilers supply steam for heating purposes only, it is estimated that 95 to 100 per cent of the steam produced will be returned as condensate so that the demineralized water requirements are small except when it is necessary to refill a boiler after draining.

One motor-driven unloading pump (50 gpm, 5 hp), two motor-driven transfer pumps (10 gpm, 250 ft TDH, 2 hp), two duplex fuel oil strainers, and two fuel oil heaters are located in the oil pump house adjacent to the fuel oil storage tanks. The two 100,000 gal fuel oil storage tanks are sufficient for two months oil supply at a maximum demand load.

4.822 Reactor Building

Reactor Operating Area. This area is provided with a separate heating and ventilating system furnishing air at 70°F by means of a supply duct system discharging air to the first floor area. Approximately 90 per cent of the air will exhaust through the experimental cubicles

to dissipate the anticipated 75 kw experimental heat load per cubicle. The remaining air exhausts through the sub-pile and control rod access rooms. Pressures in these areas are below those of all adjoining areas so that air flow is from normal personnel working areas into cubicles which are potential areas of high air activity. All air from the cubicles discharges into the cubicle exhaust header and is exhausted through the stack. The heating and ventilating equipment for this area is located in the reactor building heating and ventilating room and consists of adjustable louvers, non-freeze pre-heat steam coils, a capillary washer filter system and steam reheat coils. A supply fan of approximately 68,000 cfm is required which provides six air changes per hour, all of which are outside air.

Offices and Hallways. These areas are provided with a separate heating system furnishing air at a minimum of 70°F. Supply ducts are routed to each office, with return air ducts located in the hallways. The heating equipment is located in the heating and ventilating room and consists of adjustable outside and return air louvers, non-freeze heating coils, washable high efficiency filters, and mixing dampers. A blower of 2500 cfm provides six air changes per hour, three of which are outside air.

Experimenters' Canal Area, Hot Cell Building, Storage Canal and the Service and Mockup Areas. These areas are supplied with an additional heating system furnishing air at a minimum of 70°F by means of supply ducts located on the first floor. Flow is down through the basement levels with return air from both levels. The heating equipment is located in the heating and ventilating room and is similar to that described for the offices. A fan of approximately 75,000 cfm provides four air changes per hour, two of which are outside air.

Heating and Ventilating Controls. Controls for each system originate downstream of the heating coils. They consist of thermocouple equipped temperature recorder controllers and actuating pneumatic type modulating steam control valves to the heating coils. The reactor operating area system has an additional temperature recorder controller for the preheat steam coils.

Reactor Control and Equipment Rooms. These rooms are air conditioned by means of a multiple package air-conditioning unit. Fresh supply of air to this unit is from the reactor area supply system. Design conditions are 70°F D.B. ($\pm$ 1°) and 40 per cent R.H. for both summer and winter operation. Automatic temperature control is provided to adjust heating and cooling fluctuations. The air conditioning unit is located in the heating and ventilating equipment room. Total air circulation is six air changes per hour, two of which are outside air.

Process Water Area. This area is heated to 60°F by means of industrial unit heaters. This area is exhausted through the cubicle exhaust system in order to maintain the area at a negative pressure. Air activity problems are thus minimized in the adjoining operating areas.

4.823 Supporting Facilities

Administration and Cafeteria Building. A central steam heating system furnishing air at a minimum of 70°F is installed in this building. The unit consists of a fan section, filter box equipped with dry type washable filters, heating coils, and a damper section. It is furnished complete with automatic controls to provide heat and ventilation to the office areas. Supply and return duct systems are provided with a total air circulation of six air changes per hour, two changes being outside air. Change rooms and toilets are exhausted to the atmosphere by separate exhaust fans at twelve air changes per hour.

Warehouse and Maintenance Building. A system similar to the administration and cafeteria building is installed here with an additional wall mounted exhaust fan provided for the welding area. Total air circulation is four changes per hour, two changes being outside air.

Engineering and Laboratory Building. This building is heated to 70°F by means of industrial type heaters similar to the units for the administration and cafeteria building. Total air circulation is six air changes per hour, three changes being outside air.

Utilities Building. The utilities building houses the electrical switchgear, the two diesel generators, the makeup demineralizer, steam boilers, plant and instrument air compressors, and raw water pumps. Since it is generally a machinery area, it is heated to 60°F by means of industrial type steam unit heaters equipped with fans, dry type washable filters, non-freeze heating coils, and dampers. Fresh air intake is two air changes per hour with exhaust through power roof ventilators.

Summer ventilation required to dissipate heat from pump motors, switchgear, boilers, diesel engines, etc., will be supplied by evaporative coolers installed on the intake side of the unit heaters. Maximum ambient room temperature is held to 40°C (105°F).

System control is from a single control center. It consists of thermostats actuating modulating control valves on the steam and evaporative cooling systems, and start-stop controls for the unit heater fans and roof ventilators.

Secondary Pump House. This building, which does not require continuous occupancy, is heated to 60°F by means of industrial steam unit heaters. Ventilation is provided by gravity roof ventilators.

4.83 Plant and Instrument Air (Ref. Fig. 4.8G)

Plant and instrument air is supplied by two motor-driven air compressors (300 scfm, 150 psig, 100 hp) discharging to a 1000 cu ft air receiver located adjacent to the utilities building. The plant air system

is supplied directly from the receiver through a 2-1/2 in. plant air line. The instrument air from the plant air receiver is dried by means of either one of two silica gel driers before the air is reduced to 100 psig and distributed to the 2-1/2 in. instrument air header. One silica gel dryer is sufficient to dry the estimated instrument air demand so that the other dryer can be regenerated.

The plant air header is automatically shut off at the receiver in case the receiver pressure drops below 100 psig so that sufficient air is available for instrumentation in case of compressor or power failure. A third motor-driven air compressor (200 scfm, 150 psig, 75 hp) is supplied power from the diesel bus so that instrument air is maintained during commercial power outages.

4.84 Waste Disposal

4.841 Liquid Waste

Cold Waste (Ref. Fig. 4.8H). Non-radioactive liquids from the cooling tower, the laboratory and engineering building, the maintenance and warehouse building, and the utilities building flow directly by gravity to the plant sump. The warm plant effluents also discharge to the plant sump and are diluted with the cold wastes before being discharged to the leaching pond. Two motor-driven plant sump pumps (2000 gpm, 25 ft TDH, 20 hp) pump the liquid wastes directly to the leaching pond via a 10 in. tile line for disposal to the atmosphere by evaporation and to the subsoil by percolation. The final design area of the leaching pond will depend on the geological and climatic environment of the site selected.

The plant sump is plastic-lined to resist the corrosive demineralizer regeneration solutions. The utilities building cold drain is Duriron to resist the demineralizer caustic and acid solutions. Concrete pipe is used for all other cold building drain yard piping.

Warm Waste (Ref. Fig. 4.8H). Radioactive liquid wastes from the canal, the reactor building, the heat exchanger building, the laboratory and engineering building, and the primary coolant system degassing tank flows by gravity through 2 in. and 4 in. stainless steel piping to the 5000 gal stainless steel warm sump tank located in a shielded cubicle below the reactor building basement floor. Two motor-driven turbine pumps (200 gpm, 100 ft TDH, 7.5 hp) pump the warm wastes to the 10 in. stainless steel primary system flush line, which discharges to the plant sump. The warm sump tank is equipped with a level indicator controller which automatically starts and stops the warm sump pumps.

Hot Experimental Waste (Ref. Fig. 4.8I). Coolant and decontamination solutions from the experimental loops and the laboratories will be the only sources of wastes whose radioactivity concentrations are too high to permit ultimate discharge to the leaching pond. The hot wastes from the laboratories are estimated to be only a few gallons per week.

If experimental capsule or reactor fuel element failures contaminate the primary systems to such a degree that the primary coolant cannot be flushed directly to the leaching pond via the plant sump, the reactor will be shut down and the primary coolant circulated and decontaminated by means of the primary bypass demineralizer until the radioactivity concentrations of the primary coolant is reduced to a low enough level to be discharged to the leaching pond.

Hot wastes from experimental loops will drain via 2 in. stainless steel lines to the 1000 gal hot experimental waste sump tank located in a shielded cubicle below the reactor building basement floor. Either of two motor-driven pumps (50 gpm, 100 ft TDH, 2 hp) transfers the liquid from the sump tank to the waste storage tanks located in the yard near the heat exchanger building.

The hot experimental waste collection system is constructed of stainless steel since the decontamination solutions used on the experimental loops are highly corrosive to carbon steel.

Hot Experimental Waste Storage (Ref. Fig. 4.8I). Hot wastes from the experimental loops are stored in the hot waste storage tanks. Two stainless steel storage tanks are provided. One tank (10,000 gal) is used for the permanent storage of loop decontamination solutions. The other tank (5000 gal) is used for storage of loop coolant contaminated with fission products. Both tanks are equipped with level indicating alarms and are vented to the cubicle exhaust system.

Experimental loop coolants, contaminated with fission products, will be decontaminated by means of two resin beds containing 15 cu ft each of anion and cation resins. The fission product containing liquid will be circulated through the resin beds by means of two motor-driven pumps (50 gpm, 100 ft TDH, 2 hp) until the radioactivity has been reduced sufficiently to permit discharge of the loop water to the leaching pond.

The loop decontamination solutions cannot be decontaminated by ion exchange, since these solutions will contain large quantities of non-radioactive acids, bases, salts, and organic materials. These will be stored permanently in the 10,000 gal storage tank.

Space and connections for the installation of additional permanent storage tanks are provided. If the site selected has concentrating and storage facilities for hot wastes, the hot wastes could be transported to this facility. The storage facilities are estimated to be sufficient for two years storage of hot experimental wastes.

The most economical storage facility will have to be investigated during the first two years of operation to determine if: 1) additional storage tanks should be provided, 2) concentrating facilities

are needed, or if 3) the liquid wastes could be transported to existing facilities.

The hot experimental waste storage system is constructed of stainless steel to minimize corrosion. The resin tanks are rubber-or plastic-lined since these will be removed from the system when the ion exchange capacity is exhausted. Disposal of the resin beds and tanks is made in the burial ground.

Sanitary Waste. The sanitary wastes from the buildings drain by gravity to an 8 in. concrete sewer main and flow to a concrete lift sump at the west end of the site. Either one of two 5 hp level controlled sewage pumps discharge the raw sewage from the building to a fenced stabilization pond located west of the main plant area. The sewage pond is constructed above grade and has an area of 3.5 acres. The dikes and bottom of the pond are compacted to minimize percolation. The sewage pond effluent flows through an 8 in. concrete pipe to the leaching pond. The overflow is controlled by means of a sliding gate valve installed in the overflow lines so that the depth of the pond can be varied.

This method of sewage treatment and disposal was chosen because of the simplicity and low cost. Similar installations have been operated successfully under widely varying climatic conditions.

4.842 Gaseous Waste Disposal (Fig. 4.8J)

The gaseous waste disposal system exhausts air from potentially high air activity areas such as the experimental cubicles, the primary pipe tunnel and heat exchanger area and the sub-pile room, and purges the radioactive hot and warm waste tanks and the primary system degassing tank.

Provisions are made to exhaust the reactor working platform when the reactor vessel top closure is removed for in-tank work, so that gaseous activity in the reactor vessel is exhausted to the cubicle exhaust system and does not contaminate the building air. A portable canal exhaust hood removes radioactive gases from the surface of the canal water when ruptured capsules are stored in the canal below this hood.

Total waste gas quantity, which will be monitored prior to disposal through a 150 ft stack is estimated at 78,800 cfm. The gaseous and particulate monitor is described in further detail under "Radiation Monitoring" of this report.

Two blowers (40,000 cfm, 50 hp) are provided and operate in parallel. One motor blower is connected to the diesel power bus and the other to the commercial power bus. System flow and pressures are recorded in the primary control room.

Over-pressure safety devices (rupture discs and pressure relief valves) on the experimental loops discharge into an experimental vent header which discharge into the cubicle exhaust duct on the downstream side of the blowers. Steam and radioactive gases when released

from an experimental loop are thus vented to the stack to eliminate contamination of the experimental cubicles and equipment.

4.843 Solid Waste Disposal

A burial ground is provided near the plant for the disposal of radioactive solids. It is assumed that the site selected will permit this means of disposal. Radioactive solids are transported from the plant area by truck and placed in trenches which are then covered with earth. Experimental tubes that are no longer serviceable are buried in vertically drilled holes at the burial ground.

The burial ground is fenced and posted to restrict unauthorized human or animal entry. It is estimated that a 25 acre plot will serve for the disposal of solid wastes for a period of five to ten years.

4.85 Electric Power (Figures 4.8K and 4.8L)

The electrical system requires two sources of power; one is commerical power supplied from an assumed existing 132 kv power system and the other is diesel power supplied by diesel-driven electric generators installed at the site.

4.851 Commercial Power

The total connected plant electrical load requires the installation of two 15,000 kva transformers in an outdoor substation. The electrical loads and the power distribution are summarized schematically in Fig. 4.8K.

4.852 Diesel Power

Diesel power at 4160 volts is supplied by two heavy duty diesel generators, one of which serves as a standby unit. The critical plant and experimental loads are split between independent commercial and diesel power sources, i.e., one pump on commercial and one pump on diesel power for a system. When a commercial power failure occurs, the operating diesel generator continues to supply power to its normal connected loads. The reactor is automatically shut down on loss of commercial power or if the diesel generator fails. It is very unlikely that diesel generator failure and a commercial power outage would occur at the same time.

4.853 General

A tunnel with lay-in trays is provided for cables from the utilities building. A system of underground ducts and manholes is used for routing electrical power, communications and alarm circuits to the other site buildings.

Oil for the diesels is stored in a 100,000 gal ground-level storage tank. It is estimated that 3000 gal per day of diesel oil will be required when the diesel generator is running.

4.86 Hot Cell

A hot cell is provided in the reactor building for limited servicing of irradiation tests. These services include such items as visual and photographic examination of test specimens, disassembly and reassembly of plugs and capsules, repairing of test specimen trains, and removal of irradiated components for shipment to other laboratories.

The cell, capable of handling 10,000 to 20,000 curies of 1.5 to 3.0 mev gamma activity, is located over one end of the canal for ease of handling and minimization of accidental damage to specimen trains. The cell is constructed with walls of heavy barytes concrete 4 ft thick with three large windows and one smaller one for viewing purposes. Entrance to the cell by personnel and equipment is through large sliding steel doors in the rear wall of the cell.

Radioactive materials are charged directly into the hot cell from the canal by means of suitable hoisting and manipulating equipment. Manipulation within the cell is accomplished with a General Mills mechanical arm and a light crane operated in connection with a pair of Argonne Type Model 8B Master-Slave manipulators. The Master-Slave manipulators are installed in a sliding shield above the viewing windows. Visual and photographic examination of experiments is conducted with the aid of a thru-wall periscope located in the front of the cell.

A storage and decontamination area at the rear and a clean working area at the front of the cell are provided. The hot cell exhaust discharges through absolute filters to the cubicle exhaust system.

4.87 Radioactive Monitoring

4.871 Direct Radiation

Area monitoring is performed in various parts of the plant with ion chambers incorporating built-in calibration sources. These are adjustable from the main control panel where the contact meter relays are located. All units alarm locally as well as in the Health Physics office and those of primary importance record in the control room.

There are five ion chambers on each of the first and basement floor levels and eight ion chambers on the sub-basement level. The control panels are in the Health Physics office and two multipoint recorders are in the reactor control room.

Ten chambers are located in the heat exchanger building, two in the hot cell, and two in the utilities building. These alarm, as stated above, but do not record. Control units are locally mounted.

4.872 Air Monitoring

Constant air monitoring is accomplished by portable scintillation units. One each in the hot cell, utilities building, secondary pump house, warehouse and maintenance building, administration and cafeteria building, and two in the heat exchanger building record and alarm locally and alarm in the Health Physics office. Fourteen of the same units are located in the reactor building and record in the reactor control room.

4.873 Fission Break Detectors

There is one primary coolant fission break detector. The process water sample is continuously drawn through a pressure regulator and flow meter to the monitor which may be either an iodine or delayed neutron monitor. The activity level is continuously recorded in the reactor control room.

4.874 Waste Gas Monitoring

The waste gas monitor measures and totalizes air flow to the stack. It also monitors a continuous sample of the air stream for particulate and gaseous activity with a moving filter tape system. Scintillation counters with totalizers are used for both gas and particulate monitors. The instantaneous level of each records in the Health Physics office on a multipoint recorder.

4.875 Effluent Water Monitor

Effluent water is continuously measured for flow rate and activity. A sample whose flow is proportional to discharge rate is monitored by a scintillation system. Flow and activity are continuously multiplied and integrated to give the total curies discharged.

4.876 Personnel Monitors

Two hand-foot counters are located in the reactor building. Friskers of the quintector type are located at all reactor building exits, at elevator entrances, and at each stair well. Friskers are also provided at the main gate and cafeteria.

4.88 Communications

The communication system consists of three main parts. Two-way intercom units with call buzzers are located in all normal work areas and at all experimental control panels and are connected to the master station in the control room. The paging system utilizes the intercom units plus additional horns and speakers.

Two sound powered phone circuits connect the remote areas to the control room. It is possible to interconnect these two circuits

in the control room. These communication systems supplement a commercially installed and serviced telephone system.

In addition, a manual, automatic coding fire alarm system is installed throughout the plant. It consists of alarm boxes and bells connected to a centralized relay and terminal strip unit. Low fire-water pressure, low water level in the 2,000,000 gal storage tank, opening of cooling tower deluge valves, or the starting of either fire pump is coded.

4.89 Hydraulic Test Facility (Ref. Fig. 4.8M)

The hydraulic test facility is made up of two loops using a common pump, heat exchanger, and surge tank. One loop is used to hydraulically test and measure velocities in fuel assemblies and experimental assemblies. These assemblies are put into the removable test section with pressure tap leads running to the test panel. The other loop is used to check rod drives under operating conditions and to measure rod drop times. The loops are designed for a maximum flow rate of 800 gpm at 500 ft total discharge head. All components are stainless steel to avoid corrosion of the loop and demineralized water is used to avoid corrosion of test pieces. This facility will also be used for the research and development program.

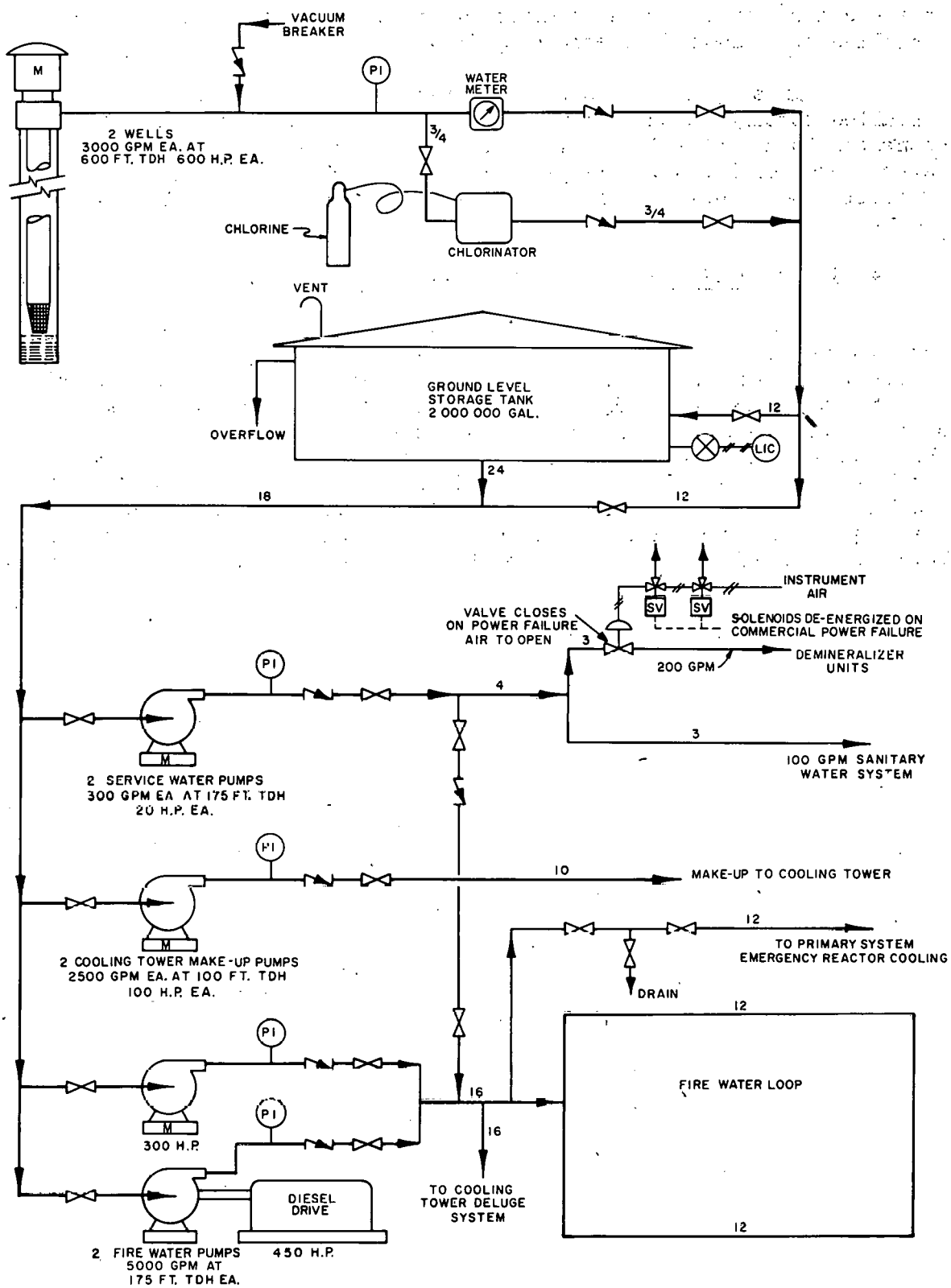

FIG. 4.8A
RAW WATER SYSTEM
FLOW DIAGRAM

P.P.CO.-C-2729

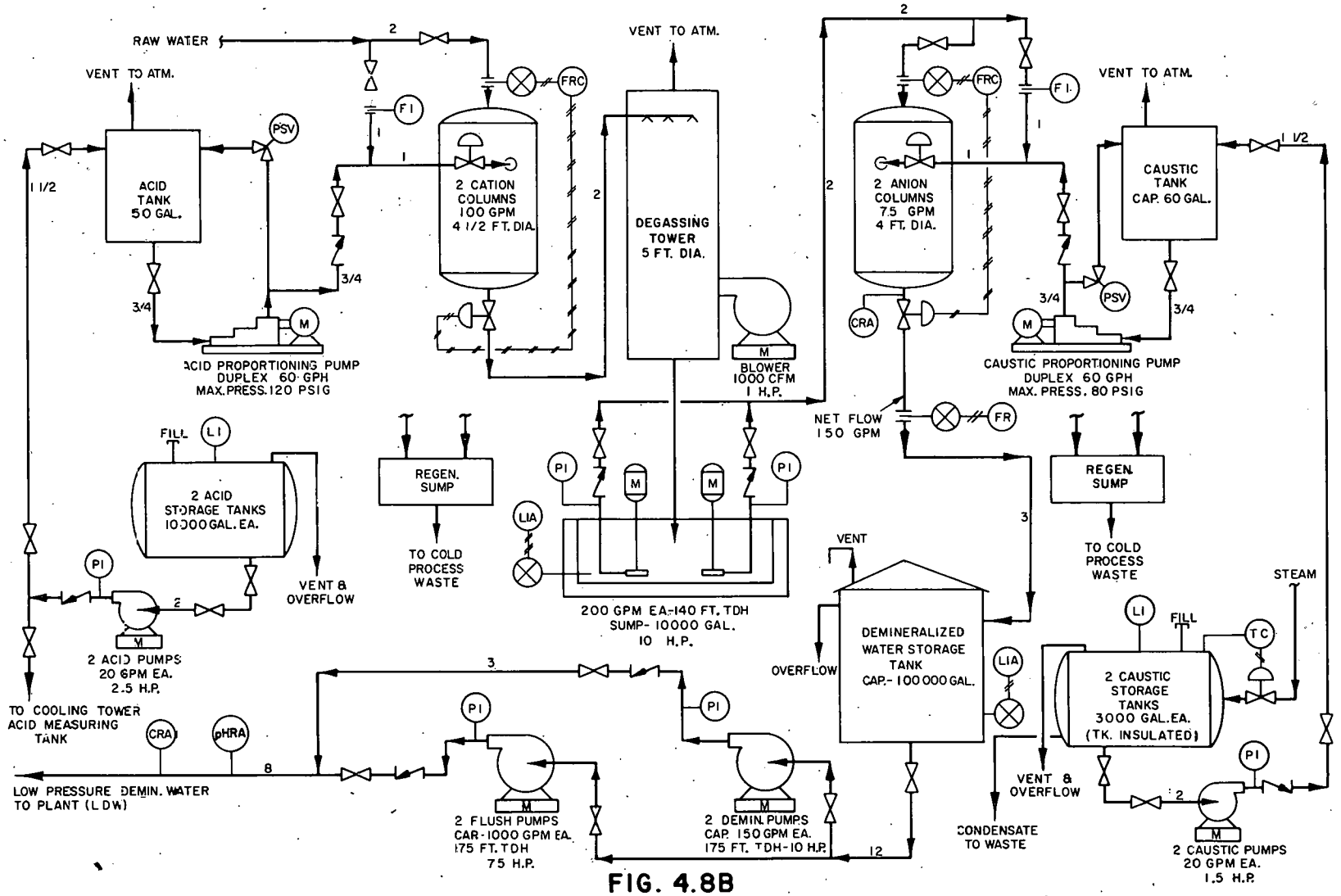

FIG. 4.8B

DEMINERALIZED WATER SYSTEM
FLOW DIAGRAM

P.P. CO. - C - 2730

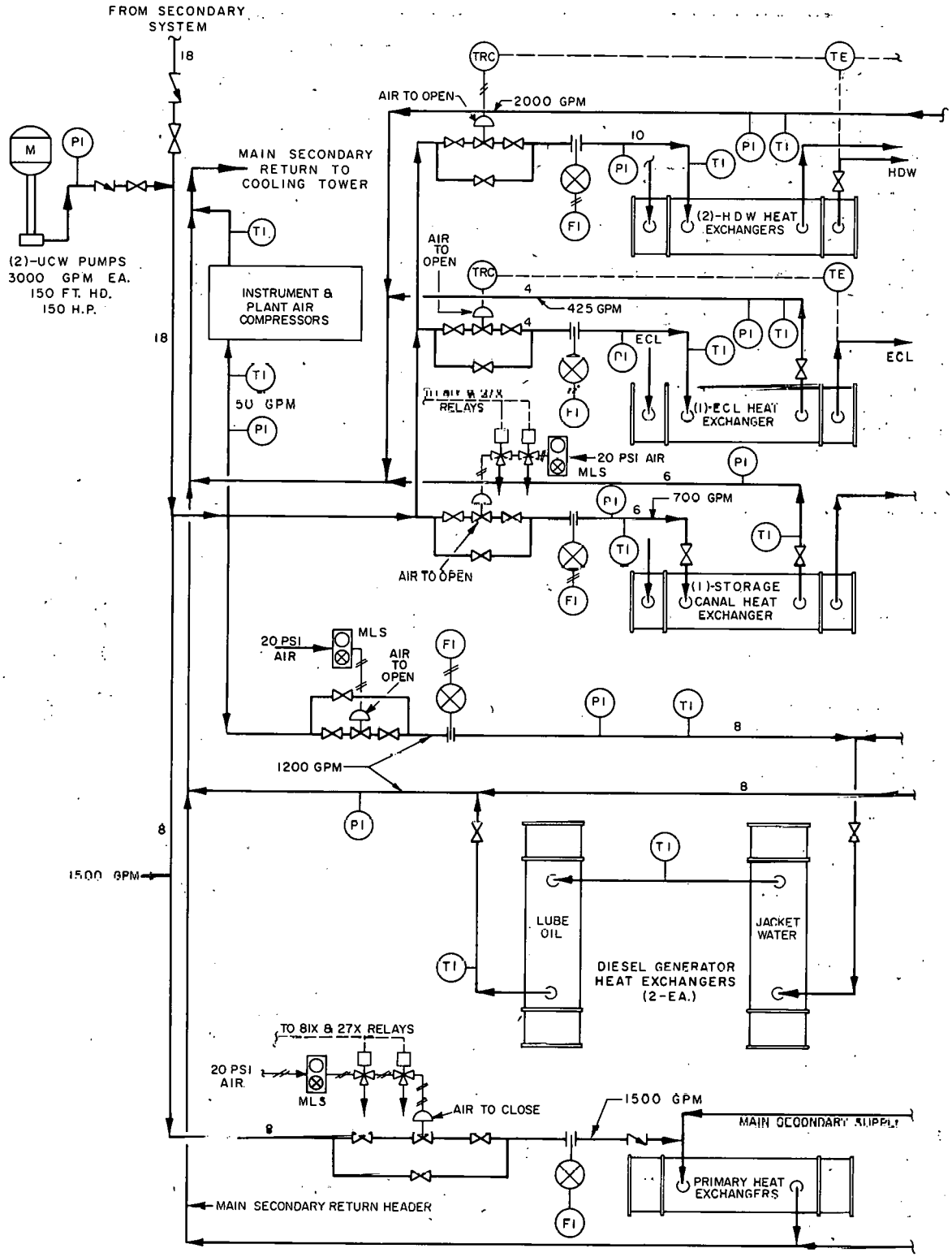

FIG. 4.8C

UTILITY COOLING WATER SYSTEM

FLOW DIAGRAM

P.P.CO.-C-2731

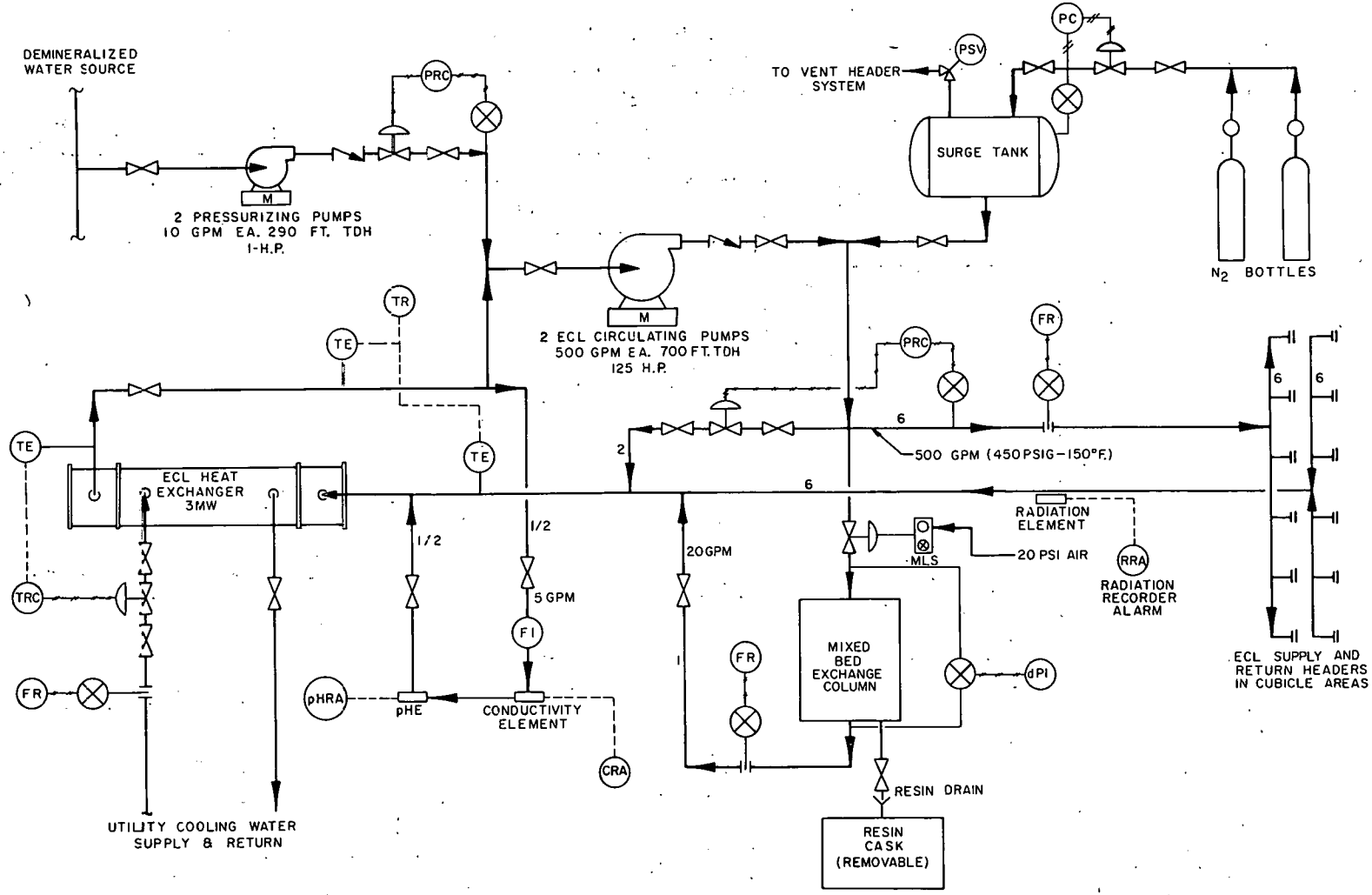

FIG. 4.8D

EXPERIMENTAL EMERGENCY COOLING LOOP FLOW DIAGRAM

PPCO.-C-2732

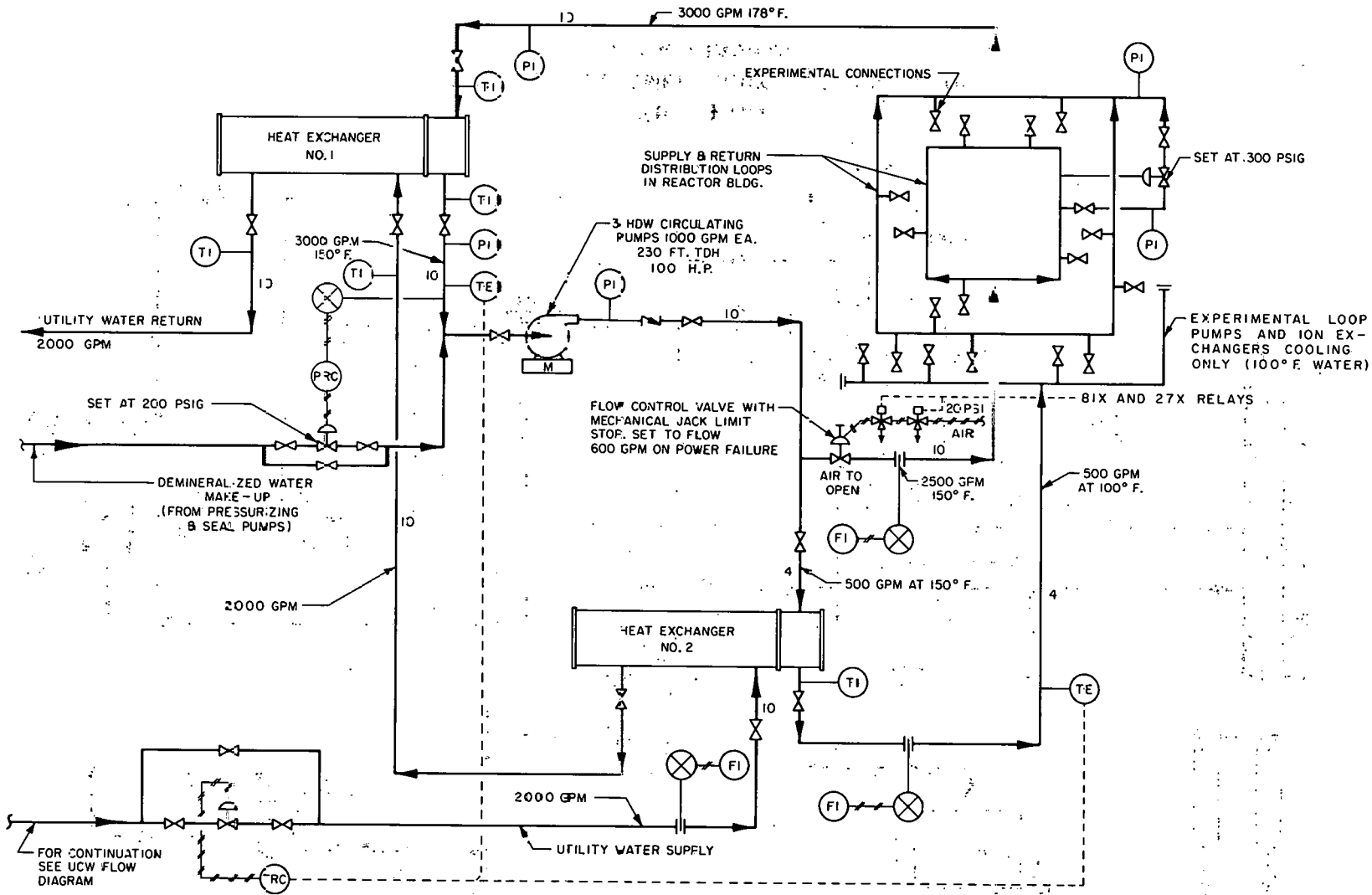

FIG. 4.8E

HIGH PRESSURE DEMINERALIZED WATER SYSTEM FLOW DIAGRAM

P. P. CO. - C - 2733

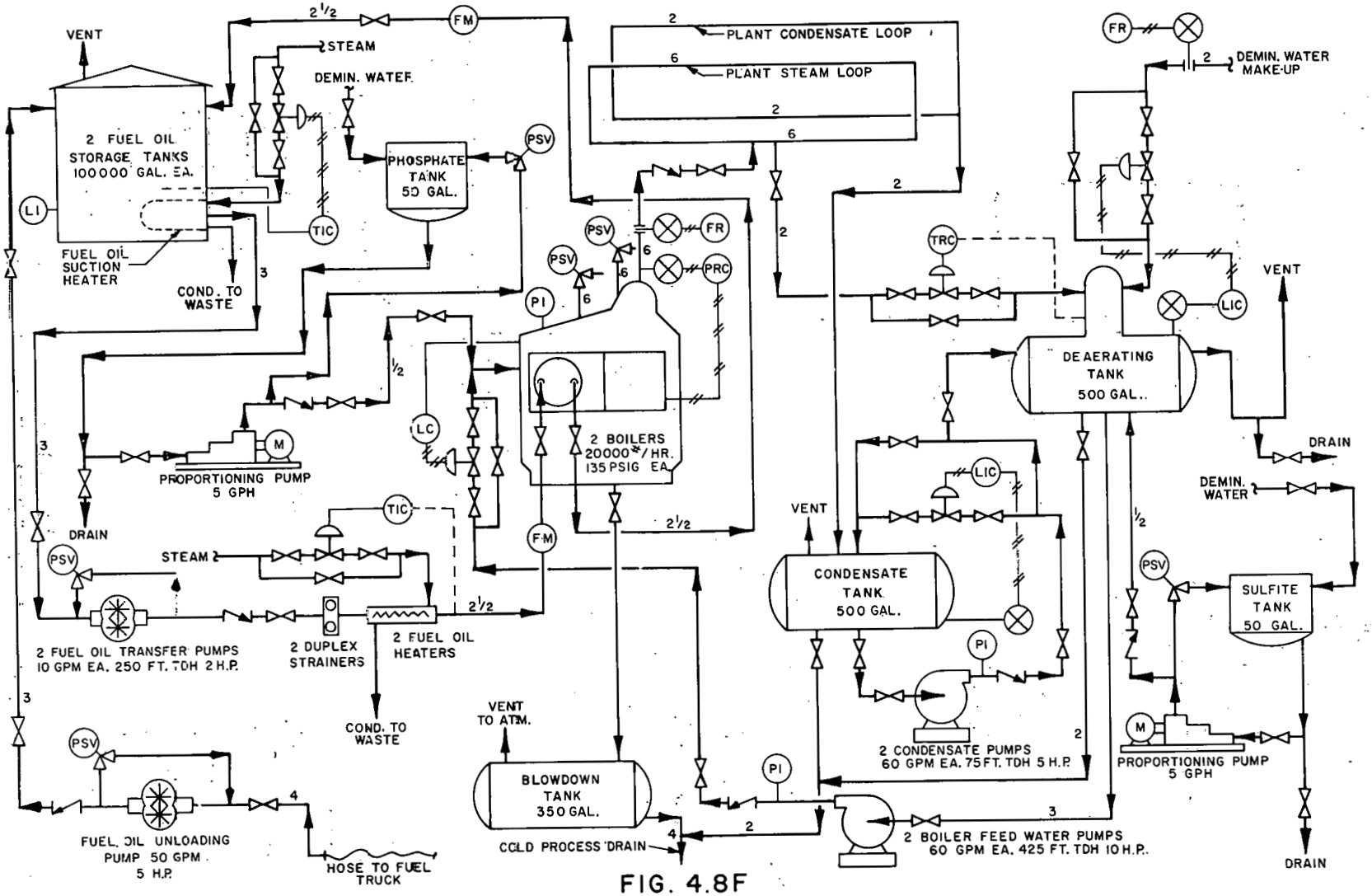

FIG. 4.8F

PLANT STEAM SYSTEM

FLOW DIAGRAM

P.P. CO.-C-2734

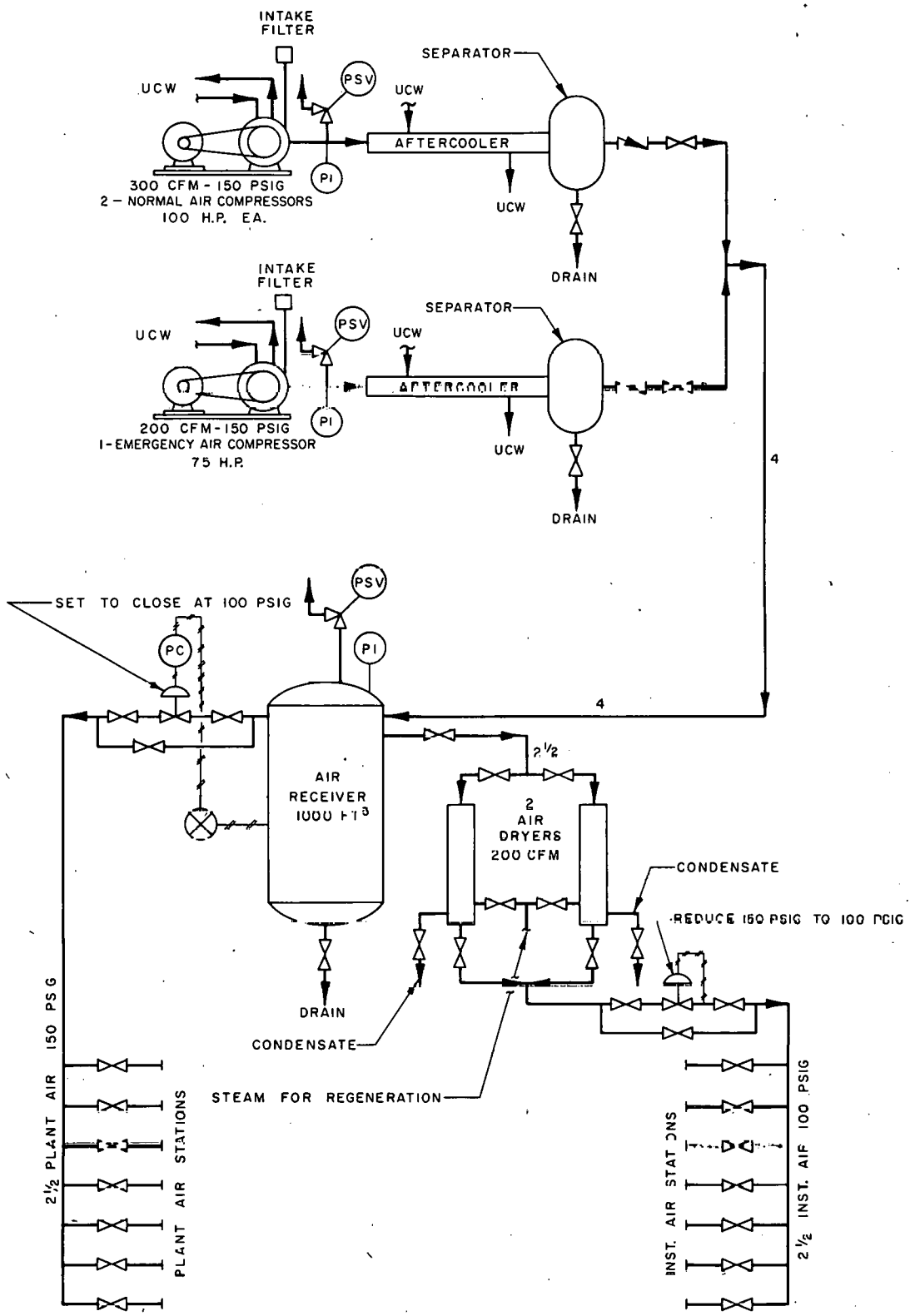

FIG. 4.8G

PLANT AND INSTRUMENT AIR SYSTEM FLOW DIAGRAM

P.P. CO.-C-2735

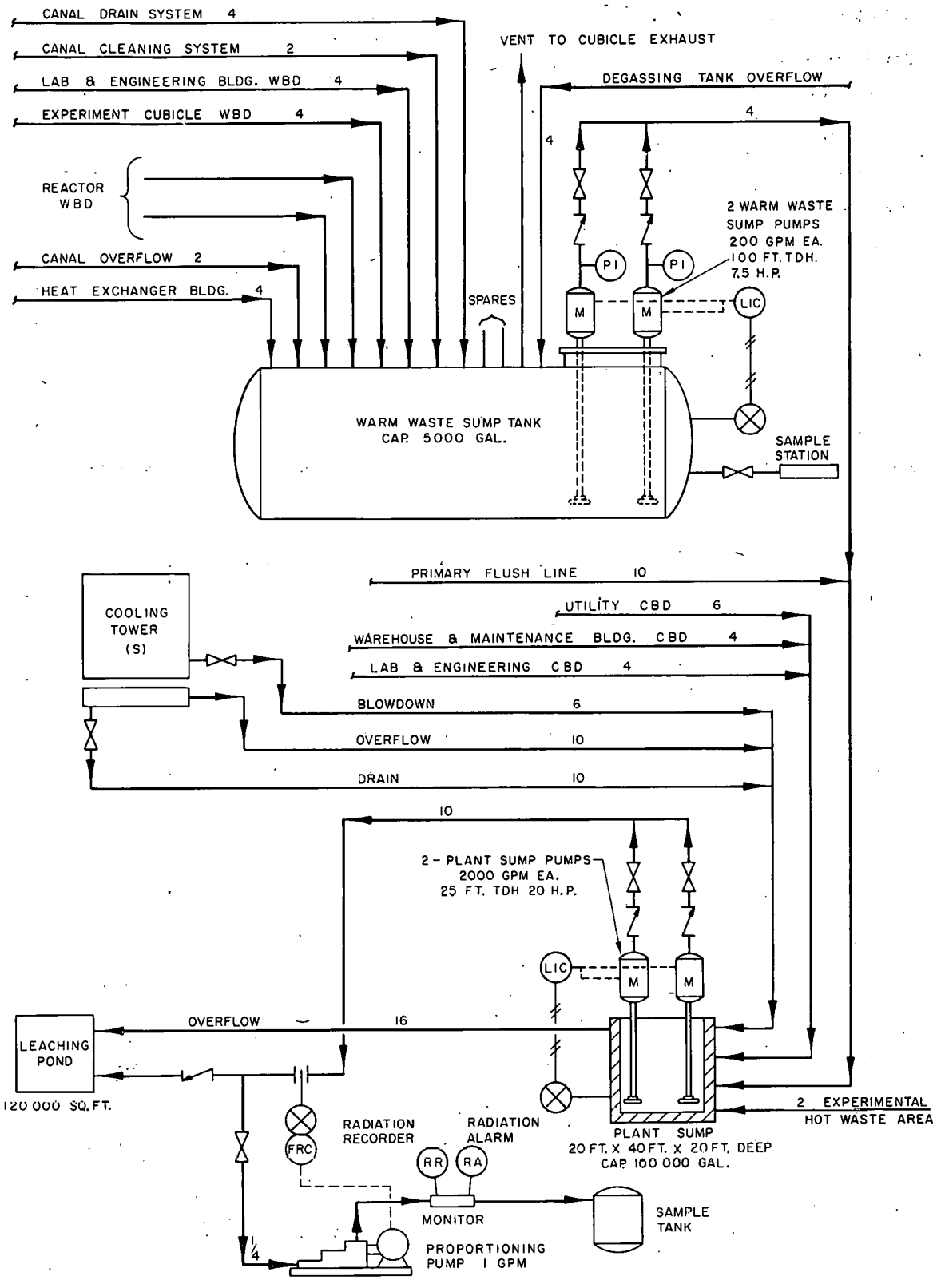

FIG. 4.8H

LIQUID WASTE DISPOSAL SYSTEM FLOW DIAGRAM

P.P.CO.-C-2736

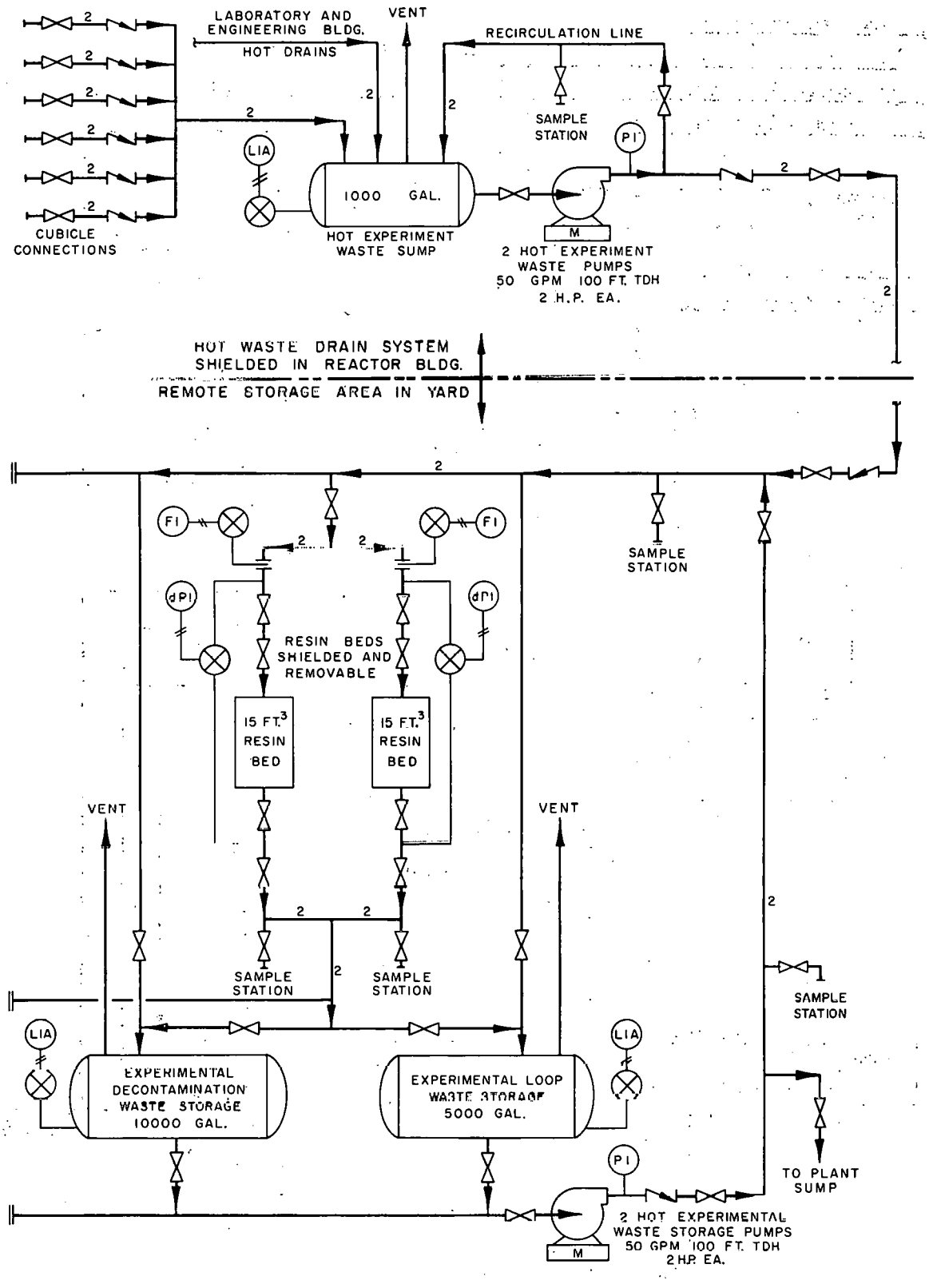

FIG. 4.8 I
EXPERIMENTAL HOT WASTE DISPOSAL SYSTEM
FLOW DIAGRAM

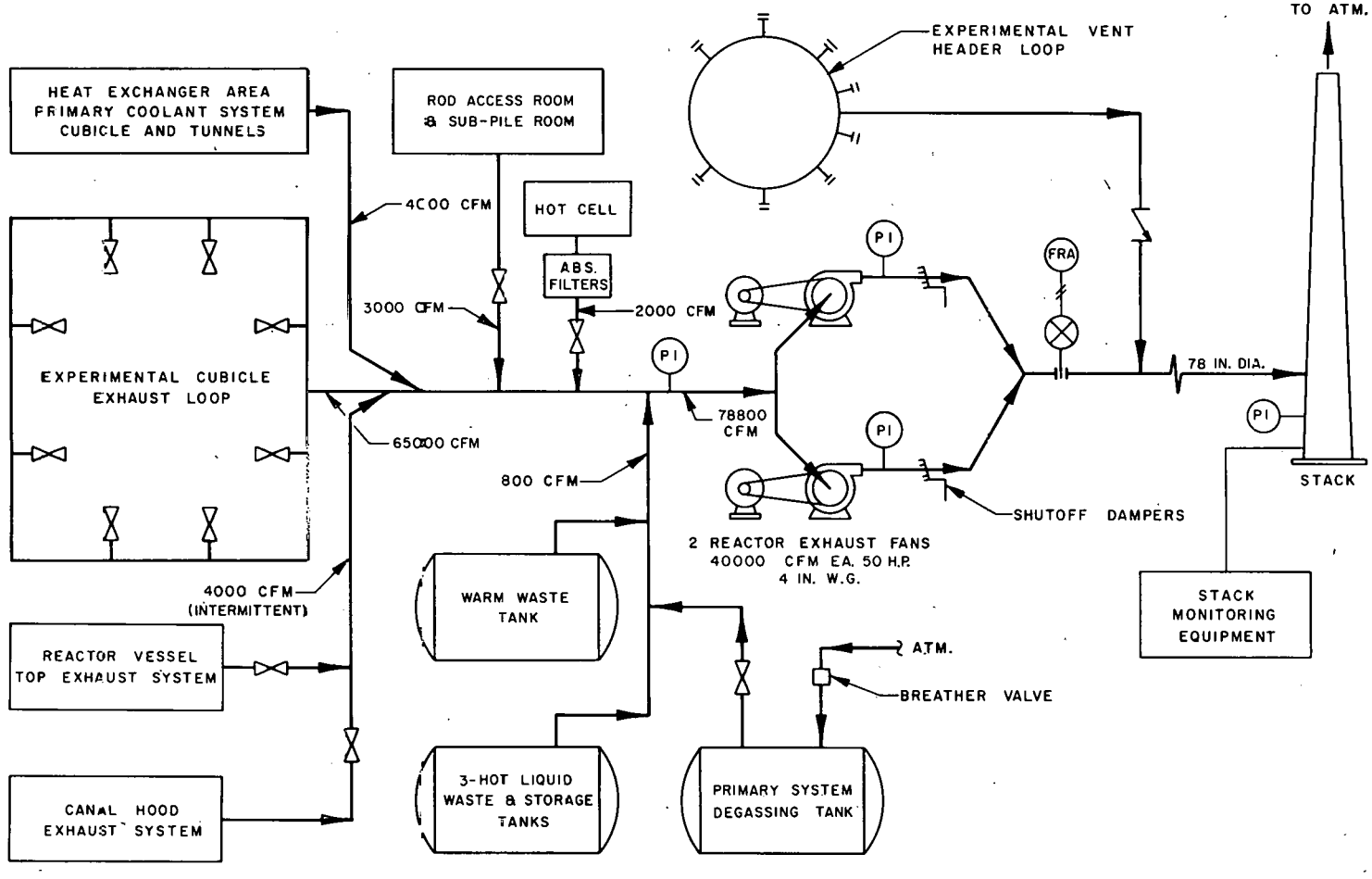

P. P. Co.-C-27,38

FIG. 4.8J
GASEOUS WASTE DISPOSAL SYSTEM
FLOW DIAGRAM

THIS PAGE

WAS INTENTIONALLY

LEFT BLANK

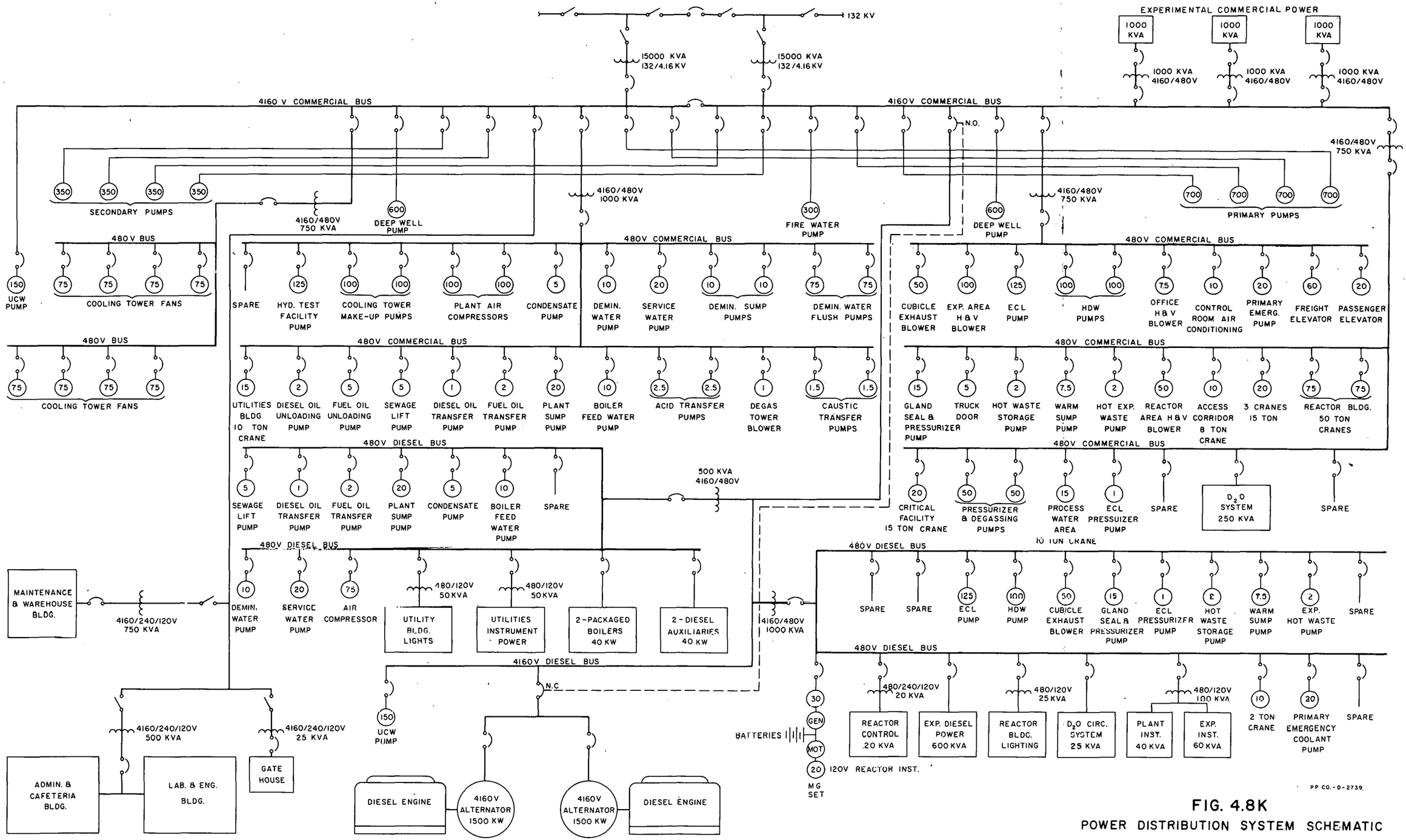

FIG. 4.8K

POWER DISTRIBUTION SYSTEM SCHEMATIC

THIS PAGE

WAS INTENTIONALLY

LEFT BLANK

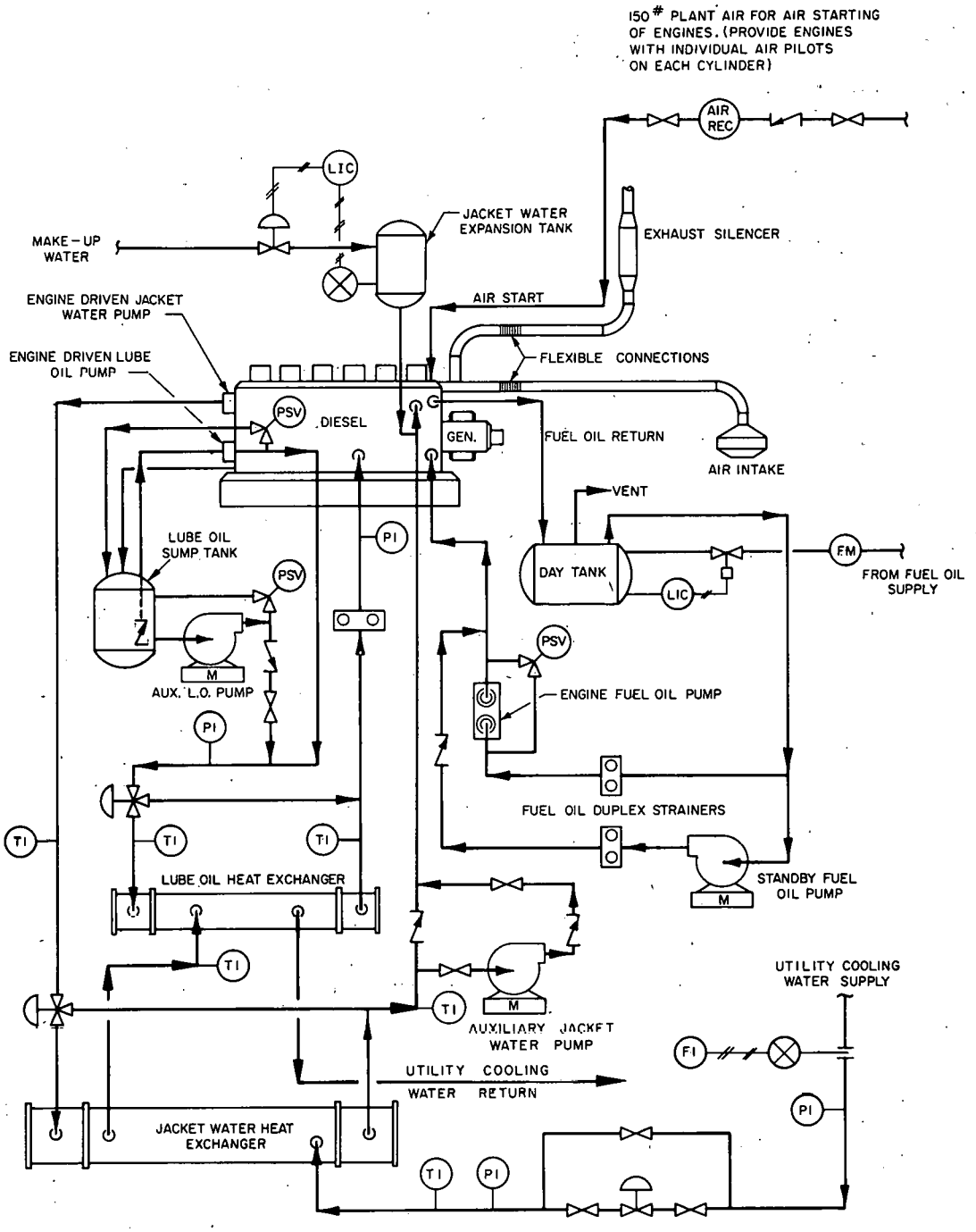

FIG. 4.8L

DIESEL GENERATORS

PROCESS FLOW DIAGRAM

P.P.CO.-C-2740

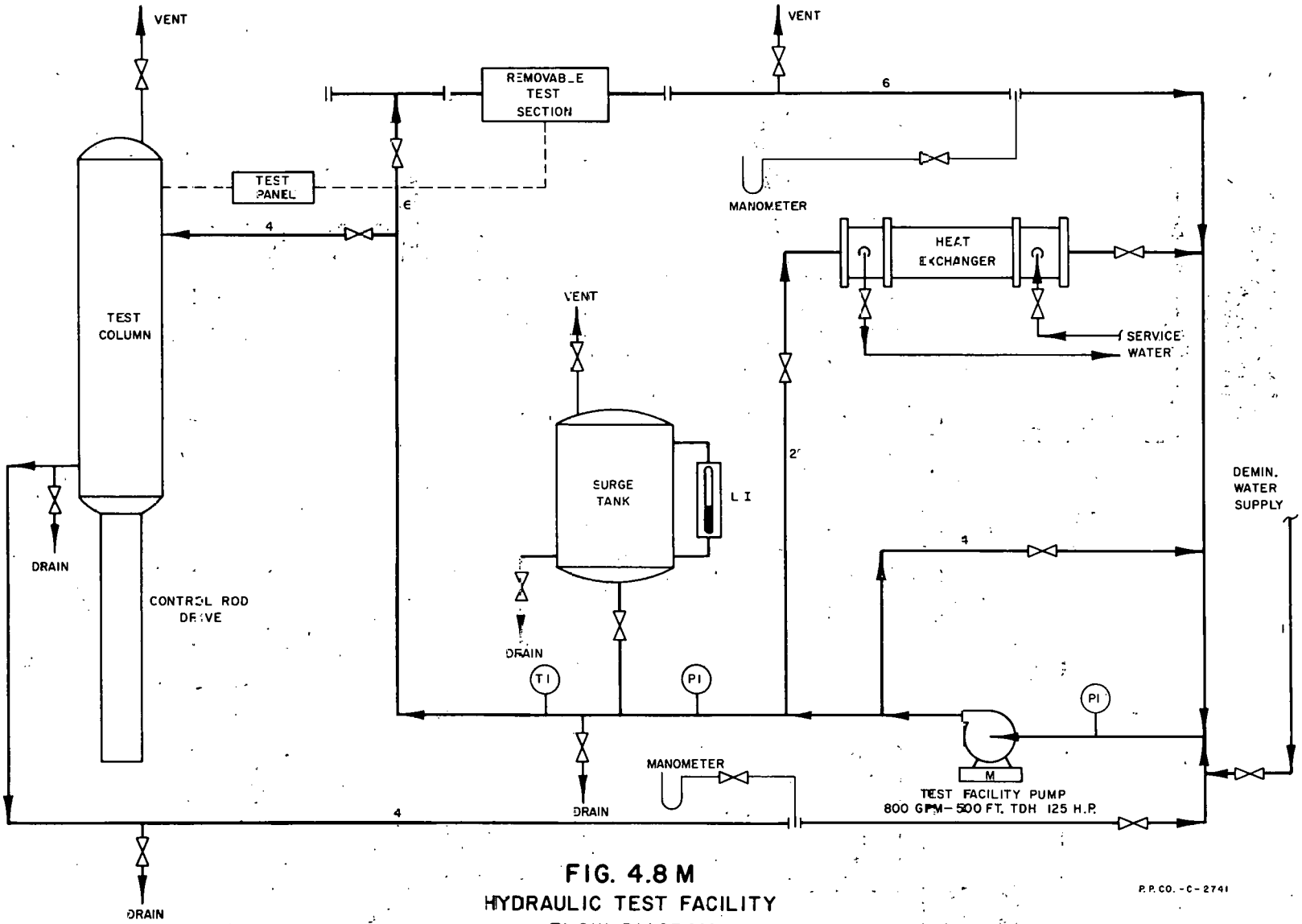

FIG. 4.8 M
HYDRAULIC TEST FACILITY
FLOW DIAGRAM

5.0 EXPERIMENTAL FACILITIES AND SERVICES

The reactor physics, mechanical layouts, supporting facilities and utilities are discussed in Sections 3.0 and 4.0. The purpose of this section is basically twofold:

1. to discuss the factors which led to the design criteria used in the other sections;

2. to describe the types of experiments which determined the design of the reactor.

5.1 Irradiation Facilities

As in all test reactors, samples are irradiated in these reactors in two different manners. The samples may be "capsules" which make use of the reactor process cooling water for heat removal or may consist of loop specimens which are essentially capsules irradiated in the high pressure water loops. One can refer to these two classes of experiments as capsules and "loop specimens", respectively, even though in some cases the capsule type may bear little resemblance to the simple sealed container which the word capsule brings to mind.

5.11 The Reactor Physics Model

In test reactor evaluation, it is extremely critical that the physics model be properly specified. This is true because of the nuclear coupling between the experiments and the test reactor itself and because the radiation characteristics of a test region are highly dependent upon the loading of the test region. For example, the neutron fluxes in a dummy filler piece in the ETR core bear little resemblance to the fluxes in typical experimental systems placed in the same hole. Physics calculations for this reactor have been made on the basis of typical high pressure water loops in the experimental holes. These loops consist of stainless steel tubes containing fuel samples. The quantity of fuel selected and the flux levels supplied are based on modern high flux testing requirements. It should be noted that both the thermal and the "fast" flux available are dependent on the annular filler media and that a variety of absolute flux levels and spectral combinations may be obtained for any particular experimental configuration by varying the annulus composition.

5.12 Capsule-Type Experiments

The concept of a capsule as used in this design is a very general one. The capsules may vary in length from a very short length to full core length; they may consist of "baskets of slugs"; they may or may not have leads (if so the leads are visualized as MTR-ETR type leads); sample diameter may vary up to 1.5 in. A capsule consisting of a number of instrumented subassemblies which must be removed from the reactor with leads intact for inspection or reassembly has also

been visualized, and provision has been made for removal of lead-type capsules and reinsertion with leads intact.

Leads are carried out through tank access nozzles to a capsule instrument panel in the second basement. Information from the capsules may also be processed in the data reduction system.

5.13 Loop Experiments - In-Pile Sections and Sub-Pile Room

The basic loop in-pile section around which this reactor is designed is a unit re-entrant from the reactor bottom head with reactor top cap penetration for experimental access (Fig. 5.1B). The tubes are insulated from the reactor water by conventional stagnant gas thermal barrier. Provision is made for shielded traps in the sub-pile room directly below the test sections. Allowance has also been made for a minimum of 1 in. of lead shielding around the experimental piping.

The test regions through the reactor core are sufficiently large to permit installation of in-pile tubes of this type having inside dimensions up to at least 2 in. in diameter. The test regions are isolated hydraulically from the reactor fuel and outside dimensions of the in-pile tubes need not meet rigid dimensional specifications. The material of construction considered for the in-pile tubes is Type 347 stainless steel. No prohibitive problems should be encountered due to gamma heat which is of the order of 20 watts/g.

The top closure plug of the loop is outside the reactor pressure vessel and reactor refueling operations and loop sample handling are relatively isolated from one another. Loop branch piping is carried from the in-pile tube to a piping corridor which surrounds the reactor.

Although the basic in-pile tube design is a unit re-entrant from the bottom, the reactor design includes access nozzles in the top of the pressure vessel and the pipe corridor also serves this region. This feature makes possible the design of experimental tubes re-entrant from the top and through loops which enter from the sub-pile room and exit from the upper nozzles or vice-versa.

5.14 Loop Piping Corridor

Around the reactor is a shielded loop piping corridor. In this area, loop piping may be manifolded, ECL tie-ins may be made, etc. This area provides isolation of a primary loop cubicle from the radioactively hot lines which exist when a loop's in-pile section is being operated on emergency cooling water.

5.15 The Loop Flow Diagram

The loop flow diagram, around which the reactor building and supporting facilities are designed, is shown in Fig. 5.1A. Scope of this conceptual design did not permit detailing the loop design, but a loop

of this basic type will permit satisfaction of all conventional 2200 psi loop requirements, i.e., all utilities, supporting facilities, and floor space are supplied and this basic loop design may be detailed using existing proven components.

The out-of-pile equipment which is visualized is capable of handling one in-pile tube 2 in. inside diameter having coolant requirements up to 150 gpm at 2200 psi and a total heat generation up to 3 Mw and maintaining conventional loop water quality. The loop would have excess cooling capacity to permit operation at low temperature about 350°F, at full power generation. This equipment could also be used to serve three or four manifolded 1 in. i.d. test loops having coolant requirements in the neighborhood of 35 gpm each and total heat generation of up to 750 kw each.

Six cubicle areas are supplied for installation of the loop equipment (see Section 5.21).

5.2 Space Allocations for Experimental Equipment

In view of the difficulties in installing, maintaining and modifying loop systems in confined areas, a special effort has been made to allow sufficient space for experimental equipment from the point of view of total square footage, geometrical configuration (e.g., minimum waste space at the "point" of pie-shaped cubicles), accessibility and proximity of the various operating areas.

5.21 The Primary Cubicles

For each loop over 750 sq ft of floor space of approximately rectangular geometry with a reasonable ratio of maximum to minimum dimension has been allocated for the loop primary cubicle. Each cubicle area contains a minimum square area of 28 ft x 28 ft. This is over 1-1/2 times the area occupied by the KAPL F-10 loop at the ETR. This area is directly adjacent to the piping corridor. Adequate floor loading will be determined in final design but should be in the order of 5000 lb/ft^2.

5.22 The Secondary (Sample) Cubicle

At least 300 sq ft of floor space directly adjacent to the primary cubicle has been allocated for a secondary cubicle to be used for the sample and the pressure instrumentation area. These areas have a minimum dimension of 10 ft on their shortest side. It is considered that the wall of the primary cubicle which is common to the secondary cubicle is accessible for primary cubicle reach rods.

5.23 Auxiliary Unshielded Equipment

At least 200 sq ft of floor space per loop has been allocated for make-up and other unshielded equipment. This space is located in the neighborhood of but not directly adjacent to the cubicle area.

5.24 Control Panels

Space is allocated for at least 30 linear ft of control panel per loop, on the same floor and in the neighborhood of the cubicle area. Suitable service and access aisles have been provided. An additional minimum of 75 sq ft of floor space has been allocated for electrical switchgear.

5.3 Supporting Facilities

Proper supporting facilities and utilities are extremely important to successful operation of a test reactor. This is particularly true during the early months of operation when oversights and inadequacies can become painfully obvious. Every effort has been made to supply all those items essential to the experimental program. (Since the discussion of the data processing system is presented in some detail, it is given in a separate section, Section 5.4.)

5.31 Analytical Laboratory

Sponsor laboratory space has been provided in the neighborhood of the sponsors offices and the experimenters canal.

5.32 Hot Cell

An experimenters hot cell has been provided. This hot cell is connected to the canal complex. Design specifications for this cell are based on the original MTR hot cell which has proved adequate for most sponsor type work.

5.33 Experimenters Canal

A section of canal for the exclusive use of the experimenters has been supplied. This canal is connected with the canal complex and is isolated from reactor operational activities.

5.34 Mockup and Pressure Test Area

A mockup and pressure test area is provided for pre-insertion assembly and testing. It was felt that a minimum of 4500 sq ft would be required since experimenters and operators, of necessity, utilize this floor space rather inefficiently (in terms of ordinary shop space). A portion of this area is isolated by a light blast shield for pneumatic testing.

5.35 Cranes

Two fifty-ton cranes with fine control on all three directions of motion are available in the reactor area and in the main canal area for handling of experimental casks. Five-ton cranes or lifts are supplied in the cubicle area. Forty-five feet of headroom is specified in

conceptual design for the heavy cranes. It is anticipated that in final design ample headroom will be allowed for discharge procedures planned at that time with a generous contingency for future discharge procedure modifications. A two-ton high crane is also included for the reactor area.

5.36 Warehouse

Warehouse facilities are extremely important since inadequate warehouse space results in inefficient operation of the experiments due to parts shortages. The warehouse included in design is visualized as containing conventional warehouse space, an isolated warm storage area for storage of contaminated reusable equipment and a cask storage area with facilities for handling and storing thirty-ton casks. The considerable headroom required by transfer casks should be kept in mind in final design.

5.37 Drafting and Reproduction

Necessary drafting and reproduction facilities for sponsor use should be included in similar plant facilities in final design.

5.38 Cask Transportation

Since site is unspecified, no provision has been made for long-haul or rail-head transportation. Facilities are supplied in the conceptual design for loading casks on trucks in the reactor building.

5.39 Hydraulic Test Facility

A hydraulic test facility for determining total flow and flow distribution within experimental test assemblies is provided.

5.310 Darkroom

Darkroom facilities for processing photographs and radiographs should be provided in final design.

5.311 Decontamination Room

A decontamination room for decontamination of experimental equipment is provided. This facility has been found very useful at MTR.

5.312 Communications System

The location of all experimental equipment for a given loop in one general area reduces the demands on the communications system but it is important that all areas containing experimental equipment be able to communicate with each other and with the reactor control room. The important outlying areas would include the reactor top, the tank nozzle area, the piping corridor and the sub-pile room.

5.313 Waste Disposal

The methods of waste disposal are a stack, underground storage and a burial ground for gaseous wastes, liquid wastes and contaminated or radioactive hardware, respectively.

Facilities for liquid waste storage and processing are sized on the basis of 250 gal loops. It was visualized that the initial fill of contaminated water in the loop could be cleaned up partially by ion exchange systems. Storage capacity in the amount of 5000 gal is supplied for this material. It was planned that radioactive wastes containing decontaminating solutions would be permanently stored. On the basis of four washes to decontaminate and one major decontamination per year for the plant, the 10,000 gal of capacity allocated amount to ten years storage.

5.4 Data Processing System for Experiments and Reactor Operations

The Data Processing System will consist of a high-speed-computer-base data system together with the required remote input stations located at each experiment area. The reactor will have a complete system for logging all required data; one electronic computer will carry out the computations. The accuracy of this system will in all cases be equal to or better than that which is available in analog instrumentation for similar measurements.

The reactor will have about six input stations located near the reactor process equipment and at the experimental facilities to receive up to 700 points of desired information from the reactor and its experimental facilities. The input stations will include precision temperature controlled junction boxes for thermocouple signals, pneumatic to electric transducers for any variable measured with pneumatic type instrumentation, and normal input terminals for electric signals already scaled to the data system input.

The Data System will provide the following functions: off-normal alarm scanning, output data logging on electric typewriters and computing.

5.41 Off-Normal Alarm Scanning

All inputs will be continuously scanned at a rate of 100 points/sec for any off-normal conditions as compared to preset values. If an alarm condition is detected, an identification light will come on as well as an audible alarm. When the channel returns to normal, the system will log out on an off-normal printer the time the channel went off-normal, the time it returned to normal and the maximum or minimum value attained during this time.

5.42 Data Logging

The system will log all channels in direct engineering units at various pre-selected time intervals. These recordings will be made on electric typewriters at a rate of 100 channels/sec from the system with

adequate buffer capacity so that the typewriters will operate at 2 channels/sec. In addition to the complete normal logging cycle, the system will contain a feature whereby any portion of the system inputs can be logged out on demand at any logging station. There will be logging stations at each major experiment control panel.

5.43 Computations

The system will contain a digital computer whereby normal operational computations such as heat flux, power generation, and fuel burnup can be computed from any input variable as well as manual entry constants. The selection of the manual entry constants in some cases will be a function of the input variables.

5.5 Utilities

The utilities are described in detail in Section 4.8. Only a few remarks need be made here.

5.51 The HDW System

The HDW (High Pressure Demineralized Water) system is designed primarily for the design shown in Fig. 5.1A, i.e., for a water-to-water heat exchange system. It does not preclude use of intermediate heat exchange media, but use of organic intermediates is a more expensive means of heat removal. The heat removal capacity of the HDW system is 16 Mw which closely represents the maximum capabilities of the loops and also allows for future expansion or conversion of capsule facilities to loops.

5.52 Emergency Cooling Loop (ECL) System

The ECL System is designed to have about 1-1/2 times the flow and heat load capacity of the ETR ECL. The reader may easily determine the many combinations of fueled and unfueled in-pile sections which this system can carry.

5.53 Failure Free Power

One important provision that may have been underestimated is that of failure free power. One tends to hold down the capacity of such power which is provided because of the high capital cost per kilowatt. This requirement should be studied very carefully in the final design.

5.54 Miscellaneous Utilities

It is not felt that more needs to be said about commercial power, instrument power, instrument air, low pressure demineralized water and utility cooling water (cooling tower water) than has been said in Section 4.8 except to make the statement which may be obvious, namely, that UCW may not be used as a substitute for HDW in water-to-water systems because of the stress corrosion problem.

5.55 The Cubicle Exhaust and Vent Header Systems

Cubicle exhaust and vent header systems are provided. The vent header system into which the experiment's pressure relief devices discharge is similar to the ETR system. A word about the design criteria for the cubicle exhaust system is in order, however. A total of 65,000 scfm will permit removal of 75 kw of loop heat as well as maintaining the required 150 ft/min air face velocity over openings in the cubicle.

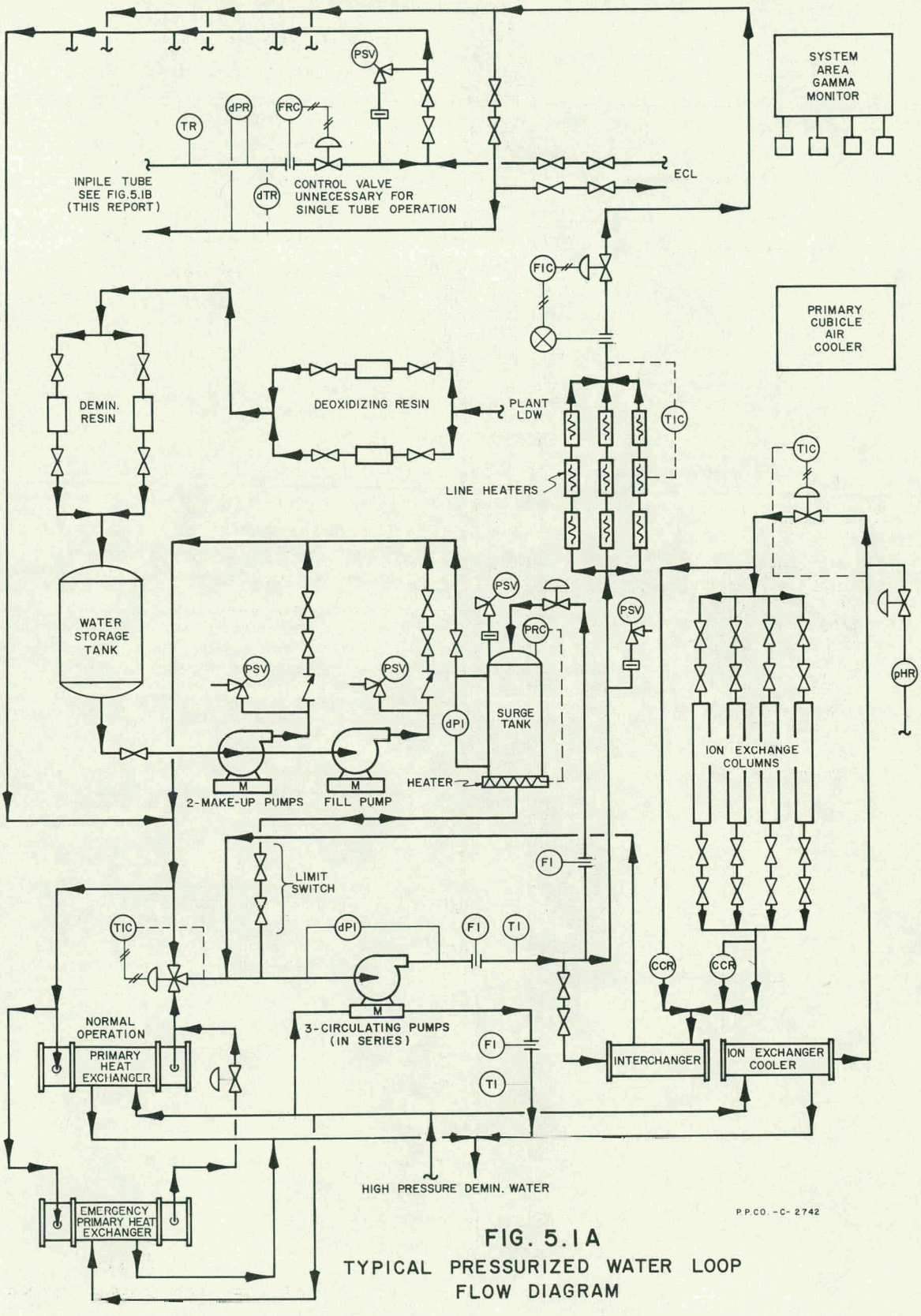

FIG. 5.1A
TYPICAL PRESSURIZED WATER LOOP
FLOW DIAGRAM

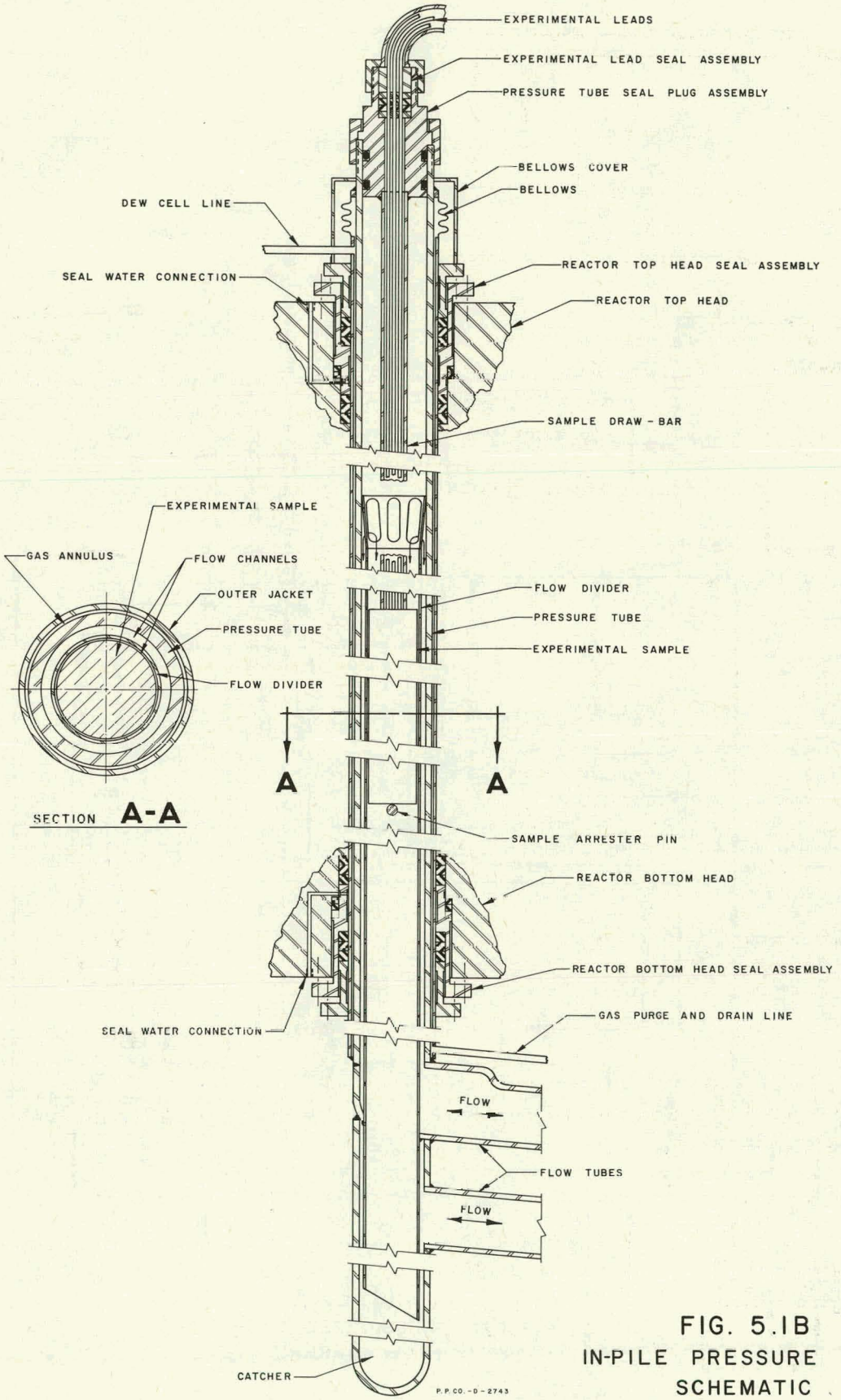

FIG. 5.1B
IN-PILE PRESSURE TUBE
SCHEMATIC

6.0 HAZARDS EVALUATION

6.1 Summary

The reactor proposed in this report utilizes design concepts which differ from those in existing testing reactors. This section considers only hazards that might arise from the unique features incorporated in the ETR II. Briefly, the areas where differences in behavior might be expected are:

1. Kinetics. Some differences are suggested because of the core material and its arrangement. The effects of these differences on the kinetics are discussed extensively in Section 6.21.

2. Transient Heat Transfer. Since portions of the core will operate at conditions nearer burnout than in ETR I, for example, the consequences of accidents involving loss of primary coolant flow and pressure, power overshoots, and accidental reactivity insertions are evaluated in Section 6.22.

3. Relation of Normal Radioactive Release to Side Location. Because there will be larger normal production of radioactive material (effluent fluids and hot waste) resulting from the operation of this plant than in the MTR and ETR, the site location with respect to disposal facilities is considered in Sections 6.31 and 6.32.

4. Abnormal Release of Fission Products. An accident involving such a release is considered in terms of the same occurrence in ETR I in Section 6.33.

A summary of the results of these studies is given here. The kinetic properties of the reactor result from the slowing down and diffusion times of neutrons in the D_2O reflector proposed. The effect of this holdup of neutrons is similar to the effect of the delayed emission of neutrons in the fission process, the differences here being two-fold: 1) the delay time is of the order of 1 msec, and 2) the number of such neutrons per fission is much larger than that of any known delayed neutron emitter.

In their study of single annulus reactors, the Internuclear Company[1] concluded that the effect of dropping the entire D_2O reflector was such as to produce a 30 per cent change in the reactivity. Roughly speaking this means that approximately 30 per cent of the neutrons, which would otherwise have been lost to the system, are returned by the D_2O reflector when it is in place. The kinetic studies which follow have used this figure of 30 per cent total leakage to demonstrate the properties that result.

---

1. C. F. Leyse et al., "An Advanced Engineering Test Reactor Design", Internuclear Company, Inc., Clayton, Missouri, Report AECU-3775, March 15, 1958.

If one considers the average fission neutron which goes out into the reflector, where it becomes thermalized and drifts back into the core, it is possible to speak of an "arrival" function which represents the average abundance as a function of time of slow neutrons returning to the core per fission event. Although the exact form of the arrival function is difficult to calculate, the kinetic behavior in the region of interest is not extremely sensitive to the particular form chosen. This has been demonstrated in the calculations of the transfer functions for several different arrival functions given in Section 6.21. It was found there that describing the behavior in terms of an equivalent seventh delayed neutron group was sufficiently accurate throughout the entire range of interest. On this basis it was found that the periods which are obtained in this system for a given reactivity step are much longer and hence more easily controlled than those of ETR I. Furthermore, because of the existence of negative void coefficients in the light water cooled fuel section, shutdown effects similar to those seen in BORAX will probably provide self-limiting behavior. In this respect ETR II appears to have the desirable long lifetime features of heavy water reactors and the prompt shutdown feature of light-water moderated systems.

In the case of loss of flow accidents, the time lapse between loss of flow and burnout is calculated to be more than 2 sec. The instruments which monitor reactor coolant flow initiate a full scram at some pre-set flow rate and if it is set at 90 per cent of full flow the safeties will begin the reactor shutdown in approximately 750 msec after loss of flow. (The scram which arises from loss of voltage to the pumps is actuated in a total of 350 msec.) Thus it seems that there is adequate time for the reactor power to be reduced to a negligible value in case of pump or motor failure. These calculations are based on actual measurements of the "coast down" of the ETR I coolant flow.

The calculations involving loss of primary coolant pressure were based on the formation of a 36 sq in. hole in the pressure vessel, somewhere above the core. Under these conditions the time lapse to burnout was calculated to be more than 7 sec. A reactor scram will be initiated by the monitoring instruments in less than 2 sec, which means that for this accident also, no damage to the reactor should occur.

Power overshoots can result from insertions of reactivity introduced either as ramps or steps. Detailed calculations have been performed using the reactor kinetics of the proposed reactor core and its heat transfer characteristics. The maximum step reactivity insertion which will not burn out the core, when operating at full power, is slightly above 0.3 per cent $\Delta k/k$. This maximum permissible step is only slightly less than the equivalent step for ETR I, and therefore appears to offer no unusual problem. From the above considerations, it appears that the reactor proposed in this report can be operated without any undue risk and can be protected adequately against the accidents resulting from malfunctions of reactor components or experiments.

The volume of radioactive effluent and hot waste from the reactor will require either its location near an authorized disposal area or the establishment of another such area.

The accidental release of an amount of fission products equal to 1 per cent of the core fission product inventory has been evaluated, and its associated hazard has been found to be similar to that of ETR I.

6.2 Reactor Behavior

6.21 Reactor Kinetic Properties

The factor in ETR II most likely to influence the short-term time response (and, therefore the high-frequency response also) is the large D_2O reflector. Neutrons which migrate into the reflector and return some time later to cause fissions exhibit properties similar to an extra group of delayed neutrons. The high bare leakage effect makes this a large group (about 30 per cent), with a time constant of about 1 msec. For the calculations, a seventh group with a delayed neutron fraction, β_7, of 0.3 and with an equivalent decay constant, λ_7, of 1000 sec^{-1} is used. Although methods exist for calculating both the frequency and time responses for six delayed groups, adding the seventh extremely large group produces its own difficulties.

The step-reactivity-time calculation is relatively easy to do, as is also the stable period (in-hour) reactivity relationship. If one assumes that there are six groups with a total delayed neutron fraction of $\beta_T = 0.0075$, plus an extra group of $\beta_7 = 0.3$, calculations reveal somewhat startling results. True prompt criticality now requires a 30 per cent reactivity insertion. Therefore, large (> 1 per cent) Δk excursions do not produce the short periods seen in a light water moderated and reflected system. Because of the short time constant of the seventh group, the behavior for small ($< .3$ per cent) Δk insertions is more like the conventional system except for a very short time after the insertion. After $1/\lambda_7$ seconds have passed, the transient power vs. time is only about a factor of two under the ordinary six delayed group case. The important fact, however, is that the power is truly less than that for the six group solution at any time, and the stable periods produced by step reactivities for the seven group case are always longer than those for the six group case. The results of some of these calculations are displayed as Figures 6.2A, 6.2B, 6.2C, and 6.2D, where Figures 6.2A through 6.2C are comparisons of stable periods for the six and seven group cases and in which the prompt neutron lifetime, ℓ, and λ_7 have been varied as parameters. These curves show the ratio of T_7/T_6, the stable periods of the two cases, versus reactivity necessary for those periods to be produced. Figure 6.2D shows the time-power curves for three cases of core kinetic parameters and two reactivities. These also confirm that the stable and transient (short time) periods are longer for the seven group cases, and that the resultant power of these reactors subjected to such reactivity steps is always lower than that of the reactor with no delayed seventh neutron group.

It has been the usual procedure in the past to set up a problem for either the ramp (runaway startup accident) or step-transient cases and solve the kinetic equations numerically with a digital computer program. The usual procedure is to allow k(t) to follow a ramp or step up to the time at which a level scram--pre-set at some n(t)--is assumed to insert the safety rods to reduce reactivity at a given rate. This will begin only after some small delay has been overcome; this delay being, for example, the release-time of an electromagnet employed to hold safety rods out of the core, as in the MTR. Estimated release time for the ETR II has been used in this report. The numerical integration programs in use, however, do not readily lend themselves to the seven group cases because of the way the computer program works. When this was discovered, a different attack was used. If the reactor kinetic equation in integral form is expressed:

$$n(t) = 1 + \int_o^t G(t-\tau)\, K(\tau)\, n(\tau)\, d\tau,$$

where G is a function of λ, β, and ℓ, a comparison of two of these integrals can be made:

$$n(t) = 1 + \int_o^t G\,(t-\tau)_7\, K(\tau)\, n(\tau)\, d\tau =$$

$$1 + \int_o^t G\,(t-\tau)_6\, K(\tau)\, n(\tau)\, d\tau,$$

wherein the parts under the integral are made numerically equal by adjusting the lifetime associated with the six group kernel. Solution of two cases (shown in Fig. 6.2E) shows that the seven group transient case of prompt neutrons lifetime $\ell_{(7)}$ of 5×10^{-5} sec behaves much the same as a six group case in which the prompt lifetime is assumed to be 3.3×10^{-4} sec.

Using this method of normalization, the complete time transients were computed for step transients of 0.3, 0.4 and 0.5 per cent reactivity. These curves are drawn in Fig. 6.2F. These curves are the ones from which some of the calculations in Section 6.22 were made. Calculations of the "startup accident" using the same parameters as in those of Fig. 6.2F appear in Fig. 6.2G for three possible ramp rates.

Since the reactor will have an automatic power level controller the frequency response was also calculated and appears in Fig. 6.2H for several cases. The curves of reactor transfer function amplitudes and their phase angles are shown compared with the ordinary six group case. Cases are calculated assuming the seventh group is simply delayed 10^{-3} sec with no decay (Case 2, Fig. 6.2H), and is delayed 10^{-4} sec and decays as $e^{-\lambda_7 t}$, where $\lambda_7 = 1000$ sec^{-1} (Case 3, Fig. 6.2H). These curves reveal two bits of information. The first is that the amplitude response of the seven group reactor is lower than that of the six group case in the region of interest, and secondly, that the most

pronounced effect of case 2 is at very high frequencies. The resonant peaks in one set of the transfer function curves result from case 2 above wherein no decay is allowed, but the reflector neutrons are simply returned after t sec. It is believed that this does not truly describe the situation and is shown only for academic interest and for comparison with the other cases. Selection of an appropriate model for such calculations is always difficult.

Some conclusions that may be drawn from the investigation, however, are listed below:

1. The reactor is less sensitive to small reactivity changes, i.e., it is "less touchy",

2. A low performance (and therefore less expensive) power level controller can be used successfully on this reactor.

3. The poisoned reflector type of reactivity shimming can be used in the day-to-day operation.

In high-flux thermal reactors the possibility of xenon instability is present under certain conditions. The proposed reactor is one in which the coupling between the various parts of the core is certainly less than it is in the MTR, for example. It is felt, however, that the coupling is tight enough to avoid the effects of xenon instability. This problem must be thoroughly investigated when the engineering design is begun.

6.22 Transient Heat Transfer

The reactor concept proposed presents transient problems which have not been duplicated by any operating research reactor. To meet the specifications in the testing facilities, the reactor must operate closer to the burnout point. The purpose of the transient heat transfer calculations is to define the margin from burnout that can be expected and to determine if presently available instrumentation will adequately protect the reactor.

There appears to be two consequences of reaching the burnout condition: 1) release of fission products and fissile material to the primary coolant, and 2) the possibility of an aluminum-water reaction with a resulting large release of energy. The admission of minute quantities of fission products and fissile materials into the primary coolant does not constitute a hazard since the light water cleanup system will adequately purify the water; this comment is based on ETR and MTR experience where such accidents are relatively commonplace. However, the burnout of a portion of a fuel plate probably results in the release of radioactivity several orders of magnitude greater than that involved in the ETR and MTR experiences. It is obviously prudent to avoid the burnout condition during any event. Operation in the nucleate boiling regime during a transient does not present any hazard since the consequences of such an activity do not appear to be hazardous.

The thermal shock that the fuel plates undergo during nucleate boiling operations is not severe apparently as evidenced by experience in the ORR and the MTR.

There are several accidents which are considered credible. They are: 1) loss of primary coolant flow, 2) loss of primary coolant pressure, and 3) an accidental power overshoot consisting of either a ramp insertion of reactivity at startup with failure of all but the top level scram or a step insertion of reactivity while operating at full power.

The loss of flow accident generally occurs because of a fault in the electrical power supply to the site. Other possibilities include the overloading of one primary circulating pump and its subsequent stoppage, failure of the main flow control valve and accidental closure or failure of one of the main block valves.

Loss of primary coolant pressure may be caused by rupturing any of the primary components, cracking a weld or the like.

An inadvertent raising of the reactor power by the operator could cause a power overshoot. Increasing the reactor power too rapidly may also result in an overshoot.

The stepwise positive addition of reactivity may occur during the removal or insertion of an experimental assembly while the reactor is operating at full power.

Burnout heat fluxes for all cases were calculated by the extended method of Bernath[1]. The set of equations is given below.

$$(Q/A)_{BO} - h_{BO} (T_w - T_b)_{BO} ,$$

where

$(Q/A)_{BO}$ = the heat flux at burnout, PCU/hr-ft^2 ,

$T_{w_{BO}}$ = wall temperature of the fuel element at burnout, ^{o}C, and

$T_{b_{BO}}$ = bulk water temperature at burnout, ^{o}C.

h_{BO}, the film coefficient at burnout in PCU/hr-ft^2-^{o}C is given by:

$$h_{BO} = 10,980 \left[D_e / (D_e + D_i) \right] + 48v/(D_e)^{0.6} ,$$

where

v = coolant velocity, ft/sec,

---

1. L. Bernath, "A Theory of Local Boiling Burnout and Its Application to Existing Data", proceedings of 3rd National Heat Transfer Conference, August 1959.

D_e = hydraulic diameter, ft, and

D_i = heated diameter = heated perimeter/π, ft.

$T_{w_{BO}}$ is given by:

$$T_{w_{BO}} = 57 \ln P - 54 P/(P + 15) - v/4,$$

where

P = pressure at the burnout point, psia.

Heat fluxes by this method were multiplied by 0.6 to allow for error in fitting to the data. The calculation, therefore, is probably conservative.

6.221 Loss of Flow Accidents

The calculations for this incident involve determining the velocity and corresponding bulk water temperature at which the burnout heat flux is equal to the operating heat flux. The burnout heat flux as a function of velocity is calculated, and from the flow coastdown curve and these calculations the time to burnout after power failure is determined. Many flow coastdown characteristics for the ETR I system have been measured using rapid response instrumentation. These curves were normalized and taken as representative for ETR II. This coastdown curve is presented in Fig. 6.2I. It has been found that the fraction of operating flow at times greater than 1 sec after pump failure in ETR I is independent of the operating flow. The measurements in ETR I should represent a good approximation of the conditions in ETR II because the primary coolant systems are expected to be similar.

The results of these calculations are summarized in Table 6.2A, and in Figure 6.2J. The time elapsed between loss of flow and burnout is greater than 2 sec. Shutdown of the reactor by means of a full scram can be accomplished within this time increment using commercially available instrumentation. The electrical power frequency can be sensed and a scram initiated following a fault in the electrical supply in 350 msec. Actual measurements of the time required to activate the frequency devices in service at ETR I have established this number. Commercially available differential pressure measuring devices are also used to protect the reactor in the event of loss of flow. The differential pressure across the reactor core is used as the primary measurement; a scram is initiated in 1 sec by these devices; this time increment is again based on measured values.

It is concluded that ETR II can be adequately protected from a loss of flow accident. It is possible that some nucleate boiling will occur during the transient, but this is not considered to be hazardous.

TABLE 6.2A

COMPARISON OF OPERATING CONDITIONS AND BURNOUT CONDITIONS

Operating power level, Mw	250
Radial max/avg power	1.56
Channel hydraulic diameter, ft	0.01258
Inlet pressure, psig	300
Coolant velocity, ft/sec	40
Nominal hot channel heat flux in millions of Btu/hr-ft^2	0.93
Nominal hot spot heat flux in millions of Btu/hr-ft^2	1.303
Burnout heat flux at normal operating conditions in millions of Btu/hr-ft^2	3.55
Ratio of burnout power at normal operating condition to normal operating power	2.725
Hot spot heat flux at burnout power level (caused by power excursion, including effect on bulk temperature) in millions of Btu/hr-ft^2	2.08
Ratio of burnout power (caused by power excursion) to normal operating power	1.595
Time to burnout after pump failure, sec	2.75
Coolant velocity at burnout resulting from pump failure, ft/sec	23.8

6.222 Loss of Pressure Accident

In order to evaluate this accident the time delay from the rupturing of the pressure vessel, above or below the core, or the inlet or outlet coolant lines to burnout is calculated from the data of Table 6.2B and the assumptions of Table 6.2C. As shown below, ETR II is adequately protected from a loss of pressure accident.

Pressure at Which Burnout Occurs. The Bernath burnout correlation, minus a 40% safety factor, is used to calculate the pressure at which burnout occurs.

$$(Q/A)_{BO} = (Q/A)_{max} = 1.303 \times 10^{6} \text{ Btu/hr-ft}^2$$

$$= (0.6)\,(1.8 \text{ Btu/PCU})\, h_{BO}\, (T_{w_{BO}} - T_{b_{max}}) \qquad (1)$$

$$T_{w_{BO}} = 57 \ln P_{BO} - 54\, P_{BO}/(P_{BO} + 15) - V/4 \qquad (2)$$

T is in ^{o}C
P is in psia
V is in ft/sec
h is in PCU/hr-ft^2-^{o}C

Substitution of Equation 2 into Equation 1 yields:

$$(Q/A)_{max} = (0.6)(1.8)(h_{BO})(57 \ln P_{BO} - 54\, P_{BO}/(P_{BO} + 15) - V/4 - T_{b_{max}}). \qquad (3)$$

Since all other quantities in Equation 3 are known (see Table 6.2B), P_{BO} may be calculated. The pressure existing above the core when burnout occurs is $P_{BO} + \Delta P_{hot\ spot}$. As shown in Fig. 6.2K, burnout occurs at 101.5 psig.

System Pressure Change After Rupture, as a Function of Time. The water lost from the system as a function of time, which is also the increase in air volume in the surge tank is given by:

$$V_{t+\delta t} = \delta t A \sqrt{2 \Delta P g} + V_t \ , \qquad (4)$$

where δt is a time interval in sec.

The initial pressure above the core is essentially the same as the pressure in the surge tank, i.e., 312.5 psia or 300 psig. The pressure-volume relationship of the air is given by the perfect gas law:

$$PV = nRT \ . \qquad (5)$$

Since n, R and T are all constant the pressure, at any time, is related to the initial pressure by:

$$P_t = P_o \left(\frac{V_o}{V_t + V_o} \right) \ , \qquad (6)$$

TABLE 6.2B

SYSTEM DATA AT NORMAL OPERATIONS

P_{inlet}	= 300 psig = 312.5 psia
$T_{w_{max}}$	= 404°F (calculated from hot-spot hot-channel analysis)
$P_{hot\ spot}$	= 259.5 psig
$(Q/A)_{max}$	= 1.303×10^6 Btu/hr-ft^2 (calculated from hot-spot hot-channel analysis)
D_e	= 0.01258 ft
D_i	= 0.197 ft = heated perimeter/π
v	= 40 ft/sec in the core*
h_{BO}	= $10{,}980 \frac{D_e}{D_e + D_i} + \frac{48v}{D_e^{0.6}}$ = 27,186 PCU/hr-ft^2-°C (Bernath correlation)
$T_{b_{max}}$	= 137°C (calculated from hot-spot hot-channel analysis) = 228°F
$T_{b_{inlet}}$	= 130°F
$\Delta P_{hot\ spot}$	= 312.5 -259.5 = 53 psi
Volume of surge tank	= 2000 gal.
Volume of air in surge tank	= 1333 gal = 178.3 ft^3

* A velocity of 40 ft/sec was used in the hazards evaluation instead of the design value of 44 ft/sec in order to obtain a more conservative hazards evaluation in case the final operating coolant velocity is less than the design value.

TABLE 6.2C

ASSUMPTIONS USED IN CALCULATING LOSS OF PRESSURE ACCIDENT

1. The maximum credible loss of pressure accident would be a rupture in the inlet line or the pressure vessel above the core.

2. A complete fracture and displacement of the inlet line is not considered credible.

3. A fracture resulting in a 36 in^2 hole in either the pressure vessel above the core or the inlet coolant line will be considered as the maximum credible accident.

4. The loss of pressure rate will be the same for the same size fracture in the pressure vessel above the core as for the inlet coolant line fracture.

5. The loss of coolant through the fracture may be calculated by assuming that the hole is equivalent to an orifice of 36 in^2 area and using the following equation:

$$V = AC\sqrt{\Delta P(2g)}$$

V = volume rate of coolant, ft^3/sec

C = discharge coefficient = 1

ΔP = pressure differential across the fracture in ft of H_2O

g = gravitational constant

A = area of fracture, ft^2

6. The coolant velocity through the core, the core power and the inlet coolant temperature remain constant during the loss of pressure; in fact, the coolant velocity decreases only slightly.

7. The surge tank responds instantaneously to any change in pressure of the coolant system.

8. The water and air in the surge tank are at the same temperature and pressure as the coolant entering the reactor.

9. The "perfect gas law" is correct for calculating P vs. V for air.

10. The effect of the system pressurizer pumps is neglected. (It takes 3 sec for the pressure loss to be detected and for the back pressure valve to close and the pumps to start.)

where V_t is the volume of water lost up to time t as determined by Equation 4 and $V_t + V_o$ is the volume of air at time t.

The volume of coolant discharged is calculated from Equation 4 starting at the time of rupture and using small time increments. The resulting pressure is calculated from Equation 6. Burnout occurs when P_t equals the pressure calculated to exist above the core at burnout ($P_{BO} + \Delta P_{hot\ spot}$). Pressure is plotted as a function of time in Fig. 6.2K and the time delay from rupture to burnout may be read directly from the curve. The figure indicates more than a 7 sec delay at full reactor power. A reactor scram can be initiated in about 2 sec, because the pressure falls about 20 per cent in the first second and thus actuates the pressure sensing instrumentation which has a time delay that should be somewhat less than 1 sec. Therefore, the reactor is adequately protected from a loss of pressure accident.

6.223 Accidental Power Overshoot

The accepted practice is to set the neutron safety levels at 1.3 times the full power level (N_f). This power level is well below the burnout value at operating coolant velocity and inlet temperature. The burnout flux is compared with the operating flux in Table 6.2A as an indication of the margin of safety during operation. Two possible methods of causing a power overshoot have been analyzed, the power overshoot resulting from a ramp insertion of reactivity at startup and that resulting from a stepwise insertion of reactivity while operating at full power. These situations represent the most severe accident believed credible. The nature of these power transients is discussed in Section 6.21.

Ramp Insertion of Reactivity. The ramp accident assumes that at source power (criticality) the rods begin driving in as a gang and that all scrams except the highest level scram, i.e., 1.3 N_f, fail. The relative power as a function of time is given in Fig. 6.2G for ramp insertions of 0.10, 0.15 and 0.20 per cent $\Delta k/k$/sec. The scram level, shown as a relative power of 10^6, is 1.3 N_f or 1.695×10^6 Btu/hr-ft^2 at the hot spot. Burnout occurs at 2.08×10^6 Btu/hr-ft^2 or at a relative power of $(2.08 \times 10^6/1.695 \times 10^6)\ 10^6 = 1.23 \times 10^6$. Figure 6.2G shows that the maximum ramp insertion that doesn't exceed burnout, i.e., $n/n_o = 1.23 \times 10^6$, is 0.1 per cent $\Delta k/k$/sec. This value has a safety factor in that the reactor self regulation, i.e., the temperature coefficient, has been intentionally neglected. If the rod drive rates are such that a ramp insertion of more than 0.1 per cent is possible, lower scrams must be operative to prevent reactor failure.

Stepwise Insertion of Reactivity. The most severe result of stepwise insertion of reactivity occurs at full power. A reactor scram is initiated at the upper level scram setting of 1.3 N_f.

Power transients produced by 0.3, 0.4 and 0.5 per cent $\Delta k/k$ step insertions are presented in Fig. 6.2F. The effect of 0.3 and 0.4 per cent step insertions on the reactor cooling has been calculated assuming that: 1) the burnout condition predicted by the Bernath

Equation represents the condition in which the boiling film completely blankets the surface, and 2) after burnout occurs negligible heat is transferred. The hot spot heat flux, at any time during the transient, is obtained from the normal operating hot spot heat flux by multiplying by the power ratio existing at the time in question.

$$Q/A_{\text{hot spot}}\ (\theta) = n/n_o\ (\theta)\ Q/A_{\text{normal hot spot}} \qquad (7)$$

The hot channel bulk water temperature rise is obtained as follows:

$$\Delta T_{b_{\text{transient}}} = \Delta T_{b_{\text{operating}}} \left[\frac{\int_{\theta-\theta t}^{\theta} \frac{P}{P_o}\, d\theta}{\theta_t} \right], \qquad (8)$$

where

θ = time,

P/P_o = ratio of power at time θ to the normal operating power (Fig. 6.2F),

θ_t = transient time of a water particle from inlet to hot spot, and

ΔT_b = hot channel bulk water temperature rise from inlet to hot spot.

Using Bernath's Equation, with the bulk water temperature calculated for the hot spot as shown above, the burnout heat flux may be calculated at any time during the transient. Burnout occurs when the hot spot heat flux equals the burnout heat flux. After burnout occurs and until the hot spot heat flux is again less than the burnout heat flux, all of the heat is assumed to be absorbed by the plate thereby increasing its temperature. The peak temperature of the plate is given by:

$$T_{\text{peak}} = T_{w_{BO}} + \int_{\theta_{BO}}^{\theta} \frac{Q/A\ (\theta)\ d\theta}{C_A}, \qquad (9)$$

where

C_A = the heat capacity of a square foot of plate surface,

Q/A and $(Q/A)_{BO}$ are determined from Equations 3, 7, and 8 and are shown in Fig. 6.2L and 6.2M for 0.3 per cent and 0.4 per cent step insertions.

In the transient produced by the insertion of 0.4 per cent reactivity, the burnout condition is reached in about 90 msec and Equation 9 indicates a peak temperature of 1125°F; this temperature is essentially the melting point of aluminum. Therefore,

a step insertion of reactivity of 0.4 per cent during operation at full power cannot be tolerated. Burnout is not reached when 0.3 per cent $\Delta k/k$ is inserted. The insertion of 0.3 per cent positive reactivity would not result in either a release of fission products into the primary coolant or a metal-water reaction and should therefore be safe. This value has the same safety factor as the ramp insertion, i.e., the reactor self regulation due to its negative temperature coefficient has been purposely neglected.

6.3 Effluent Control and Area Location

Effluent control and solid wastes are of concern in the location of a reactor plant, along with an evaluation of the behavior of an airborne cloud of fission products which would be produced by an incident involving the reactor.

6.31 Liquid Waste

The largest contributor of liquid waste is the reactor coolant system under normal conditions. The second largest source is the complement of loop experiments. Discharge of radioactive liquid from the reactor and loops is discussed in Section 4.8. Hazards to the reactor and experimental equipment from the loops themselves cannot be fully evaluated here. Three experiments approved for insertion in the MTR-ETR have been selected as ones more or less typical of the type proposed for ETR II, and their hazards studies are offered as references in which the problems involved are well handled and for which detailed analyses have been made:

1. S. Cohen, GEH-ETR-6 x 9, IDO-16506,
2. R. J. Flygare, ETR Hazards Study of KAPL F-10, IDO-16507, and
3. R. L. Gump, ETR Hazards Analysis of WAPD-M-13, IDO-16503.

6.32 Solid Waste

It is concluded from experience that the reactor will produce large amounts of radioactive trash in the form of capsules, fuel element end boxes, parts of loop experiments, etc. These and the large quantities of blotting paper and other decontamination aids must be transported to an authorized AEC burial ground. It is desirable, therefore, to consider the proximity of the nearest burial ground to any proposed reactor location.

6.33 Gross Fission Product Release

According to the established custom in the preparation of hazards analyses for reactors of this type, the location of the test reactor must be studied in deail in regard to the exposure of off-site personnel. It is important--particularly in the hypothetical incident in which a large amount of fission products could be released

in one act to the atmosphere--that the site be located so as to keep the off-site exposure below the established maximum. Site location of the plant in this respect would necessarily follow the same considerations posed for the MTR and ETR. The meteorology of the selected site will be a prime consideration, of course, and such a study cannot be included in the scope of the conceptual design report. Exposures to on-site personnel will be controlled by existing AEC regulations and personnel monitoring would proceed as it does in the MTR-ETR complex.

Since the reactor operates at a power only slightly higher than ETR I, an accident to the reactor resulting in exposure to off-site personnel would be expected to bring about the same exposure as could be expected from such an accident in ETR I.

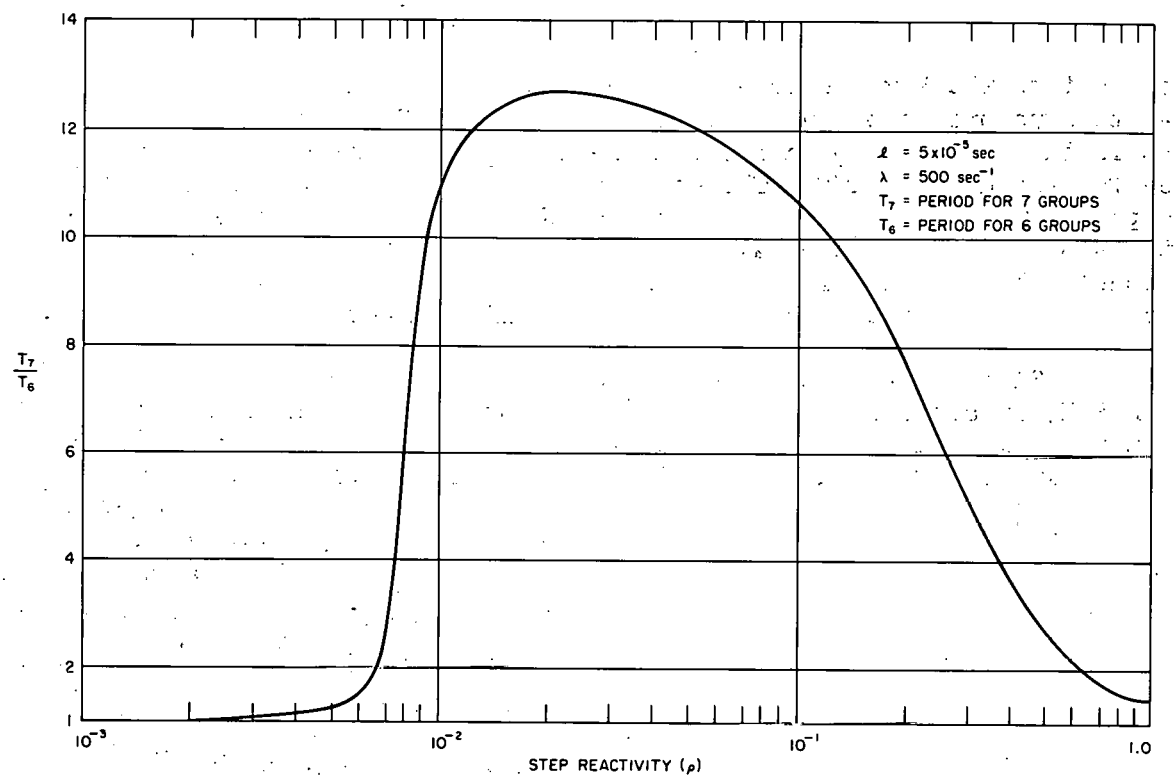

FIG. 6.2 A

RATIO OF STABLE PERIODS vs. REACTIVITY STEP

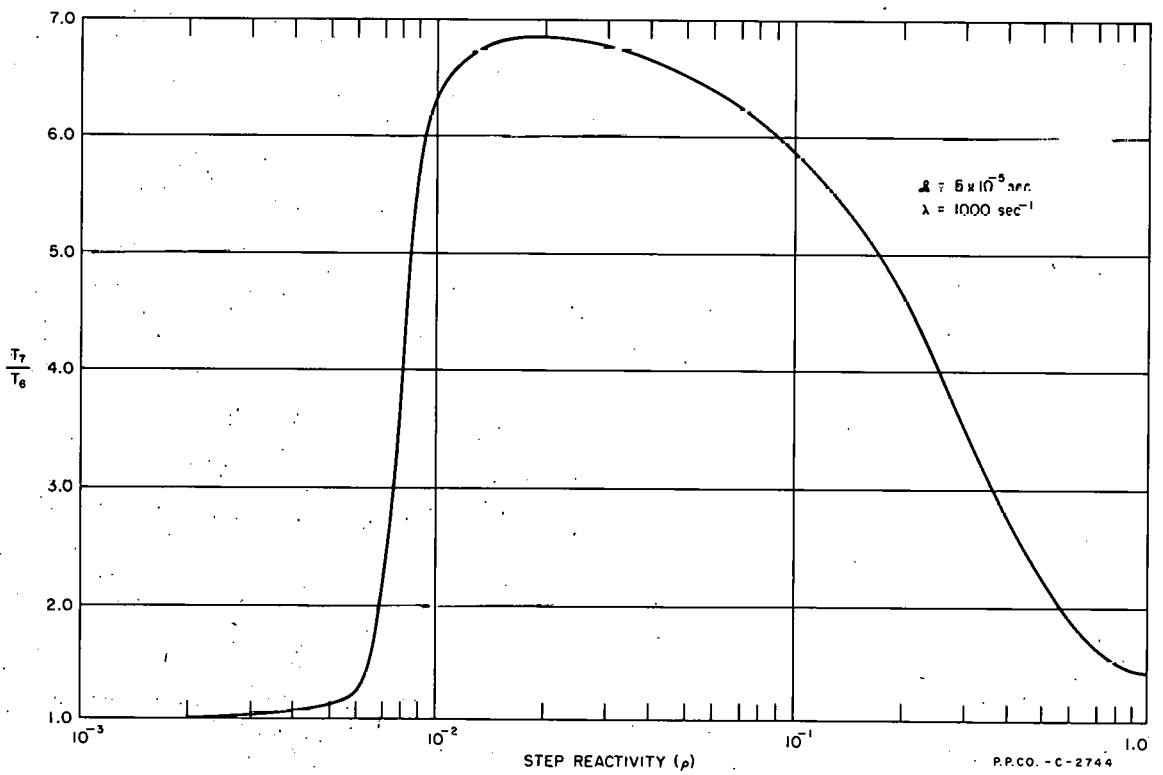

FIG. 6.2 B

RATIO OF STABLE PERIODS vs. REACTIVITY STEP

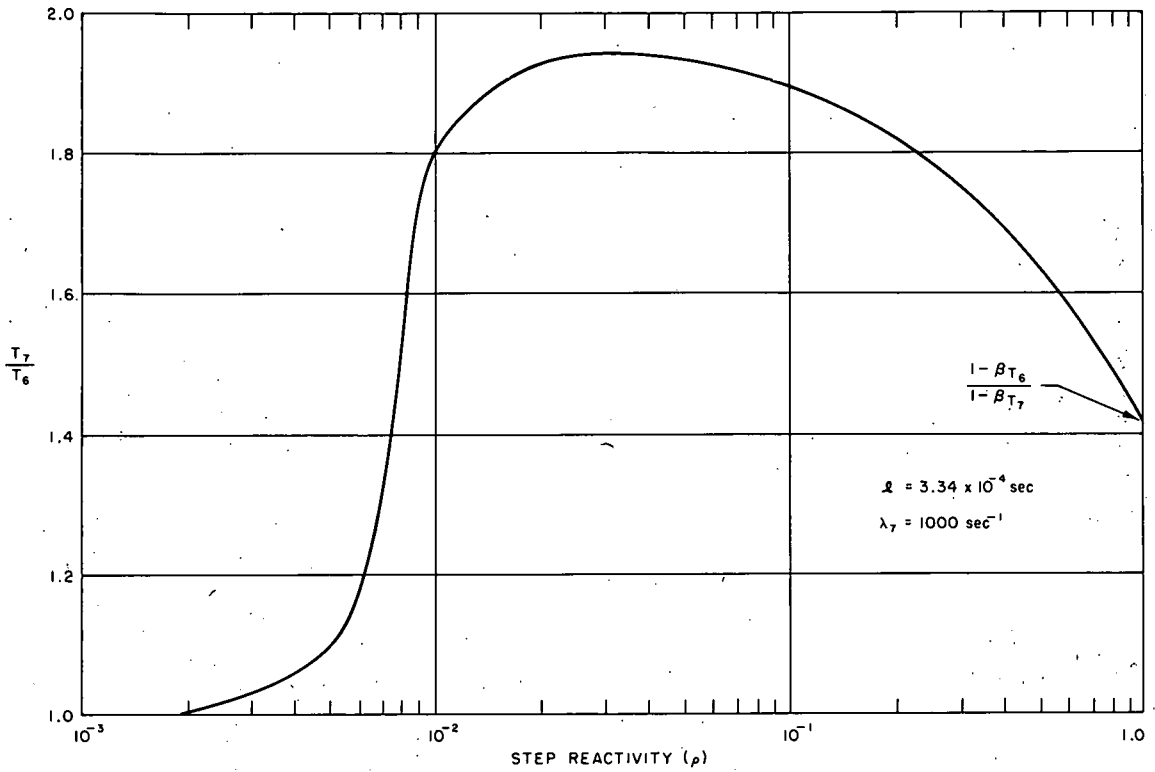

FIG. 6.2 C

RATIO OF STABLE PERIODS vs. REACTIVITY STEP

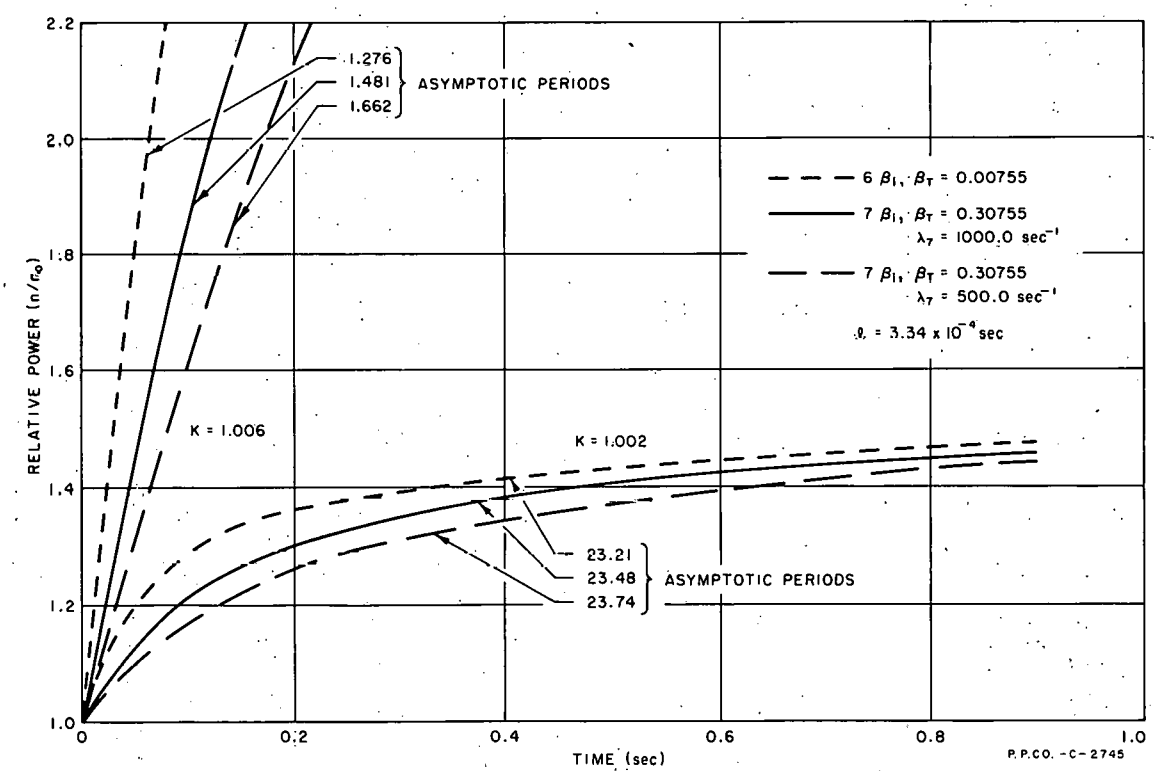

FIG. 6.2 D

COMPARISON OF STEP TRANSIENTS FOR TWO REACTIVITIES

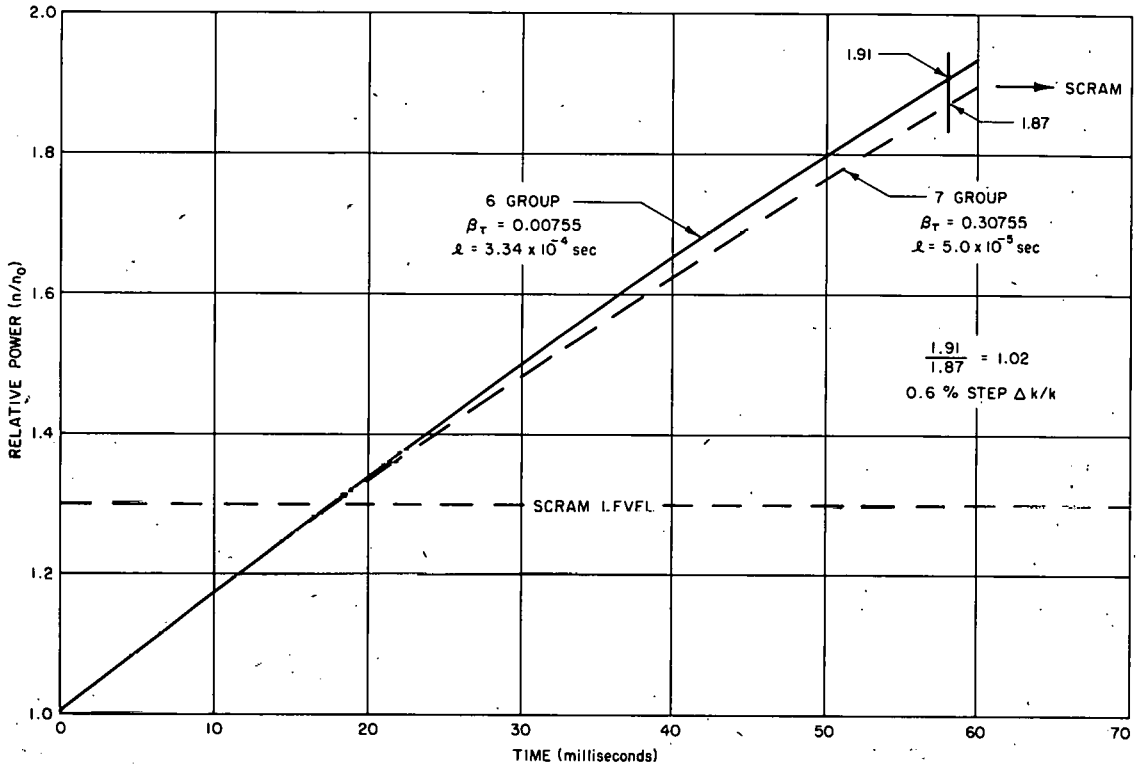

FIG. 6.2 E

COMPARISON OF STEP TRANSIENTS FOR SIX AND SEVEN GROUPS

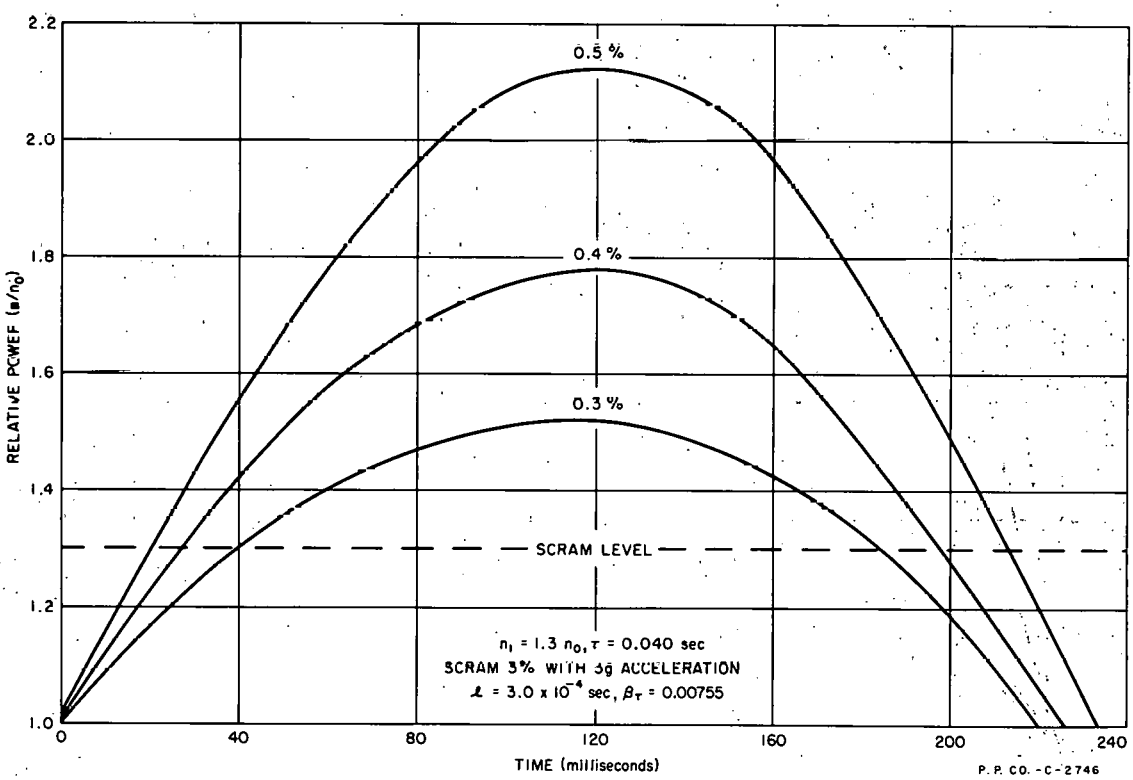

FIG. 6.2 F

STEP REACTIVITY TRANSIENT POWER OVERSHOOTS

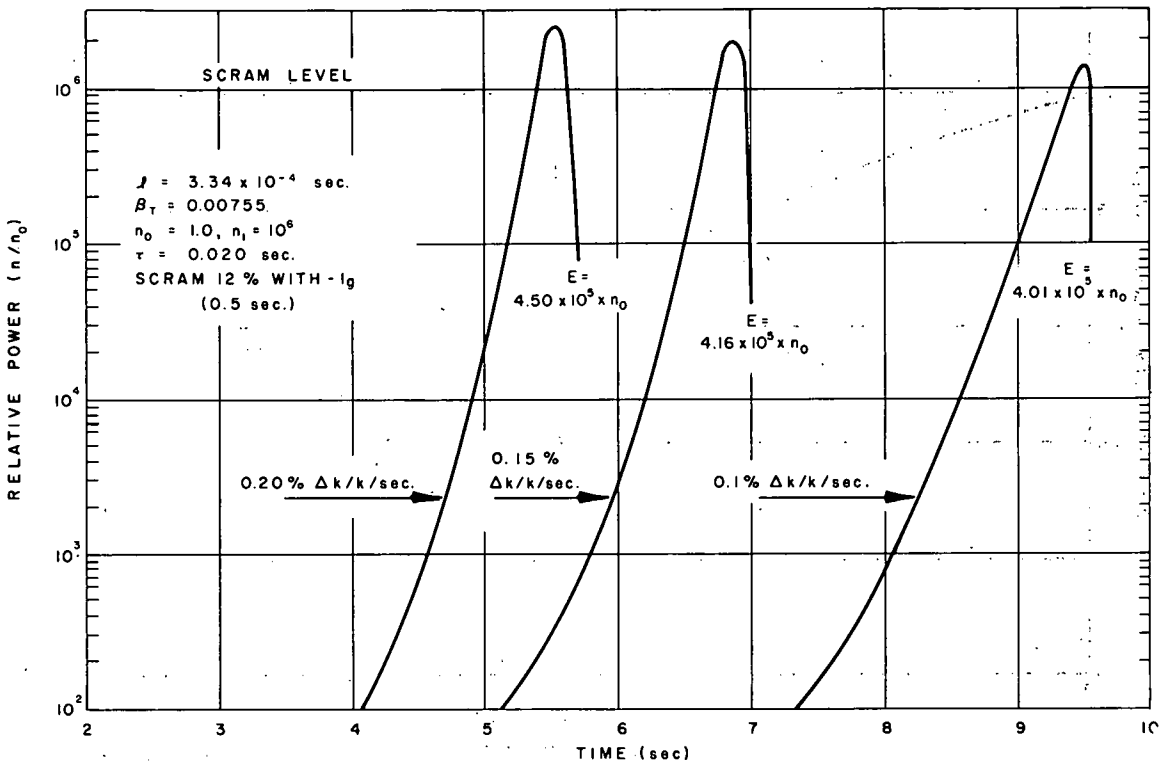

FIG. 6.2G

STARTUP ACCIDENT POWER CURVES FOR THREE RAMP RATES

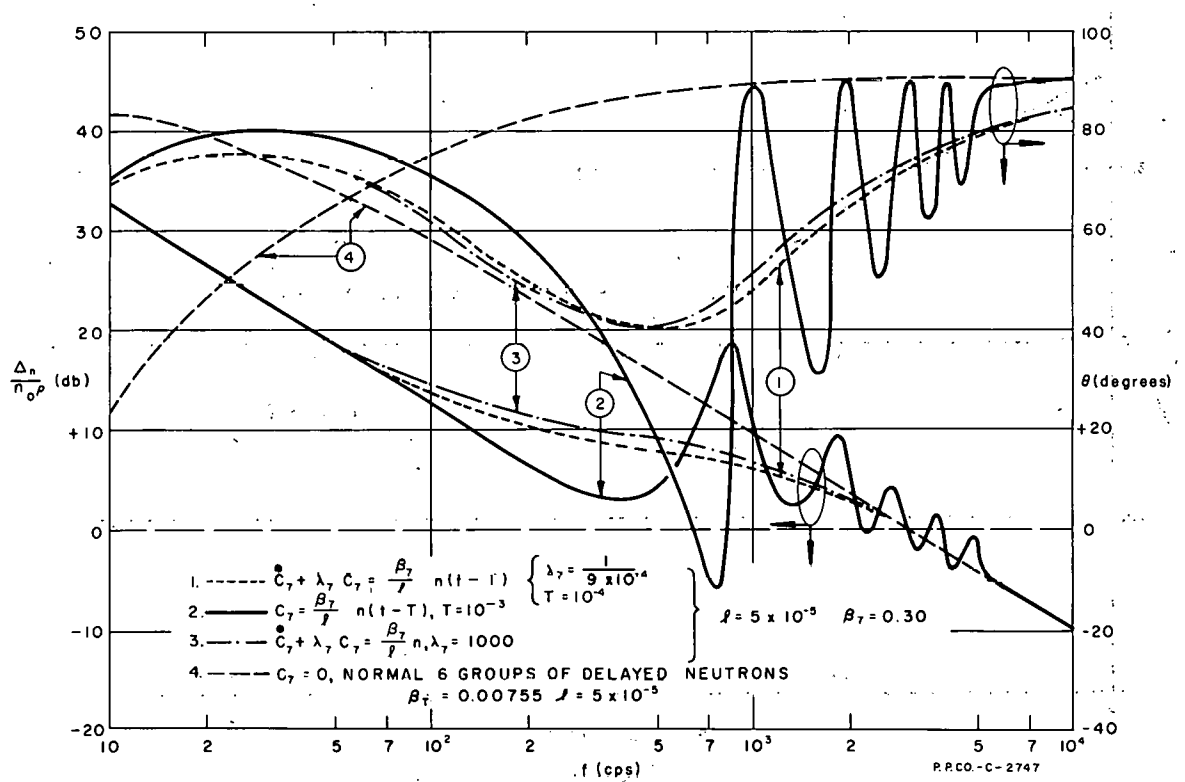

FIG. 6.2H

ZERO POWER REACTOR FREQUENCY RESPONSES

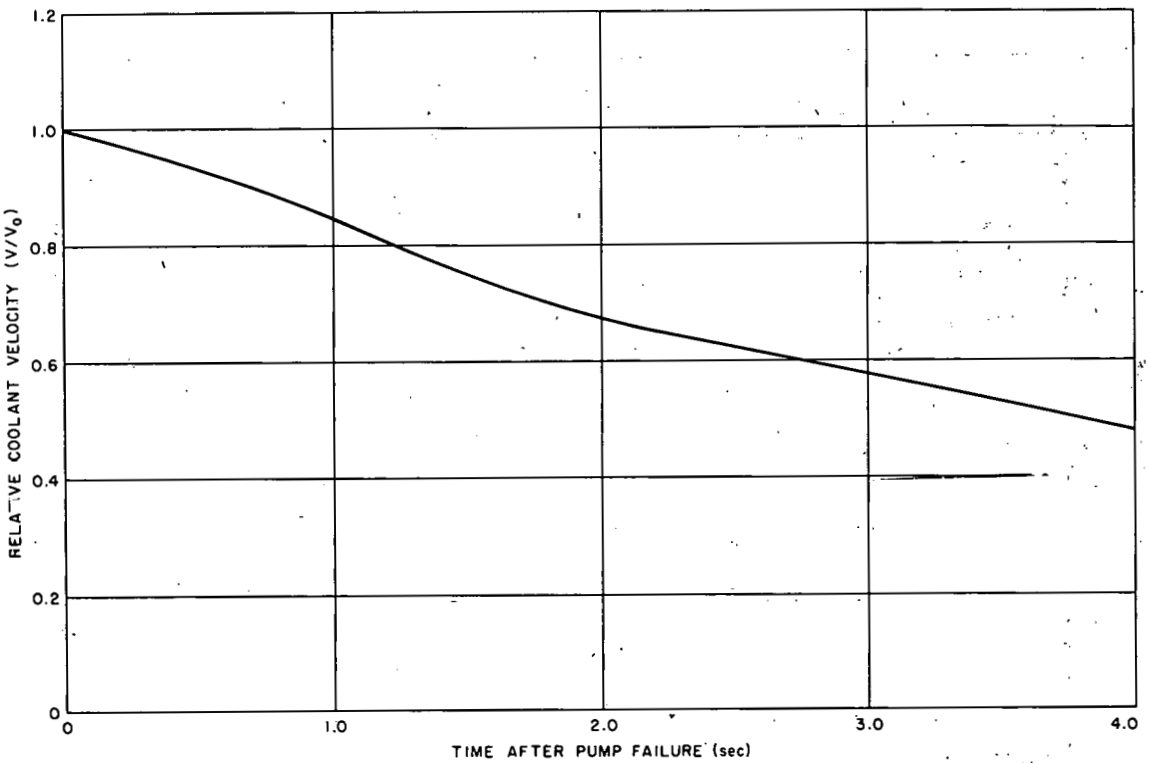

FIG. 6.2 I
FLOW DECAY IN ETR-I

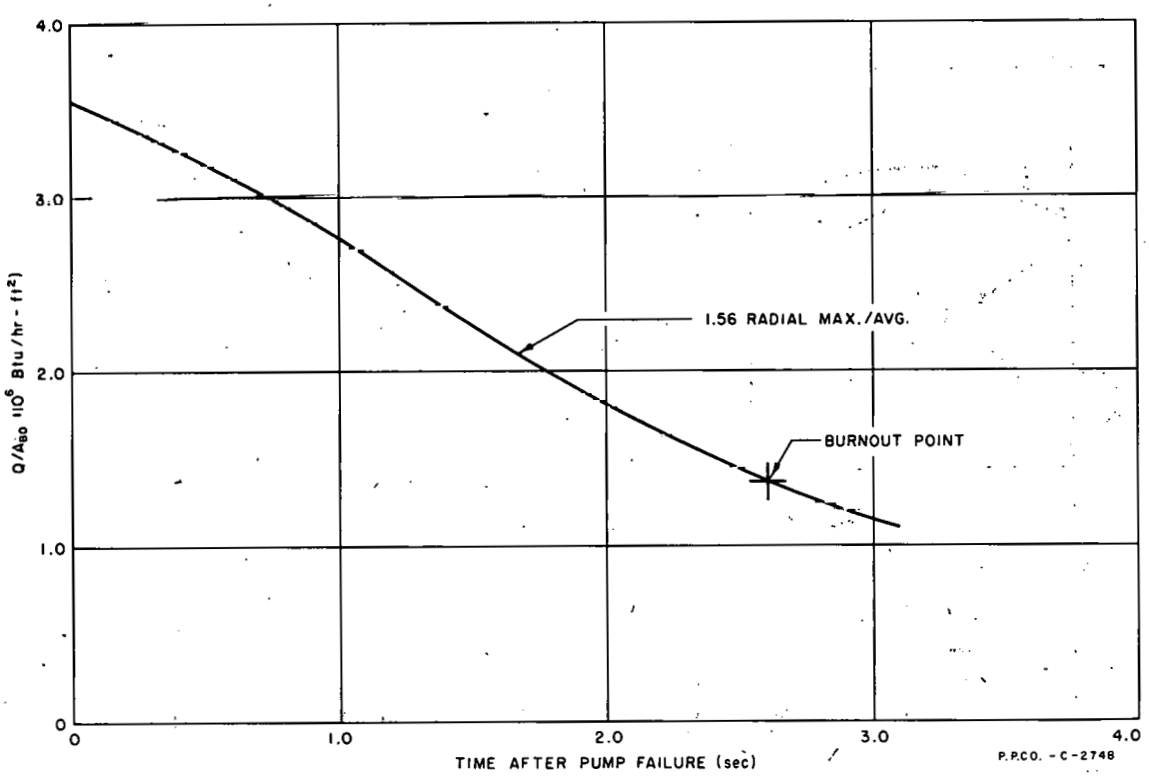

FIG. 6.2 J
BURNOUT IN LOSS OF FLOW ACCIDENT

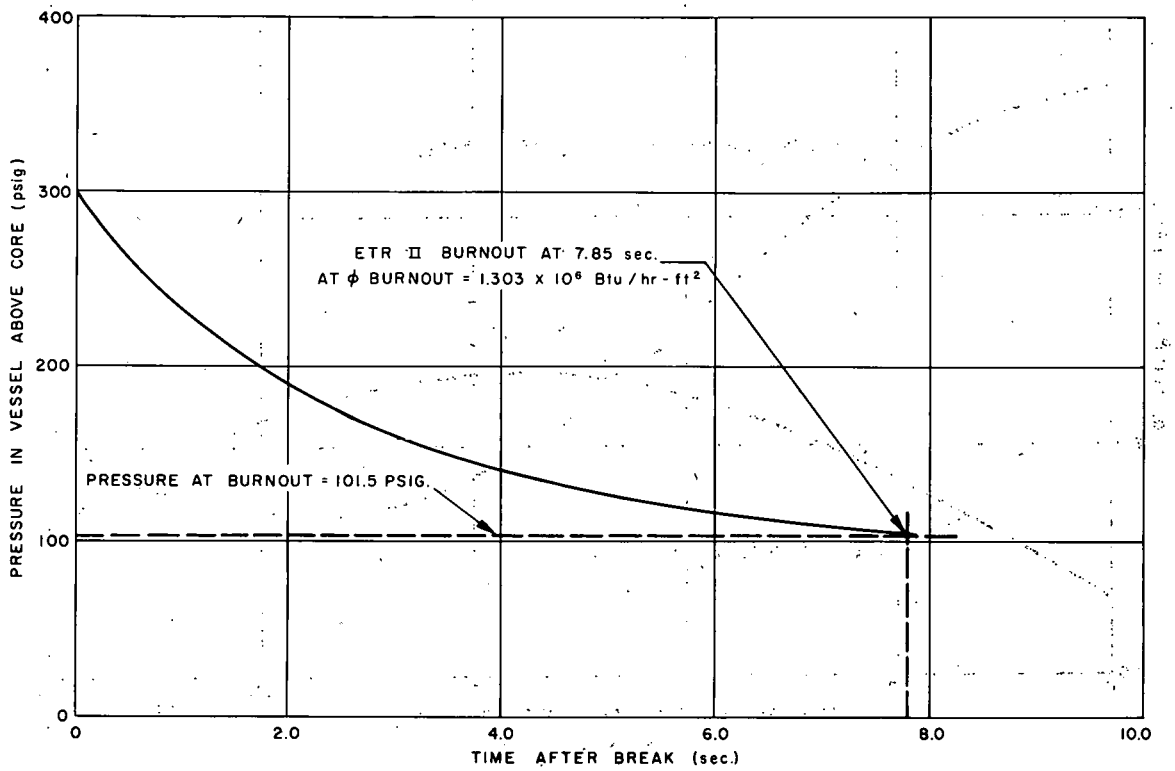

FIG. 6.2 K

LOSS OF PRESSURE ACCIDENT PRESSURE vs. TIME FOR 36 in^2 BREAK IN THE PRESSURE VESSEL ABOVE THE CORE

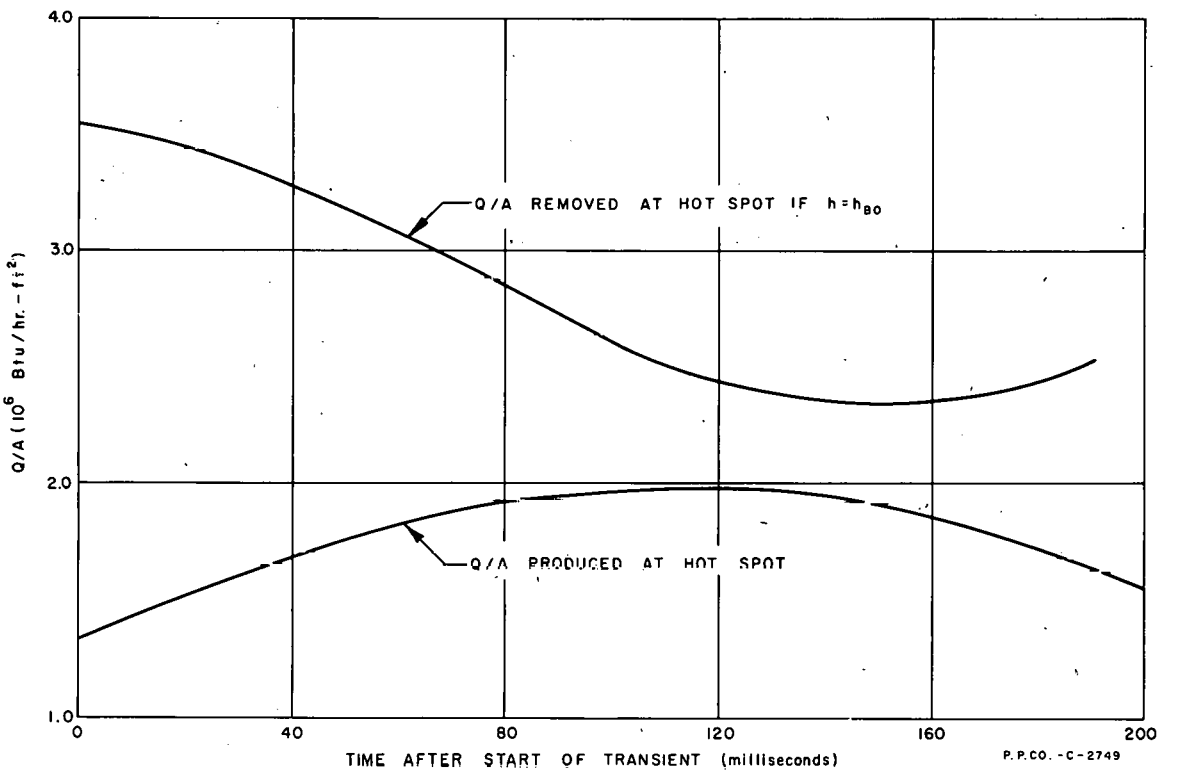

FIG. 6.2 L

HEAT FLUX IN CORE DURING POWER TRANSIENT FROM STEP INSERTION OF 0.3% Δ k/k

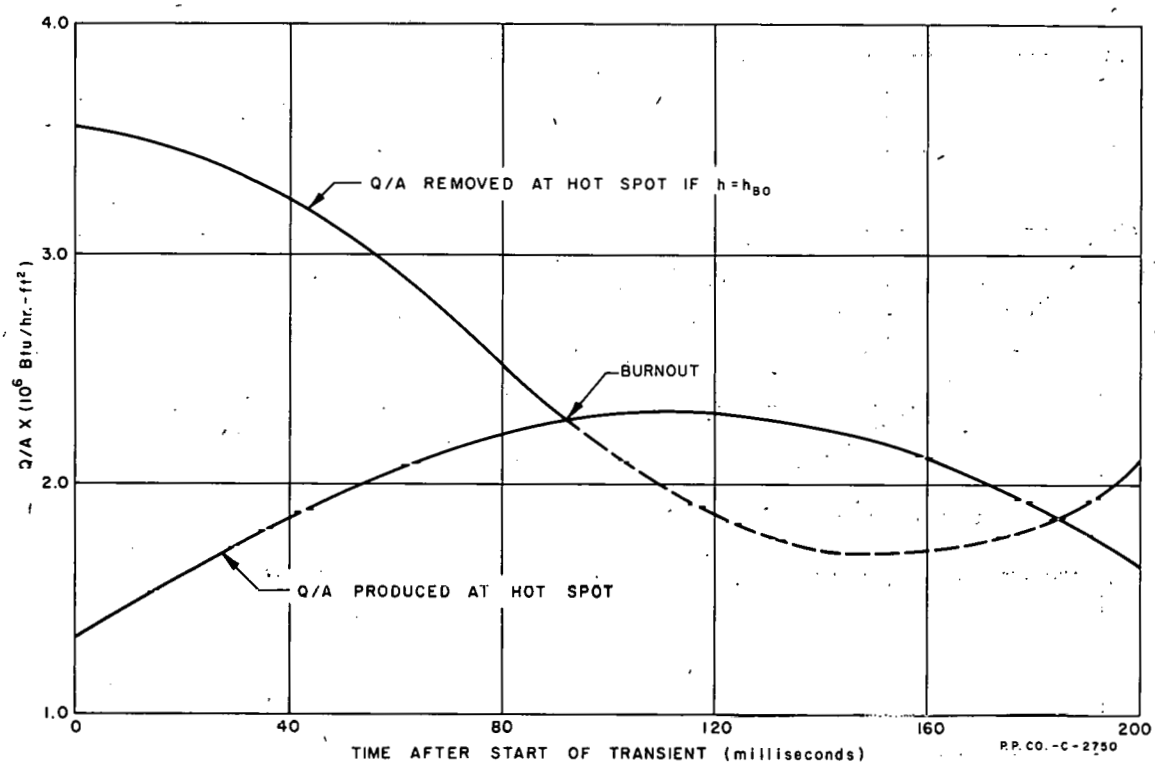

FIG. 6.2 M

BURNOUT IN CORE DURING POWER TRANSIENT FROM STEP INSERTION OF 0.4% Δ k/k

7.0 ACKNOWLEDGMENTS

To G. M. Kavanagh, I. F. Zartman and Doyle Rauch of AEC Nuclear Technology for their guidance and suggestions concerning the scope of this study.

To D. G. Boyer of AEC-IDO for his valuable services in obtaining information and clarifications of project objectives.

Special acknowledgment for their contributions is accorded to the two consultants from the Internuclear Company who worked with the Phillips staff during the project: B. H. Leonard, Jr. (Reactor Design) and T. L. Francis (Reactor Physics).

THIS PAGE

WAS INTENTIONALLY

LEFT BLANK

8.0 APPENDICES

8.1 Quality Control of Boron in Recent ETR Elements

February 26, 1960

Boron Content of ETR Fuel Assemblies
and ETR Control Rod Fuel Sections
Contract C-217
WMH-26-60A

Mr. F. E. Watson, Jr.
General Electric Company
Atomic Power Equipment Department
Post Office Box 234
San Jose 12, California

Dear Sir:

The results of the ETR Critical Facility's measurements of boron in ETR core fuel assemblies and ETR control rod fuel sections recently shipped to us are as follows:

400 g elements

Fuel Element No.	Boron Content (grams)	Fuel Element No.	Boron Content (grams)
U-756	2.12	U-796	2.04
760	2.06	800	2.05
764	2.19	804	2.04
768	2.10	808	2.06
772	2.15	812	2.06
776	2.19	816	2.01
780	2.02	820	2.08
784	2.09	824	2.04
788	2.09	828	2.01
792	2.10	831	2.11

160 g Control Rod Section

Section No.	Boron Content (grams)	Section No.	Boron Content (grams)
U-125	0.78	U-141	0.84
129	0.82	145	0.80
133	0.82	149	0.80
137	0.85		

Very truly yours,

WMHawkins:hj
/HK

Manager, Division Engineering
Atomic Energy Division

cc: Messrs. F. E. Watson, Jr.
R. L. Doan, Phillips

8.2 History and Need of Very High Flux Test Reactors

The need for higher neutron fluxes than obtainable in the MTR and ETR has been recognized by the Commission and its contractors for a number of years. Based on experimenters' requests and operating experience, Phillips Petroleum Company replied to a request from the AEC on the needs for advanced testing reactors and on the testing conditions they should fulfill. A report[1] issued in May, 1956, suggested in essence that an advanced test reactor be designed and constructed which provides thermal and fast neutron fluxes in the 10^{15} to 10^{16} n/cm^2-sec range, and emphasis be placed on smaller test holes of about 3 in. x 3 in. cross section. More recently J. A. Lane, ORNL,[2] reviewed the need for very high fluxes and the type of reactors being planned in the United States to obtain these fluxes. He also concluded that neutron fluxes in the 10^{15} to 10^{16} range were needed for isotope production, chemistry studies, cross section measurement and fuel element testing. In the latter part of 1958 the AEC issued a "Request for Proposals to Supply Irradiation Services" to commercial suppliers. Appendix A of this request contained NR test requirements for very high neutron fluxes. These requirements have since been revised and new requirements are reported in an AEC letter from NR to DRD[3].

Definitive work on very high flux testing reactors for fuel element experiments was initiated in 1956 when the AEC requested four companies to study, independently, reactor concepts which would provide unperturbed thermal fluxes above 10^{15} n/cm^2-sec in certain specific loop type experiments. The specifications called for:

1. an unperturbed flux of 10^{15} n/cm^2-sec in a 3 in. and a 4 in., 2000 psia, 500 to 600°F, circulating light water loops,

2. an unperturbed flux of 1.5×10^{15} n/cm^2-sec in three 6 in. x 6 in. and one 4 in. x 4 in. versatile gas or liquid metal loops; the gas loop to operate at 2200°F and 300 psia, and the liquid metal loop at 1500°F and 300 psia, and

3. an unperturbed flux of 10^{15} n/cm^2-sec in a 3 in. liquid metal loop.

ASTRA[4] recommended a graphite-moderated and -reflected homogeneous-fuel-type reactor. The large graphite core was penetrated by parallel Zircalloy tubes through which flowed a heavy-water solution of uranyl

---

1. J. R. Huffman, W. P. Connor, G. H. Hanson, "Advanced Testing Reactors", Phillips Petroleum Company, Idaho Falls, Idaho, Report IDO-16353, May 28, 1956.
2. J. A. Lane, "The Design and Need for Ultra High Flux Reactors", ORNL, presented at Symposium on Experience in the Use of Research Reactors, Harwell, England, June 11, 1959.
3. I. H. Mandil, "Revised NR Requirements for an Advanced Test Reactor", Letter to G. M. Kavanagh, AEC-DRD, August 28, 1959.
4. R. G. Mallon, J. Saldick, R. E. Gibbons, "Conceptual Design of an Advanced Engineering Test Reactor", Advanced Scientific Techniques Research Associates, Milford, Connecticut, Report NYO-4849, March 1, 1957.

sulfate. Total reactor power was estimated to be 220 Mw. Nine vertical through-holes of various sizes, having thermal neutron fluxes greater than 1 x 10^{15} n/cm^2-sec were provided. Plant capital cost was estimated at $30,000,000, and a large development program was inherent in the use of a circulating homogeneous fuel solution.

Aeronutronic Systems, Inc.[1] recommended a homogeneous reactor system. The uranyl-sulfate solution in D_2O was circulated through the core and external circuit. The seven experimental loops were inserted into the center of the spherical reactor. At full reactor power of 500 Mw, the unperturbed thermal neutron flux in the central core region was estimated to be 6 x 10^{15} n/cm^2-sec. Plant capital cost was estimated to be over $60,000,000, and a large development program was inherent in this design also.

Curtiss-Wright Corporation[2] recommended a large heterogeneous fuel-type reactor with a heavy-water moderator-reflector. The seven experimental loops were located at the center of the cylindrical core. The reactor power varied from 520 to 360 Mw over an operating cycle to produce a usable thermal neutron flux ranging from 1 x 10^{15} to above 2 x 10^{15} n/cm^2-sec.

Internuclear Company[3,4] recommended a complex of seven small separate "flux-trap" type reactors contained in a single large biological shield. Each reactor consisted of a cylindrical annular core of aluminum plate-type fuel elements (MTR-type), cooled with H_2O, reflector-moderated outside the core with D_2O, with H_2O annulus just inside the core and a central test loop. The inner H_2O annulus thermalizes the fast flux causing the thermal flux to peak in the water annulus and providing a high thermal flux in the test region.

A single size reactor was recommended for all loops. At a total power of 500 to 900 Mw, the unperturbed thermal neutron fluxes of 1 to 1.5 x 10^{15} n/cm^2-sec were obtained in the test loops. Reflector control was suggested whereby the outer portion of the moderator reflector was poisoned with boric acid for shim control and a pure inner portion could be dropped for safety control.

In a continuing effort on the flux-trap type reactor, Internuclear Company[5] in 1957-1958 prepared a conceptual design to fulfill the test

---

1. "A Selection Study for an Advanced Engineering Test Reactor", Aeronutronic Systems, Inc. (Subsidiary of Ford Motor Company), Glendale, California, Report AECU-3478, March 29, 1957.
2. "A Conceptual Design Study of an Advanced Engineering Test Reactor", Curtiss-Wright Corporation, Research Division, Quehanna, Pennsylvania, Report CWR-464 (Del.) May 1, 1957.
3. O. J. Elgert, C. F. Leyse, D. G. Ott, "Preliminary Investigation for an Advanced Engineering Test Reactor", Internuclear Company, Clayton, Missouri, Report AECU-3427, February 22, 1957.
4. C. F. Leyse, B. H. Leonard, ibid, Report AECU-3427 (Add.), April 16, 1957.
5. C. F. Leyse, et al., "An Advanced Engineering Test Reactor Design", Internuclear Company, Clayton, Missouri, AECU-3775, March 15, 1958.

requirements of the seven loops described previously. At the same time American Standard[1] reviewed the test reactor complex design recommended by Internuclear Company in the original study.

The Internuclear Company conceptual design again consisted of seven, single-annulus fuel, flux-trap reactors. Two core sizes were recommended, one to provide a 7 in. diameter test hole and the other a 4 in. diameter. The total design power for the complex of reactors was calculated to be 980 Mw. Major features of this design were the use of involute-curved fuel plates to provide a uniform core region, thereby reducing hydraulic problems and increasing heat transfer area, and a non-uniform fuel loading in the plates to flatten radial power distribution. Internuclear Company at present is continuing work on this test reactor complex concept under an existing AEC contract.

The National Laboratories have been interested in very high flux reactors for a number of years. Work on the Mighty Mouse Reactor[2] was initiated by ANL in about 1956. A number of other studies on very high flux reactors have since been reported by the National Laboratories. J. A. Lane's talk, reference 2 on first page of this section, summarizes the high flux test reactors and includes a list of the very high flux reactors being planned in the United States. Those scheduled for construction by the National Laboratories and their completion dates are:

1. B^2R^2, 1962 (BNL),

2. HFIR, 1963 (ORNL), and

3. AHFR, 1964 (ANL).

The B^2R^2 reactor is proposed for beam type experiments. The reactor core consists of ETR type fuel elements, 17 in. long, and is cooled, moderated and reflected with D_2O. The maximum thermal flux may reach 1×10^{15} n/cm^2-sec some distance in the reflector.

The HFIR uses the internal flux trap principle to obtain unperturbed neutron fluxes up to 5×10^{15} n/cm^2-sec for the production of heavy elements and other isotopes. Design features have not yet been established except that it will be a single-annular-type core about one foot long with a center flux-trap island (similar to the Internuclear test reactor complex described previously).

The AHFR will be used for physical science research. The core employs conventional ETR type fuel elements, has a center flux-trap island, is H_2O cooled and moderated, and is beryllium reflected. A

---

1. M. McVey, et al., "Evaluation of an Advanced Engineering Test Reactor Design", American-Standard, Mountain View, California, Report ASAE-S-11, July 15, 1958.
2. L. E. Link, et al., "The Mighty Mouse Research Reactor Preliminary Design Study", Argonne National Laboratory, Lemont, Illinois, Report ANL-5688, March, 1957.

number of beam tubes terminate in the reflector, a 1.5 in. diameter central thimble is located in the flux-trap island and a number of other smaller experimental facilities are provided. The maximum unperturbed thermal neutron flux is estimated to be about 3 to 4 x 10^{15} n/cm^2-sec.

Other groups also have studied very high flux reactors. In 1956 a group of students at Oak Ridge School of Reactor Technology prepared a design of a heavy-water, heterogeneous-fuel, cylindrical flux-trap reactor[1]. Their calculations indicated that a reactor with an 80 cm diameter central hole and operating at 425 Mw could deliver the following average thermal fluxes in 10 cm diameter experiments: in thorium, 5.8 x 10^{14}; MTR fuel element, 2.2 x 10^{15}; and in bismuth, 3.9 x 10^{15}. The following year another group of students prepared a design of a double-slab-type flux-trap reactor[2] which has interesting possibilities, particularly for long cores to accommodate long experiments. The same year, Phillips Petroleum Company made an exploratory study of coolant-moderator and flux-trap materials for very high flux reactors[3], which showed their effect on attainable neutron fluxes (and the required reactor operating powers) as a function of the diameter of the central experimental hole and its contained experiment. A symposium on "Ultra High Flux Research Reactors" was held in December of 1957 and a transcript of the ORNL seminars was issued the following year.[4] In May, 1959, a Test Reactors Meeting for Industry was held in Idaho Falls, Idaho; these papers are recorded in report IDO-16520.[5]

---

1. R. D. Cheverton, et al., "High Flux Research Reactor", Oak Ridge School of Reactor Technology, Oak Ridge, Tennessee, Report CF-56-8-206, August, 1956.
2. W. L. Carter, et al., "Design Study of an Advanced Test Reactor -- Reactor Design and Feasibility Study", Oak Ridge School of Reactor Technology, Oak Ridge, Tennessee, Report ORNL-CF-57-8-5, August, 1957.
3. R. J. Howerton, G. H. Hanson, W. P. Connor, "Parameters of High Flux Testing Reactors", Phillips Petroleum Company, Idaho Falls, Idaho, IDO-16406, August 23, 1957.
4. J. A. Lane, Summary of Seminars on "Ultra High Flux Research Reactors", ORNL-CF-58-7-117, July 31, 1958.
5. "Test Reactors Meeting for Industry", Report IDO-16520, May 13-15, 1959.

8.3 Reactor Physics - Constants and Methods (Ref. Tables 8.3A through 8.3F)

8.31 "Handbook" Reactor Constants

The constants for pure D_2O were obtained from ANL-5800[1]. The borated D_2O constants were assumed to be the same as for pure D_2O except for Σ_a thermal, which was computed by assuming a saturated solution of boric acid in D_2O and adding the Maxwellian averaged cross section of the resulting boron to that of the pure D_2O.

The constants for beryllium-water mixtures and beryllium-D_2O mixtures were obtained as follows:

'Values for τ for Be-H_2O mixtures were taken from a report by McMurry[2], while McMurry's method was used to calculate values of τ for Be-D_2O mixtures.

Values of D were obtained from the formula,

$$D_{mix} = \frac{1}{\sum_i \frac{Fi}{Di\ pure}} ,$$

where

Fi = volume fraction of substance i, and

Di pure = diffusion coefficient of pure substance i.

The constants used for pure beryllium were $D_f = 0.685$ and $D_s = 0.618$.

Reflector savings for all compositions were assumed to be 15 cm, a value lying between the value for pure water and that of pure D_2O, since in most of the computations there are both water and D_2O present in the reactor. However, for the 4 ft core height the perpendicular buckling is affected only slightly by the value of reflector savings.

8.32 ETR II Two-Dimensional Cases Studied

Tables 8.3E and 8.3F present the PDQ cases for the 3 in. and 2 in. reference cores.

---

1. Reactor Physics Constants, ANL-5800.

2. H. L. McMurry, "The Age in Beryllium-Water Mixture", Phillips Petroleum Company, Idaho Falls, Idaho, Report IDO-16067, March, 1953.

TABLE 8.3A

ETR II FUEL CONSTANTS

Composition		J-1	J-2	J-3	J-4
Wt. % U in Meat		20% U	30% U	40% U	50% U
Fast Group	$\nu\Sigma_f$	0.00413	0.006975	0.01020	0.01410
	D	2.18	2.1791	2.1791	2.1770
	Σ_R	0.02299	0.02404	0.023421	0.02174
	Σ_a	0.00305	0.004489	0.006351	0.008599
Thermal Group	$\nu\Sigma_f$	0.182	0.2673	0.3694	0.48523
	D	0.349	0.3635	0.3730	0.3767
	Σ_a	0.096	0.1389	0.1889	0.24612

TABLE 8.3B

ETR II CORE STRUCTURE CONSTANTS

Composition		K-1	K-2	K-3	K-4
		Aluminum	Stainless Steel	Borated Stainless Steel	Cadmium
Fast Group	D	20.0	0.758	1.897	Same as fuel
	Σ_R	0.002214	0.00252	0.0025	Same as fuel
	Σ_a	0.000071	0.00305	0.1506	0.03972
Thermal Group	D	2.080	0.366	0	0
	Σ_a	0.0098	0.0913	0.4695*	0.4695*

* Black Boundary condition.

TABLE 8.3C

ETR II TEST CELL CONSTANTS

Composition		L-1	L-2	L-3	L-4	L-5
		Test Cell M/W = 0.4	Loop Type A-1	Loop Type A-3	Loop Type A-5	Loop Type A-6
Fast Group	$\nu\Sigma_f$	.000074	0.000717	0.001433	0.0021498	0.002578
	D	1.6241	1.0542	1.0542	1.0542	1.0542
	Σ_R	0.03555	0.023119	0.023119	0.023119	0.023119
	Σ_a	0.001161	0.002766	0.00311	0.003455	0.003662
Thermal Group	$\nu\Sigma_f$	.000990	0.020844	0.041687	0.06253	0.075
	D	0.2370	0.2988	0.2988	0.2988	0.2988
	Σ_a	0.015940	0.089667	0.099699	0.10973	0.11573

M/W ratio for compositions L-2 through L-5 was 1.0

TABLE 8.3D

ETR II MODERATOR CONSTANTS

200°F

Composition		M-1	M-2	M-3	M-4	M-5	M-6	M-7	M-8	M-9
		Pure Water	90% H_2O + 10% Al	40% H_2O + 60% Al	40% Borated H_2O + 60% Al	6% H_2O + 94% Be	Pure D_2O	Borated D_2O	20% D_2O + 80% Be	20% Borated D_2O + 80% Be
Fast Group	D	1.3975	1.50	2.4332	2.4332	0.7037	1.352	1.352	0.76	0.76
	Σ_R	0.04703	0.0425	0.019028	0.019028	0.008796	0.009143	0.009143	0.00742	0.00742
	Σ_a	0.000781	0	0.000335	0.005217	0.000001	0.000001	0.0001	0	0
Thermal Group	D	0.1765	0.17697	0.4308	0.4308	0.531	0.90	0.90	0.6593	0.6593
	Σ_a	0.016340	0.016868	0.01292	0.1243	0.001975	0.000058	0.2731	0.0007908	0.0554

TABLE* 8.3E

REGIONAL COMPOSITIONS FOR ETR II PDQ CASES, 3-INCH REFERENCE CORE

Problem No.	1	2	3	4	5	6	7
Eigenvalue	1.220	1.268	1.296	1.233	1.176	1.1407	1.0457
1 Center Test Cell	L-1	L-1	L-1	L-1	L-1	L-1	L-1
2 Lobe Test Cell	L-1	L-1	L-1	L-1	L-1	L-1	L-1
3 Side Test Cell	L-1	L-1	L-1	L-1	L-1	L-1	L-1
4 Fuel Concentration, wt. %	30	40	50	50	50	30	30
5 Inner Reflector	H_2O	H_2O	H_2O	H_2O	H_2O	Be+D_2O	Be+D_2O
6 Intermediate Reflector	Be	Be	Be	Be	Be	B-D_2O	B-D_2O
7 Outer Reflector	B-D_2O	B-D_2O	B-D_2O	B-D_2O	B-D_2O	B-D_2O	B-D_2O
8 Center Filler Annulus	H_2O	H_2O	H_2O	H_2O	H_2O	H_2O	H_2O
9 Lobe Filler Annulus	H_2O	H_2O	H_2O	H_2O	H_2O	H_2O	H_2O
10 Side Filler Annulus	**	**	**	**	**	**	**
11 Neck Filler	H_2O	H_2O	H_2O	H_2O	H_2O	H_2O	H_2O
12 Pressure Tube, Half Cylin.	ss	ss	ss	B-ss	B-ss	B-ss	B-ss
13 Pressure Tube, Half Cylin.	ss	ss	ss	ss	ss	ss	ss
14 Pressure Tube	ss	ss	ss	ss	ss	ss	ss
15 Cadmium Blades	Out	Out	Out	Out	In	Out	In

Problem No.	8	9	10	11	12	13	14
Eigenvalue	1.1223	1.1489	1.2860	1.2941	1.1480	1.0970	1.0338
1 Center Test Cell	L-1	L-1	L-1	L-1	L-1	L-1	L-1
2 Lobe Test Cell	L-1	L-1	L-1	L-1	L-1	L-1	L-1
3 Side Test Cell	L-1	L-1	L-1	L-1	L-1	L-1	L-1
4 Fuel Concentration, wt. %	30	30	30	30	30	30	30
5 Inner Reflector	Be+(B-D_2O)	Be+(B-D_2O)	Be+D_2O	Be+D_2O	Be+(B-D_2O)	Be+(B-D_2O)	Be+(B-D_2O)
6 Intermediate Reflector	B-D_2O	B-D_2O	Be+D_2O	Be+D_2O	Be+(B-D_2O)	Be+(B-D_2O)	Be+(B-D_2O)
7 Outer Reflector	B-D_2O	B-D_2O	D_2O	D_2O	B-D_2O	B-D_2O	B-D_2O
8 Center Filler Annulus	H_2O	H_2O	H_2O	H_2O	H_2O	H_2O	H_2O
9 Lobe Filler Annulus	H_2O	H_2O	H_2O	H_2O	H_2O	H_2O	H_2O
10 Side Filler Annulus	**	**	**	**	**	**	**
11 Neck Filler	H_2O	H_2O	H_2O	Be+D_2O	H_2O	Be+(B-D_2O)	Be+(B-D_2O)
12 Pressure Tube, Half Cylin.	B-ss	ss	ss	ss	B-ss	B-ss	B-ss
13 Pressure Tube, Half Cylin.	ss	B-ss	B-ss	B-ss	ss	ss	ss
14 Pressure Tube	ss	ss	ss	ss	ss	ss	ss
15 Cadmium Blades	Out	Out	Out	Out	Out	Out	In

* The composition designations in this table are defined at the bottom of Table 8.3F.

** There was no side filler annulus for these cases, and regions 5, 6, and 7 extended over the volume of region 10.

TABLE* 8.3F

REGIONAL COMPOSITIONS FOR ETR II PDQ CASES, 2-INCH REFERENCE CORE

Problem No.	15	16	17	18	19	20
Eigenvalue	1.2014	1.3082	1.2190	1.1402	0.8964	0.9558
1 Center Test Cell	L-1	L-1	L-1	L-1	L-1	L-1
2 Lobe Test Cell	L-1	L-1	L-1	L-1	L-1	L-1
3 Side Test Cell	L-1	L-1	L-1	L-1	L-1	L-1
4 Fuel Concentration, wt. %	30	30	30	20	30	30
5 Inner Reflector	Be+D_2O	Be+D_2O	Be+D_2O	Be+D_2O	Be+(B-D_2O)	Be+(B-D_2O)
6 Intermediate Reflector	Be+D_2O	Be+D_2O	Be+D_2O	Be+D_2O	Be+(B-D_2O)	Be+(B-D_2O)
7 Outer Reflector	D_2O	D_2O	D_2O	D_2O	B-D_2O	B-D_2O
8 Center Filler Annulus	H_2O	Be+D_2O	H_2O	H_2O	H_2O	H_2O
9 Lobe Filler Annulus	H_2O	Be+D_2O	H_2O	H_2O	H_2O	H_2O
10 Side Filler Annulus	**	**	**	**	**	**
11 Neck Filler	H_2O	Be+D_2O	Be+D_2O	Be+D_2O	Be+(B-D_2O)	Be+(B-D_2O)
12 Pressure Tube, Half Cylin.	ss	ss	ss	ss	B-ss	B-ss
13 Pressure Tube, Half Cylin.	B-ss	B-ss	B-ss	B-ss	ss	ss
14 Pressure Tube	ss	ss	ss	ss	ss	ss
15 Cadmium Blades	Out	Out	Out	Out	In	Out

Problem No.	21	22	23	24	25
Eigenvalue	0.8551	1.272	1.046	1.199	1.245
1 Center Test Cell	L-1	A-3	A-3	A-3	A-3
2 Lobe Test Cell	L-1	A-5	A-5	A-5	A-1
3 Side Test Cell	L-1	A-6	A-6	A-6	A-6
4 Fuel Concentration, wt. %	20	30	30	30	30
5 Inner Reflector	Be+(B-D_2O)	D_2O	B-D_2O	D_2O	D_2O
6 Intermediate Reflector	Be+(B-D_2O)	D_2O	B-D_2O	D_2O	D_2O
7 Outer Reflector	B-D_2O	D_2O	D_2O	D_2O	D_2O
8 Center Filler Annulus	H_2O	.4H_2O+Al	.4H_2O+Al	.4H_2O+Al	.4H_2O+Al
9 Lobe Filler Annulus	H_2O	.4H_2O+Al	.4H_2O+Al	.4H_2O+Al	.9H_2O+Al
10 Side Filler Annulus	**	.4H_2O+Al	.4H_2O+Al	.4H_2O+Al	.4H_2O+Al
11 Neck Filler	Be+(B-D_2O)	.4H_2O+Al	.4H_2O+Al	.4(B-H_2O)+Al	.4H_2O+Al
12 Pressure Tube, Half Cylin.	B-ss	ss	ss	ss	ss
13 Pressure Tube, Half Cylin.	ss	ss	ss	ss	ss
14 Pressure Tube	ss	ss	ss	ss	ss
15 Cadmium Blades	Out	Out	Out	Out	Out

* The composition designations in this table are related to those in Tables 8.3A through 8.3D by,

20 = J-1	ss = K-2	A-3 = L-3	.9H_2O+Al = M-2	D_2O = M-6
30 = J-2	B-ss = K-3	A-5 = L-4	.4H_2O+Al = M-3	B-D_2O = M-7
40 = J-3	L-1 = L-1	A-6 = L-5	.4(B-H_2O)+Al = M-4	Be+D_2O = M-8
50 = J-4	A-1 = L-2	H_2O = M-1	Be = M-5	Be+(B-D_2O) = M-9

** There was no side filler annulus for these cases, and regions 5, 6, and 7 extended over the volume of region 10.

8.4 ETR Critical Facility, Reactor Physics Measurements

It was recognized that four 6 in. x 6 in. experimental spaces, surrounded with ETR fuel elements or control rods placed in the corners of the ETRC core and coupled with eight more fuel elements, making a fifth 6 in. x 6 in. experimental space, would approximate the geometry of the four-lobe ETR II with 3 in. element thickness and a beryllium reflector. After preliminary reactivity measurements in the ETRC showed that an approximate loading could be made critical with two additional fuel elements, it was decided that critical experiments would be performed. The ideal geometry is shown in Figures 8.4E-I (Core I).

Because the program being carried out in support of ETR I by the ETRC is quite pressing, only one week of ETRC time was allotted for the measurements reported herein. Therefore, it was not possible to make all the studies desired. Also, because time was limited, no modifications were made to the ETRC. With the exception of two experiment mockups, all materials used, e.g., fuel elements and control rods, were standard ETR or ETRC components.

8.41 Description of the Facility and Components

The ETRC is a low power, highly enriched, water cooled and moderated, beryllium-beryllium oxide reflected reactor. It is a full scale nuclear mockup of the core and reflector of its parent reactor, the ETR. In fact it is more than just a mockup because most of the in-pile components (fuel elements and control rods) are identical to those in the parent reactor. For reasons of economy there are, however, slight modifications in the reflector. Over a period of several years, experiments have displaced enough 3 in. square beryllium pieces from the MTR to provide a complete reflector for the ETRC. These, however, make up only a 3 in. reflector as compared to 4-1/2 in. in the ETR. The remaining 1-1/2 in. are made up of canned beryllium oxide. Around the beryllium-beryllium oxide reflector is an aluminum reflector. The physical arrangements of the standard ETRC core and reflector are shown in Fig. 8.4A. The physical arrangement of the core, its support structure, control bridge, etc., is shown in Fig. 8.4B. A more detailed description of the facility can be found in IDO-16332[1].

With the exception of the experiment mockup, the core components (fuel elements, control rod fuel sections and guide tubes, and aluminum filler pieces) are standard ETR or ETRC components. The ETRC filler pieces are made of aluminum and have machined slots. These slots simulate the coolant passages in ETR filler pieces. The water volume associated with these pieces is 20 per cent of the total volume (metal-water ratio = 4). In all loadings studied an aluminum filler piece was also desired in grid position I-9 where a control rod guide tube is located. Aluminum plates were inserted in this guide tube to displace enough water to duplicate the metal-water ratio of the standard filler pieces.

---

1. D. R. deBoisblanc, et al., "The Engineering Test Reactor Critical Facility Hazards Summary Report", Phillips Petroleum Company, Idaho Falls, Idaho, Report IDO-16332, March 27, 1957.

The fuel elements which were used in these measurements contained 320 g U-235 and on the average 1.7 g natural boron. In addition, six elements with the same U-235 content but which contained no boron were used to shim the reactor by loading them with boron impregnated polyethylene tapes. The control rod fuel sections used contained 130 g U-235 and on the average 0.68 g natural boron. Drawings of the fuel element, and control rod fuel section and its guide tube are shown in Figures 8.4C and 8.4D.

The experiment mockups were made from stock aluminum rod (2.5 in. diameter) and schedule 40 stainless steel pipe (3.06 in. i.d. and 3.5 in. o.d.).

8.42 Loading Configurations

Inasmuch as no control rods are currently planned in the fuel region for the ETR II it would have been desirable to mockup the core completely with fuel elements in the arrangement shown in Figure 8.4E-I. This was impossible in these critical experiments, however, because the safety rods were necessary for shutdown and because time did not permit removing the control rod guide tubes to permit insertion of fuel elements in those control rod positions which did not contain safety rods. The fuel arrangement desired intersected ten control rod positions. Fortunately, all four safety rod positions (H-7, K-9, G-11, M-11) and a driven shim (gray) rod position (H-13) were located in fueled regions. The remaining five positions contained fixed control rod fuel sections. As was mentioned previously, the other six guide tubes remained in the core but were water filled. These six tubes are not shown in the figures.

Because of these considerations, plus the boron built into the ETR elements, it was not possible to achieve criticality with the desired loading configuration. As a result, two extra elements had to be added. Because adding these elements produce flux distributions different from those in the desired loading, two loadings in which the two elements were placed in different locations were studied to determine the effects of these elements. In one loading the elements were located in the center experimental space so that almost symmetrical neutron flux distributions would be produced. In the second, the elements were located in the experimental space in diametrically opposite lobes. These loading arrangements are shown in Figure 8.4E-II and -III respectively. The effects on the neutron flux of removing the beryllium reflector from one of the lobes were also studied. The loading used for this study was the same as that in Figure 8.4E-II, except that one-fourth of the reflector was removed. This arrangement is shown as a separate loading in Figure 8.4E-IV.

8.43 Neutron Flux and Power Distribution

Thermal neutron flux distributions were measured to determine 1) the power densities required to obtain a thermal flux of 10^{15} n/cm^2-sec in a hypothetical loop experiment, 2) the flux gradients that could be

expected from narrow fueled regions, and 3) the effects of the reflector on the flux in an experiment located within a lobe. Most of the detailed measurements were made in and around the NE* quadrant, or lobe, which contained no control rod fuel sections. In fuel elements where detailed measurements were not made, only one measurement was made at the midplane in the center of the element. As will be seen in detail flux plots, this is the minimum flux within the element at the horizontal midplane.

8.431 Experimental Procedures and Treatment of Data

The thermal neutron flux distributions were determined from the activity of irradiated gold foils, and bare and cadmium covered gold wires. The foils are 5/32 in. diameter by 0.005 in. thick. The cadmium ratios were determined from 0.040 in. diameter gold wires, 3 in. long, the center of which were covered with a cadmium sleeve (0.020 in. wall and 1 in. long). After irradiation, the wires were cut into 1/4 in. sections and the average activity of the bare and covered sections were used to calculate the cadmium ratios. The cadmium ratios from sleeves have been normalized against standard cadmium covered foils.

The foils and wires, with cadmium sleeves, were taped with plastic electricians tape to either lucite strips, aluminum strips, or directly on an experiment. The lucite strips were used where measurements were made within a fuel element. These strips were inserted in the fuel element coolant channels and were designed to position the neutron detectors within $\pm$ 0.03 in. of the desired location. The aluminum strips were used where measurements were desired in a water space. These strips, containing the detectors, were taped on some object, usually a fuel element, such that they protruded into the desired region.

The activity of all the foils was first converted to relative flux distribution by use of the cadmium ratios and was then normalized to a Maxwellian-averaged flux of 10^{15} n/cm^2-sec in the experiment mockup in the NE lobe. In some of the figures, a given value (usually the minimum) is normalized to unity so that the flux gradient is more easily determined.

8.432 Results

The pertinent neutron flux data which were measured in these experiments are presented in Figures 8.4F through 8.4N.

It can be seen in Figures 8.4F and 8.4G that maximum-to-minimum flux in the NE lobe is not appreciably affected by the rearrangement of elements from Loading II to Loading III but is significantly increased by the removal of the beryllium reflector as is evidenced in Figure 8.4H. It is significant, however, that even

---

* The top of the page is assumed to be North in this description. This conforms to the physical orientation of ETR I.

though there is a pronounced gradient across the lobe, the max/avg flux around the aluminum cylinder is only 1.05 in Loading II and changes to only 1.10 in Loading IV, which has a quite different power distribution. This is illustrated in a circumferential flux plot in Figure 8.4I. An E-W traverse through the lobe is shown in Figure 8.4J. This property has been recognized as a most important feature of ETR II and is discussed more completely in Section 3.2.

It can be seen in the detailed flux traverses in Figures 8.4K and 8.4L that undesirable flux gradients exist within the fuel elements. For example, the maximum-to-minimum flux within the fuel element in position N-6 is 1.9. This indicates the desirability of graduating the fuel density and increasing the absorption cross section of the fuel element side plates by the addition of burnable poison or possibly fuel.

A typical vertical traverse, shown in Figure 8.4M, has approximately the same shape and max/avg flux (1.40) as traverses measured in ETR loadings.

A flux traverse measured in grid positions H-10, J-10, and K-10 is shown in Figure 8.4N merely to indicate the amount of flux peaking in a 3 in. x 3 in. space containing an aluminum filler piece with a M/W ratio of four.

8.433 Power Calculations

Various factors associated with power distributions have been calculated and are summarized in Table 8.4A. Total power is shown for the most balanced loading only since the other cores are not considered representative of the manner in which ETR II will be loaded. Of considerable significance is the fact that even though the max/avg in the NE lobe varied from 1.54 to 2.35, the power in that lobe required to produce the same experimental flux changed only 10 per cent.

To make these power calculations, special considerations were required. The thermal neutron flux values shown in the diagrams of the three experimental loadings (Figures 8.4F, 8.4G, and 8.4H) were all measured at the center of the fuel elements and normalized to a thermal flux of 1×10^{15} n/cm^2-sec at the center of the mockup loop in the NE lobe. For power calculations each value had to be corrected to an average thermal flux per element. Although the max/avg ratios of the vertical flux profiles are essentially constant throughout the core, this is not true of the individual (within each element) horizontal profiles, as shown in Figures 8.4K and 8.4L. For this reason, the correction factor used to obtain an average flux from the measured value at the center of the element depended upon the particular location of the element in the core. These factors (over-all center-to-average) ranged from 0.77 to 0.98.

TABLE 8.4A

POWER DISTRIBUTIONS

	NE LOBE*			FULL CORE
	Loading II	Loading III	Loading IV	Loading II
Total Power	72 Mw	77 Mw	70 Mw	335 Mw (425)**
Horizontal Max/Avg Power	1.62	1.54	2.35	2.61

* 12 Elements: K-5 to 8, N-5 to 8, L-5 and 8, and M-5 and 8.

** Power of core loading II corrected to 4 ft length.

In calculating power, an empirically determined correction factor was included to account for the contribution of epithermal neutrons to the total fission rate. The fission rate due to epithermal neutrons is 10 per cent of that due to thermal neutrons. The U-235 fission cross section at 2200 meters/sec (580 barns) was corrected by the usual factors to a Maxwellian-averaged value at 75°F. Using this cross section, the measured flux ratios, and correcting to a core length of 4 ft gave a power level of 425 Mw. In Section 3.2 a calculation of a 3 in. four-lobe reactor similar to ETR II gave a value of 220 Mw. Even with allowance for the difference in neutron temperature (75°F in the ETRC, 200°F in the ETR II) and computational uncertainties, the advantage of the more symmetric geometry is evident.

8.44 Critical Mass - Measurements and Calculations

It was mentioned above that the four-lobe geometry shown in Figure 8.4E-I (Core I) needed two additional fuel elements in the center of the core for criticality (Positions J-9 and H-10). This loading (Core II, Figure 8.4E-II) was critical with the driven shim rod in Position H-13 at 17.5 in. (full travel 36 in.). All other rods were fully withdrawn, i.e., the fuel sections on all other rods were in the core.

Forty-two of the forty-eight fuel elements in Core II were standard ETR fuel elements with an average of 1.72 g of natural boron (ranging from 1.60 to 1.86 g). The remaining six elements, like the former in all other respects, were fabricated without boron. Since the

shim rod was worth only 0.3 per cent $\Delta k/k$, the coarse shimming was done by adding boron impregnated polyethylene tapes to the six unborated elements. The U-235 mass in this loading (48 fuel elements and 9-1/2 control rod fuel sections) is 16,600 g. The critical mass of the cold clean unborated loading with the configuration of Core I was derived by calculating the excess reactivity this configuration would have had if there had been no boron in the fuel elements. This excess reactivity is then used to calculate the amount of fuel which would have to be removed uniformly from Core I (46 elements, 10 control rod fuel sections - 16,020 g) to reduce its excess reactivity to zero, or in other words, k_{eff} to unity. Table 8.4B is an itemized list of the results of these calculations using a theoretical approach in one case and an empirical approach in another. As shown, the cold clean unborated critical masses by the two methods are in good agreement.

TABLE 8.4B

CRITICAL MASS CALCULATIONS

	Empirical	Theoretical
Removing boron	+ 0.0906 $\Delta k/k$	+ 0.0860 $\Delta k/k$
Removing extra elements	- 0.0445	- 0.0355
Complete withdrawal of shim rod	+ 0.0016	+ 0.0016 (same)
Total excess reactivity	+ 0.0477 $\Delta k/k$	+ 0.0521 $\Delta k/k$
Excess fuel	2760 g	3340 g
Critical mass (16,020 - Excess fuel)	13,260 g	12,680 g

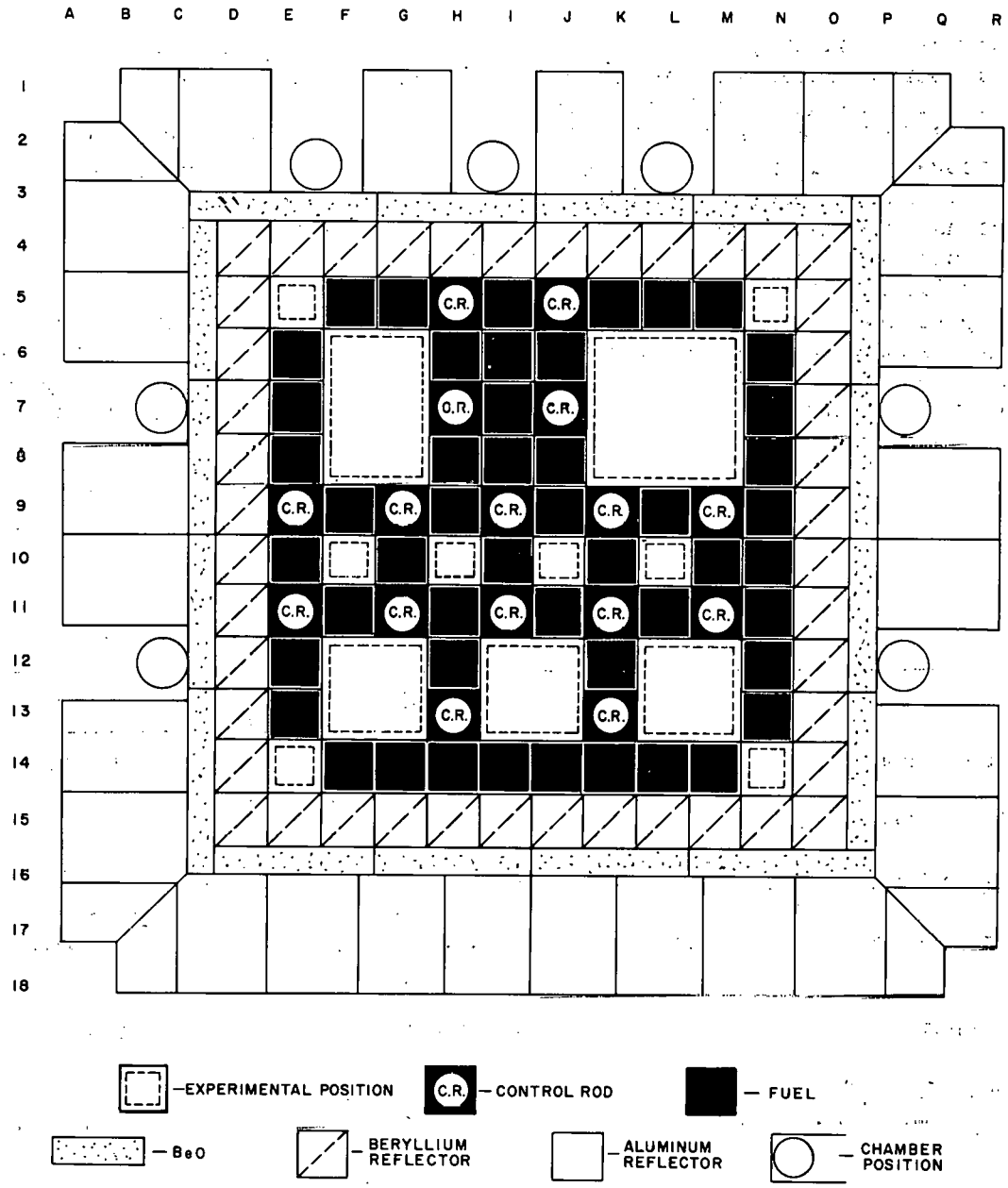

FIG. 8.4A

ETRC CORE DIAGRAM

PP CO-C-2751

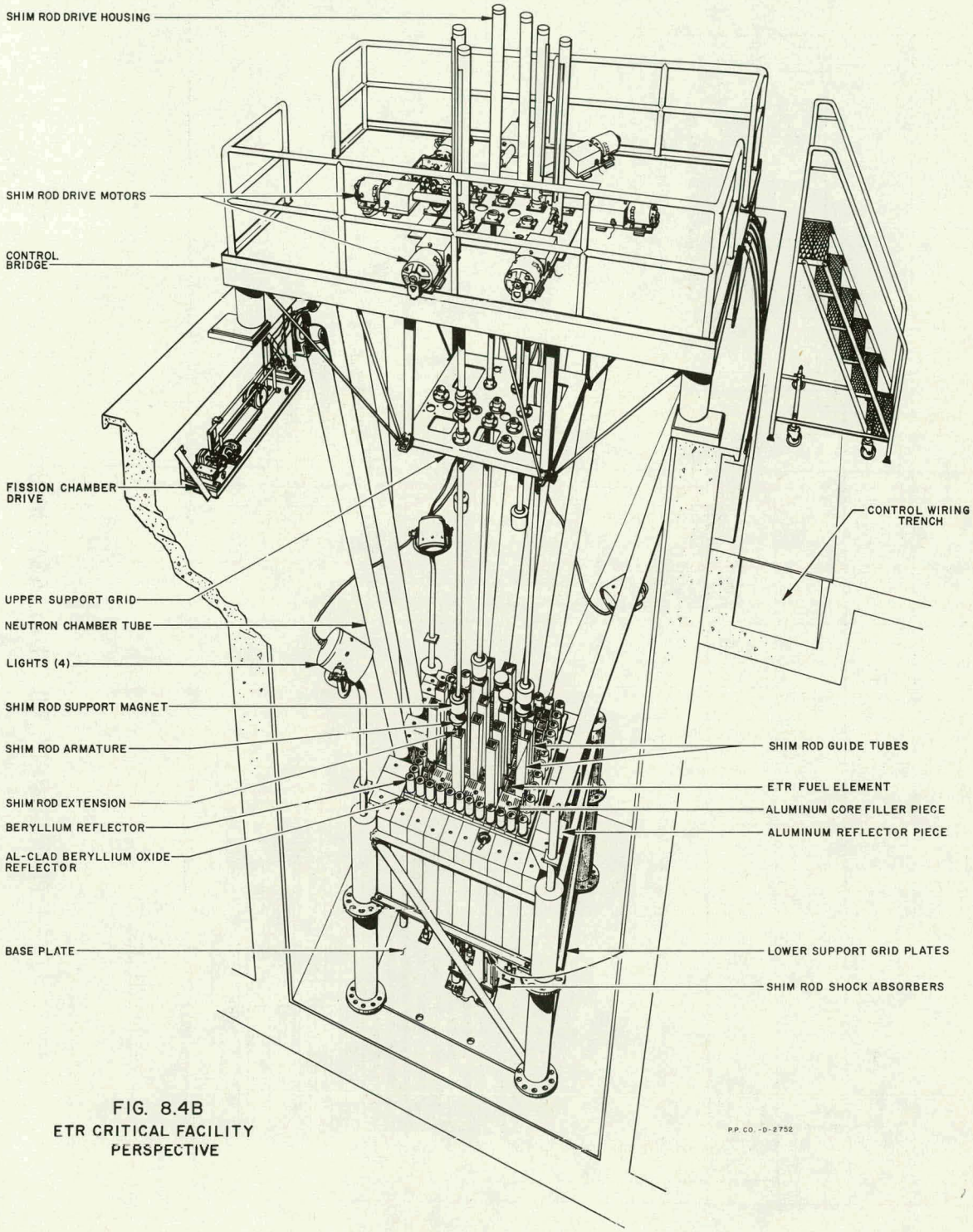

FIG. 8.4B
ETR CRITICAL FACILITY
PERSPECTIVE

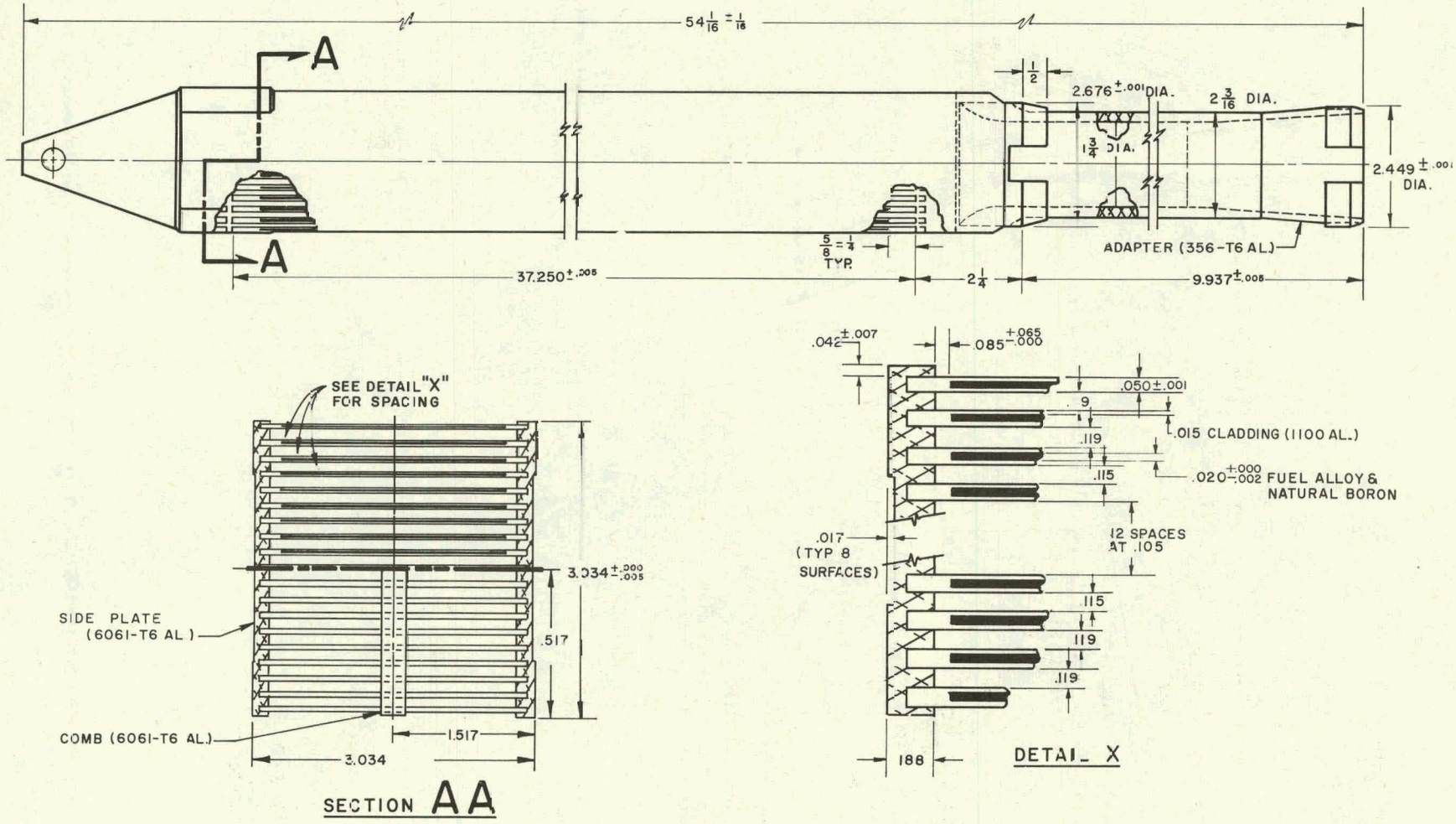

P.P. CO. - C - 2753

FIG. 8.4C

ETR-I AND ETRC FUEL ASSEMBLY

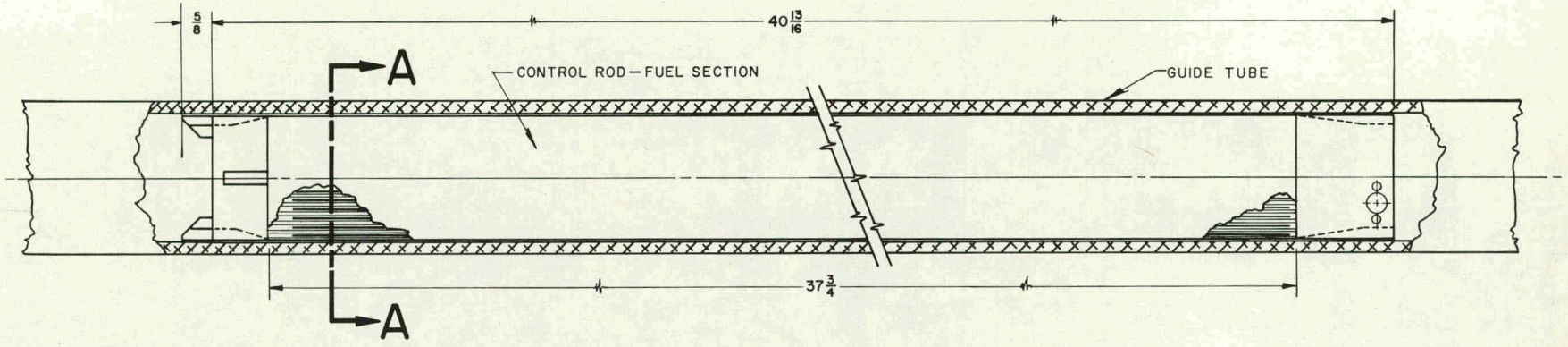

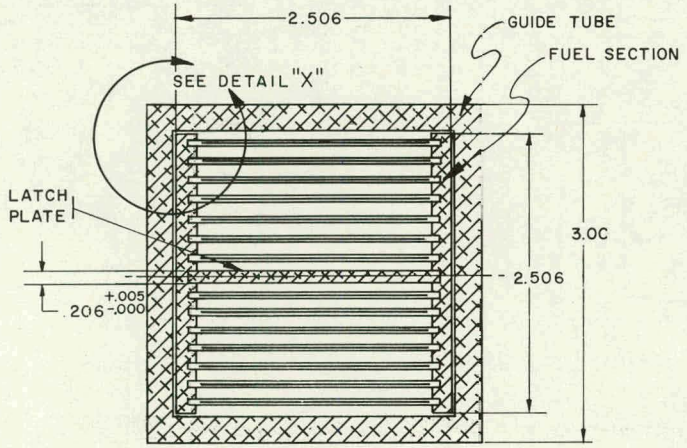

SECTION A-A

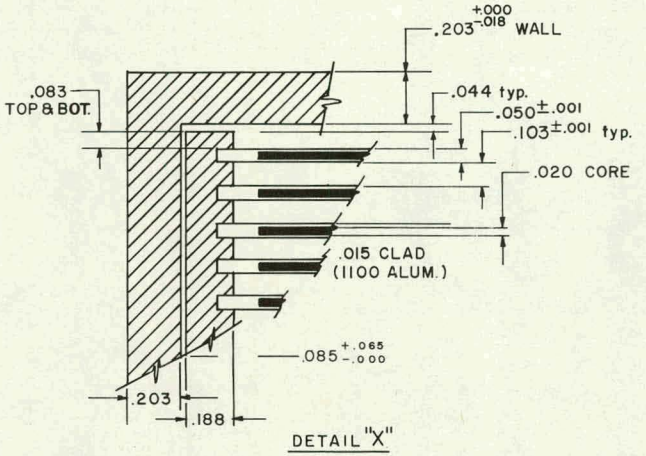

DETAIL "X"

FIG. 8.4D

P.P.CO.-C-2754

ETR-I AND ETRC CONTROL ROD
FUEL SECTION AND GUIDE TUBE

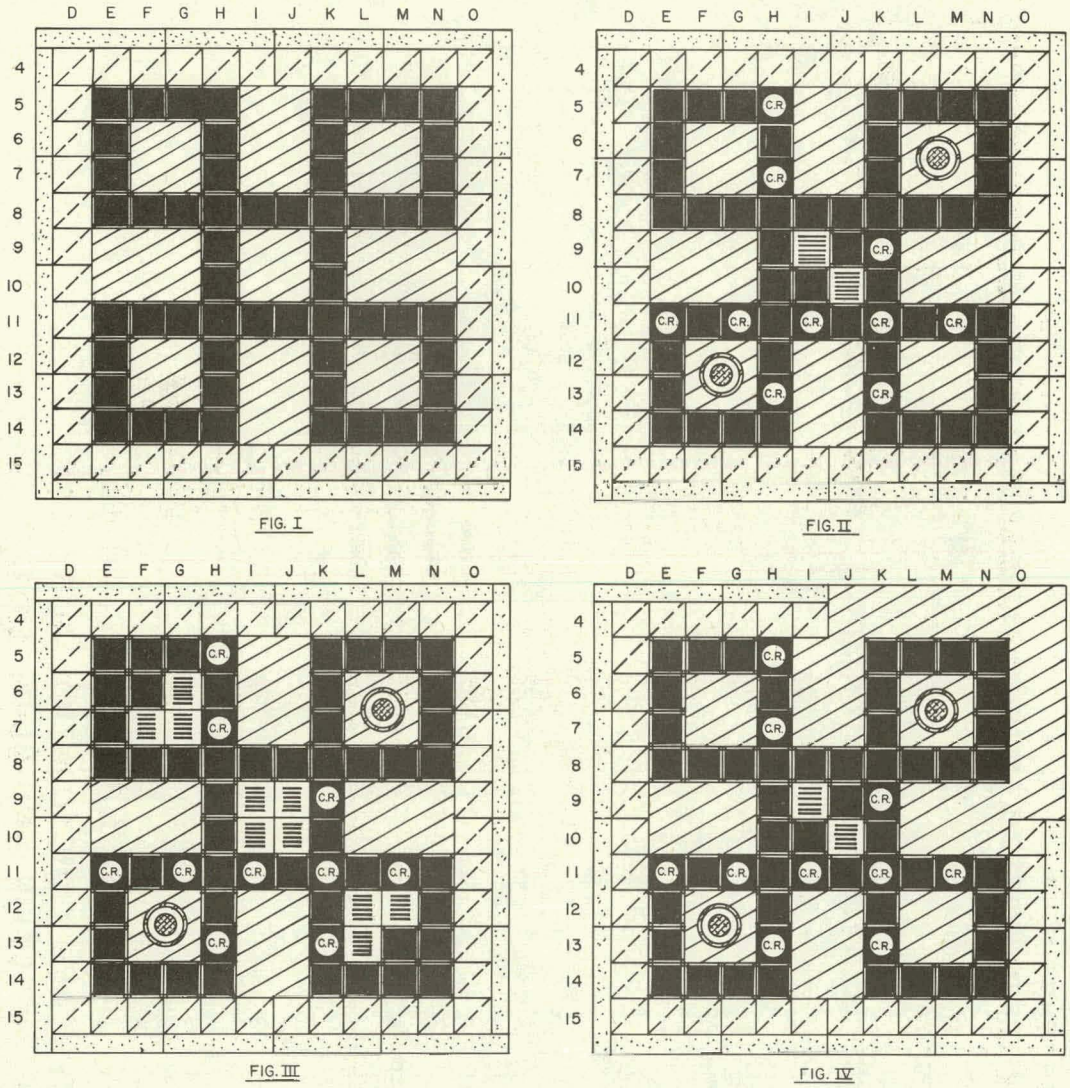

FIG. 8.4E

P.P. CO-C-2755

MOCKUP LOADING IN THE ETR C

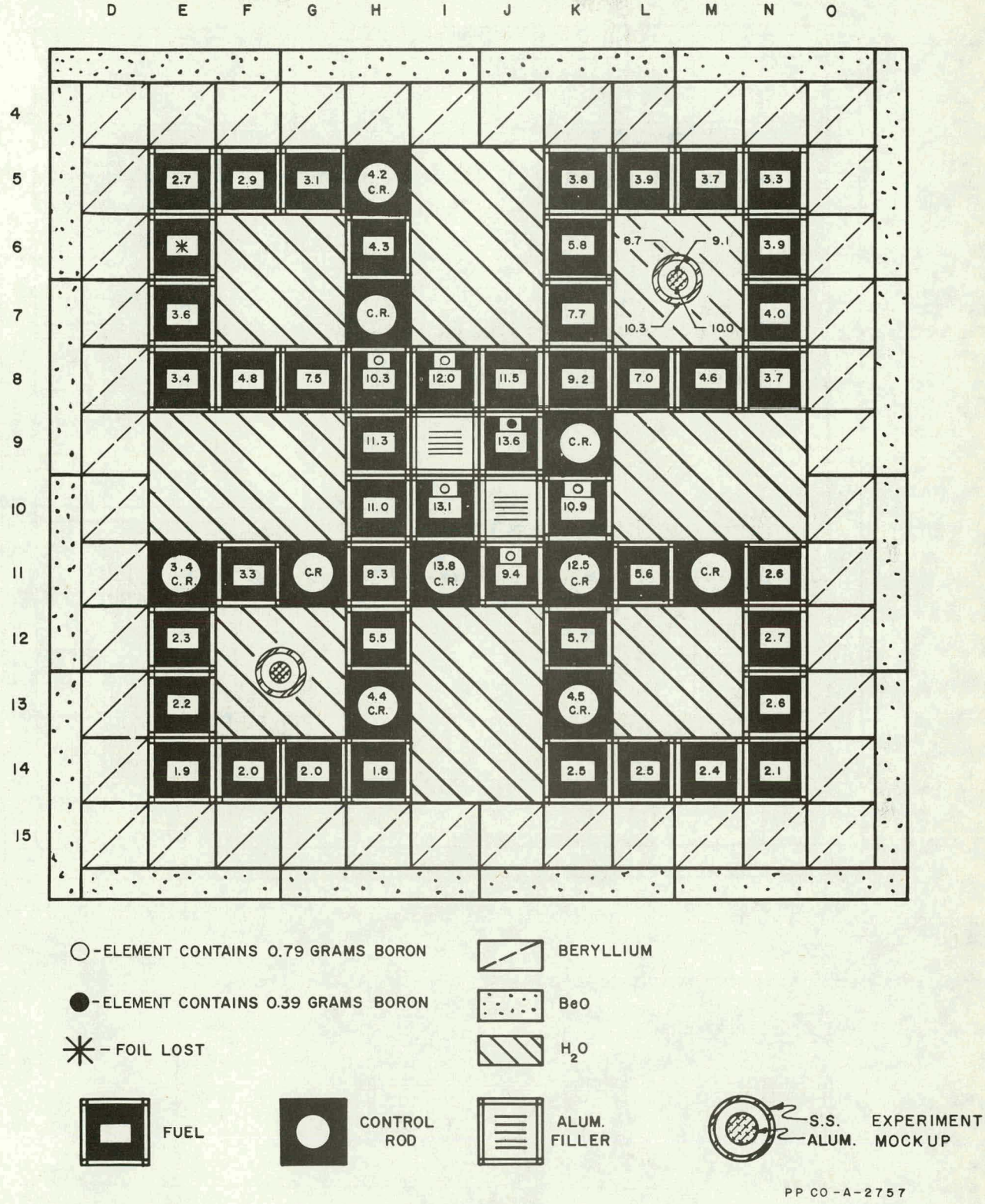

FIG. 8.4F

LOADING II MIDPLANE THERMAL NEUTRON FLUX, 10^{14} n/cm^2-sec.

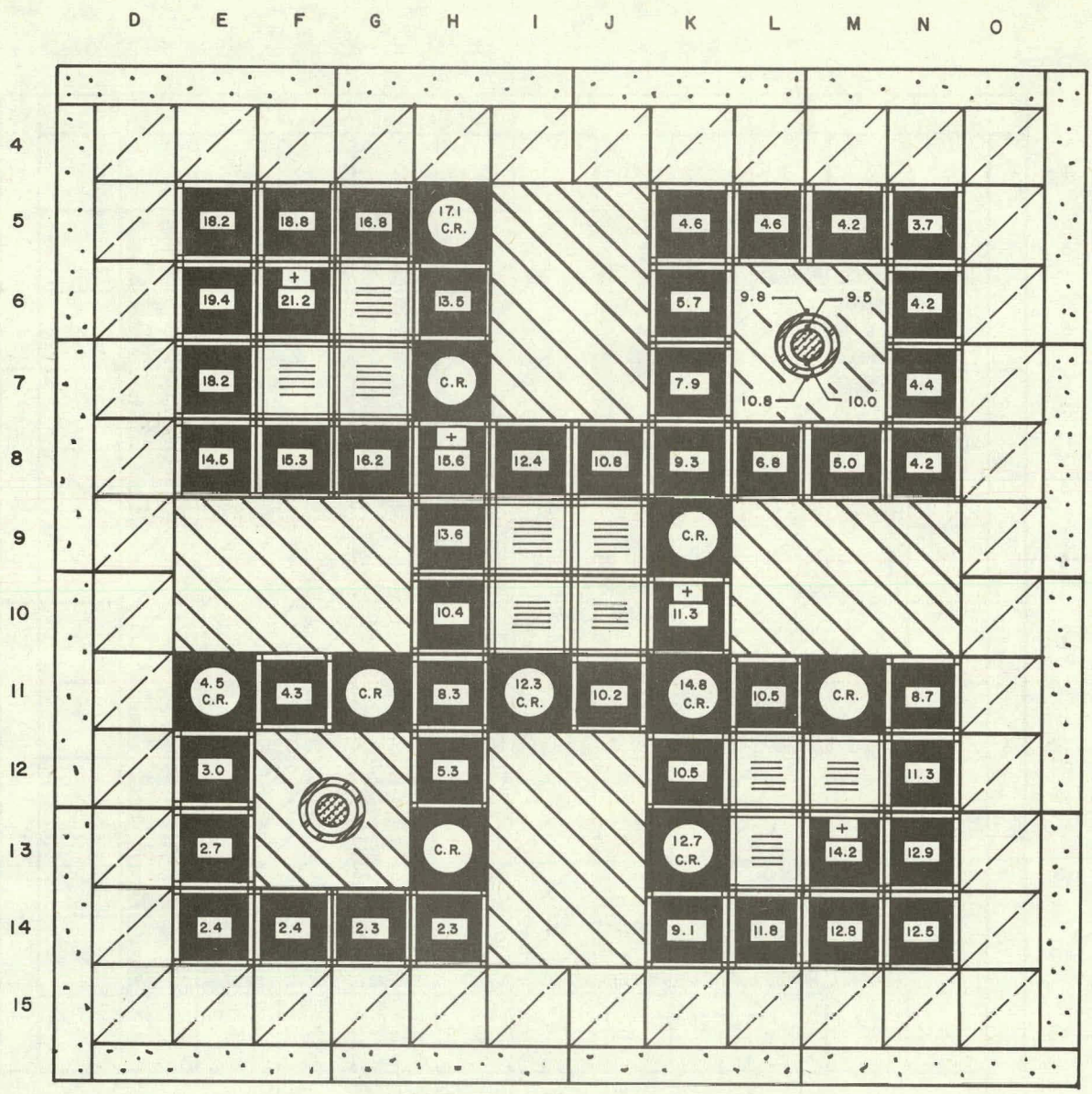

+ — ELEMENT CONTAINS NO BORON

BeO

BERYLLIUM

H_2O

FUEL

CONTROL ROD

ALUM. FILLER

S.S. ALUM. EXPERIMENT MOCKUP

P.P.CO-A-2758

FIG. 8.4G

LOADING III MIDPLANE THERMAL NEUTRON FLUX, 10^{14} n/cm^2 - sec.

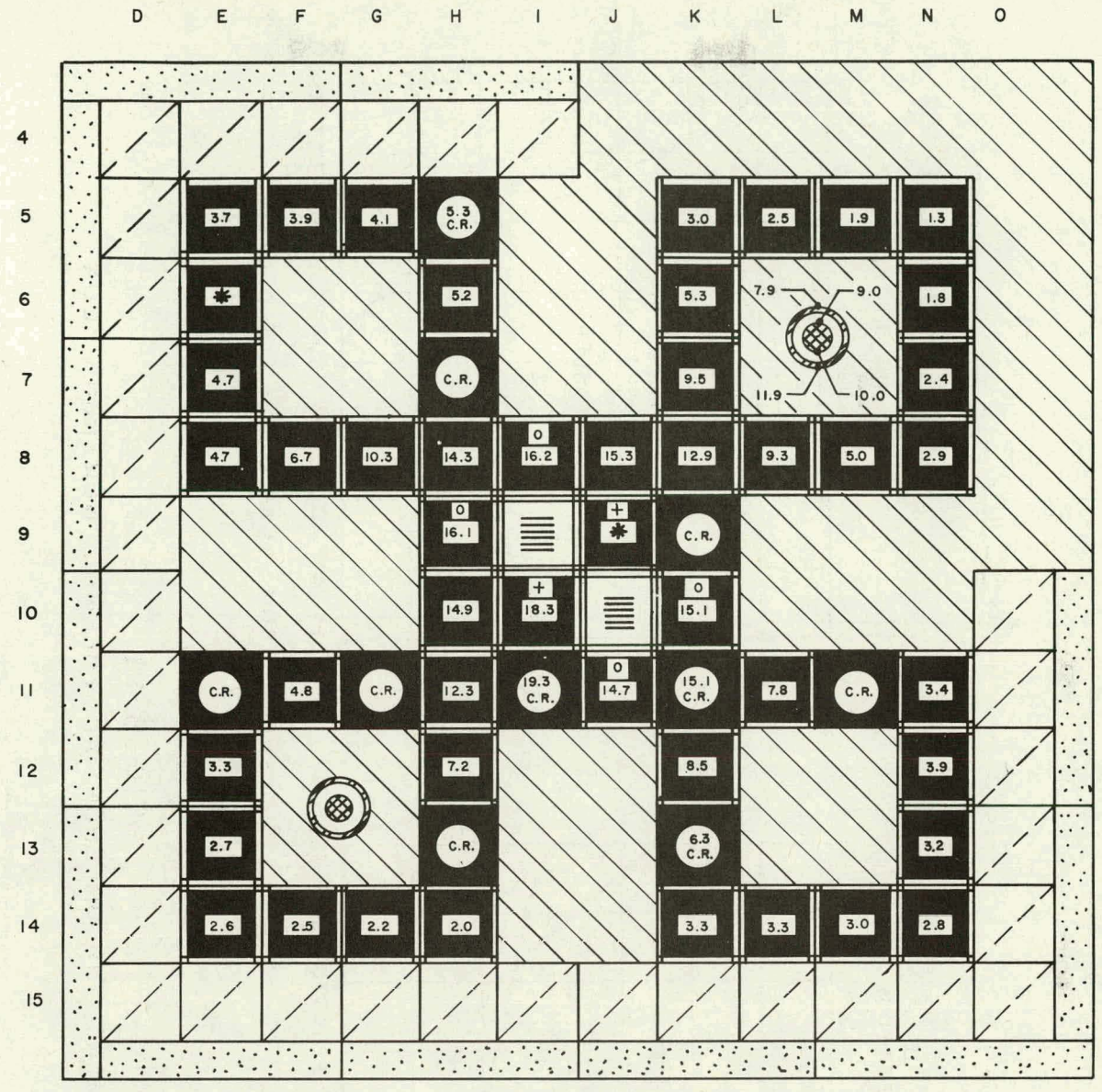

FIG. 8.4H

LOADING IV MIDPLANE THERMAL NEUTRON FLUX, 10^{14} n/cm^2 - sec.

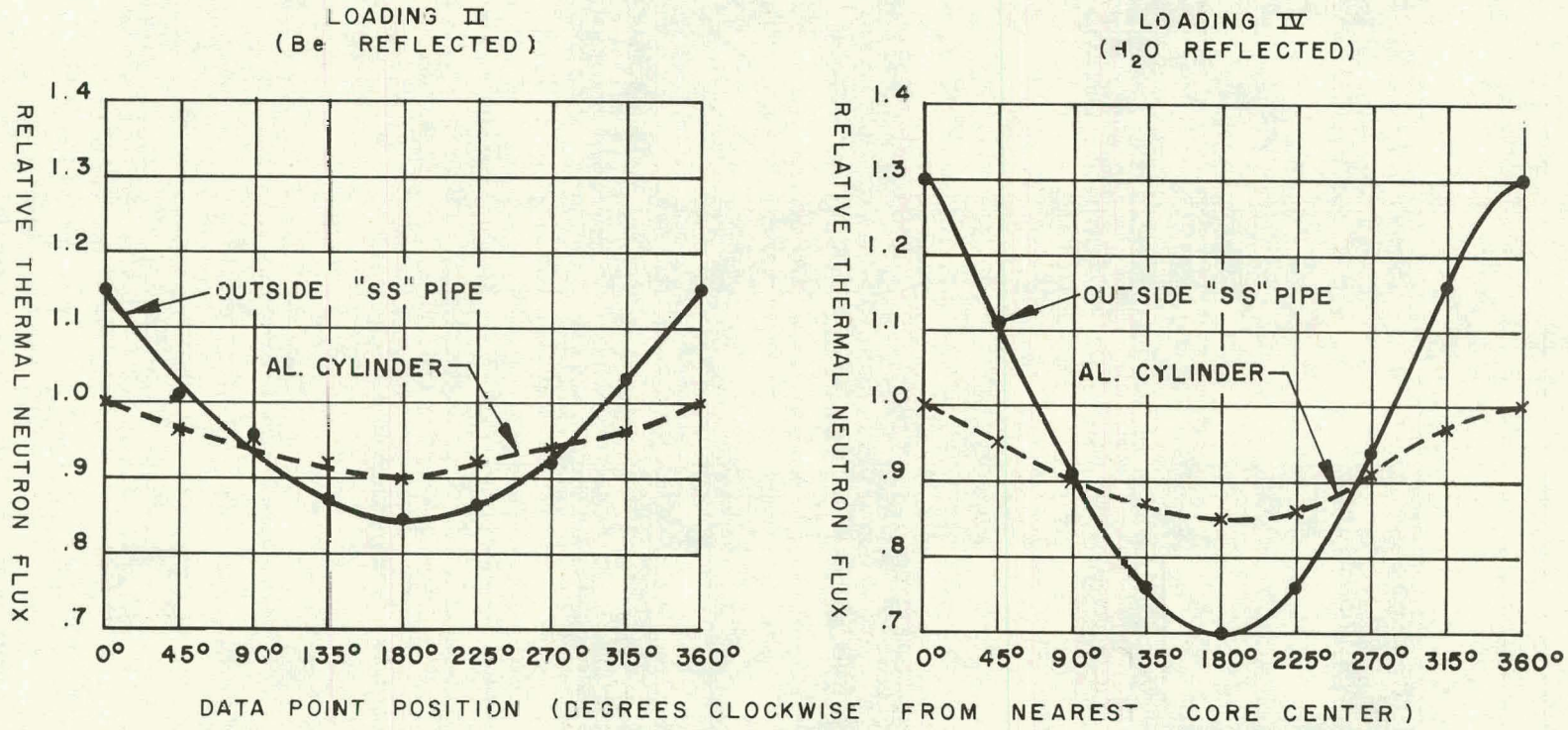

PPCO-A-2760

FIG. 8.4 I

EXPERIMENT CIRCUMFERENTIAL THERMAL NEUTRON FLUX

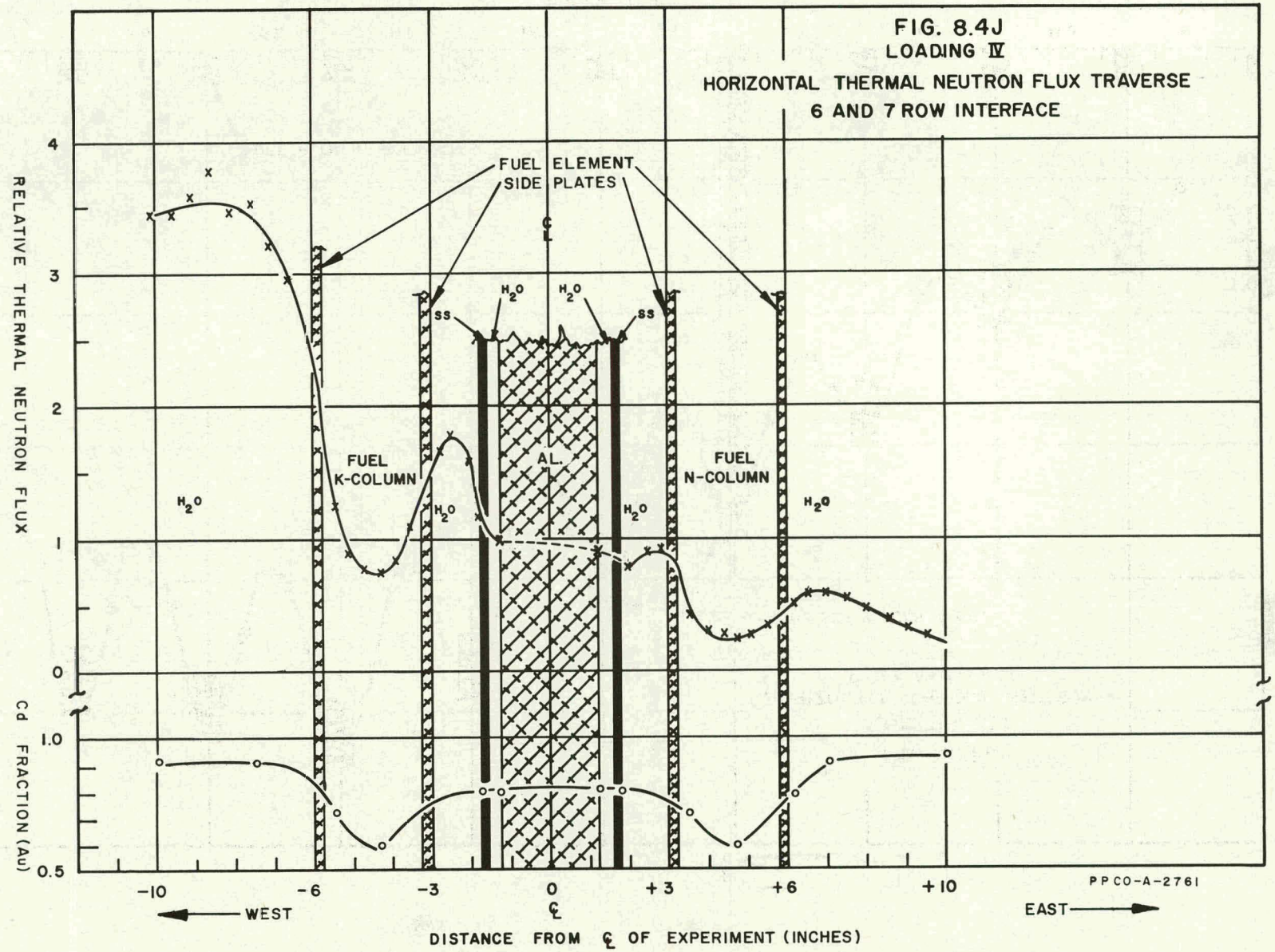
FIG. 8.4J
LOADING IV
HORIZONTAL THERMAL NEUTRON FLUX TRAVERSE
6 AND 7 ROW INTERFACE
RELATIVE THERMAL NEUTRON FLUX
Cd FRACTION (Au)
FUEL ELEMENT SIDE PLATES
FUEL K-COLUMN
AL.
FUEL N-COLUMN
SS
H2O
H2O
H2O
H2O
H2O
H2O
4
3
2
1
0
1.0
0.5
-10
-6
-3
0
+3
+6
+10
WEST
EAST
DISTANCE FROM ℄ OF EXPERIMENT (INCHES)
PPCO-A-2761

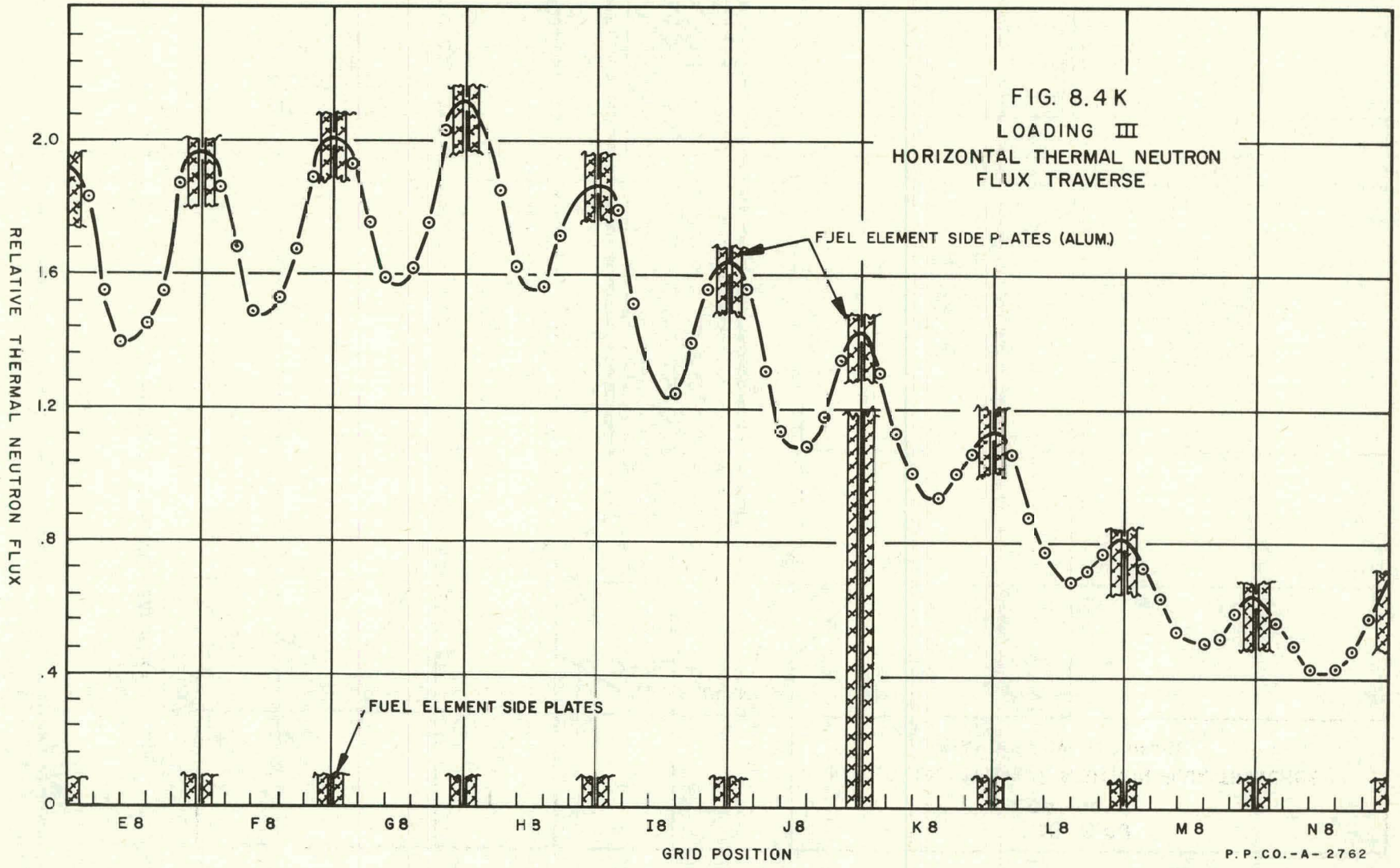
FIG. 8.4 K
LOADING III
HORIZONTAL THERMAL NEUTRON
FLUX TRAVERSE
FUEL ELEMENT SIDE PLATES (ALUM.)
FUEL ELEMENT SIDE PLATES
RELATIVE THERMAL NEUTRON FLUX
2.0
1.6
1.2
.8
.4
0
E 8
F 8
G 8
H 8
I 8
J 8
K 8
L 8
M 8
N 8
GRID POSITION
P. P. CO.-A- 2762

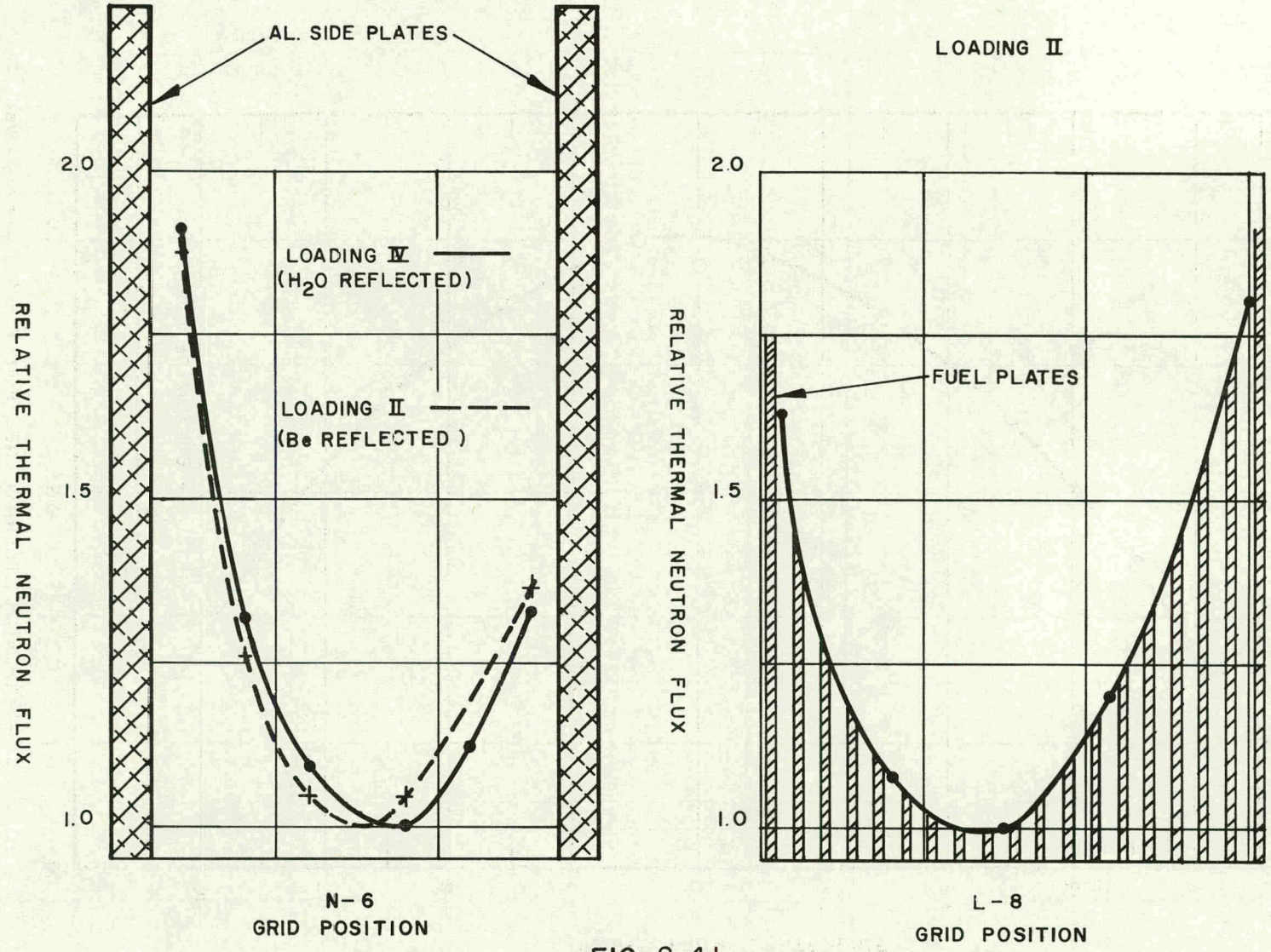

FIG. 8.4L

FUEL ELEMENT THERMAL NEUTRON FLUX TRAVERSES

P.P.CO.-A-2763

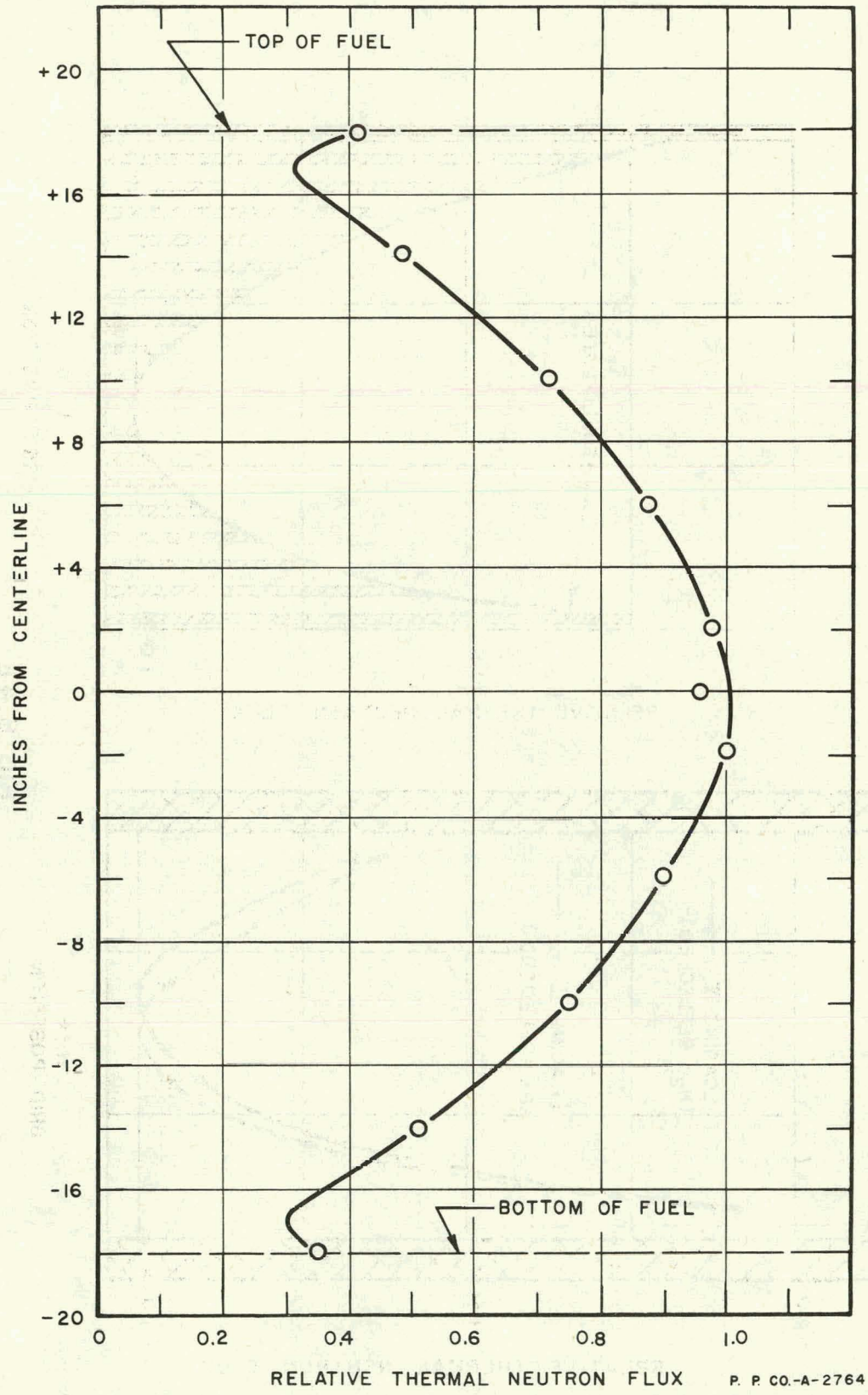

FIG. 8.4M

TYPICAL VERTICAL NEUTRON FLUX DISTRIBUTION

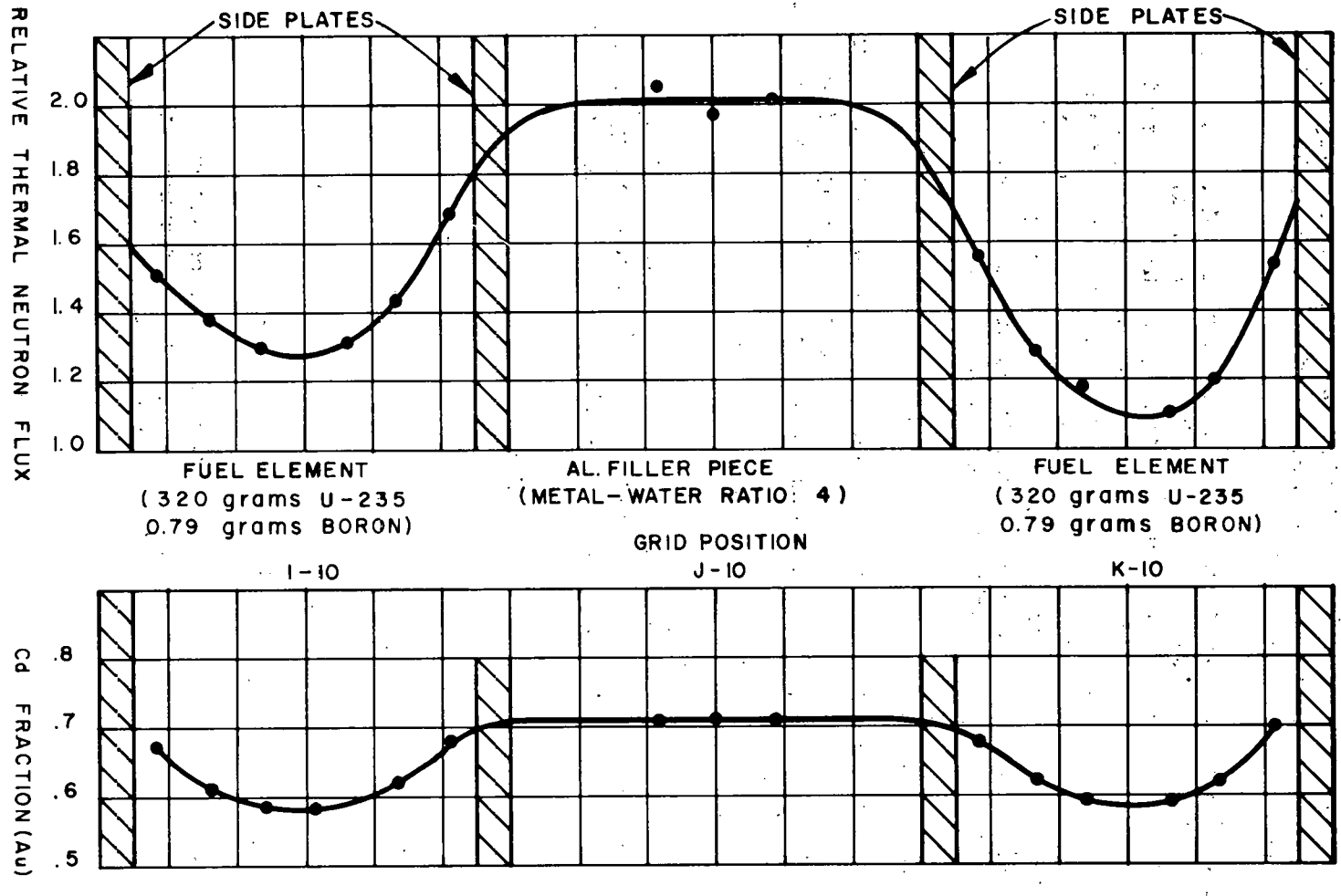

FIG. 8.4 N

HORIZONTAL THERMAL NEUTRON FLUX TRAVERSE
LOADING II

P.P.CO.-A-2765

8.5 Two-Dimensional Computation of Four-Lobe ETR Geometry

A four-group, two-dimensional calculation was made duplicating ETR Critical Facility Loading II described in Section 8.4. The IBM 704 code PDQ02[1] was utilized for this calculation.

Loading II went critical with the shim rod in position H-13 at 17.5 in.; however, for the two-dimensional calculation this rod was assumed to be fully withdrawn and the position filled with the 130 g shim fuel section. It was necessary to extend and deform the volumes of the "Experiment Mockup" in the NE and SW lobes for the calculation in order to fit the available mesh spacing. A schematic diagram of the core is shown in Figure 8.5A. Aluminum guide tubes were present in Loading II in positions E-9, G-9, J-5, J-7, and M-9. These tubes are not shown in Figure 8.5A but the calculation included these tube regions.

8.51 Nuclear Constants

The nuclear constants which were used are listed in Table 8.5A. The constants for the fast groups (1, 2, and 3) were obtained by using the IBM 650 code MUFT III. The thermal constants (Group 4) are Maxwellian-averaged values at 20°C.

8.52 Critical Mass

The eigenvalue obtained from the PDQ calculation was 1.037, indicating a supercritical core. The "critical mass" corresponding to an eigenvalue of 1.000 can be approximated by using the following equation.

$$\frac{\Delta K}{K} = (1 - f)\,\frac{\Delta M}{M},$$

where

$$\frac{\Delta K}{K} = 0.037,$$

thermal utilization, f, = 0.75, and

total U-235 mass, M, = 16.66 kg.

ΔM is found to be 2.46 kg, corresponding to a computed "critical mass" for this core of 14.2 kg of U-235. This compares to the measured value of 16.6 kg as given in Section 8.44.

---

1. G. G. Bilodeau, W. R. Cadwell, J. P. Dorsey, J. G. Fairey and R. S. Varga, "PDQ-An IBM 704 Code to Solve the Two-Dimensional Few-Group Neutron-Diffusion Equation", WAPD-TM-70, August, 1957.

TABLE 8.5A

NUCLEAR CONSTANTS USED IN ETRC-PDQ CALCULATION

Composition		Group 1	Group 2	Group 3	Group 4
Water	D	2.2895	1.10486	0.59419	0.161
	Σ_a	0.001415	0.000012	0.000942	0.01911
	Σ_R	0.1036	0.14941	0.15022	---
Aluminum	D	24.0	6.76	4.55	4.00
	Σ_a	0	0	0.00017	0.0139
	Σ_R	0.00181	0.00181	0.000403	---
BeO	D	2.6832	0.6861	0.621232	0.552
	Σ_a	0.001862	0	0	0.000510
	Σ_R	0.03057	0.019195	0.010634	---
Beryllium	D	3.30	0.59764	0.500	0.411
	Σ_a	0.000028	0	0.000021	0.0015
	Σ_R	0.03324	0.031737	0.01938	---
320 g fuel element with 1.7 g of boron in element	D	3.1145	1.32939	0.76278	1.27061
	Σ_a	0.001042	0.000383	0.00644	0.1158
	Σ_R	0.06439	0.090134	0.087554	---
	$\nu\Sigma_f$	0.000548	0.000715	0.009446	0.182
320 g fuel element with 0.8 g boron present in polyethylene strips	D	3.1151	1.3296	0.763	1.30055
	Σ_a	0.001041	0.000379	0.006357	0.1096
	Σ_R	0.06439	0.09013	0.08775	---
	$\nu\Sigma_f$	0.000548	0.000715	0.00945	0.182
320 g fuel element with 0.4 g boron present in polyethylene strips	D	3.11537	1.32972	0.763105	1.3144
	Σ_a	0.001041	0.000377	0.00623	0.1069
	Σ_R	0.06439	0.09013	0.087833	---
	$\nu\Sigma_f$	0.000548	0.000715	0.009452	0.182
130 g shim rod fuel section	D	3.70843	1.48852	0.88673	0.32323
	Σ_a	0.000697	0.000158	0.002963	0.05676
	Σ_R	0.0493	0.068	0.067	---
	$\nu\Sigma_f$	0.000222	0.00029	0.003851	0.07206
Experiment mockup	D	2.792	1.3283	0.73716	0.40903
	Σ_a	0.000307	0.000015	0.002806	0.06385
	Σ_R	0.04559	0.03962	0.03745	---
Aluminum filler (Al + 20% H_2O)	D	5.2365	1.72671	1.14286	0.650
	Σ_a	0.000285	0.000002	0.000333	0.01385
	Σ_R	0.0236	0.03226	0.0322	---
Water plus aluminum guide tube	D	2.63182	1.20199	0.66664	0.19933
	Σ_a	0.001108	0.000009	0.000792	0.01813
	Σ_R	0.084	0.1195	0.120	---

8.53 Neutron Flux

To compare the PDQ values of thermal neutron flux distribution with the measured distribution, the PDQ values were normalized by multiplying them by the ratio of the measured thermal neutron flux in position K-8 to the corresponding PDQ value. The calculated values of thermal neutron flux are shown in Fig. 8.5A.

8.54 Reactor Power

The total reactor power was calculated from the formula:

$$\text{power} = C \sum_{i=1}^{4} \int_V \Sigma_{fi} \Phi_i \, dV \quad ,$$

where

Σ_{fi} = the macroscopic fission cross section for neutron energy group i as taken from Table 8.5A. ν was assumed to be equal to 2.47 for all groups,

Φ_i = neutron flux in energy group i normalized to measured values by the thermal group ratio in position K-8, and

C = conversion factor to convert fissions/sec to power.

Using the above formula and constants, the reactor power corresponding to the thermal neutron fluxes given in Fig. 8.5A was calculated to be 330 Mw. A value of 335 Mw as listed in Table 8.4A was obtained from the measured neutron fluxes. In a similar manner the power generated in the NE lobe was calculated to be 73 Mw, compared to 72 Mw listed in Table 8.4A. The power generated in several fuel elements including those around the NE lobe was also calculated and is listed in Table 8.5B along with values obtained in ETRC Loading II. Also listed in Table 8.5B are calculated values of power density at the center of several fuel elements and the ratio of power produced by above thermal fissions to the power produced by thermal fissions at the center of the elements.

TABLE 8.5B

COMPARISON OF CALCULATED AND MEASURED ETRC

FUEL ELEMENT POWERS

Fuel Element Position	Power Generated Within Element, Mw		Power Density at Center of Element Mw/liter	Ratio - Above Thermal Fissions / Thermal Fissions
	PDQ Calculation	ETRC Measured		
E-8	4.81		1.12	0.0564
F-8	7.00		1.63	0.0517
G-8	9.08		2.15	0.0554
H-8	9.56		2.35	0.0678
I-8	11.18		2.76	0.0627
J-8	10.75		2.64	0.0672
K-8	9.39	9.81	2.31	0.0713
L-8	9.18	9.51	2.18	0.0559
M-8	7.00	6.29	1.63	0.0533
N-8	5.05	4.55	1.18	0.0560
K-7	9.23	8.97		
K-6	7.31	6.72		
K-5	5.19	4.52		
L-5	4.72	5.01		
M-5	4.12	4.68		
N-5	3.34	3.75		
N-6	4.08	4.36		
N-7	4.62	4.41		

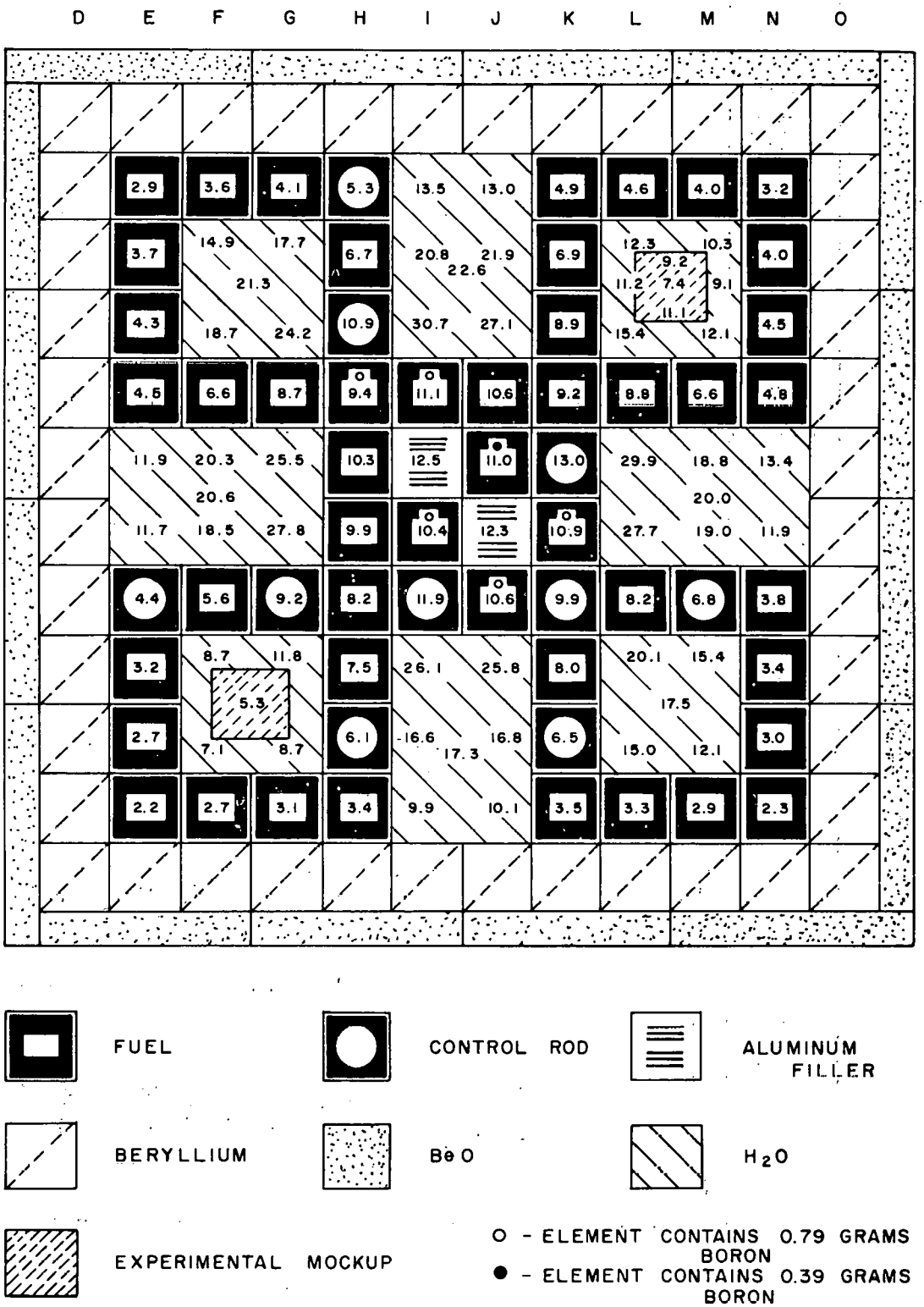

FIG. 8.5 A

P.P.CO.-A-2766

MIDPLANE THERMAL NEUTRON FLUX AT A REACTOR POWER OF 330 MEGAWATTS (UNITS OF 10^{14} NEUTRONS / cm^2 - sec)

8.6 Fuel Element Supplement

8.61 Other Designs Considered

8.611 Rectangular Elements

Rectangular fuel elements were considered for use in the ETR II. These elements have the advantage of easy construction and interchangeability between the concave and convex fuel annuli. However, the wasted space between the fuel elements which results from fitting rectangular elements into annular segments reduces the over-all core efficiency and thereby negates the advantages of the simple construction. If rectangular fuel elements of the MTR type were specified for the ETR II, they would be required to have a local power density approximately 24 per cent greater than that required for the equivalent circular segment fuel element. Also, those segments of the fuel annulus which would contain no fuel because of the use of rectangular fuel elements would probably cause an undesirable shifting of the neutron flux distribution.

The rectangular elements are ideally suited for a square-lobe configuration such as mocked up in the ETRC (Fig. 8.4E). However, this configuration is not recommended for ETR II because of the high total power and high maximum power density required (Re: Table 8.4A).

8.612 Tubular Elements

Bundles of tubes in various arrangements were also considered for the reactor core. If it were possible to obtain adequate strength in these tube bundles without the use of side plates or exterior shells, then the tube bundles would be superior to the equivalent plate designs. However, tube bundles of the required length and diameter, fabricated by existing techniques, do not have sufficient strength to withstand the hydraulic forces without side plates or shells. Once these shells are added, the tube bundles have no superiority over equivalent plate designs, and the added complexity of the tubes makes them less desirable than the plate type element.

8.613 Involute Elements

One of the most promising type of fuel elements considered for uniformly loaded annular fuel elements was the involute element of a design similar to that proposed by Internuclear Company, Inc. (Report AECU-3775). However, the involute element could not be adapted for efficient use in the ETR II core because of the reversal of the direction of curvature of the fuel elements within the core.

8.62 Discussion of Materials Considered

8.621 Fuel Cladding and Side Plates

Aluminum alloys have been recommended for fuel cladding and side plates because of their low neutron cross section, availability,

low cost, ease of fabrication, and adequate mechanical and chemical properties.

The corrosion resistance of aluminum to high temperature water is determined primarily by the purity and the metallurgical condition of the metal. High temperature heat treatment seriously impairs resistance and leads to intergranular attack, whereas cold work is beneficial. The presence of iron and silicon either as impurity or alloy additions improves the resistance of aluminum to corrosion below 400°F. Above this temperature intergranular penetration occurs although such elements as nickel, iron, titanium, copper, cobalt, molybdenum, or tungsten may be added to eliminate this; nickel being the most effective. Al-Fe-Ni type alloys have been developed which show very good corrosion resistance to water at temperatures up to 680°F.

Since the maximum temperature of the fuel plates under operating conditions is in the range of disintegration of 1100 aluminum alloy and in the range of high strength loss for the 6061 age-hardened alloy, an X8001 aluminum alloy containing 1 per cent nickel is recommended. The corrosion of this alloy changes from localized penetration at grain boundaries and blister formation to the more desirable uniform overall attack. The corrosion of X8001 alloy has been studied by various groups with the rate being about 0.2 mil/month under static conditions. Flow velocities up to 20 ft/sec show an increased rate of about three fold. Corrosion of aluminum alloys during higher flow velocities and increased temperatures should be incorporated in a research and development program.

Increased corrosion resistance can be obtained by adding small amounts of Ti and Be to X8001 or by using X8002 or X8003 aluminum alloys. Under aqueous static conditions at 600°F, the corrosion resistance of X8002 and X8003 alloys are respectively five-fold and sixteen-fold that of X8001 alloy. The X8003 alloy would have the disadvantage of being more expensive because of the special fabricating processes involved.

Aluminum alloys having improved mechanical properties over the 1100 alloy at high temperatures must be used to increase the strength of alumimum clad fuel plates for high operating temperatures. Table 8.6A compares the strength of several aluminum alloys at various temperatures. Although other aluminum alloys with good high temperature strengths might have been included in Table 8.6A, the good corrosion resistance of the alloys shown makes them logical choices for the ETR II.

8.622 Fuels

Two types of metallurgical structures for the fuel material have been considered, uranium-aluminum alloys and uranium oxide dispersed in an aluminum matrix. When uranium-aluminum alloys are prepared containing greater than 13 weight per cent uranium, some fabrication difficulties may be encountered. These hypereutectic alloys are strong and brittle due to the intermetallic compound UAl_4. Rapid cooling of these high uranium alloys tends to suppress the peritectic reaction

TABLE 8.6A

STRENGTHS OF ALUMINUM ALLOYS[1,2]

Alloys	Yield Strength, psi				
	75°F	300°F	400°F	500°F	600°F
1100 Al					
"O" Condition	5000	4500	3500	2000	1500
H-14 Condition	17,000	12,000	7000	2500	1500
H-18 Condition	22,000	14,000	4000	2000	1500
X8001					
Forged (F)	17,800	13,700	9400	6000	3200
Extruded (F)	6300				2800
X8002 H-18 Condition	28,800		12,000	7200	5600
6061 Al					
"O" Condition	8000				
T-4 Condition	21,000				
T-6 Condition	40,000	29,000	15,000	5000	2500
M457 Extruded (F)					6100
M257 Extruded (F)	24,000		18,000	16,000	15,000
M470 Extruded (F)	29,000				21,000
M430 Extruded (F)	35,000		30,000	27,000	23,000

1. "Alcoa Aluminum Handbook", Aluminum Company of America, Pittsburgh, Pennsylvania, 1959.

2. W. W. Binger, Alcoa--personal communication.

occurring at 750°C and prevent UAl_3 from reacting with Al to produce UAl_4. Suppressing the peritectic reaction produces a more ductile material which makes it possible to hot roll U-Al alloys containing up to 35 weight per cent uranium. Uranium-aluminum alloys containing greater than 35 weight per cent uranium can be fabricated by using ternary additions (Ge, Zr, Sn, Si) to suppress the peritectic reaction, thus allowing the primary nucleating compound UAl_3 to be retained as the stable phase. Experimental studies have shown that a 48 weight per cent U-Al alloy containing 3 weight per cent silicon can be successfully hot rolled.

A 35 weight per cent U-Al alloy contains approximately 52 weight per cent of the intermetallic compound UAl_4 unless some suppression is obtained. Without any suppression of the UAl_4 compound, the high yield strength of the core alloy and the low strength of the cladding produces "dog boning". Such non-uniform deformation is not pronounced in plates containing 10 to 20 weight per cent U-Al alloys because of close matching of the yield strength and ductility of these alloys with 1100 Al containment materials. By using an aluminum alloy such as X8001 for both cladding and matrix, dog boning can be reduced; and, if one controls the fabrication techniques, a fuel element containing up to 35 weight per cent uranium in U-Al alloys can be fabricated.

If fuel loadings requiring higher uranium content are necessary, the plates can be fabricated using UO_2-Al dispersion cores containing up to 60 weight per cent UO_2. Highly enriched UO_2 costs more than the metal, and rejected plates prepared by powder techniques must be chemically recovered rather than recycled directly into the melt as is the case with the alloy. Although the powder metallurgy plates are more costly, they are superior to the alloy because of less dog boning, and burnable poisons can be added with much greater accuracy and greater uniformity than with the alloys. Also, gradients in fuel concentration can be easily employed if desired. Fuel plates containing fuel gradations as large as 30 weight per cent have been produced by the powder technique. Other advantages which might be considered are that fewer steps are employed in preparation of plates and that less scrap is formed in the processing of plates.

8.63 Extension to Higher Power Operation

From a heat removal standpoint, reactor power could be increased, if desirable, in one or more of many ways. The easiest method of increasing reactor power would be to increase the coolant velocity. This would require no modifications to the core or to the element, except for possible modification in the total fuel loading. At the present state of reactor technology, 45 to 50 ft/sec appears to be the maximum practical coolant velocity for use with Al plates. The reactor tank pressure may also be increased, which would allow a corresponding increase in the maximum wall temperature. However, again current

technology for aluminum clad fuel plates limits the maximum, practical wall temperature to approximately 475°F and therefore little additional gain may be made by increasing the tank pressure above 300 psi without changing the cladding materials.

The greatest potential increase in core power may be obtained through the use of variable fuel and/or poison loadings throughout the fuel elements. If the fuel and/or poison concentration is held constant in any given fuel plate, but is adjusted from plate-to-plate so that the maximum heat flux is the same for each plate, then the power of ETR II could be increased by a factor of approximately 1.5. Such a variation from plate-to-plate is entirely practical and may be accomplished through the use of standard fabrication techniques. If the fuel and/or poison is also varied lengthwise in each plate, the reactor power may be increased by an additional factor of approximately 1.3. However, the longitudinal variation within a single plate may cause considerable fabrication difficulties which would necessitate a development program and cause an increase in the cost of the element. In any event, deviation from uniform fuel loadings would cause some variation of the reactor flux, and for each proposed case of variable loadings, flux calculations would be necessary to determine the detailed effect of the variable fuel and/or poison loadings.

8.7 Reactor Cooling

8.71 Introduction

The hydraulic and heat transfer performance of several different fuel element geometries was determined during this study. This work was undertaken to facilitate the selection of a fuel element which is expected to operate satisfactorily at the specified conditions.

The general criteria used to establish the fuel element geometry and operating conditions of the primary coolant are discussed in Section 4.3, 4.5, and 8.6. The physics requirements are discussed in Section 3.0 and the core configuration which the fuel element must fit is discussed in Section 2.0.

Standard non-isothermal, turbulent hydraulic calculations have been made to determine the core pressure drop and the absolute pressure at the hot-spot.

8.72 Circular Segment Heat Transfer

An explanation of the method used to calculate the wall temperature is presented here since it differs slightly from that sometimes used. The nominal wall temperature at the point of maximum power density is calculated from the following equation.

$$T_w = T_{in} + \Delta T_b + \Delta T_f \quad ,$$

or

$$T_w = T_{in} + \left(\frac{\Phi_{max}}{\Phi_{avg}}\right)_{II} \frac{(Q/A)A'}{V\rho C_p \alpha} + 0.90 \left(\frac{\Phi_{max}}{\Phi_{avg}}\right)_{H} \left(\frac{\Phi_{max}}{\Phi_{avg}}\right)_{V} \frac{(Q/A)}{h} \quad ,$$

where

T_w = wall temperature,

T_{in} = inlet temperature,

ΔT_b = bulk water temperature rise to the point in question,

Q/A = total reactor power divided by total reactor heat transfer area,

A' = heat transfer area in hot channel from top of channel to hot spot,

V = coolant velocity,

ρ = coolant density,

C_p = coolant heat capacity,

α = cross sectional flow area of hot channel,

$\left(\frac{\Phi_{max}}{\Phi_{avg}}\right)_H$ = horizontal power density ratio, max/avg,

$\left(\frac{\Phi_{max}}{\Phi_{avg}}\right)_V$ = vertical power density ratio, max/avg, and

h = heat transfer coefficient evaluated at a film temperature equal to $\frac{1}{2}(T_{in} + \Delta T_b + T_w)$.

To each of the terms in this equation is applied its maximum deviation for the hot-spot hot-channel analysis. These uncertainty terms are grouped together in $\Pi(F_b)$ and $\Pi(F_h)$. The heat transfer coefficient is now evaluated at the hot-spot film temperature, i.e.,

$$\frac{1}{2}\left[T_{in} + \Delta T_{add} + \Pi(F_b)\,\Delta T_b + T_{w_{max}}\right].$$

The equation, containing the uncertainty factors, for the maximum wall temperature becomes:

$$T_{w_{max}} = T_{in} + \Delta T_{add} + \Pi(F_b)\,\Delta T_b + 0.90\,\Pi(F_h)\left(\frac{\Phi_{max}}{\Phi_{avg}}\right)_V\left(\frac{\Phi_{max}}{\Phi_{avg}}\right)_H \frac{Q/A}{h},$$

where

$T_{w_{max}}$ = maximum creditable wall temperature,

ΔT_{add} = variation of inlet bulk water temperature,

$\Pi(F_b)$ = product of all hot-channel factors, and

$\Pi(F_h)$ = product of all hot-spot factors.

The hot-channel, hot-spot and power distribution factors used in the heat transfer analysis are cited in Table 4.5A. Most of these factors are based upon MTR-ETR experience. The power distribution factors are set by physics studies.

Several of the factors are set by the fuel assembly specifications. These are: fuel content per plate, fuel core alloy thickness, and fuel segment angle. In calculating the hot channel factor for the hydraulic diameter variation it was assumed that the velocity was directly proportional to the square root of the hydraulic diameter. The cross sectional area variation of a coolant channel must be included since it is necessary to convert from a measured, or calculated, linear velocity to a mass rate of flow.

The net heat generation factor (0.90) results from the fact that not all of the reactor heat is generated in the fuel core alloy.

The modified Colburn equation was used to calculate the heat transfer coefficient;

$$\frac{hD}{k} = 0.023\ Re^{0.8}\ Pr^{0.3} \quad ,$$

where

h = heat transfer coefficient, Btu/hr-ft^2-$^\circ$F,

D = hydraulic diameter, ft,

k = thermal conductivity, Btu/hr-ft^2-$^\circ$F/ft,

Re = Reynolds number, and

Pr = Prandtl modulus.

All the physical properties were evaluated at the film temperature. The coefficient calculated by this equation has an uncertainty of ± 20 per cent or a hot-spot factor of 1.25 to account for the variation in the experimental measurements and also since a recent investigator[1] has found that the modified Colburn equation predicts heat transfer coefficients which are larger than those that were measured in geometries similar to those studied here. Table 8.7A and Figures 8.7A and 8.7B summarize the results of the calculations for the selected geometry and inlet coolant conditions. In Fig. 8.7C, the maximum permissible power density is correlated with the channel thickness for different linear velocities and reactor inlet pressures. Table 8.7B cites the lateral differential pressures that were calculated for various cases. It appears that the element selected can be expected to withstand the hydraulic forces developed during normal operation.

8.73 Maximum Power Density

A limited number of heat transfer and hydraulic calculations were made utilizing the following assumptions: 1) the maximum operable wall temperature was 500°F and 2) the maximum permissible core pressure

---

1. S. Levy, R. O. Niemi, R. A. Fuller, "Heat Transfer to Water in Thin Rectangular Channels" Journal of Heat Transfer, No. 81, p. 129-43, 1959

TABLE 8.7A

ETR II CIRCULAR-SEGMENT FUEL ELEMENT*

Coolant Vel. ft/sec	$(Q/A)_{avg}$** Btu/hr ft^2	Maximum Allowable Core Power Mw	Average** Power Density (Mw/liter)	Maximum Power Density (Mw/liter)	T_{wall} (^oF)	Flow Thru Fuel Core (gpm)	Core Δp (psi)
30	5.34×10^5	224	0.85	1.86	432	17,330	45.5
40	6.7×10^5	281	1.07	2.34	424	23,110	76.1
50	7.85×10^5	330	1.25	2.73	414	28,890	115

* Experimental Conditions

Fuel element sector	$= 45^o$
Fuel element thickness	= 2.5 in.
Number of plates	= 19
Thickness of plates	= 0.050 in.
Thickness of channels	= 0.0775 in.
Inlet water temperature	= 130°F
Inlet water pressure	= 300 psig
Metal-to-water ratio	= 0.80
$(\Phi max/\Phi avg)_V$	= 1.4
$(\Phi_{max}/\Phi_{avg})_H$	= 1.56

** Average over entire core.

TABLE 8.7B

LATERAL DIFFERENTIAL PRESSURES FOR VARIOUS DESIGN AND OPERATING CONDITIONS

Velocity ft/sec	Channel Thickness in.	Lateral Differential Pressure psi
40	0.100	2.9
40	0.090	3.2
40	0.084	3.5
40	0.0775	3.8
30	0.0775	2.1
50	0.0775	5.9

drop was 100 psi. The calculations were made for the hot channel only and were done to indicate the maximum density that could be obtained with reasonable assurance that the fuel elements would operate satisfactorily. Four foot and six foot core lengths were considered.

The hot-channel and hot-spot factors that were used are cited in Table 4.5A. An axial maximum-to-average power density ratio of 1.35 was assumed. The fraction of total power generated in the fuel plates was assumed to be 0.90.

The results of these calculations are presented in Table 8.7C. It can be seen from these results that changing the channel size does not affect the operable power density significantly if the core pressure drop and maximum wall temperature are held constant. Increasing the length to 6 ft from 4 ft decreases the allowable maximum power density by about one Mw/liter for the two cases compared.

TABLE 8.7C

SUMMARY OF MAXIMUM POWER DENSITY CALCULATIONS FOR CIRCULAR-SEGMENT FUEL ELEMENT

Coolant Channel Thickness, in.	Average Fuel Core Alloy Length, in.	Coolant* Velocity, ft/sec	Average Power Density, Mw/liter	Maximum Power Density,** Mw/liter	Lateral Pressure Differential, psi
0.060	48	40	2.56	3.46	4.0
0.080	48	45	2.61	3.52	3.3
0.100	48	51	2.71	3.66	3.2
0.060	72	33	1.72	2.32	
0.080	72	38	1.92	2.59	

* Core Pressure Drop = 100 psi

** Inlet Water Temperature = 130°F

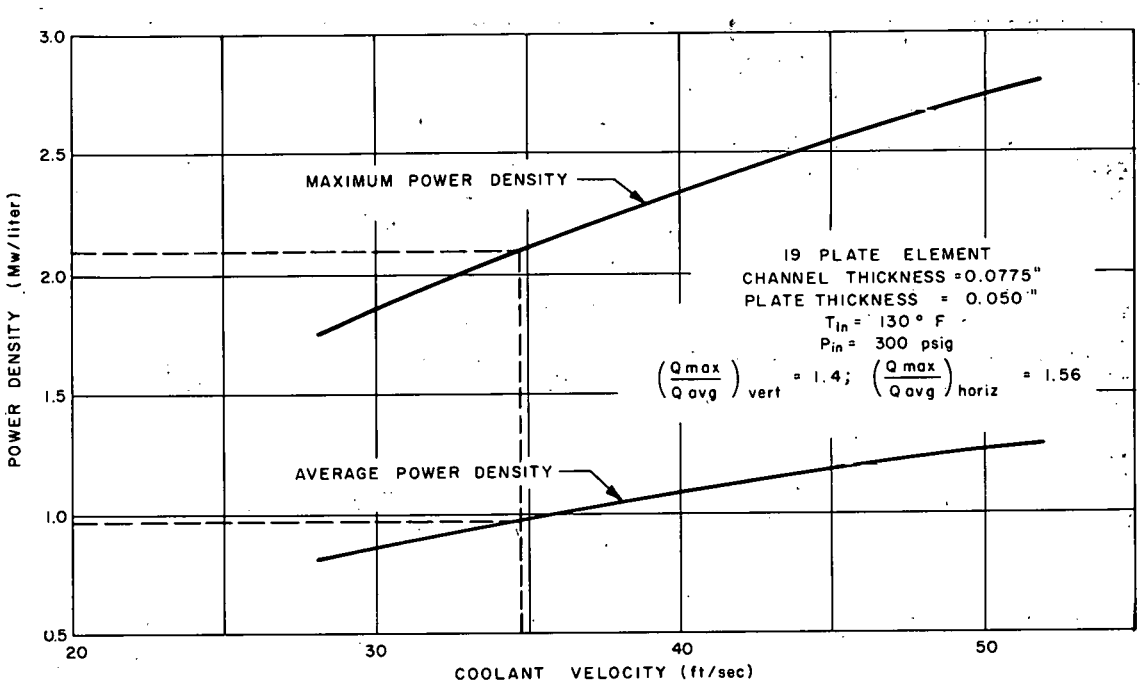

FIG. 8.7 A

ALLOWABLE POWER DENSITY vs COOLANT VELOCITY

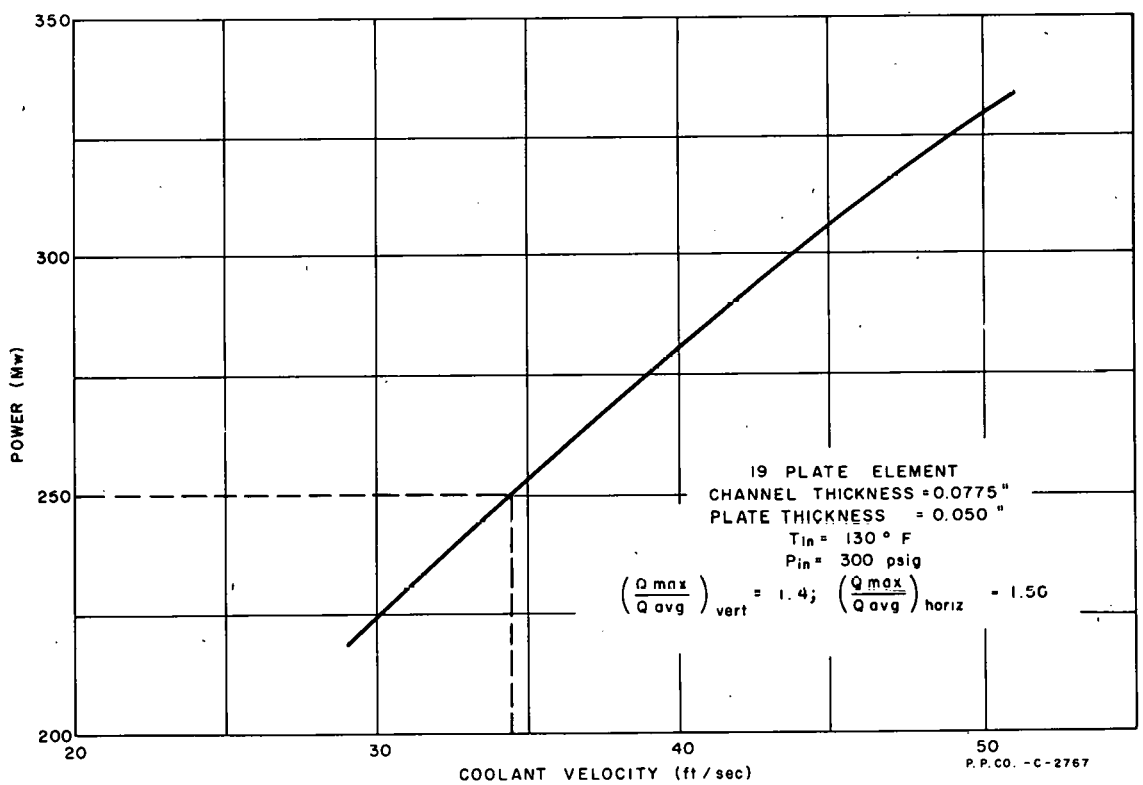

FIG. 8.7 B

TOTAL ALLOWABLE REACTOR POWER vs COOLANT VELOCITY

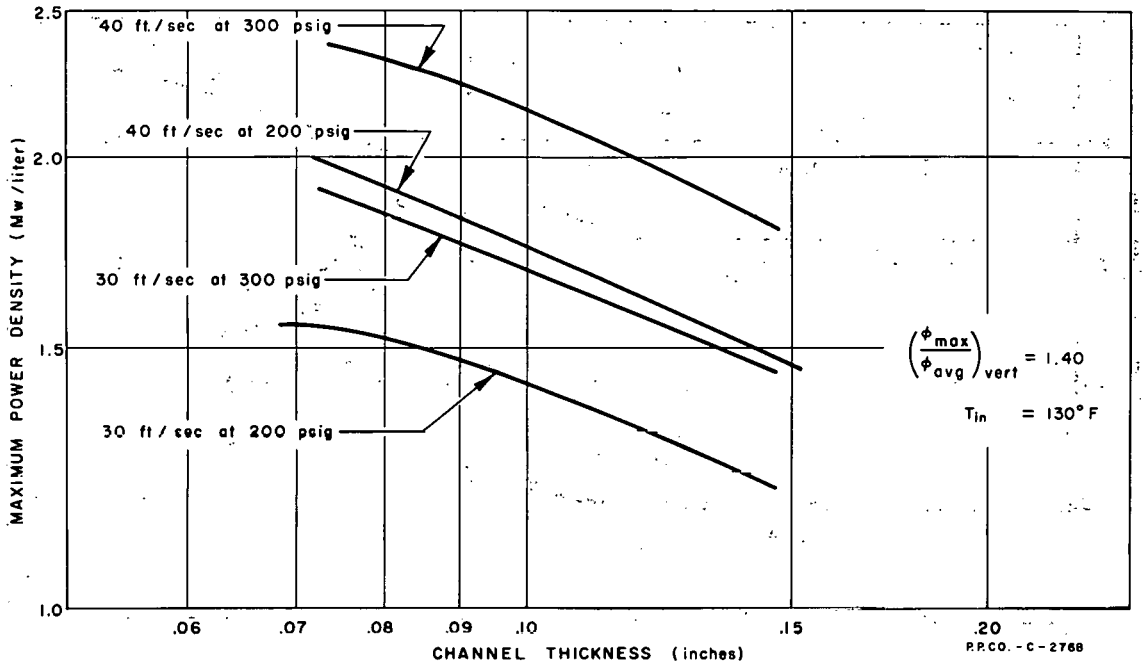

FIG. 8.7 C

MAXIMUM ALLOWABLE POWER DENSITY vs CHANNEL THICKNESS

8.8 Materials of Construction

Requirements for high neutron flux and test loop pressure can result in relatively high combined stresses in the reactor vessel and the in-pile loop tubes. In the design of the four-lobe reactor wherein the vessel wall is removed from the vicinity of the fuel so that the internal heating rate is low (< 2.0 watts/cc) stainless steel (Type 304L or 347) is recommended as the pressure vessel construction material.

The specifications for decontamination of the in-pile loops necessitate the use of stainless steel (Type 304L or 347) as the construction material for the loops and when subjected to the maximum design conditions of pressure, thermal, and combined stress are designed for a definite fatigue life of 65,000 cycles according to tentative design criteria.

8.81 Internal Heating Rate

Heat generation rates in the four-lobe core pressure vessel were calculated from the flux equations given by Rockwell.[1] Each lobe of the four-lobe was assumed to be an evenly distributed cylindrical source. Core buildup was derived from plane isotropic buildup factors for lead.[2] Point isotropic buildup factors were used in the aluminum[3] and plane isotropic buildup factors in water reflectors.[2] Sources for prompt and fission product gammas were from Rockwell.[1] The source was based on a power density of 1000 watts/cc.

Neutron heating was calculated for elastic and inelastic scattering and capture. Scattering heating assumed all collisions of fast neutrons were first collisions in the tank near the core.

The results are as follows:

Four-Lobe (Vessel outside outer reflector)	Total Heating watts/g
Average for vessel with 59 in. diameter	0.11
Average for vessel with 75 in. diameter	0.021

1. T. Rockwell, "Reactor Shielding Design Manual", D. VanNostrand, 1956
2. S. Presser, P. S. Mittelman, C. R. Berndtson, "Plane Isotropic Build-up Factors for Lead and Water with Application to Shielding Calculations", NDA-10-144, 1954
3. H. Goldstein and J. E. Wilkins, "Calculations of the Penetration of Gamma Rays", NYO-3075, 1954

8.82 Material Selection

With potentially high thermal stresses from internal heat generation and with high strength at temperature required, the combined stresses in various materials were compared with the maximum allowable stress values at temperature as required by the ASME "Boiler and Pressure Vessel Code".[1] For those designs in which the pressure vessel is inside the outer reflector so that the internal heat generation is greater than 2 watts/g (see Table 8.8C) the total stress in a stainless steel pressure vessel becomes greater than the allowable stress, while the total stress in an aluminum alloy vessel is less than the allowable stress. In the design wherein the vessel is outside the outer reflector so that attenuation of neutrons and gammas in the water and possibly the thermal shield occurs, steel as a material for the pressure vessel shell is more attractive. According to a prominent fabricator of aluminum shapes, the largest tubes extruded are 24 in. o.d. so that allowable stresses for vessel shells in excess of 24 in. according to ASME code would be based on the annealed value.

In Table 8.8A are thermal stress factors and ASME code allowable shell thickness for various materials at several tube diameters for the following design conditions:

Internal Pressure	425 psig
External Pressure	0 psig
Maximum Metal Temperature	200°F

It is noted that high strength aluminum alloys offer an advantage in reduced thermal stress by greater than a factor of 15.

The corrosion resistance of these alloys at 200°F should be adequate, although the possibility for stress corrosion does exist. The beneficial effects of copper additions to aluminum and especially of nickel on the corrosion resistance in high purity water at elevated temperatures has been noted by several authors.[2,3]

8.83 Stresses in Reactor Core Vessel and Loop Tubes

The stresses in the loop tube and the reactor pressure vessel were studied to determine the thermal and pressure stresses. The methods of calculation are briefly described.

---

1. ASME Boiler and Pressure Vessel Code 1956 Section VIII Unfired Pressure Vessels.
2. R. L. Dillon, R. E. Wilson, W. H. Troutner, "High Temperature Aqueous Corrosion of Commerical Aluminum Alloys", HW-27636, January 11, 1956.
3. J. E. Draley and W. E. Ruther, "Corrosion Resistant Aluminum Above 200°C", ANL-5430, July 15, 1955.

TABLE 8.8A

THERMAL STRESS FACTORS AND ASME CODE

ALLOWABLE SHELL THICKNESS AT 200°F

Materials	Tube Diameter i.d. in in.	Thickness in.	$\frac{\alpha E}{k\,(1-\nu)}$
Aluminum Alloys			
1100-0	26.3	3.52	1.62
2014-T6	22.0	0.33	2.34
5052-H34	22.0	0.58	2.62
6061-T6	22.0	0.55	2.25
2018-T6	22.0		2.28
5454-0	26.3	0.99	2.89
	40.5	1.52	2.89
	59.0	2.21	2.89
	75.0	2.81	2.89
	88.5	3.32	2.89
Stainless Steel Type 347			
	40.5	0.59	38
	59.0	0.85	38
	75.0	1.08	38
	88.5	1.28	38

8.831 Material Property Values

The property values assumed for the aluminum alloys and for stainless steel are temperature dependent. The values used in the calculations are given in Table 8.8B (for temperature range 77-212°F).

8.832 Uniform Internal Heating

The rate of internal heat generation will not be uniform through the metal due to attenuation so that the heat generation will be higher at the surface. Since cooling is also accomplished at the surface, the temperature distribution through the metal will be less than for uniform heat generation. A value of thermal stress leading to conservative design will therefore be obtained by an assumption of uniform internal heat generation.

TABLE 8.8B

PROPERTY VALUES OF VARIOUS ALLOYS USED IN THERMAL STRESS CALCULATIONS

Property Values	2014-T6	5454-0	Stainless Steel
Coefficient of Thermal Expansion, in./in.^{o}F	13.3×10^{-6}	14.0×10^{-6}	9.0×10^{-6}
Modulus of Elasticity, psi	10.6×10^{6}	10.3×10^{6}	28×10^{6}
Poisson's Ratio	0.33	0.33	0.29
Thermal Conductivity, Btu/hr-ft-^{o}F	89.5	74.5	9.4

The formula used assumes that the cylinder is free to expand in an axial direction, that the vessel is relatively long, and that the variation in temperature along the axis is gradual so that axial temperature differences do not cause appreciable stresses. The maximum tangetial stress in a hollow tube is given[1] by:

$$\sigma = \frac{\alpha E}{(1-\nu)} \left\{ \frac{q}{8k} \left[b^2 + a^2 - \left(\frac{b^2 - a^2}{\ell n\ b/a} \right) \right] + (T_b - T_a) \left[\frac{b^2}{b^2 - a^2} - \frac{1}{\ell n\ b^2/a^2} \right] \right\} ,$$

where

σ = the longitudinal and tangential stress, psi,
α = coefficient of thermal expansion, in./in.^{o}F,
E = modulus of elasticity, psi,
k = thermal conductivity, Btu/hr-ft-^{o}F,
ν = Poisson's ratio,
q = heat generation per unit volume, Btu/hr-ft^{3},
b = outside radius of the tube, ft,
a = inside radius of the tube, ft, and
T = temperature at the surface denoted, ^{o}F.

Stresses due to transmitted heat will be reflected by a thermal gradient across the cylinder wall.

8.833 Stresses Due to Pressure

When hydrostatic pressures are applied to either surface of the cylinder, the tangential stress is computed by the formula:

1. R. Daane, "Nuclear Engineering Handbook", edited by H. Etherington, p. 9-112, 1958.

$$\sigma_\theta = \frac{a^2 P_a - b^2 P_b}{b^2 - a^2} - \frac{(P_b - P_a)\, a^2 b^2}{r^2 (b^2 - a^2)} \quad ,$$

where

P = pressure at the surface denoted, psi.

Where the pressure is an internal pressure only and the thickness is small compared to the radius, the above formula reduces to the familiar formula for loop stress:

$$S = PR/h \quad ,$$

where

S = the tangential stress, psi,
P = internal pressure, psi,
R = inside radius, in., and
h = thickness, in.

8.834 Combined Stresses

When the stresses in a structure occur as a result of more than one type of load, the resultant stress in the material is obtained by superposition of the primary or colinear stresses. The tangential pressure and thermal stresses can therefore be added algebraically to find the combined stress. If this stress is the numerical maximum, it can then be compared with the allowable stress values at temperature as required by the ASME, "Boiler and Pressure Vessel Code".

The pressure and thermal stresses as functions of wall thicknesses are shown by Figures 8.8A and 8.8B, for an internal heat generation rate of 2.5 watts/g.

8.835 Reactor Core Vessel

In the ETR II the diameter of the pressure vessel limits the use of heat treated high strength aluminum alloys. The advantages of these alloys are indicated in Table 8.8C. Design Conditions:

Internal Pressure	425 psi
Metal Temperature	200°F
Wall Temperature Difference	10°F

It is readily seen that the high strength aluminum alloys have a distinct advantage in meeting ASME code requirements at the higher internal heating rates. However, as the pressure vessel is moved away from the fuel annulus and the heating rate decreases, the advantage changes to the use of stainless steel (Type 304L or 347) because of its proven

ability as construction material in reactor pressure vessels. The predictable better resistance to stress corrosion conditions under irradiation makes Type 304L or 347 stainless steel the preferred material at low (< 2.0 watts/cc) heating rates, see Table 8.8C.

TABLE 8.8C

COMPARISON OF TOTAL STRESS WITH ALLOWABLE STRESS

FOR VARIOUS MATERIALS AND VESSEL DIAMETERS

Material	Internal Heating watts/cc	Inside Diameter in.	Thickness* in.	Total Stress psi	Allowable Stress** psi
Aluminum Alloys					
2014-T6	90	12	0.40	9,800	21,600
2014-T6	90	22.5	0.50	14,000	21,600
2014-T6	20	22.5	0.50	10,600	21,600
5454-0	20	26.3	1.0	9,910	11,150
5454-0	6.7	40.5	1.6	9,000	11,150
5454-0	0.29	59	2.3	6,600	11,150
5454-0	0.055	75	3.0	6,500	11,150
	20	40.5	0.60	31,400	28,100
Stainless Steel	0.9	59	0.9	15,800	28,100
Type 347	0.17	75	1.2	14,900	28,100

* Thickness equal to or greater than ASME Code requires.

** Allowable stress is 1.5 times S value in Table 23, Section VIII, ASME Code.

8.836 Loop Tubes

In order that the entire loop system containing primary coolant may be decontaminated with various chemical procedures, the in-pile loop tubes should be constructed of high alloy steels.

The pressure and thermal stresses for loop tubes of various thicknesses are given in Fig. 8.8C for the following design conditions:

Internal Pressure	2200 psig
External Pressure	0 psig
Uniform Internal Heat Generation	20 watts/g
Maximum Metal Temperature	500°F
Internal Diameter	3.018 in.

The requirement of maximum loop water coolant temperature of 650°F can be met by providing an adiabatic inside wall (stagnant water

layer or gas barrier) so that the thermal stresses were calculated for cooling from the outside wall only. A comparison of total stress with allowable stress[1] (1.5S) is given in Table 8.8D for stainless steel.

TABLE 8.8D

COMPARISON OF TOTAL STRESS WITH ALLOWABLE STRESS

Material	Inside Diameter in.	Thickness* in.	Total Stress psi	Allowable Stress** psi
Type 347 S.S.	3.018	0.241	82,800	22,800
Type 316 S.S.	3.068	0.216	70,000	25,800

* Thickness equal to or greater than required by ASME Code.
** Allowable combined stress is 1.5 times S value from Table 23, Section VIII, ASME Code.

It is seen from the above Table that with these design conditions even the strongest (Type 316) 3 in. stainless steel schedule-forty pipe (0.216 in. wall thickness) does not meet the allowable stress requirements of the ASME Code; neither will a thicker wall, as is seen from Fig. 8.8C. Although construction of the loop tube from Type 347 stainless steel requires a thicker wall to meet the pressure stress requirements, its known corrosion and fatigue life behavior under irradiation makes it the preferred material of construction for the loop tubes. Reduction of the thermal stress even by reduction of the temperature difference across the wall to 10°F, does not result in a combined stress within ASME code. Design of the loop tubes with high thermal heating rates must therefore be made in accordance with tentative methods involving allowable-pressure and tentative-fatigue design procedures.

Stainless steel loop tubes with design characteristics similar to those indicated in Table 8.8D are now being used successfully in reactors. The justification entails calculation of the fatigue life from the strain cycling that occurs since the combined stresses exceed the proportional limit, e.g., the yield strength for Type 316 stainless steel at 500°F is 27,000 psi.[2] This design procedure has not as yet been accepted by ASME but is used by the Bureau of Ships.[3] Following the procedure of Coffin,[4] the fatigue life for Type 347 stainless steel

1. Interpretations of ASME Boiler and Pressure Vessel Code, Case 1273N.
2. Reactor Handbook of Materials, U.S. AEC McGraw-Hill Printing Company. p. 274, 1955.
3. "Tentative Structural Design Basis for Reactor Pressure Vessels and Directly Associated Components" dated December 1, 1958, Bureau of Ships.
4. L. F. Coffin, "Design Aspects of High Temperature Fatigue with Particular Reference to Thermal Stresses", Trans. ASME Vol. 78, p. 527, 1956.

under the conditions of Table 8.8D is 65,000 cycles. For a yield stress of Type 347 stainless steel of 32,000 psi and pressure and thermal stress values from Fig. 8.8C for a thickness of 0.241 in. the progressive expansion of the loop tubes may be examined following the method of Miller[1] with the result that cyclic growth does not occur for a linear or parabolic temperature variation in the metal.

From the above considerations the loop tube should be constructed of Type 347 stainless steel with a thickness of 0.241 in. for the 3 in. i.d. tubes.

---

1. D. R. Miller, "Thermal-Stress Ratchet Mechanism in Pressure Vessels", KAPL-1955, August 12, 1958.

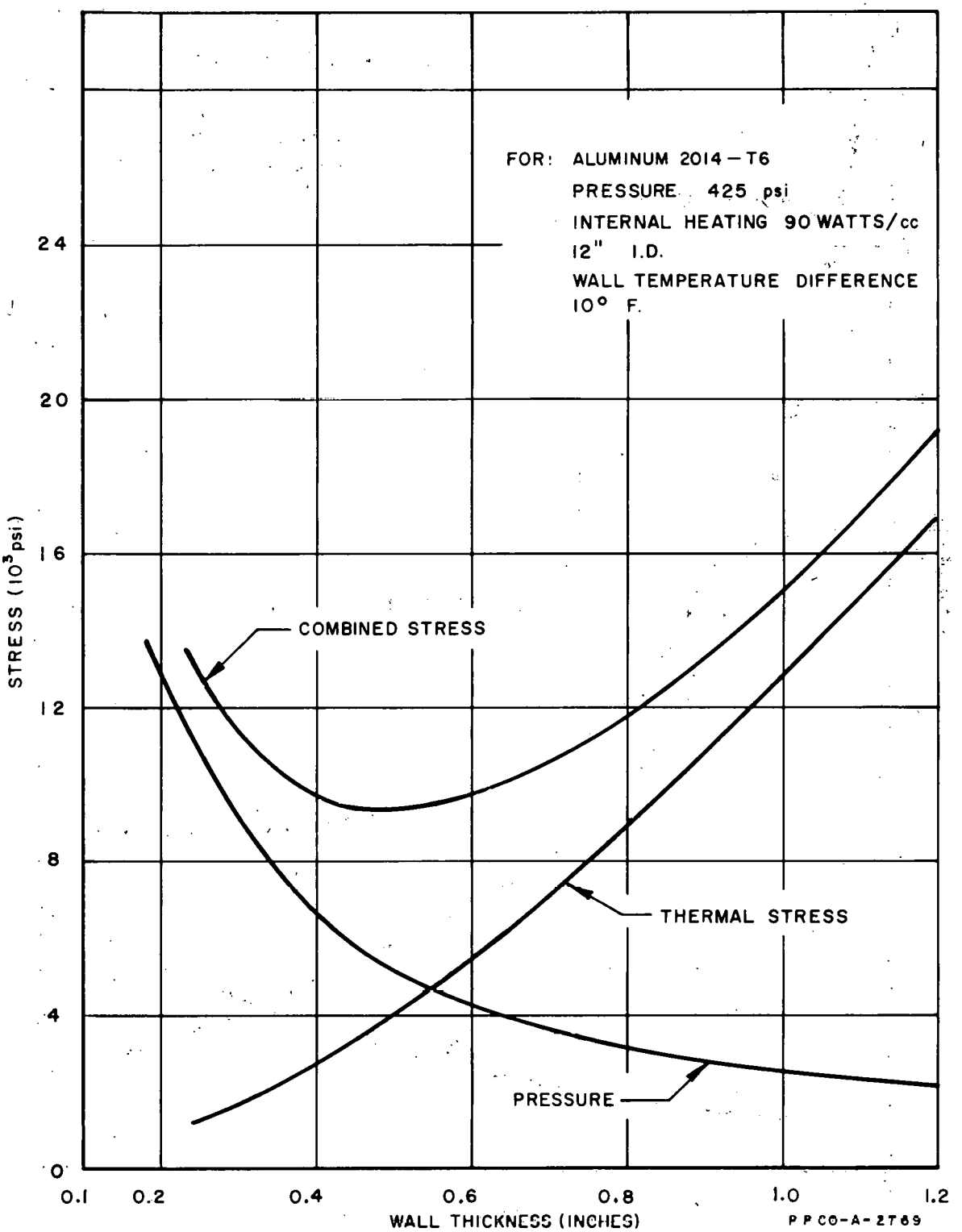

FIG. 8.8 A

TANGENTIAL STRESSES IN REACTOR PRESSURE VESSEL VERSUS WALL THICKNESS

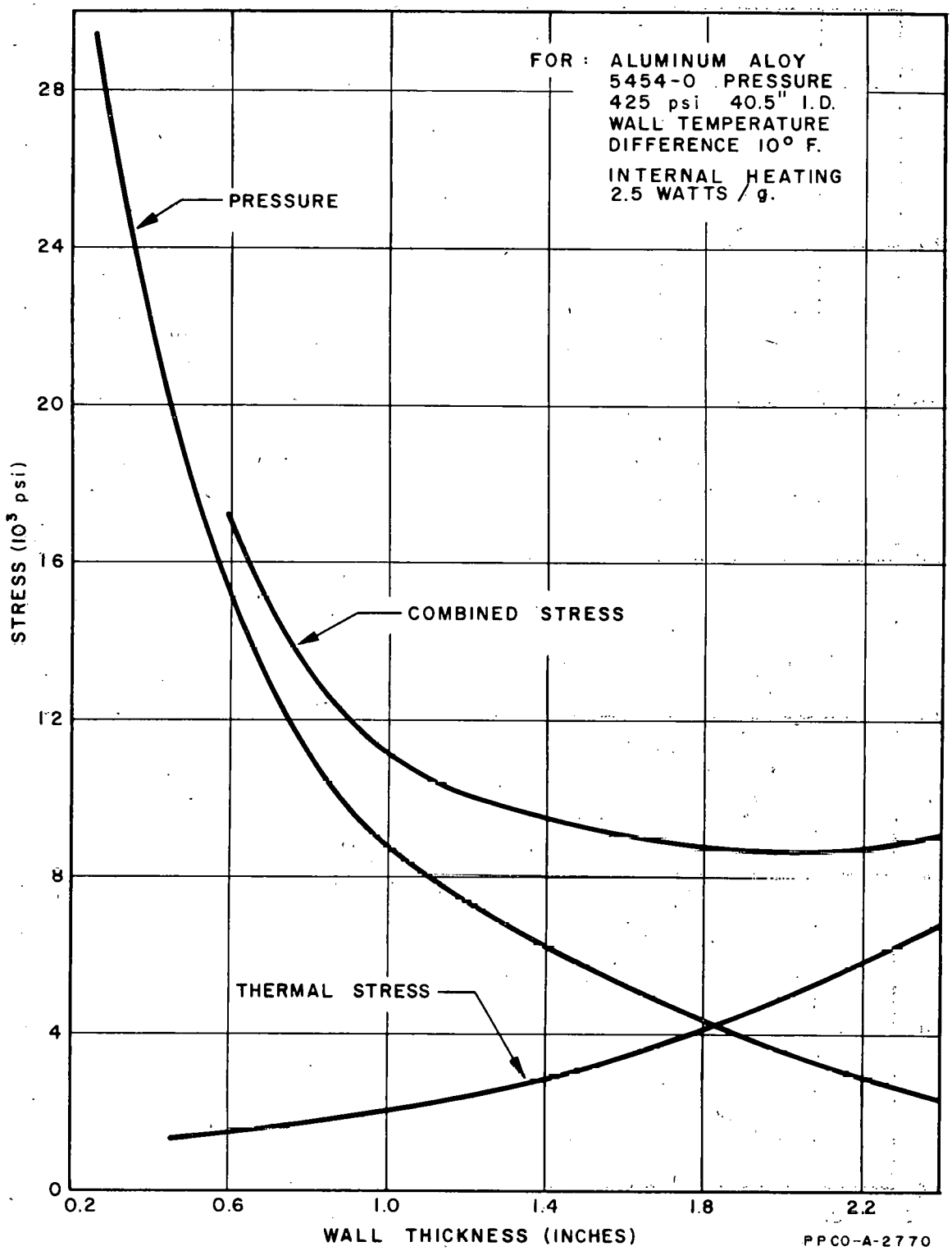

FIG. 8.8 B

TANGENTIAL STRESSES IN REACTOR PRESSURE VESSEL VERSUS WALL THICKNESS

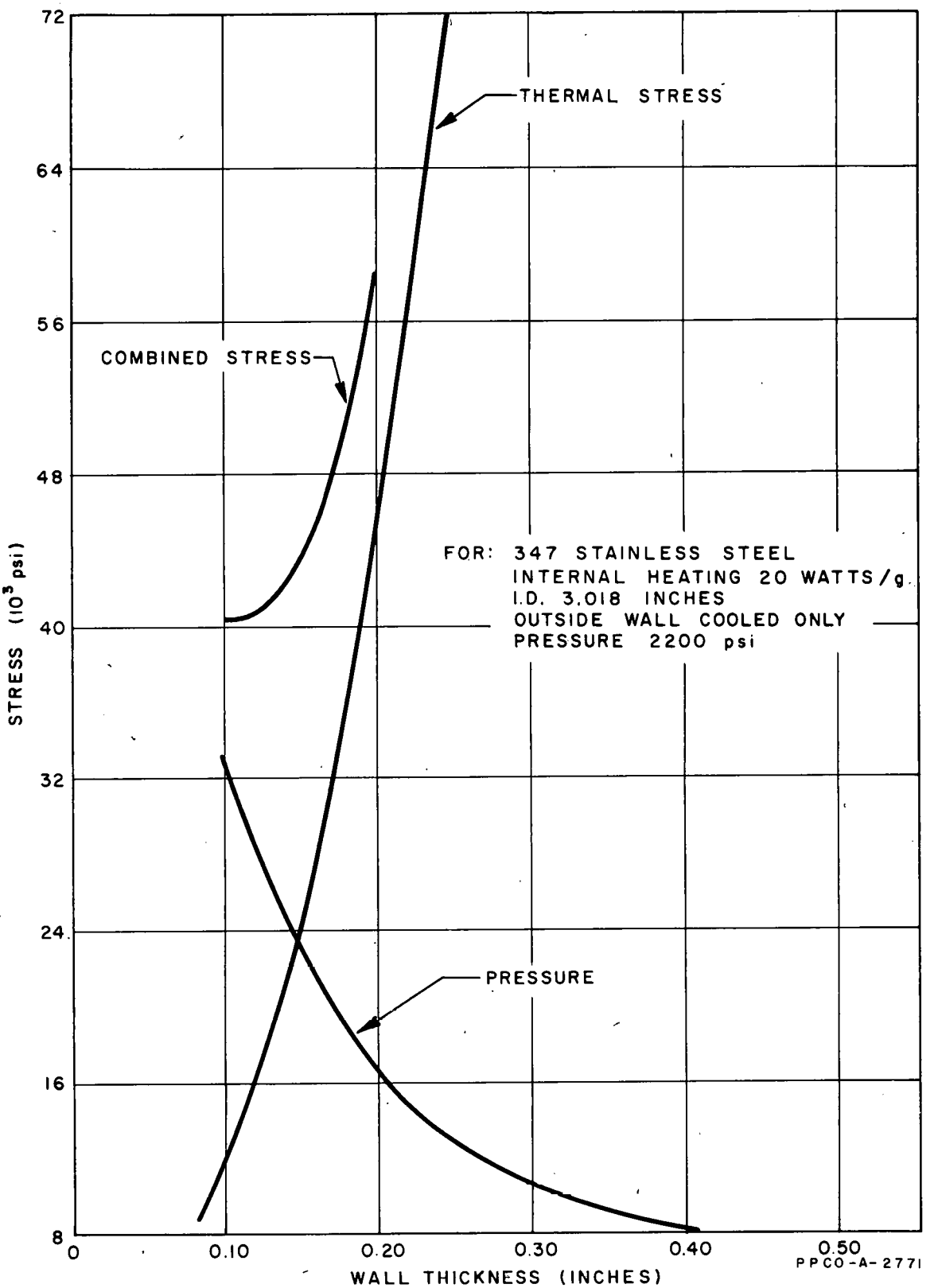

FIG. 8.8 C
TANGENTIAL STRESSES IN IN-PILE LOOP TUBE
VERSUS WALL THICKNESS

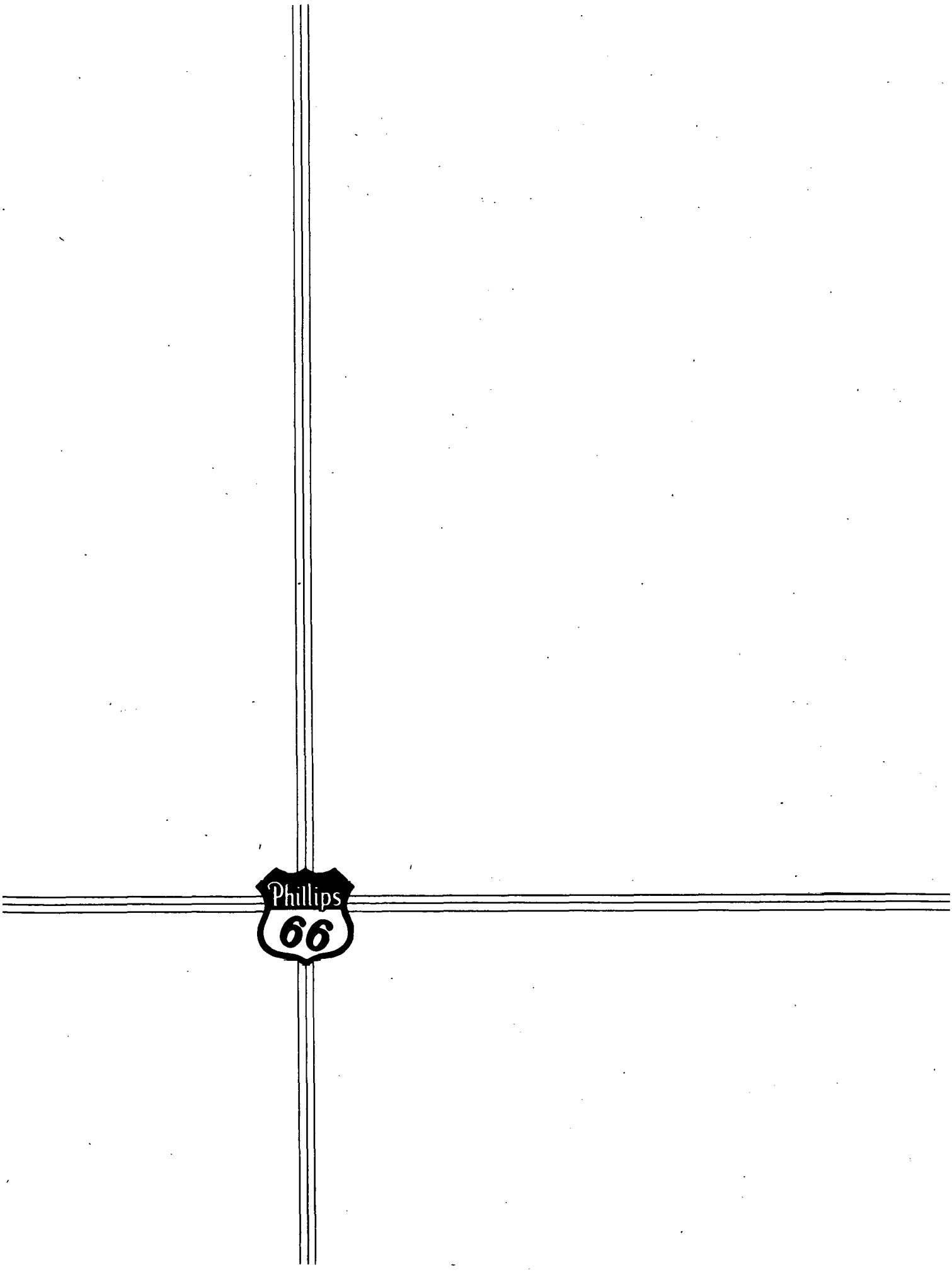
Phillips
66